Defining the Ubiquitin and E2-Enzyme Requirements for APC/C-Mediated Degradation of Cyclin B1

Dissertation Advisor: Dr. Randall W. King Author: Nevena Dimova

Defining the ubiquitin and E2-enzyme requirements for APC/C-mediated degradation of cyclin B1

Abstract

Post-translational modification of proteins with ubiquitin regulates many aspects of cell physiology, including protein degradation. A uniform polyubiquitin chain that is linked through Lys48 has been widely accepted as central for recognition and destruction by the 26S proteasome. Work in more recent years has demonstrated that the repertoire of proteolytic signals may encompass chains of other linkage types, including Lys11-linked ubiquitin chains and short assemblies of mixed linkage. In this dissertation I examine whether catalysis mediated by the Anaphase-Promoting Complex/Cyclosome (APC/C) is dependent on polyubiquitination and whether the proteolytic machinery exerts a requirement for specific ubiquitin linkages to efficiently degrade cyclin B1.

In chapter II, I describe a novel method in which *Xenopus* cell-cycle extracts are made largely dependent on exogenous ubiquitin by inhibiting ubiquitin recycling, allowing us to evaluate the relative contribution of distinct ubiquitin linkages in APC/C-mediated ubiquitination and degradation. Utilizing this approach, in chapter III, I found that the conjugation of single ubiquitin moieties to multiple lysine residues in cyclin promotes efficient degradation of cyclin B1 in mitotic *Xenopus* extracts. Lysine11-ubiquitin chain-formation becomes essential to proteasomal targeting only when the number of available lysine residues in cyclin B1 is

restricted. Analysis in a reconstituted system revealed that APC/C catalyzes multiple monoubiquitination with rapid kinetics and species bearing four or more monoubiquitins on distinct lysines are recognized by ubiquitin receptors. These multiply monoubiquitinated species are rapidly degraded by purified proteasomes.

In chapter IV, I examine the role of distinct E2 enzymes in APC/C-dependent proteolysis. I demonstrate that the chain-extending E2 UBE2S and long Lys11-linked ubiquitin assemblies are dispensable for cyclin B1 degradation, but become increasingly important with restriction of the number of ubiquitination sites. Our findings support a model where through attachment of monoubiquitin to multiple lysine residues, and possibly elaboration of some short chains, UBCH10, or possibly members of the UBC4/5 family, cooperate with the APC/C to generate a robust proteolytic signal on cyclin B1.

Table of Contents:

List of Tables and Figures:

Acknowledgments

First I would like to thank my advisor Dr. Randy King. He has been a truly great mentor in every aspect. Randy has been very supportive along every step of my graduate career. During the last five and a half years of work in the laboratory, Randy has exerted profound influence on me, which is not limited to my research projects, but also extends to my view of science. He has encouraged me to always identify and pursue important questions and has demonstrated to me how to tackle scientific questions in a systematic way. He has also conveyed the importance of designing experiments in a rigorous way and has taught me to interpret data in a critical manner. His love for teaching and passion for science have been an inspiration to me.

I would like to thank the members of my dissertation advisory committee – Dr. Dan Finley, Dr. Sam Reck-Peterson and Dr. Jagesh Shah. They have always been very supportive and enthusiastic about my projects. Their guidance has been greatly valuable for the progress of my work. In spite of their busy schedules, they have always found time to discuss questions about this work or my professional growth.

I could have not asked for better colleagues in the laboratory. Although the makeup of the laboratory has changed over the years of my graduate work, all of my colleagues have been truly great scientists to work with and amazing friends. They have all been very supportive and always ready to help. I would like to give special thanks to Dr. Nathaniel Hathaway who was a graduate student at the time I joined the lab. Nate is a very talented scientist and a great teacher. Working closely with him, I learned a great deal and gathered the confidence that I can pursue the answers to important scientific questions. The degradation assays part of this project would not have been possible without the proteasomes Dr. Byung-Hoon Lee provided. Byung-Hoon, who has a joint appointment with the Finley lab, has been a great colleague. I am very happy to have worked with Dr. Katherine Sackton. She invested a great amount of time and efforts examining the stability of

different lysine mutants of cyclin B1 in human cells. Dr. Kathleen Pfaff has been very helpful with different aspects of my project. There are so many good things I can say about Dr. Frederic Sigoillot. In addition to sharing a lot about French culture and cuisine, he has been enthusiastic about sharing his knowledge and experience. Whether I had a question regarding formatting figures or needed help with a protein purification, he has been there for me. I would like to acknowledge Xing Zeng who is a classmate of mine and did his graduate work in the lab. I thank Xing for insightful discussions and collaboration on different aspects of our projects. Also, I would like to say that without the undergraduate students Lillian Zhao, Maia Anderson, Shantanu Gaur, the lab would not have so much fun.

I feel privileged to have done my graduate work in the Department of Cell Biology. I would like to give special thanks to our collaborators – Dr. Steve Gygi and Dr. Dan Finley, and the members of their laboratories. At the heart of this project has been work carried out by a talented scientist – Dr. Donald Kirkpatrick. Also, more recently my project has benefited significantly from collaborations with Dr. Mike Aguiar. It has been a pleasure to also work with scientists in Dr. Dan Finley's lab, in particular Dr. Suzanne Elsasser, Dr. Jessica Robert and Dr. Bradley Pearse. Their expertise in the proteasome field has been of great value to my research.

I would like to thank my friends and family for their unconditional love and support. Even thousands of miles away from home, I have been blessed to have my family's support along this long journey. This dissertation is dedicated to my parents -Rositssa and Varbin, and to my brothers – Matey and Lyubomir.

Chapter I: Introduction

Nevena Dimova

Protein modification by ubiquitin

Ubiquitination (also known as ubiquitylation) is a powerful mechanism for regulating essentially all aspects of cell physiology, including cell division, apoptosis, transcription, signal transduction and the modulation of diverse metabolic pathways (Ciechanover, 2005b; Johnson, 2002; Kerscher et al., 2006; Pickart and Fushman, 2004). The covalent attachment of ubiquitin (Ub) to substrate proteins is mediated by an enzymatic cascade that is tightly regulated in a spatial and temporal manner and is characterized by a high degree of specificity for the substrates it modulates. The best-studied result of this modification is the targeting of ubiquitin-tagged proteins for proteasomal degradation. Other important advances since the seminal work focused on understanding the energy-dependent proteolytic activity found in reticulocyte extracts (Ciechanover, 2005a; Ciechanover, 2005b; Ciechanover et al., 1984a; Hershko, 2005) were the discovery of non-degradative functions for ubiquitin and the discovery of ubiquitin-like proteins. How the ubiquitin signal assembled on a substrate is read by different downstream effectors and modulates the fate and/or function of the modified protein remains a central theme in the ubiquitin field.

Ubiquitin is a small 76 amino-acid protein first purified during the isolation of thymopoietin by Goldstein and colleagues (Goldstein, 1974). The high evolutionary sequence conservation (Schlesinger and Goldstein, 1975; Wilkinson et al., 1986), likely unparalleled among known proteins, indicates the central role of ubiquitin-conjugation pathways to normal cell function. Even though this protein may not be as ubiquitous as was initially thought, the name aptly reflects its representation in a variety of cellular tissues and organisms (Goldstein, 1974; Goldstein et al., 1975). Several ubiquitin-like proteins (UBLs) have also been identified, including NEDD8, SUMO and ISG15, which share a characteristic three-dimensional fold with ubiquitin but are otherwise distinct (Kerscher et al., 2006; Schulman and Harper, 2009). The overall structure of this ~8.5-kDa heat-stable protein is extremely compact and tightly-hydrogen bonded with only its C-terminal tail, which is accessed by enzymes, protruding from the molecule

(Vijay-Kumar et al., 1987). The stability of ubiquitin is likely further enhanced by the pronounced hydrophobic core (Vijay-Kumar et al., 1987). Subsequent work has indicated that the structural constraints required for proper conjugation or recognition of ubiquitin by downstream effectors are quite strict. Different surfaces revealed in the crystal structure of ubiquitin (Vijay-Kumar et al., 1987) have been implicated in distinct cellular processes. The hydrophobic patch surrounding residues Leu8, Ile44 and Val70 is important for recognition of ubiquitin chains by proteasome-associated ubiquitin receptors and proteasome-mediated degradation (Beal et al., 1996; Beal et al., 1998; Lam et al., 1997a; Sloper-Mould et al., 2001). The surface surrounding Ile44 has also been implicated in internalization of activated plasma-membrane receptors (Shih et al., 2000; Sloper-Mould et al., 2001). Residues Phe4 and Asp58 have been demonstrated to be critical for non-proteolytic functions of ubiquitin (Lee et al., 2006; Penengo et al., 2006; Shih et al., 2000; Sloper-Mould et al., 2001).

An important breakthrough early in the field of ubiquitin research was the discovery that a single ubiquitin molecule can be covalently linked to histones, particularly to histones H2A and H2B (Hershko and Ciechanover, 1998). This and subsequent work revealed that, in most cases, ubiquitin is conjugated to substrates via an isopeptide bond between the activated carboxy-terminal glycine (Gly76) of ubiquitin and an ε-amino group of a lysine (Lys) residue in a substrate (Ciechanover et al., 1984a; Ciechanover et al., 1980; Goldknopf and Busch, 1977; Hershko and Ciechanover, 1998; Hershko et al., 1981; Hunt and Dayhoff, 1977). In some cases, ubiquitin is conjugated to the α-amino group of the target substrate (Ciechanover and Ben-Saadon, 2004; Hershko et al., 1984), and there are a few examples of attachment to threonine, serine or cysteine residues (Cadwell and Coscoy, 2005; Carvalho et al., 2007; Grou et al., 2008; Shimizu et al., 2010; Wang et al., 2007). Ubiquitin itself contains seven Lys residues, at positions 6, 11, 27, 29, 33, 48, and 63, which can function as acceptor sites for another ubiquitin moiety during the assembly of ubiquitin chains**.** All seven potential ubiquitin-ubiquitin linkages have been found to exist *in vivo* (Peng et al., 2003; Xu et al., 2009)**.** Because of the possible variations

in the sites and type of ubiquitination, the potential repertoire of ubiquitin signals is vast and an outstanding challenge for the ubiquitin field is to understand how these modifications dictate distinct fates of target proteins.

Molecular players in ubiquitin-chain assembly and disassembly

The organization of the ubiquitin-conjugation system is hierarchical. The enzymes involved in the cascade reaction of ubiquitin transfer onto substrates (Figure 1.1) were purified by Hershko, Ciechanover and colleagues (Ciechanover et al., 1982; Hershko et al., 1983). In the first step, the ubiquitin-activating enzyme (E1) forms a ternary complex consisting of E1-ubiquitin thioester with ubiquitin-AMP bound (Bedford et al., 2011; Ciechanover et al., 1984a; Hershko and Ciechanover, 1998).The activated ubiquitin is subsequently passed to one of a number of distinct ubiquitin-conjugating (E2) enzymes by transthiolation to a conserved cysteine (Cys) of the E2. The E2 proteins catalyze substrate modification in conjunction with a ubiquitin-protein ligase (E3). For the ~60 members of homologous to E6-AP C-terminus (HECT) family E3s, ubiquitin is shuttled from an E2 to a catalytic Cys in the HECT domain of the E3 before being attached to a substrate (Bedford et al., 2011; Hershko and Ciechanover, 1998; Kerscher et al., 2006; Scheffner et al., 1995). Most E3s, however, contain a really interesting new gene (RING) domain or a structurally related U-box and act as scaffold, bringing a substrate and ubiquitin-charged E2 in proximity and activating the E2 to transfer ubiquitin to a Lys residue in the substrate (Bedford et al., 2011; Kerscher et al., 2006; Pickart, 2001). Ubiquitin chains nucleated on the substrate can be further elaborated by the activity of chain-elongating (E4) enzymes (Crosas et al., 2006; Koegl et al., 1999). Removal of ubiquitin groups which may modulate ubiquitin signaling is carried out by deubiquitinating enzymes (also referred to as deubiquitinases or DUBs) (Amerik and Hochstrasser, 2004; Finley, 2009; Komander et al., 2009; Lam et al., 1997b; Nijman et al., 2005). By processing ubiquitin or ubiquitin-like gene products to yield the

free monomer form (Ozkaynak et al., 1987; Ozkaynak et al., 1984) and by recycling ubiquitin from existing conjugates (Komander et al., 2009), deubiquitinases play a critical role in ubiquitin homeostasis and the proper functioning of the ubiquitin-conjugation cascade.

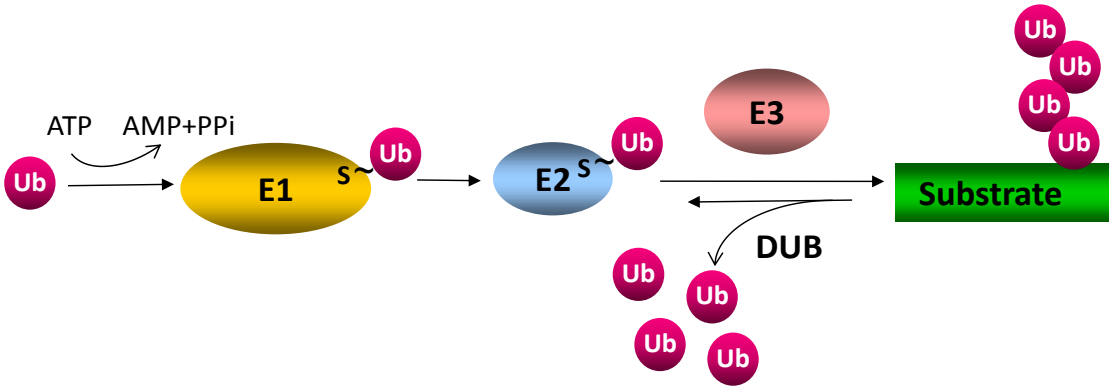

Figure 1.1 Schematic overview of ubiquitination. In the first step, a ubiquitin-activating (E1) enzyme uses ATP to form a thioester bond between the Cys residue (denoted with S) at its active site and the carboxyl terminus of ubiquitin (Ub). The activated ubiquitin is then transferred to the Cys residue in the active site of a ubiquitin-conjugating (E2) enzyme, which in turn cooperates with ubiquitin-protein (E3) ligases to catalyze substrate modification. Removal of ubiquitin groups from substrates, which may modulate the downstream fate of a substrate and is important for maintaining steady-state ubiquitin levels, is carried out by deubiquitinating enzymes or DUBs.

In contrast to the small number of E1 enzymes known to operate in the ubiquitin-proteasome system (UPS) (Ciechanover et al., 1984b; Finley et al., 1984; Jin et al., 2007), there are at least 38 E2s encoded by the human genome (Ye and Rape, 2009). Active E2 enzymes possess a conserved core ubiquitin-conjugating (UBC) domain, which contains the catalytic Cys residue and interacts with E1s (Ye and Rape, 2009). After accepting ubiquitin transiently, E2s engage with a cognate E3 enzyme to catalyze substrate ubiquitination. A single ubiquitin ligase can work in conjunction with more than one E2 to ubiquitinate substrates, as seen for the anaphase-promoting complex/cyclosome (APC/C or APC) which interacts with members of the E-2C and UBC4/5 families of E2 enzymes (Kirkpatrick et al., 2006). Also, a sole E2 can function

with several different E3s – this is observed most dramatically with E2s from the UBC4/5 (also referred to as UBE2D) class (Brzovic et al., 2006; Garnett et al., 2009; Kirkpatrick et al., 2006). A central question in the field remains how the limited number of E2s pair up with the much greater number of putative ubiquitin ligases in a specific and regulated manner.

Because of their role as the ultimate arbiters of substrate selection for ubiquitination, much of the initial work focused on E3s, and E2s were often viewed as simple carriers of activated ubiquitin with auxiliary roles. There is emerging evidence that contradicts this early image of E2s by revealing the complex interactions they carry out and important roles they have in substrate ubiquitination. Indeed, it is now evident that E2 enzymes can actively influence the linkage specificity and length of ubiquitin polymers. Ubiquitin-chain formation requires E3s to first nucleate chains by modifying a substrate lysine, and subsequently to elongate chains by targeting lysine residues in ubiquitin. To catalyze these complex reactions, the ubiquitin system has evolved different strategies. Some E2 enzymes such as yeast Cdc34 catalyzes both chain nucleation and elongation to form Lys48-linked chains on SCF substrates (Gazdoiu et al., 2007; Petroski and Deshaies, 2005; Saha et al., 2011). In contrast to Cdc34, some E2s appear to have dedicated roles in ubiquitin-chain initiation or elongation. An example that is particularly important to our work and will be discussed in further detail in a subsequent section is typified by yeast APC/C which uses Ubc4 to transfer ubiquitin onto Lys residues in cyclin B1 and Ubc1 to elaborate homotypic Lys48-linked ubiquitin chains (Rodrigo-Brenni and Morgan, 2007). In this context, regulating the availability of the two E2s is predicted to impact the outcome of the ubiquitination reaction. It is an interesting possibility that such a mechanism of APC/C activity with dependence on multiple E2 enzymes has evolved to more tightly regulate substrate modification and the ensuing cellular consequences.

Synthesizing ubiquitin chains of a distinct topology is another intrinsic property of many E2 enzymes. To form specific ubiquitin-ubiquitin linkages, the E2 may orient the acceptor ubiquitin in a way that exposes the favored Lys residue to its active site (Eddins et al., 2006;

Petroski and Deshaies, 2005). Some E2s exhibit specificity for assembling free chains of a distinct linkage without the aid of an E3 and that linkage specificity is not altered by binding to their cognate E3s (Chen and Pickart, 1990; Wickliffe et al., 2011a). Because ubiquitinated substrates may be sorted into different pathways based on diverse polyubiquitin structures (Pickart and Fushman, 2004), E2s can be viewed as regulators of ubiquitin signaling owing to their capacity to build specific chains. It is important, however, to determine whether the assembly of ubiquitin chains of specific linkage simply reflects intrinsic properties of the E2 rather than a requirement imposed by downstream effectors.

Ubiquitin-conjugating enzymes may also influence the processivity of ubiquitination, defined as the number of ubiquitin molecules that are attached to substrates during a single binding to an E3 (Carroll and Morgan, 2002; Rape et al., 2006). Processivity of ubiquitination depends on the binding affinity of substrates as well as the availability and kinetic properties of E2 enzymes (Rape et al., 2006). Very processive substrates will acquire their functional ubiquitin tag in a single substrate-E3 binding event (Pierce et al., 2009; Rape et al., 2006). In contrast, more distributive substrates will continuously shuttle on and off the ligase complex in order to achieve their functional ubiquitination status and be potentially exposed to the activity of DUBs. Thus the processivity with which a substrate acquires its functional ubiquitin signal is likely to directly influence the downstream fate of the substrate. E2 enzymes have evolved different mechanisms to enhance the processivity of ubiquitination, including the binding of E3s using multiple independent binding sites to increase affinity, recognition of substrate and ubiquitin motifs, oligomerization of ubiquitin-charged E2s and pre-assembly of ubiquitin polymers on their active sites followed by *en bloc* transfer to the substrate (Ye and Rape, 2009).

How do properties of E2 enzymes that determine the balance of multiple monoubiquitination versus assembly of ubiquitin chains of specific length and topology affect ubiquitin-receptor binding and proteasomal degradation of substrates? In the work presented in

this dissertation, we address this question in the context of APC-mediated proteolysis of cyclin B1.

Ubiquitin-signal topology and proteasome targeting

Over a decade after the discovery of the ubiquitin pathway, it was realized that ubiquitin can be appended not only to different cellular proteins, but also to other ubiquitin moieties forming polyubiquitin structures (Chau et al., 1989; Hershko and Heller, 1985). This raised the question as to whether a unique ubiquitin tag signals destruction by the proteasome. Indeed, in the context of an engineered substrate Arg-βgal, the assembly of a polyubiquitin chain was critical for proteasomal degradation (Chau et al., 1989). In this context, lysine-to-arginine substitution at Lys48 of ubiquitin abrogated both ubiquitin-polymer formation and substrate proteolysis (Chau et al., 1989). Based on this and subsequent studies (Thrower et al., 2000), a model emerged where a polymer of 4 or more ubiquitin groups linked through Lys48 is required for efficient substrate degradation by the proteasome. Whether ubiquitin signals of different architecture were sufficient for proteasomal targeting was not addressed in these studies. Nevertheless, Lys48-linked chains became widely viewed as the canonical proteolytic signal. This model was further corroborated by work demonstrating that Lys48 of ubiquitin was important for bulk protein turnover and essential, albeit not sufficient, for proper cell-cycle progression in *S. cerevisiae* (Finley et al., 1994; Xu et al., 2009). The mitotic phenotype observed in UbK48R mutants where cells displayed two-lobed nuclei and remained arrested in medial nuclear division (Finley et al., 1994) is reminiscent of that observed upon deletion of the gene encoding the E2 Ubc1 (Rodrigo-Brenni and Morgan, 2007). For timely mitotic exit in these cells, the activity of the Lys48 chain-extending E2 Ubc1 in promoting proteolysis of APC substrates was found critical (Rodrigo-Brenni and Morgan, 2007). These and other studies underscore that the ubiquitin signal assembled on substrates is a function of the different E2-E3 complexes and poise the question

whether ubiquitin structures other than Lys48-linked chains can target substrates to the proteolytic machinery. Assigning the proteasomal signaling function to a specific Lys48-linked polymeric unit was a particularly attractive model as it also explained how a single ubiquitin can act as a functionally distinct signal in non-proteolytic processes. Similarly, to monoubiquitination and multiple monoubiquitination (Robzyk et al., 2000; Terrell et al., 1998), polymers assembled through Lys63 of ubiquitin have been implicated in mostly non-proteolytic roles (Deng et al., 2000; Hofmann and Pickart, 1999; Pickart and Fushman, 2004; Spence et al., 2000; Spence et al., 1995; Yang et al., 2009) (Figure 1.2).

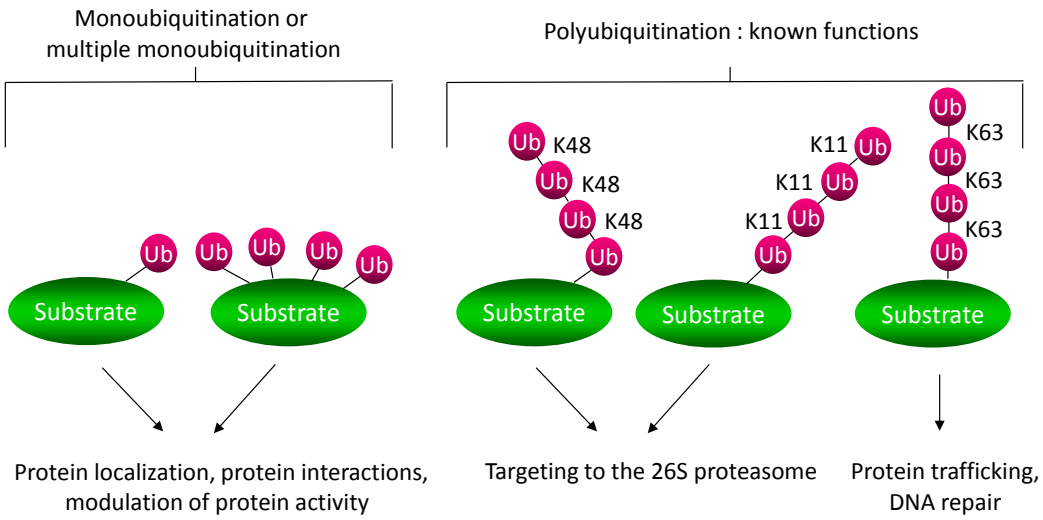

Figure 1.2 The ubiquitin code. Ubiquitin is usually conjugated to the ε-amino group of a lysine (Lys) residue in a substrate (Hershko and Ciechanover, 1998). Ubiquitin itself contains seven Lys residues, at positions 6, 11, 27, 29, 33, 48, and 63, which can function as acceptor sites for another ubiquitin moiety during the assembly of ubiquitin chains**.** In the classical model, a uniform K48-linked ubiquitin polymer is required for substrate recognition and destruction by the 26S proteasome (Chau et al., 1989; Thrower et al., 2000; Finley et al., 1994). Work in more recent years has demonstrated that the repertoire of proteolytic signals may encompass chains of other linkage types, including K11-linked ubiquitin chains (Xu et al., 2009). Polymers built through K63 of ubiquitin have been suggested to have non-proteolytic roles in orchestrating different steps of DNA repair (Spence et al., 1995; Hofmann and Pickart, 1999) , kinase activation (Deng et al., 2000), protein trafficking (Pickart and Fushman, 2004; Yang et al., 2009) and translation (Spence et al., 2000). Similarly, the transfer of a single ubiquitin moiety to one (monoubiquitination) or to multiple sites (multiple monoubiquitination) in a substrate has long been implicated in mostly non-proteolytic processes, such as epigenetic control (Robzyk et al., 2000) and receptor endocytosis (Terrell et al., 1998).

How can we detect different ubiquitin topologies and gain understanding of their functional significance in the cell? One approach has involved large-scale analyses and characterization of protein ubiquitination using quantitative mass-spectrometry techniques (Kim et al., 2011; Peng et al., 2003; Xu et al., 2009). Such studies have revealed a striking and unexpectedly high abundance of non-Lys48 ubiquitin linkages, especially Lys11 linkages (Peng et al., 2003; Xu et al., 2009). Moreover, Lys11-linked chains have been implicated in a broad range of physiological processes, including cell division and endoplasmic reticulum-associated degradation (ERAD) (Behrends and Harper, 2011; Wickliffe et al., 2011b; Xu et al., 2009). A critical issue with these methodologies is that they are concentration-sensitive and thus better at identifying more abundant conjugates in the cell, while not detecting all short-lived proteins such as cell-cycle regulators (Peng et al., 2003). Also, while such analyses are integral to our understanding of the global ubiquitin landscape in the cell, they may not accurately reflect the behavior of individual proteins. For instance, no significant changes in total levels of Lys63 linkages are observed upon proteasomal inhibition (Xu et al., 2009), even though these are capable of supporting degradation by the proteasome (Baboshina and Haas, 1996; Hofmann and Pickart, 2001).

Another approach to studying protein ubiquitination may be to integrate large-scale analyses with work detailing individual pathways. A method that has allowed significant progress in characterizing ubiquitin conjugates and mapping precise sites of ubiquitination is the absolute quantification of ubiquitin by mass spectrometry (Ub-AQUA) (Kirkpatrick et al., 2005; Kirkpatrick et al., 2006). This quantitative mass-spectrometry technique uses isotope-labeled internal standard peptides to quantify tryptic peptides that are derived from the digestion of any given sample. By comparison to the known amount of isotope-labeled standards, the exact amount of any given peptide in a sample can be quantitated. By applying the law of conservation of mass, one can use this method to quantify the absolute amount of any given substrate, ubiquitin, and the relative proportion of each of the seven potential ubiquitin-ubiquitin linkages.

In the work presented in this dissertation, we have combined analysis of processes reconstituted *in vitro* and Ub-AQUA analysis with studies in the *Xenopus* system to delineate how the E3 ligase APC/C mediates ubiquitination and degradation of cyclin B1.

Studying the role of distinct ubiquitin topologies in protein breakdown in physiological settings has proven to be challenging. This can be attributed, in part, to the dynamic nature and fast kinetics of the ubiquitination and proteolytic events. Another factor that hinders our understanding of ubiquitin-mediated proteolysis has been the lack of methods allowing the ubiquitin pool available in a physiological setting to be modulated in a precise and controlled manner. Dominant-negative effects may be hard to observe when conducted in a background that contains wild-type ubiquitin. Meanwhile, ubiquitin homeostasis, through *de novo* protein synthesis and recycling from existing conjugates, is tightly regulated, rendering ubiquitin depletion hard to achieve. Thus, we need novel approaches for ubiquitin replacement to examine the effects of ubiquitin mutants on degradation in a physiological context.

The proteasome - a complex protein-degrading machinery

The 26S proteasome, an intricate molecular machine of over 2.5 MDa, is the proteolytic arm of the UPS (Waxman et al., 1987). It functions primarily to degrade damaged, misfolded and short-lived regulatory proteins bearing ubiquitin modifications. The proteasome also regulates the state of cells by eliminating key cell-cycle regulators such as cyclins and securin. While existing in multiple forms, the proteasome is a composite of two major assemblies - the 28-subunit core particle (also known as the 20S particle) and the 19-subunit regulatory particle (also known as the 19S particle or PA700) (Finley, 2009; Weissman et al., 2011).The catalytic activity of the proteasome is contained within the barrel-shaped structure of the core particle (Bedford et al., 2011; Finley, 2009; Weissman et al., 2011).

How does this complex machinery discern ubiquitin tags with proteolytic versus non-proteolytic functions, ensuring substrates are not inadvertently degraded? Entrance to the catalytic chamber is directed by factors within the regulatory particle, which recognize and process polyubiquitinated substrates (Finley, 2009; Weissman et al., 2011). Another function of the 19S complex is to remove and recycle ubiquitin from proteolytic substrates concomitantly or prior to their translocation into the core. The third key function of this subcomplex is to promote substrate unfolding and translocation into the core (Finley, 2009; Weissman et al., 2011). The 19S particle is more heterogeneous and unstable as compared to the catalytic core with some of its components in sub-stoichiometric amounts and interchanging with the cytosol (Elsasser and Finley, 2005; Finley, 2009; Leggett et al., 2002; Schmidt et al., 2005). These findings have important implications about the adaptability of the proteasome in response to changing cellular signaling. In the work presented in this dissertation, we attempt to explore how the presence of proteasome-associated DUB activity may influence the recognition and degradation of a ubiquitin-tagged substrate.

Once associated with proteasomal subunits, substrates may have their ubiquitin chains extensively remodeled through opposing ubiquitin-ligase and deubiquitinating activities (Crosas et al., 2006). Whether the delivery pathway to the proteasome influences the nature and extent of ubiquitin-polymer remodeling and how substrate specificity is enforced remain poorly understood. However, there is an emerging view that remodeling of the ubiquitin tag by the proteasome, during a kinetically defined time window, can influence the fate of substrates. Remodeling of the ubiquitin signal can, in part, be carried out by the three deubiquitinases found in mammalian proteasomes: RPN11, USP14, and UCH37 (Finley, 2009; Komander et al., 2009; Lee et al., 2010b). UCH37 and USP14 associate reversibly with the proteasome, whereas RPN11 is a stoichiometric subunit (Finley, 2009). Essential for proteasome function (Finley, 2009; Verma et al., 2002; Yao and Cohen, 2002), the metalloenzyme RPN11 promotes substrate degradation by removing ubiquitin moieties, which may not be easily threaded through the

narrow translocation channel (Finley, 2009; Lander et al., 2012; Verma et al., 2002; Yao and Cohen, 2002).

The activity of UCH37 and USP14 may stimulate breakdown of some substrates, while antagonize that of others (Hanna et al., 2006; Jacobson et al., 2009; Lam et al., 1997b; Lee et al., 2010a; Leggett et al., 2002). UCH37 has been implicated as an editing activity for the proteasome by selectively removing ubiquitin groups from oligoubiquitinated substrates and allowing them to escape degradation (Lam et al., 1997b). It remains to be determined, however, whether in the cellular context, UCH37 could provide a means for the proteolytic machinery to discriminate against substrates bearing multiple monoubiquitins or short ubiquitin chains. In contrast, USP14 is thought to act on more heavily ubiquitinated substrates. By trimming of substrate-bound ubiquitin chains, USP14 has been suggested to potentially govern the degradation rates of numerous substrates (Hanna et al., 2006; Lee et al., 2010a). Unexpectedly, USP14 was also found to delay substrate degradation through a non-catalytic mechanism (Hanna et al., 2006; Lee et al., 2010a). While these effects are not well understood, they may be related to the chain-trimming activity of USP14 and may also help the cell recycle ubiquitin especially under conditions of ubiquitin deficiency. Consistent with such a role, the expression of Ubp6 (the yeast orthologue of USP14) is upregulated and loading onto the proteasome elevated following depletion of free ubiquitin levels (Hanna et al., 2007). A number of important questions about the proteolytic machinery remain unresolved. Which proteins are substrates of the different DUBs on the proteasome and how substrate specificity and selectivity are enforced? Also, how do the number and spatial arrangement of ubiquitin monomers on a substrate affect its recognition and processing by the proteasome?

An important question is how ubiquitin-tagged proteins are correctly targeted to the proteasome holoenzyme for destruction. One potential solution to this complex problem is the recruitment of the ubiquitin-conjugation machinery in the vicinity in the proteasome. In fact, the E2 UBC4 (Chuang and Madura, 2005) and the APC (Seeger et al., 2003) (also N.D., R.W.K.,

unpublished observations), among other enzymes (Finley, 2009), have been observed to directly associate with the proteasome. The functional significance of these interactions has not been elucidated, but they may allow ubiquitination and subsequent degradation to be spatially linked within the cell. An alternative pathway for target delivery to the proteasome may be dependent on the activity of ubiquitin-receptor proteins. The proteasome appears to recognize ubiquitinated substates via both intrinsic ubiquitin-receptor subunits and by transiently associating shuttling factors (Elsasser and Finley, 2005). Rpn10 (Deveraux et al., 1994; Elsasser and Finley, 2005; Young et al., 1998) and Rpn13 (Husnjak et al., 2008; Schreiner et al., 2008) are the two currently known intrinsic ubiquitin receptors, whereas Rad23, Dsk2, and Ddi1 (Elsasser and Finley, 2005) are shuttling proteins.

The "shuttle" proteins are thought to function in capturing of ubiquitinated substrates remotely from the proteasome and escorting them to this complex. The ubiquitin-associated (UBA) domains in these proteins recognize the ubiquitin tag, whereas the ubiquitin-like (UBL) domains bind to the proteasome (Finley, 2009; Hicke et al., 2005; Schauber et al., 1998). *In vitro* studies suggest some ubiquitin-binding domains (UBDs) bind polyubiquitin preferentially to monoubiquitin, and may even exhibit preference for specific ubiquitin linkages (Hicke et al., 2005). Supporting the view of Lys48-linked chains as the principal proteolytic signal, some studies suggest that proteasome-associated receptor proteins may preferentially recognize Lys48 linkages (Raasi et al., 2004; Raasi and Pickart, 2003; Varadan et al., 2004). In a cellular context, it is likely that the specificity and affinity of binding may require that UBL/UBA proteins recognize binding determinants not only in the ubiquitin tag but also in the modified substrate. Substrate specificity (Verma et al., 2004) may be further enforced by subcellular localization of ubiquitin receptors or their interactions with E3 ubiquitin ligases. Importantly, ubiquitin receptors have the potential to recognize a vast array of ubiquitin signals through multiple UBDs joined by flexible linker regions (Kang et al., 2007; Wang et al., 2005) and by multimerization with other receptors (Kang et al., 2007; Kang et al., 2006). The presence of multiple ubiquitin-interacting

motifs in receptors such as RPN10 may provide additional avidity in recognition of targets, particularly those targets bearing either a polyubiquitin structure or multiple monoubiquitins (Finley, 2009; Harper and Schulman, 2006).

In the work presented in this dissertation, we investigate whether ubiquitin receptors Rad23 and Rpn10 exert a requirement for ubiquitin-chain formation for binding to ubiquitinated cyclin B1. We also sought to understand whether the proteolytic machinery exerts a requirement for specific ubiquitin topologies for cyclin degradation.

Orchestration of the cell cycle by the anaphase-promoting complex

Cyclins are a diverse family of proteins whose defining feature is that they bind and direct the activity of members of the cyclin-dependent kinase (CDK) family. Oscillations in their levels help to generate strictly controlled changes in the enzymatic activity of CDKs which modulate the phosphorylation state, and thereby the state of activation, of proteins that control cell-cycle processes. The M-phase cyclins typified by cyclin B in vertebrates (Clb1-4 in budding yeast) accumulate as the cell approaches mitosis, peaking at metaphase. The periodic rise and fall in cyclin levels and its striking disappearance at the end of each mitosis in early sea urchin embryos led to the discovery of this critical cell-cycle regulator (Evans et al., 1983). Subsequent studies found cyclin B to form a complex with CDK1 initially termed maturation promoting factor and now referred to as M-phase promoting factor (MPF) (Gautier et al., 1990; Gautier et al., 1988; Lohka et al., 1988). The activity of cyclin B1-CDK complexes is responsible for the striking cellular changes that lead to assembly of the mitotic spindle and the alignment of sister-chromatid pairs on the spindle at metaphase. In addition to driving the cell to metaphase, the complex activates the system that degrades its cyclin subunit and orchestrates exit from both mitosis and meiosis (Glotzer et al., 1991; Hershko et al., 1991; Murray et al., 1989).

The Anaphase-Promoting Complex/Cyclosome (APC/C or APC) was identified in *Xenopus* and clam extracts as the cyclin B1 specific ubiquitin ligase responsible for MPF inactivation upon mitotic exit (King et al., 1995; Sudakin et al., 1995). The E3 ligase activities of Skp1-Cullin-F-box complex (SCF) family and the APC have long been recognized to be crucial to cell-cycle progression and regulation (Harper et al., 2002; Lipkowitz and Weissman, 2011; Peters, 2006; Skaar and Pagano, 2009). Consistent with this, the genetic inactivation of APC causes cell-cycle arrest in all species in which it has been investigated so far, ranging from yeast to mouse (Peters, 2006). In addition to regulating mitosis and meiosis, the APC has been implicated in post-mitotic processes including dendrite formation in neurons, metabolic, and learning and memory processes (Barford, 2011b).

The APC is a ~1.5 MDa complex, composed of at least 13 subunits (Peters, 2006). The size and unusual complexity of this E3 ubiquitin ligase has limited structural studies. The essential roles of APC constituent proteins pose further challenges in using native systems to study the complex. A recombinant expression system was recently generated that allowed the reconstitution of a functional APC in milligram quantities (Schreiber et al., 2011). This is exciting advance as the system may allow defined manipulation of APC complexes and facilitate studies of how APC subunits assemble and interact with co-activators, substrates and regulatory factors.

APC-mediated coordination of cell-cycle progression is achieved through the temporal regulation of APC activity and substrate specificity. One aspect of temporal regulation of the ligase activity is achieved through a combination of two structurally related co-activators Cdc20 and Cdc20 homolog 1 (Cdh1), coupled to protein phosphorylation. The two co-activator subunits have opposing activity profiles. Cdc20 activates the APC at the onset of mitosis, when APC subunits are phosphorylated and Cdh1 activity is low owing to its CDK-mediated phosphorylation. After CDK activity is diminished during mitotic exit, Cdh1 forms a complex with APC, which ubiquitinates Cdc20, leading to APC^{Cdc20} inactivation. The co-activators help recruit substrates to the ligase complex. Indeed, multiple lines of evidence suggest that the co-

activator directly bind APC substrates via its WD40-repeat domain so at least part of the function of the co-activator appears to be a substrate adaptor (Burton and Solomon, 2001; Buschhorn et al., 2011; da Fonseca et al., 2011; Kraft et al., 2005). The co-activators recognize two characteristic sequence elements found in APC substrates, namely a destruction box (D box; RxxLxxI/VxN) (Glotzer et al., 1991; King et al., 1996), and a KEN box (KENxxxN/D) (Pfleger and Kirschner, 2000; Pfleger et al., 2001). Whereas Cdc20 specifically recognizes the D-box motif, Cdh1 appears to prefer the KEN box, but also recognizes the D-box (Peters, 2006; Pfleger et al., 2001).

The reversible association of co-activators with the APC presents one level of regulation of APC activity. Another level of APC control is provided by pseudo-substrate inhibitors such as early mitotic inhibitor 1 (Emi1). By preventing productive interactions of substrates with the catalytic module or interfering with recruitment of E2 enzymes (Barford, 2011b), such pseudo-substrates can block APC-mediated ubiquitination and proteolysis. A similar concept of inhibition may apply to another critical APC regulatory system, the mitotic checkpoint complex (MCC) (Barford, 2011b; Kim and Yu, 2011). Consistent with this idea, elegant structural work reveals that checkpoint proteins inhibit APC catalysis at least in part by preventing substrate binding (Herzog et al., 2009).

According to electron microscopy studies, APC/C complexes more commonly resemble an asymmetric triangular structure, composed of a platform and an arc lamp domain that together enclose a central cavity (Dube et al., 2005; Passmore et al., 2005). Apc1, together with Apc4 and Apc5, function as a scaffolding-like assembly subunit linking the catalytic module formed from Apc2, Apc11 and Apc10 (Doc1) with the TPR subunits Cdc16, Cdc23, Cdc27 found in the arc-lamp domain (Barford, 2011b; Dube et al., 2005; Herzog et al., 2009; Schreiber et al., 2011; Thornton et al., 2006; Vodermaier et al., 2003). The tetratricopeptide repeats (TPR) found in APC/C subunits are 34-amino acid motifs that generate super-helical structures, facilitating protein-protein interactions (Barford, 2011a).

The catalytic core of the anaphase-promoting complex consists of Apc2 and Apc11. Apc2, a member of the cullin protein family, associates with the RING H2-finger domain in Apc11, which in turn recruits E2 ubiquitin-conjugating enzymes (Peters, 2006). Interestingly, Apc2-Apc11 alone can support ubiquitin ligation, albeit with diminished substrate specificity (Tang et al., 2001; Yu et al., 1998). Elegant structural work recently revealed that the cullin-RING module was in close vicinity to the core APC/C subunit Apc10 (Doc1) (Buschhorn et al., 2010; da Fonseca et al., 2011). Apc10 was earlier demonstrated to play a role in substrate recruitment to the ligase and processive substrate ubiquitination (Carroll et al., 2005; Carroll and Morgan, 2002; Passmore et al., 2003), but how it performs these functions remained poorly understood. In this context, a model emerging from recent studies suggests that Apc10 promotes processive substrate ubiquitination by forming part of a bipartite substrate receptor on the APC/C, composed of Apc10's ligand binding region (Au et al., 2002; Buschhorn et al., 2011; Carroll et al., 2005; Carroll and Morgan, 2002; Chao et al., 2012; da Fonseca et al., 2011; Wendt et al., 2001) and the WD40 propeller domain of the co-activator protein (Buschhorn et al., 2011; da Fonseca et al., 2011; Kraft et al., 2005; Matyskiela and Morgan, 2009). Interestingly, substrate binding was found to induce conformational changes in Apc2-Apc11 (Buschhorn et al., 2011) which may be coupled with proper substrate recognition and efficient ubiquitin transfer to substrate residues.

Another layer of interactions important for APC/C activity are those with E2 ubiquitin-conjugating enzymes. Members of the UBC4/5 (King et al., 1995) and E-2C (Aristarkhov et al., 1996; Townsley et al., 1997; Yu et al., 1996) families (in particular human UBCH5 and UBCH10, respectively) have long been recognized as E2 partners for the APC/C. While in a reconstituted system both classes of E2s can support APC/C-dependent ubiquitination (Garnett et al., 2009; Kirkpatrick et al., 2006; Mathe et al., 2004; Summers et al., 2008; Yu et al., 1996; Zeng et al., 2010), which E2 enzyme(s) work with the APC/C *in vivo* remains an open question. Genetic evidence from *S. pombe* and *D. melanogaster* supports the notion that members of the E-

2C family, Ubc11 and Vihar, are most likely to be physiologically relevant (Mathe et al., 2004; Osaka et al., 1997) .Consistent with this, the spatiotemporal pattern of the E-2C protein Vihar distribution and proteolysis closely resembles that for cyclin B1 (Mathe et al., 2004) and a dominant-negative form of the enzyme results in stabilization of APC/C substrates (Townsley et al., 1997). Unlike in simpler model organisms, the importance of UBCH10 for mitosis in human cells has been disputed (Rape and Kirschner, 2004; Walker et al., 2008). An N-terminal extension found in UBCH10, but not in members of the UBC4/5 family, has been proposed to regulate the ubiquitination activity of the APC/C and the sensitivity of the ligase to checkpoint control (Summers et al., 2008).

The set of distinct E2 ubiquitin-conjugating enzymes suspected to function in APC/C-mediated catalysis was recently expanded. In budding yeast, Ubc1 functions as a supplementary E2 enzyme that elongates ubiquitin chains initiated by the proximally-acting E2 Ubc4 (Rodrigo-Brenni and Morgan, 2007). In higher eukaryotes, it has been proposed that another E2 UBE2S is important in elaborating Lys11-linked ubiquitin chains on APC/C-substrates (Garnett et al., 2009; Williamson et al., 2009; Wu et al., 2010). In this model, UBCH10 is proposed to initiate monoubiquitination of the substrate, with UBE2S then extending Lys11-linked ubiquitin chains that signal degradation by the proteasome (Garnett et al., 2009; Jin et al., 2008; Williamson et al., 2009; Wu et al., 2010). Consistent with this idea, depletion of UBE2S from *Drosophila* S2 cells results in a strong delay in a metaphase-like state and stabilization of cyclin B1 at the spindle poles, among other mitotic defects (Williamson et al., 2009). In contrast, UBE2S has a nonessential function in APC/C-mediated proteolysis of cyclin B1 during normal mitosis in human HeLa cells (Garnett et al., 2009). These findings imply instead that UBE2S becomes important for substrate proteolysis under conditions where APC/C activity is compromised such as during recovery from drug-induced spindle assembly checkpoint (SAC) activation. The spindle checkpoint detects inappropriate attachment and tension between chromosomal kinetochores and microtubules and delays segregation of sister chromatids by inhibiting APC-mediated

ubiquitination of securin and cyclin B1 (Kim and Yu, 2011; Musacchio and Salmon, 2007). Under such conditions of low APC/C activity, UBE2S may be priming APC/C molecules for rapid and processive ubiquitination of substrates and may be promoting degradation by enhancing the rate of ubiquitination relative to that of deubiquitination. A possible role of UBE2S in silencing the SAC has not been elucidated. Together these findings imply that the contribution of UBE2S and Lys11-linked chains in the degradation of APC/C substrates may be organism-and condition-specific, and that there may not be a uniform requirement for UBE2S in all systems or circumstances.

Role of ubiquitin-chain formation in cyclin B1 proteolysis

Previous work revealed that in contrast to the SCF-ligase complex which cooperates with the E2 Cdc34 to assemble homogeneous Lys48-linked chains on substrates (Petroski and Deshaies, 2005), the APC works in conjunction with UBCH10 and UBCH5 and modifies cyclin B1 with chains of complex topology (Figure 1.3) (Kirkpatrick et al., 2006). Surprisingly, the ubiquitin signal assembled on cyclin B1 consists of ubiquitin-ubiquitin linkages through Lys11 and Lys63 in addition to Lys48 (Kirkpatrick et al., 2006). Analysis of cyclin ubiquitination revealed a two-stage ubiquitination process, where initially the APC/C facilitates transfer of ubiquitin monomers to multiple lysine residues on cyclin B1, followed by extension of short ubiquitin chains (Kirkpatrick et al., 2006). Under conditions where the assembly of proteolytic signal is non-processive and requires rebinding to the ubiquitin ligase, this pathway, as opposed to the rapid elongation of a single chain, may allow the APC/C to more precisely control the spatiotemporal pattern of substrate proteolysis. In the context of cyclin B1, the short ubiquitin polymers generated by UBCH10 or UBC4 present an efficient proteolytic signal (Kirkpatrick et al., 2006). Interestingly, these assemblies are remodeled by the opposing activities of proteasome-associated E4 chain-elongating enzyme Hul5 (KIAA10) and the deubiquitinase USP14 (Crosas et

al., 2006; Hanna et al., 2006; Leggett et al., 2002; You and Pickart, 2001). In these studies, perhaps the most surprising finding was that Lys48-linked ubiquitin polymers were dispensable for binding of modified cyclin B1 to ubiquitin receptors and rapid degradation by the proteasome (Kirkpatrick et al., 2006). As only few other substrates were known at the time to be degraded independent of Lys48-chain formation (Baboshina and Haas, 1996; Guterman and Glickman, 2004; Hershko and Heller, 1985; Hofmann and Pickart, 2001), this in-depth analysis of cyclin B1 set out the stage to explore the significance of different ubiquitin linkages in APC-mediated proteolysis.

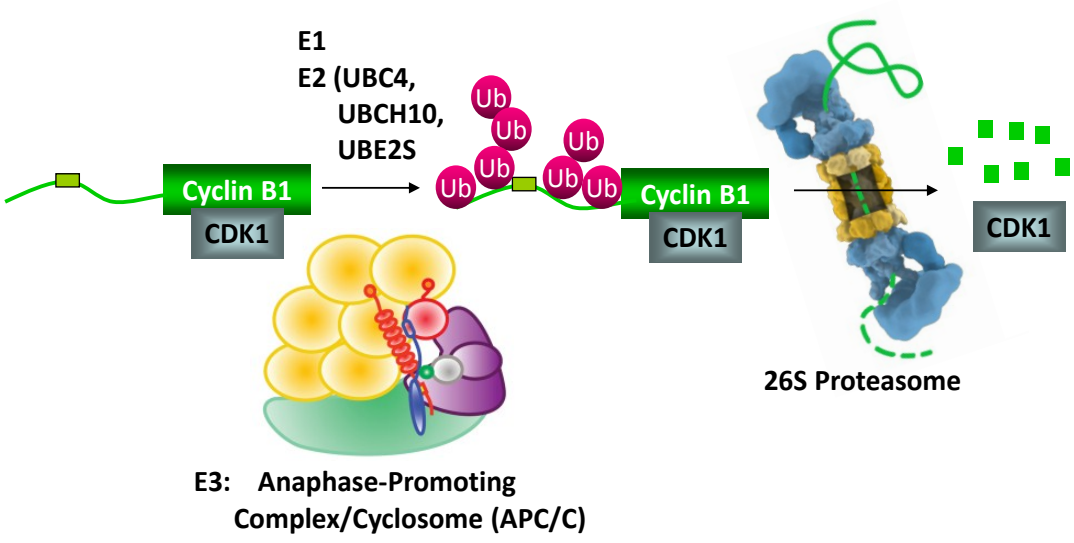

Figure 1.3 APC/C-dependent proteolysis of cyclin B1. The APC/C cooperates with ubiquitin-conjugating enzymes from the E-2C and UBC4/5 families (in particular, human UBCH10 and UBCH5, respectively) to catalyze chain formation through three lysine residues of ubiquitin (K11, K48 and K63) (Kirkpatrick et al., 2006) . UBCH10 or UBCH5 builds multiple short ubiquitin chains on cyclin B1, which are sufficient to target the protein for degradation by the proteasome. In this context, K48-linked ubiquitin polymers are dispensable for binding of modified cyclin B1 to ubiquitin receptors and degradation by the proteasome (Kirkpatrick et al., 2006) . More recent work indicates that a second E2 enzyme, UBE2S, is important in elaborating K11-linked ubiquitin chains on APC/C-substrates (Garnett et al., 2009; Williamson et al., 2009; Wu et al., 2010). In this model, UBCH10 is proposed to initiate monoubiquitination of the substrate, with UBE2S then extending K11-linked ubiquitin chains that signal degradation by the proteasome.

The ability of the APC, in conjunction with the E2 UBCH10, to extend multiple short ubiquitin chains through lysines 11, 48 and 63 of ubiquitin *in vitro* (Kirkpatrick et al., 2005) raises the question as to whether Lys11-chain formation is indeed required for proteolysis of APC/C substrates, and if so, whether this requirement arises from a specific role of UBE2S, or because Lys11 is one of three sites used by UbcH10 (Jin et al., 2008; Kirkpatrick et al., 2005). Also, are any of these ubiquitin linkages functioning as the major degradative element? We sought to address these questions using *Xenopus* egg extracts as a model system. Studies of the role of ubiquitin topology in substrate turnover in *Xenopus* extract are hampered by the presence of endogenous ubiquitin. Seeking to understand whether APC/C-dependent proteolysis is strictly dependent upon polyubiquitination and whether the proteolytic machinery exerts a requirement for Lys11 or other Ub-Ub linkages to efficiently degrade cyclin B1, we developed a novel approach where *Xenopus* extracts are made largely dependent on exogenous ubiquitin. Treatment of *Xenopus* extract with ubiquitin-vinyl sulfone (UbVS), a general inhibitor of ubiquitin isopeptidases (Borodovsky et al., 2001), blocked cyclin B1 proteolysis in a manner that could be fully rescued by exogenous ubiquitin. For our analysis, we used full-length cyclin B1 and CDK1, expressed in insect cells and combined to produce MPF (Kirkpatrick et al., 2006). The studies with active MPF were nicely complemented with the use of an N-terminal fragment (1-88 amino acids) of cyclin B1 which we extensively characterized and found to mimic the ubiquitination and degradation patterns of the full-length protein. To quantitatively evaluate the role of different ubiquitin structures in targeting cyclin B1 for degradation, we expressed and purified ^{35}S-labeled cyclin B1 and measured its proteolysis in *Xenopus* extract by monitoring release of radioactive soluble counts. Surprisingly, using the UbVS system we found that Lys11-linked ubiquitin chains were not required for efficient cyclin B1 degradation. Furthermore, we were fascinated with the robust rates of proteolysis a chain-terminating ubiquitin (Ub^{triR}), which blocks all possible sites of chain elongation by UBCH10, UBC4/5, and UBE2S, supported.

Cyclin B1 has some particularly interesting features that may play a role in regulating its localization in the cell and interactions with other proteins, as well as its stability. The function of accepting ubiquitin appears to be fulfilled by lysine residues found in the non-conserved regions neighboring the degron (Glotzer et al., 1991; King et al., 1996). Positioned in the vicinity of the D-box or KEN-box motif, the TEK box has been proposed as a new interaction motif directing the chain-initiation event (Jin et al., 2008). However, the potential contribution of the lysine residue found in this motif to proteolysis of different APC substrates remains to be addressed and may provide a better understanding of how the integrity of the motif is essential to UBCH10-dependent conjugation and proteasomal degradation (Jin et al., 2008). For cyclin B1, the unstructured N-terminal region upstream of the cyclin box provides a platform containing 18 lysine residues; 15 of these lysine residues are located within the first 88 amino acids close to the destruction box. Intriguingly, there are patterns of lysine clustering that appear to be fairly well conserved in different species and whose significance has not been elucidated. We hypothesized that the lysine profile of cyclin B1 provides a platform upon which a proteolytic signal consisting of multiple monoubiquitins or short ubiquitin chains can be assembled, obviating the need for the formation of long Lys11-linked ubiquitin chains. In the work presented in this dissertation, we examined how cyclin B1 proteolysis is influenced by the number of available ubiquitination sites. To this end, we generated a series of cyclin mutants containing lysine-to-arginine substitutions at particular residues guided by mass spectrometry analysis of the ubiquitination sites in the substrate. Our findings suggested that ubiquitin-chain formation is not essential for cyclin B1 proteolysis, unless the number of available lysine residues is restricted and that multiple monoubiquitination constitutes an efficient proteolytic signal in this context.

What the ubiquitination status of cyclin B1 upon its docking at the proteasome is and what ubiquitin requirements the proteolytic machinery itself may be imposing on the APC for efficient degradation of cyclin B1 have remained poorly understood. To further evaluate the relevance of different chain structures as a targeting signal for degradation, we sought to

reconstitute different steps of the pathway *in vitro*. In ubiquitination reconstituted with recombinant E1, E2s, and ubiquitin, the APC/C, immunopurified from mitotic *Xenopus* extracts where it is activated by Cdc20, can rapidly attach mono-ubiquitin to multiple lysines in cyclin B1. Cyclin modified with 4 or more ubiquitin moieties on distinct lysines was recognized by various ubiquitin receptors. Consistent with experiments in *Xenopus* extract, multiply monoubiquitinated cyclin B1 species were efficiently degraded by purified human proteasomes in the absence of the proteasome-associated deubiquitinating enzyme USP14. Surprisingly, we found that USP14 suppressed degradation of multiply monoubiquitinated cyclin B1 to a similar extent as that of polyubiquitinated species, suggesting that USP14 can efficiently remove monoubiquitin. However, such deubiquitinating activity did not appear to strongly antagonize proteasome function in *Xenopus* extract as our findings presented in this dissertation suggest. We further pursued identification of deubiquitinating enzyme(s) that may modulate the rate of cyclin degradation in the *Xenopus* extract.

In conclusion, in chapter II we present our work on developing and characterizing the UbVS system. This includes work detailing the behavior of an N-terminal fragment of cyclin B1 and our approach to quantitatively analyze its degradation. In the study presented in chapter III we sought to evaluate the role of different ubiquitin linkages in cyclin B1 proteolysis. We demonstrate that conjugation of ubiquitin moieties to multiple lysine residues of cyclin B1 provides an alternative degradation pathway for cyclin B1 that does not require chain extension by the Lys11-specific E2 enzyme UBE2S. Lys11-ubiquitin chain formation becomes essential only when the number of available lysine residues in cyclin B1 is restricted. We postulate that high local density of ubiquitin, whether attached as monomers along the substrate or linked to each other in a polymer, is sufficient to target a substrate for proteolysis. In chapter IV we further examine the relative contribution of different E2 enzymes for APC/C-mediated ubiquitination and degradation in the *Xenopus* extract.

References

Amerik, A. Y., and Hochstrasser, M. (2004). Mechanism and function of deubiquitinating enzymes. Biochim Biophys Acta *1695*, 189-207.

Aristarkhov, A., Eytan, E., Moghe, A., Admon, A., Hershko, A., and Ruderman, J. V. (1996). E2-C, a cyclin-selective ubiquitin carrier protein required for the destruction of mitotic cyclins. Proc Natl Acad Sci U S A *93*, 4294-4299.

Au, S. W., Leng, X., Harper, J. W., and Barford, D. (2002). Implications for the ubiquitination reaction of the anaphase-promoting complex from the crystal structure of the Doc1/Apc10 subunit. J Mol Biol *316*, 955-968.

Baboshina, O. V., and Haas, A. L. (1996). Novel multiubiquitin chain linkages catalyzed by the conjugating enzymes E2EPF and RAD6 are recognized by 26 S proteasome subunit 5. J Biol Chem *271*, 2823-2831.

Barford, D. (2011a). Structural insights into anaphase-promoting complex function and mechanism. Philos Trans R Soc Lond B Biol Sci *366*, 3605-3624.

Barford, D. (2011b). Structure, function and mechanism of the anaphase promoting complex (APC/C). Q Rev Biophys *44*, 153-190.

Beal, R., Deveraux, Q., Xia, G., Rechsteiner, M., and Pickart, C. (1996). Surface hydrophobic residues of multiubiquitin chains essential for proteolytic targeting. Proc Natl Acad Sci U S A *93*, 861-866.

Beal, R. E., Toscano-Cantaffa, D., Young, P., Rechsteiner, M., and Pickart, C. M. (1998). The hydrophobic effect contributes to polyubiquitin chain recognition. Biochemistry *37*, 2925-2934.

Bedford, L., Lowe, J., Dick, L. R., Mayer, R. J., and Brownell, J. E. (2011). Ubiquitin-like protein conjugation and the ubiquitin-proteasome system as drug targets. Nat Rev Drug Discov *10*, 29-46.

Behrends, C., and Harper, J. W. (2011). Constructing and decoding unconventional ubiquitin chains. Nat Struct Mol Biol *18*, 520-528.

Borodovsky, A., Kessler, B. M., Casagrande, R., Overkleeft, H. S., Wilkinson, K. D., and Ploegh, H. L. (2001). A novel active site-directed probe specific for deubiquitylating enzymes reveals proteasome association of USP14. Embo J *20*, 5187-5196.

Brzovic, P. S., Lissounov, A., Christensen, D. E., Hoyt, D. W., and Klevit, R. E. (2006). A UbcH5/ubiquitin noncovalent complex is required for processive BRCA1-directed ubiquitination. Mol Cell *21*, 873-880.

Burton, J. L., and Solomon, M. J. (2001). D box and KEN box motifs in budding yeast Hsl1p are required for APC-mediated degradation and direct binding to Cdc20p and Cdh1p. Genes Dev *15*, 2381-2395.

Buschhorn, B. A., Petzold, G., Galova, M., Dube, P., Kraft, C., Herzog, F., Stark, H., and Peters, J. M. (2010). Substrate binding on the APC/C occurs between the coactivator Cdh1 and the processivity factor Doc1. Nat Struct Mol Biol *18*, 6-13.

Buschhorn, B. A., Petzold, G., Galova, M., Dube, P., Kraft, C., Herzog, F., Stark, H., and Peters, J. M. (2011). Substrate binding on the APC/C occurs between the coactivator Cdh1 and the processivity factor Doc1. Nat Struct Mol Biol *18*, 6-13.

Cadwell, K., and Coscoy, L. (2005). Ubiquitination on nonlysine residues by a viral E3 ubiquitin ligase. Science *309*, 127-130.

Carroll, C. W., Enquist-Newman, M., and Morgan, D. O. (2005). The APC subunit Doc1 promotes recognition of the substrate destruction box. Curr Biol *15*, 11-18.

Carroll, C. W., and Morgan, D. O. (2002). The Doc1 subunit is a processivity factor for the anaphase-promoting complex. Nat Cell Biol *4*, 880-887.

Carvalho, A. F., Pinto, M. P., Grou, C. P., Alencastre, I. S., Fransen, M., Sa-Miranda, C., and Azevedo, J. E. (2007). Ubiquitination of mammalian Pex5p, the peroxisomal import receptor. J Biol Chem *282*, 31267-31272.

Chao, W. C., Kulkarni, K., Zhang, Z., Kong, E. H., and Barford, D. (2012). Structure of the mitotic checkpoint complex. Nature *484*, 208-213.

Chau, V., Tobias, J. W., Bachmair, A., Marriott, D., Ecker, D. J., Gonda, D. K., and Varshavsky, A. (1989). A multiubiquitin chain is confined to specific lysine in a targeted short-lived protein. Science *243*, 1576-1583.

Chen, Z., and Pickart, C. M. (1990). A 25-kilodalton ubiquitin carrier protein (E2) catalyzes multi-ubiquitin chain synthesis via lysine 48 of ubiquitin. J Biol Chem *265*, 21835-21842.

Chuang, S. M., and Madura, K. (2005). Saccharomyces cerevisiae Ub-conjugating enzyme Ubc4 binds the proteasome in the presence of translationally damaged proteins. Genetics *171*, 1477-1484.

Ciechanover, A. (2005a). Early work on the ubiquitin proteasome system, an interview with Aaron Ciechanover. Interview by CDD. Cell Death Differ *12*, 1167-1177.

Ciechanover, A. (2005b). Proteolysis: from the lysosome to ubiquitin and the proteasome. Nat Rev Mol Cell Biol *6*, 79-87.

Ciechanover, A., and Ben-Saadon, R. (2004). N-terminal ubiquitination: more protein substrates join in. Trends Cell Biol *14*, 103-106.

Ciechanover, A., Elias, S., Heller, H., and Hershko, A. (1982). "Covalent affinity" purification of ubiquitin-activating enzyme. J Biol Chem *257*, 2537-2542.

Ciechanover, A., Finley, D., and Varshavsky, A. (1984a). The ubiquitin-mediated proteolytic pathway and mechanisms of energy-dependent intracellular protein degradation. J Cell Biochem *24*, 27-53.

Ciechanover, A., Finley, D., and Varshavsky, A. (1984b). Ubiquitin dependence of selective protein degradation demonstrated in the mammalian cell cycle mutant ts85. Cell *37*, 57-66.

Ciechanover, A., Heller, H., Elias, S., Haas, A. L., and Hershko, A. (1980). ATP-dependent conjugation of reticulocyte proteins with the polypeptide required for protein degradation. Proc Natl Acad Sci U S A *77*, 1365-1368.

Crosas, B., Hanna, J., Kirkpatrick, D. S., Zhang, D. P., Tone, Y., Hathaway, N. A., Buecker, C., Leggett, D. S., Schmidt, M., King, R. W.*, et al.* (2006). Ubiquitin chains are remodeled at the proteasome by opposing ubiquitin ligase and deubiquitinating activities. Cell *127*, 1401-1413.

da Fonseca, P. C., Kong, E. H., Zhang, Z., Schreiber, A., Williams, M. A., Morris, E. P., and Barford, D. (2011). Structures of APC/C(Cdh1) with substrates identify Cdh1 and Apc10 as the D-box co-receptor. Nature *470*, 274-278.

Deng, L., Wang, C., Spencer, E., Yang, L., Braun, A., You, J., Slaughter, C., Pickart, C., and Chen, Z. J. (2000). Activation of the IkappaB kinase complex by TRAF6 requires a dimeric ubiquitin-conjugating enzyme complex and a unique polyubiquitin chain. Cell *103*, 351-361.

Deveraux, Q., Ustrell, V., Pickart, C., and Rechsteiner, M. (1994). A 26 S protease subunit that binds ubiquitin conjugates. J Biol Chem *269*, 7059-7061.

Dube, P., Herzog, F., Gieffers, C., Sander, B., Riedel, D., Muller, S. A., Engel, A., Peters, J. M., and Stark, H. (2005). Localization of the coactivator Cdh1 and the cullin subunit Apc2 in a cryo-electron microscopy model of vertebrate APC/C. Mol Cell *20*, 867-879.

Eddins, M. J., Carlile, C. M., Gomez, K. M., Pickart, C. M., and Wolberger, C. (2006). Mms2-Ubc13 covalently bound to ubiquitin reveals the structural basis of linkage-specific polyubiquitin chain formation. Nat Struct Mol Biol *13*, 915-920.

Elsasser, S., and Finley, D. (2005). Delivery of ubiquitinated substrates to protein-unfolding machines. Nat Cell Biol *7*, 742-749.

Evans, T., Rosenthal, E. T., Youngblom, J., Distel, D., and Hunt, T. (1983). Cyclin: a protein specified by maternal mRNA in sea urchin eggs that is destroyed at each cleavage division. Cell *33*, 389-396.

Finley, D. (2009). Recognition and processing of ubiquitin-protein conjugates by the proteasome. Annu Rev Biochem *78*, 477-513.

Finley, D., Ciechanover, A., and Varshavsky, A. (1984). Thermolability of ubiquitin-activating enzyme from the mammalian cell cycle mutant ts85. Cell *37*, 43-55.

Finley, D., Sadis, S., Monia, B. P., Boucher, P., Ecker, D. J., Crooke, S. T., and Chau, V. (1994). Inhibition of proteolysis and cell cycle progression in a multiubiquitination-deficient yeast mutant. Mol Cell Biol *14*, 5501-5509.

Garnett, M. J., Mansfeld, J., Godwin, C., Matsusaka, T., Wu, J., Russell, P., Pines, J., and Venkitaraman, A. R. (2009). UBE2S elongates ubiquitin chains on APC/C substrates to promote mitotic exit. Nat Cell Biol *11*, 1363-1369. Epub 2009 Oct 1311.

Gautier, J., Minshull, J., Lohka, M., Glotzer, M., Hunt, T., and Maller, J. L. (1990). Cyclin is a component of maturation-promoting factor from Xenopus. Cell *60*, 487-494.

Gautier, J., Norbury, C., Lohka, M., Nurse, P., and Maller, J. (1988). Purified maturation-promoting factor contains the product of a Xenopus homolog of the fission yeast cell cycle control gene cdc2+. Cell *54*, 433-439.

Gazdoiu, S., Yamoah, K., Wu, K., and Pan, Z. Q. (2007). Human Cdc34 employs distinct sites to coordinate attachment of ubiquitin to a substrate and assembly of polyubiquitin chains. Mol Cell Biol *27*, 7041-7052.

Glotzer, M., Murray, A. W., and Kirschner, M. W. (1991). Cyclin is degraded by the ubiquitin pathway. Nature *349*, 132-138.

Goldknopf, I. L., and Busch, H. (1977). Isopeptide linkage between nonhistone and histone 2A polypeptides of chromosomal conjugate-protein A24. Proc Natl Acad Sci U S A *74*, 864-868.

Goldstein, G. (1974). Isolation of bovine thymin: a polypeptide hormone of the thymus. Nature *247*, 11-14.

Goldstein, G., Scheid, M., Hammerling, U., Schlesinger, D. H., Niall, H. D., and Boyse, E. A. (1975). Isolation of a polypeptide that has lymphocyte-differentiating properties and is probably represented universally in living cells. Proc Natl Acad Sci U S A *72*, 11-15.

Grou, C. P., Carvalho, A. F., Pinto, M. P., Wiese, S., Piechura, H., Meyer, H. E., Warscheid, B., Sa-Miranda, C., and Azevedo, J. E. (2008). Members of the E2D (UbcH5) family mediate the ubiquitination of the conserved cysteine of Pex5p, the peroxisomal import receptor. J Biol Chem *283*, 14190-14197.

Guterman, A., and Glickman, M. H. (2004). Complementary roles for Rpn11 and Ubp6 in deubiquitination and proteolysis by the proteasome. J Biol Chem *279*, 1729-1738.

Hanna, J., Hathaway, N. A., Tone, Y., Crosas, B., Elsasser, S., Kirkpatrick, D. S., Leggett, D. S., Gygi, S. P., King, R. W., and Finley, D. (2006). Deubiquitinating enzyme Ubp6 functions noncatalytically to delay proteasomal degradation. Cell *127*, 99-111.

Hanna, J., Meides, A., Zhang, D. P., and Finley, D. (2007). A ubiquitin stress response induces altered proteasome composition. Cell *129*, 747-759.

Harper, J. W., Burton, J. L., and Solomon, M. J. (2002). The anaphase-promoting complex: it's not just for mitosis any more. Genes Dev *16*, 2179-2206.

Harper, J. W., and Schulman, B. A. (2006). Structural complexity in ubiquitin recognition. Cell *124*, 1133-1136.

Hershko, A. (2005). Early work on the ubiquitin proteasome system, an interview with Avram Hershko. Interview by CDD. Cell Death Differ *12*, 1158-1161.

Hershko, A., and Ciechanover, A. (1998). The ubiquitin system. Annu Rev Biochem *67*, 425-479.

Hershko, A., Ciechanover, A., and Rose, I. A. (1981). Identification of the active amino acid residue of the polypeptide of ATP-dependent protein breakdown. J Biol Chem *256*, 1525-1528.

Hershko, A., Ganoth, D., Pehrson, J., Palazzo, R. E., and Cohen, L. H. (1991). Methylated ubiquitin inhibits cyclin degradation in clam embryo extracts. J Biol Chem *266*, 16376-16379.

Hershko, A., and Heller, H. (1985). Occurrence of a polyubiquitin structure in ubiquitin-protein conjugates. Biochem Biophys Res Commun *128*, 1079-1086.

Hershko, A., Heller, H., Elias, S., and Ciechanover, A. (1983). Components of ubiquitin-protein ligase system. Resolution, affinity purification, and role in protein breakdown. J Biol Chem *258*, 8206-8214.

Hershko, A., Heller, H., Eytan, E., Kaklij, G., and Rose, I. A. (1984). Role of the alpha-amino group of protein in ubiquitin-mediated protein breakdown. Proc Natl Acad Sci U S A *81*, 7021-7025.

Herzog, F., Primorac, I., Dube, P., Lenart, P., Sander, B., Mechtler, K., Stark, H., and Peters, J. M. (2009). Structure of the anaphase-promoting complex/cyclosome interacting with a mitotic checkpoint complex. Science *323*, 1477-1481.

Hicke, L., Schubert, H. L., and Hill, C. P. (2005). Ubiquitin-binding domains. Nat Rev Mol Cell Biol *6*, 610-621.

Hofmann, R. M., and Pickart, C. M. (1999). Noncanonical MMS2-encoded ubiquitin-conjugating enzyme functions in assembly of novel polyubiquitin chains for DNA repair. Cell *96*, 645-653.

Hofmann, R. M., and Pickart, C. M. (2001). In vitro assembly and recognition of Lys-63 polyubiquitin chains. J Biol Chem *276*, 27936-27943.

Hunt, L. T., and Dayhoff, M. O. (1977). Amino-terminal sequence identity of ubiquitin and the nonhistone component of nuclear protein A24. Biochem Biophys Res Commun *74*, 650-655.

Husnjak, K., Elsasser, S., Zhang, N., Chen, X., Randles, L., Shi, Y., Hofmann, K., Walters, K. J., Finley, D., and Dikic, I. (2008). Proteasome subunit Rpn13 is a novel ubiquitin receptor. Nature *453*, 481-488.

Jacobson, A. D., Zhang, N. Y., Xu, P., Han, K. J., Noone, S., Peng, J., and Liu, C. W. (2009). The lysine 48 and lysine 63 ubiquitin conjugates are processed differently by the 26 s proteasome. J Biol Chem *284*, 35485-35494.

Jin, J., Li, X., Gygi, S. P., and Harper, J. W. (2007). Dual E1 activation systems for ubiquitin differentially regulate E2 enzyme charging. Nature *447*, 1135-1138.

Jin, L., Williamson, A., Banerjee, S., Philipp, I., and Rape, M. (2008). Mechanism of ubiquitin-chain formation by the human anaphase-promoting complex. Cell *133*, 653-665.

Johnson, E. S. (2002). Ubiquitin branches out. Nat Cell Biol *4*, E295-298.
Kang, Y., Chen, X., Lary, J. W., Cole, J. L., and Walters, K. J. (2007). Defining how ubiquitin receptors hHR23a and S5a bind polyubiquitin. J Mol Biol *369*, 168-176.

Kang, Y., Vossler, R. A., Diaz-Martinez, L. A., Winter, N. S., Clarke, D. J., and Walters, K. J. (2006). UBL/UBA ubiquitin receptor proteins bind a common tetraubiquitin chain. J Mol Biol *356*, 1027-1035.

Kerscher, O., Felberbaum, R., and Hochstrasser, M. (2006). Modification of proteins by ubiquitin and ubiquitin-like proteins. Annu Rev Cell Dev Biol *22*, 159-180.

Kim, S., and Yu, H. (2011). Mutual regulation between the spindle checkpoint and APC/C. Semin Cell Dev Biol *22*, 551-558.

Kim, W., Bennett, E. J., Huttlin, E. L., Guo, A., Li, J., Possemato, A., Sowa, M. E., Rad, R., Rush, J., Comb, M. J.*, et al.* (2011). Systematic and quantitative assessment of the ubiquitin-modified proteome. Mol Cell *44*, 325-340.

King, R. W., Glotzer, M., and Kirschner, M. W. (1996). Mutagenic analysis of the destruction signal of mitotic cyclins and structural characterization of ubiquitinated intermediates. Mol Biol Cell *7*, 1343-1357.

King, R. W., Peters, J. M., Tugendreich, S., Rolfe, M., Hieter, P., and Kirschner, M. W. (1995). A 20S complex containing CDC27 and CDC16 catalyzes the mitosis-specific conjugation of ubiquitin to cyclin B. Cell *81*, 279-288.

Kirkpatrick, D. S., Gerber, S. A., and Gygi, S. P. (2005). The absolute quantification strategy: a general procedure for the quantification of proteins and post-translational modifications. Methods *35*, 265-273.

Kirkpatrick, D. S., Hathaway, N. A., Hanna, J., Elsasser, S., Rush, J., Finley, D., King, R. W., and Gygi, S. P. (2006). Quantitative analysis of in vitro ubiquitinated cyclin B1 reveals complex chain topology. Nat Cell Biol *8*, 700-710.

Koegl, M., Hoppe, T., Schlenker, S., Ulrich, H. D., Mayer, T. U., and Jentsch, S. (1999). A novel ubiquitination factor, E4, is involved in multiubiquitin chain assembly. Cell *96*, 635-644.

Komander, D., Clague, M. J., and Urbe, S. (2009). Breaking the chains: structure and function of the deubiquitinases. Nat Rev Mol Cell Biol *10*, 550-563.

Kraft, C., Vodermaier, H. C., Maurer-Stroh, S., Eisenhaber, F., and Peters, J. M. (2005). The WD40 propeller domain of Cdh1 functions as a destruction box receptor for APC/C substrates. Mol Cell *18*, 543-553.

Lam, Y. A., DeMartino, G. N., Pickart, C. M., and Cohen, R. E. (1997a). Specificity of the ubiquitin isopeptidase in the PA700 regulatory complex of 26 S proteasomes. J Biol Chem *272*, 28438-28446.

Lam, Y. A., Xu, W., DeMartino, G. N., and Cohen, R. E. (1997b). Editing of ubiquitin conjugates by an isopeptidase in the 26S proteasome. Nature *385*, 737-740.

Lander, G. C., Estrin, E., Matyskiela, M. E., Bashore, C., Nogales, E., and Martin, A. (2012). Complete subunit architecture of the proteasome regulatory particle. Nature *482*, 186-191.

Lee, B. H., Lee, M. J., Park, S., Oh, D. C., Elsasser, S., Chen, P. C., Gartner, C., Dimova, N., Hanna, J., Gygi, S. P.*, et al.* (2010a). Enhancement of proteasome activity by a small-molecule inhibitor of USP14. Nature *467*, 179-184.

Lee, M. J., Lee, B. H., Hanna, J., King, R. W., and Finley, D. (2010b). Trimming of ubiquitin chains by proteasome-associated deubiquitinating enzymes. Mol Cell Proteomics *10*, R110 003871.

Lee, S., Tsai, Y. C., Mattera, R., Smith, W. J., Kostelansky, M. S., Weissman, A. M., Bonifacino, J. S., and Hurley, J. H. (2006). Structural basis for ubiquitin recognition and autoubiquitination by Rabex-5. Nat Struct Mol Biol *13*, 264-271.

Leggett, D. S., Hanna, J., Borodovsky, A., Crosas, B., Schmidt, M., Baker, R. T., Walz, T., Ploegh, H., and Finley, D. (2002). Multiple associated proteins regulate proteasome structure and function. Mol Cell *10*, 495-507.

Lipkowitz, S., and Weissman, A. M. (2011). RINGs of good and evil: RING finger ubiquitin ligases at the crossroads of tumour suppression and oncogenesis. Nat Rev Cancer *11*, 629-643.

Lohka, M. J., Hayes, M. K., and Maller, J. L. (1988). Purification of maturation-promoting factor, an intracellular regulator of early mitotic events. Proc Natl Acad Sci U S A *85*, 3009-3013.

Mathe, E., Kraft, C., Giet, R., Deak, P., Peters, J. M., and Glover, D. M. (2004). The E2-C vihar is required for the correct spatiotemporal proteolysis of cyclin B and itself undergoes cyclical degradation. Curr Biol *14*, 1723-1733.

Matyskiela, M. E., and Morgan, D. O. (2009). Analysis of activator-binding sites on the APC/C supports a cooperative substrate-binding mechanism. Mol Cell *34*, 68-80.

Murray, A. W., Solomon, M. J., and Kirschner, M. W. (1989). The role of cyclin synthesis and degradation in the control of maturation promoting factor activity. Nature *339*, 280-286.

Musacchio, A., and Salmon, E. D. (2007). The spindle-assembly checkpoint in space and time. Nat Rev Mol Cell Biol *8*, 379-393.

Nijman, S. M., Luna-Vargas, M. P., Velds, A., Brummelkamp, T. R., Dirac, A. M., Sixma, T. K., and Bernards, R. (2005). A genomic and functional inventory of deubiquitinating enzymes. Cell *123*, 773-786.

Osaka, F., Seino, H., Seno, T., and Yamao, F. (1997). A ubiquitin-conjugating enzyme in fission yeast that is essential for the onset of anaphase in mitosis. Mol Cell Biol *17*, 3388-3397.

Ozkaynak, E., Finley, D., Solomon, M. J., and Varshavsky, A. (1987). The yeast ubiquitin genes: a family of natural gene fusions. Embo J *6*, 1429-1439.

Ozkaynak, E., Finley, D., and Varshavsky, A. (1984). The yeast ubiquitin gene: head-to-tail repeats encoding a polyubiquitin precursor protein. Nature *312*, 663-666.

Passmore, L. A., Booth, C. R., Venien-Bryan, C., Ludtke, S. J., Fioretto, C., Johnson, L. N., Chiu, W., and Barford, D. (2005). Structural analysis of the anaphase-promoting complex reveals multiple active sites and insights into polyubiquitylation. Mol Cell *20*, 855-866.

Passmore, L. A., McCormack, E. A., Au, S. W., Paul, A., Willison, K. R., Harper, J. W., and Barford, D. (2003). Doc1 mediates the activity of the anaphase-promoting complex by contributing to substrate recognition. EMBO J *22*, 786-796.

Penengo, L., Mapelli, M., Murachelli, A. G., Confalonieri, S., Magri, L., Musacchio, A., Di Fiore, P. P., Polo, S., and Schneider, T. R. (2006). Crystal structure of the ubiquitin binding domains of rabex-5 reveals two modes of interaction with ubiquitin. Cell *124*, 1183-1195.

Peng, J., Schwartz, D., Elias, J. E., Thoreen, C. C., Cheng, D., Marsischky, G., Roelofs, J., Finley, D., and Gygi, S. P. (2003). A proteomics approach to understanding protein ubiquitination. Nat Biotechnol *21*, 921-926.

Peters, J. M. (2006). The anaphase promoting complex/cyclosome: a machine designed to destroy. Nat Rev Mol Cell Biol *7*, 644-656.

Petroski, M. D., and Deshaies, R. J. (2005). Mechanism of lysine 48-linked ubiquitin-chain synthesis by the cullin-RING ubiquitin-ligase complex SCF-Cdc34. Cell *123*, 1107-1120.

Pfleger, C. M., and Kirschner, M. W. (2000). The KEN box: an APC recognition signal distinct from the D box targeted by Cdh1. Genes Dev *14*, 655-665.

Pfleger, C. M., Lee, E., and Kirschner, M. W. (2001). Substrate recognition by the Cdc20 and Cdh1 components of the anaphase-promoting complex. Genes Dev *15*, 2396-2407.

Pickart, C. M. (2001). Mechanisms underlying ubiquitination. Annu Rev Biochem *70*, 503-533.

Pickart, C. M., and Fushman, D. (2004). Polyubiquitin chains: polymeric protein signals. Curr Opin Chem Biol *8*, 610-616.

Pierce, N. W., Kleiger, G., Shan, S. O., and Deshaies, R. J. (2009). Detection of sequential polyubiquitylation on a millisecond timescale. Nature *462*, 615-619.

Raasi, S., Orlov, I., Fleming, K. G., and Pickart, C. M. (2004). Binding of polyubiquitin chains to ubiquitin-associated (UBA) domains of HHR23A. J Mol Biol *341*, 1367-1379.

Raasi, S., and Pickart, C. M. (2003). Rad23 ubiquitin-associated domains (UBA) inhibit 26 S proteasome-catalyzed proteolysis by sequestering lysine 48-linked polyubiquitin chains. J Biol Chem *278*, 8951-8959.

Rape, M., and Kirschner, M. W. (2004). Autonomous regulation of the anaphase-promoting complex couples mitosis to S-phase entry. Nature *432*, 588-595.

Rape, M., Reddy, S. K., and Kirschner, M. W. (2006). The processivity of multiubiquitination by the APC determines the order of substrate degradation. Cell *124*, 89-103.

Robzyk, K., Recht, J., and Osley, M. A. (2000). Rad6-dependent ubiquitination of histone H2B in yeast. Science *287*, 501-504.

Rodrigo-Brenni, M. C., and Morgan, D. O. (2007). Sequential E2s drive polyubiquitin chain assembly on APC targets. Cell *130*, 127-139.

Saha, A., Lewis, S., Kleiger, G., Kuhlman, B., and Deshaies, R. J. (2011). Essential role for ubiquitin-ubiquitin-conjugating enzyme interaction in ubiquitin discharge from Cdc34 to substrate. Mol Cell *42*, 75-83.

Schauber, C., Chen, L., Tongaonkar, P., Vega, I., Lambertson, D., Potts, W., and Madura, K. (1998). Rad23 links DNA repair to the ubiquitin/proteasome pathway. Nature *391*, 715-718.

Scheffner, M., Nuber, U., and Huibregtse, J. M. (1995). Protein ubiquitination involving an E1-E2-E3 enzyme ubiquitin thioester cascade. Nature *373*, 81-83.

Schlesinger, D. H., and Goldstein, G. (1975). Molecular conservation of 74 amino acid sequence of ubiquitin between cattle and man. Nature *255*, 42304.

Schmidt, M., Hanna, J., Elsasser, S., and Finley, D. (2005). Proteasome-associated proteins: regulation of a proteolytic machine. Biol Chem *386*, 725-737.

Schreiber, A., Stengel, F., Zhang, Z., Enchev, R. I., Kong, E. H., Morris, E. P., Robinson, C. V., da Fonseca, P. C., and Barford, D. (2011). Structural basis for the subunit assembly of the anaphase-promoting complex. Nature *470*, 227-232.

Schreiner, P., Chen, X., Husnjak, K., Randles, L., Zhang, N., Elsasser, S., Finley, D., Dikic, I., Walters, K. J., and Groll, M. (2008). Ubiquitin docking at the proteasome through a novel pleckstrin-homology domain interaction. Nature *453*, 548-552.

Schulman, B. A., and Harper, J. W. (2009). Ubiquitin-like protein activation by E1 enzymes: the apex for downstream signalling pathways. Nat Rev Mol Cell Biol *10*, 319-331.

Seeger, M., Hartmann-Petersen, R., Wilkinson, C. R., Wallace, M., Samejima, I., Taylor, M. S., and Gordon, C. (2003). Interaction of the anaphase-promoting complex/cyclosome and proteasome protein complexes with multiubiquitin chain-binding proteins. J Biol Chem *278*, 16791-16796.

Shih, S. C., Sloper-Mould, K. E., and Hicke, L. (2000). Monoubiquitin carries a novel internalization signal that is appended to activated receptors. Embo J *19*, 187-198.

Shimizu, Y., Okuda-Shimizu, Y., and Hendershot, L. M. (2010). Ubiquitylation of an ERAD substrate occurs on multiple types of amino acids. Mol Cell *40*, 917-926.

Skaar, J. R., and Pagano, M. (2009). Control of cell growth by the SCF and APC/C ubiquitin ligases. Curr Opin Cell Biol *21*, 816-824.

Sloper-Mould, K. E., Jemc, J. C., Pickart, C. M., and Hicke, L. (2001). Distinct functional surface regions on ubiquitin. J Biol Chem *276*, 30483-30489.

Spence, J., Gali, R. R., Dittmar, G., Sherman, F., Karin, M., and Finley, D. (2000). Cell cycle-regulated modification of the ribosome by a variant multiubiquitin chain. Cell *102*, 67-76.

Spence, J., Sadis, S., Haas, A. L., and Finley, D. (1995). A ubiquitin mutant with specific defects in DNA repair and multiubiquitination. Mol Cell Biol *15*, 1265-1273.

Sudakin, V., Ganoth, D., Dahan, A., Heller, H., Hershko, J., Luca, F. C., Ruderman, J. V., and Hershko, A. (1995). The cyclosome, a large complex containing cyclin-selective ubiquitin ligase activity, targets cyclins for destruction at the end of mitosis. Mol Biol Cell *6*, 185-197.

Summers, M. K., Pan, B., Mukhyala, K., and Jackson, P. K. (2008). The unique N terminus of the UbcH10 E2 enzyme controls the threshold for APC activation and enhances checkpoint regulation of the APC. Mol Cell *31*, 544-556.

Tang, Z., Li, B., Bharadwaj, R., Zhu, H., Ozkan, E., Hakala, K., Deisenhofer, J., and Yu, H. (2001). APC2 Cullin protein and APC11 RING protein comprise the minimal ubiquitin ligase module of the anaphase-promoting complex. Mol Biol Cell *12*, 3839-3851.

Terrell, J., Shih, S., Dunn, R., and Hicke, L. (1998). A function for monoubiquitination in the internalization of a G protein-coupled receptor. Mol Cell *1*, 193-202.

Thornton, B. R., Ng, T. M., Matyskiela, M. E., Carroll, C. W., Morgan, D. O., and Toczyski, D. P. (2006). An architectural map of the anaphase-promoting complex. Genes Dev *20*, 449-460.

Thrower, J. S., Hoffman, L., Rechsteiner, M., and Pickart, C. M. (2000). Recognition of the polyubiquitin proteolytic signal. EMBO J *19*, 94-102.

Townsley, F. M., Aristarkhov, A., Beck, S., Hershko, A., and Ruderman, J. V. (1997). Dominant-negative cyclin-selective ubiquitin carrier protein E2-C/UbcH10 blocks cells in metaphase. Proc Natl Acad Sci U S A *94*, 2362-2367.

Varadan, R., Assfalg, M., Haririnia, A., Raasi, S., Pickart, C., and Fushman, D. (2004). Solution conformation of Lys63-linked di-ubiquitin chain provides clues to functional diversity of polyubiquitin signaling. J Biol Chem *279*, 7055-7063.

Verma, R., Aravind, L., Oania, R., McDonald, W. H., Yates, J. R., 3rd, Koonin, E. V., and Deshaies, R. J. (2002). Role of Rpn11 metalloprotease in deubiquitination and degradation by the 26S proteasome. Science *298*, 611-615.

Verma, R., Oania, R., Graumann, J., and Deshaies, R. J. (2004). Multiubiquitin chain receptors define a layer of substrate selectivity in the ubiquitin-proteasome system. Cell *118*, 99-110.

Vijay-Kumar, S., Bugg, C. E., and Cook, W. J. (1987). Structure of ubiquitin refined at 1.8 A resolution. J Mol Biol *194*, 531-544.

Vodermaier, H. C., Gieffers, C., Maurer-Stroh, S., Eisenhaber, F., and Peters, J. M. (2003). TPR subunits of the anaphase-promoting complex mediate binding to the activator protein CDH1. Curr Biol *13*, 1459-1468.

Walker, A., Acquaviva, C., Matsusaka, T., Koop, L., and Pines, J. (2008). UbcH10 has a rate-limiting role in G1 phase but might not act in the spindle checkpoint or as part of an autonomous oscillator. J Cell Sci *121*, 2319-2326.

Wang, Q., Young, P., and Walters, K. J. (2005). Structure of S5a bound to monoubiquitin provides a model for polyubiquitin recognition. J Mol Biol *348*, 727-739.

Wang, X., Herr, R. A., Chua, W. J., Lybarger, L., Wiertz, E. J., and Hansen, T. H. (2007). Ubiquitination of serine, threonine, or lysine residues on the cytoplasmic tail can induce ERAD of MHC-I by viral E3 ligase mK3. J Cell Biol *177*, 613-624.

Waxman, L., Fagan, J. M., and Goldberg, A. L. (1987). Demonstration of two distinct high molecular weight proteases in rabbit reticulocytes, one of which degrades ubiquitin conjugates. J Biol Chem *262*, 2451-2457.

Weissman, A. M., Shabek, N., and Ciechanover, A. (2011). The predator becomes the prey: regulating the ubiquitin system by ubiquitylation and degradation. Nat Rev Mol Cell Biol *12*, 605-620.

Wendt, K. S., Vodermaier, H. C., Jacob, U., Gieffers, C., Gmachl, M., Peters, J. M., Huber, R., and Sondermann, P. (2001). Crystal structure of the APC10/DOC1 subunit of the human anaphase-promoting complex. Nat Struct Biol *8*, 784-788.

Wickliffe, K. E., Lorenz, S., Wemmer, D. E., Kuriyan, J., and Rape, M. (2011a). The mechanism of linkage-specific ubiquitin chain elongation by a single-subunit E2. Cell *144*, 769-781.

Wickliffe, K. E., Williamson, A., Meyer, H. J., Kelly, A., and Rape, M. (2011b). K11-linked ubiquitin chains as novel regulators of cell division. Trends Cell Biol *21*, 656-663.

Wilkinson, K. D., Cox, M. J., O'Connor, L. B., and Shapira, R. (1986). Structure and activities of a variant ubiquitin sequence from bakers' yeast. Biochemistry *25*, 4999-5004.

Williamson, A., Wickliffe, K. E., Mellone, B. G., Song, L., Karpen, G. H., and Rape, M. (2009). Identification of a physiological E2 module for the human anaphase-promoting complex. Proc Natl Acad Sci U S A *106*, 18213-18218.

Wu, T., Merbl, Y., Huo, Y., Gallop, J. L., Tzur, A., and Kirschner, M. W. (2010). UBE2S drives elongation of K11-linked ubiquitin chains by the anaphase-promoting complex. Proc Natl Acad Sci U S A *107*, 1355-1360.

Xu, P., Duong, D. M., Seyfried, N. T., Cheng, D., Xie, Y., Robert, J., Rush, J., Hochstrasser, M., Finley, D., and Peng, J. (2009). Quantitative proteomics reveals the function of unconventional ubiquitin chains in proteasomal degradation. Cell *137*, 133-145.

Yang, W. L., Wang, J., Chan, C. H., Lee, S. W., Campos, A. D., Lamothe, B., Hur, L., Grabiner, B. C., Lin, X., Darnay, B. G., and Lin, H. K. (2009). The E3 ligase TRAF6 regulates Akt ubiquitination and activation. Science *325*, 1134-1138.

Yao, T., and Cohen, R. E. (2002). A cryptic protease couples deubiquitination and degradation by the proteasome. Nature *419*, 403-407.

Ye, Y., and Rape, M. (2009). Building ubiquitin chains: E2 enzymes at work. Nat Rev Mol Cell Biol *10*, 755-764.

You, J., and Pickart, C. M. (2001). A HECT domain E3 enzyme assembles novel polyubiquitin chains. J Biol Chem *276*, 19871-19878.

Young, P., Deveraux, Q., Beal, R. E., Pickart, C. M., and Rechsteiner, M. (1998). Characterization of two polyubiquitin binding sites in the 26 S protease subunit 5a. J Biol Chem *273*, 5461-5467.

Yu, H., King, R. W., Peters, J. M., and Kirschner, M. W. (1996). Identification of a novel ubiquitin-conjugating enzyme involved in mitotic cyclin degradation. Curr Biol *6*, 455-466.

Yu, H., Peters, J. M., King, R. W., Page, A. M., Hieter, P., and Kirschner, M. W. (1998). Identification of a cullin homology region in a subunit of the anaphase-promoting complex. Science *279*, 1219-1222.

Zeng, X., Sigoillot, F., Gaur, S., Choi, S., Pfaff, K. L., Oh, D. C., Hathaway, N., Dimova, N., Cuny, G. D., and King, R. W. (2010). Pharmacologic inhibition of the anaphase-promoting complex induces a spindle checkpoint-dependent mitotic arrest in the absence of spindle damage. Cancer Cell *18*, 382-395.

Chapter II: Development and characterization of the UbVS system

Nevena Dimova

Abstract

Covalent attachment of ubiquitin to proteins regulates a myriad of cellular processes by influencing activity, localization and stability of substrates. Ubiquitin can be appended to proteins as single moieties or as ubiquitin polymers of specific length and linkage type. The widely accepted view supported by early studies was that Lys63-linked ubiquitin polymers have non-proteolytic roles, whereas Lys48-linked assemblies serve as the principal signal for substrate degradation by the 26S proteasome. While appealing in its simplicity, it is now evident that this model does not reflect the wealth of information different ubiquitin signals encode. Recent work has revealed that the proteasome has the capacity to recognize and degrade substrates bearing ubiquitin modifications other than homogenous Lys48-linked ubiquitin chains. In this study, we establish and characterize a novel approach to studying the role of ubiquitin-chain synthesis in targeting of substrates to the proteasome. Global inhibition of deubiquitinases with ubiquitin vinyl sulfone (UbVS) rendered *Xenopus* egg extracts dependent on exogenous ubiquitin to promote cyclin B1 proteolysis. Detailed characterization of the system suggested that it can be a valuable approach in defining the role of ubiquitin-chain formation in APC/C-dependent ubiquitination and degradation.

Introduction

Ubiquitin is a highly conserved 76 amino-acid protein which can be conjugated posttranslationally to other proteins via an isopeptide linkage between its carboxy-terminal glycine and, most typically, the ε-amino group of a lysine (Lys) in a substrate (Ciechanover et al., 1984; Ciechanover et al., 1980; Goldknopf and Busch, 1977; Hershko and Ciechanover, 1998; Hershko et al., 1981; Hunt and Dayhoff, 1977). Ubiquitin itself contains seven Lys residues, at positions 6, 11, 27, 29, 33, 48, and 63, allowing the assembly of ubiquitin polymers and a diverse array of ubiquitin signals (Pickart and Fushman, 2004). Posttranslational modification by ubiquitin is utilized in many cellular pathways, but the role of ubiquitin in selective, intracellular protein degradation remains its best-understood function. In the classical model, a chain of four ubiquitin molecules linked through Lys48 is required for efficient recognition and degradation by the 26S proteasome (Chau et al., 1989; Finley et al., 1994; Thrower et al., 2000). The development of novel mass spectrometry techniques (Kirkpatrick et al., 2005; Kirkpatrick et al., 2006; Peng et al., 2003; Xu et al., 2009) and biochemical reagents (Matsumoto et al., 2010; Newton et al., 2008) has been vital to recent work demonstrating that the repertoire of proteolytic signals may encompass chains of other linkage types, including Lys11-linked ubiquitin chains (Baboshina and Haas, 1996; Garnett et al., 2009; Jin et al., 2008; Matsumoto et al., 2010; Williamson et al., 2009; Wu et al., 2010; Xu et al., 2009) or short chains of mixed linkage (Kirkpatrick et al., 2006). Congruent with the widely accepted view that ubiquitin-polymer structure is required for high-affinity binding to the proteasome, the attachment of a single ubiquitin to one (monoubiquitination) or to multiple sites (multiple monoubiquitination) has been implicated in mostly non-proteolytic processes.

The cell cycle must proceed in an orderly fashion to maintain genomic integrity and to prevent dysregulated proliferation. Fundamental to this is the precisely timed destruction of key regulators, including cyclins, cyclin-dependent kinase inhibitors and securin. Many of these

regulators are substrates of the anaphase-promoting complex/cyclosome (APC/C or APC), a multisubunit RING E3 ubiquitin ligase. In an event critical for anaphase entry, the APC/C and cognate E2 ubiquitin-conjugating enzymes catalyze the ubiquitination of cyclin B1 targeting it to the 26S proteasome for degradation (Barford, 2011; Glotzer et al., 1991; Harper et al., 2002; Hershko et al., 1991; Peters, 2002; Peters, 2006). The ubiquitin signal assembled on cyclin B1 *in vitro* was previously revealed to comprise of monoubiquitin appended to multiple distinct lysines in the substrate, as well as some short chains linked through Lys11, Lys48 and Lys63 (Kirkpatrick et al., 2006). While starkly different from canonical proteolytic signals consisting of a single homogeneous ubiquitin chain, the ubiquitin signal built on cyclin B1 supports rapid degradation by the 26S proteasome (Kirkpatrick et al., 2006). More recent studies have implicated a role of the Lys11-linkage specific E2 UBE2S and chain synthesis it promotes in APC/C-dependent proteolysis (Garnett et al., 2009; Matsumoto et al., 2010; Wickliffe et al., 2011a; Wickliffe et al., 2011b; Williamson et al., 2009; Wu et al., 2010; Ye and Rape, 2009). At least in some biological contexts, however, turnover of APC/C substrates and normal mitosis can occur in the absence of UBE2S or Lys11-linked polyubiquitination (Garnett et al., 2009; Jin et al., 2008).

Dissecting the contribution of different ubiquitin linkages to proteasomal recognition and degradation in intricate systems such as whole cells or cellular extracts is complicated in part by the pool of endogenous ubiquitin. Maintenance of steady-state ubiquitin levels is crucial in physiological settings and is regulated at multiple levels, the most important of which are *de novo* synthesis of ubiquitin (Simon et al., 1999; Watt and Piper, 1997) and ubiquitin recycling mediated by deubiquitinating enzymes (Finley, 2009; Hanna et al., 2007). Such pathways pose challenges to studying the role of ubiquitin topology in proteasomal targeting and their robustness renders it a non-trivial task to induce ubiquitin deficiency. To gain better understanding of the role of specific ubiquitin linkages in cyclin B1 proteolysis, we developed and characterized a

novel approach where *Xenopus* extracts are made largely dependent on exogenous ubiquitin by restricting the recycling of endogenous ubiquitin.

Results

Developing a quantitative assay to measure cyclin proteolysis in *Xenopus* cell-cycle extract

The heterogeneous nature of the ubiquitin signal built on cyclin B1 in *Xenopus* extract renders visualization of ubiquitinated species by western blot analysis challenging. Furthermore, the ubiquitin tag assembled on substrates may not promote their degradation. To assess the contribution of different ubiquitin linkages specifically in cyclin B1 turnover, we developed a quantitative assay to measure cyclin B1 degradation products. We metabolically labeled an N-terminal fragment of cyclin B1 with ^{35}S in *E. coli*, purified the protein, and measured its proteolysis in *Xenopus* extract by monitoring release of trichloroacetic-acid (TCA) soluble counts.

We first examined whether this N-terminal fragment of cyclin B1, similar to the full-length protein, was degraded in an APC/C-dependent fashion. When added to interphase extract, a state in which the APC/C is inactive, cycB1-NT remained stable, but was rapidly degraded upon entry of extract into mitosis (Figure 2.1a). Furthermore, pre-treatment of mitotically-arrested extract with a small-molecule inhibitor of the APC/C TAME (Zeng and King, 2012; Zeng et al., 2010) (Figure 2.1b) or concomitant addition of identical unlabeled N-terminal fragment largely stabilized the radiolabeled cycB1-NT (Figure 2.1d), consistent with a requirement for APC/C-mediated ubiquitination to stimulate substrate degradation. In contrast, proteolysis was not effectively competed by a destruction-box (D-box) mutant (Figure 2.1d). Interestingly, these competition experiments revealed differing efficiencies of inhibition, suggesting cyclin B1 fragments from different species may bind the APC with different affinities. Difference in binding affinities may stem from the sequence variation distinguishing the D-box motif of the sea urchin protein from that of the human cyclin B1. Alternatively, sea urchin cyclin B1 is relatively lysine-poor in its N-terminal domain, containing only 10 lysine residues, raising

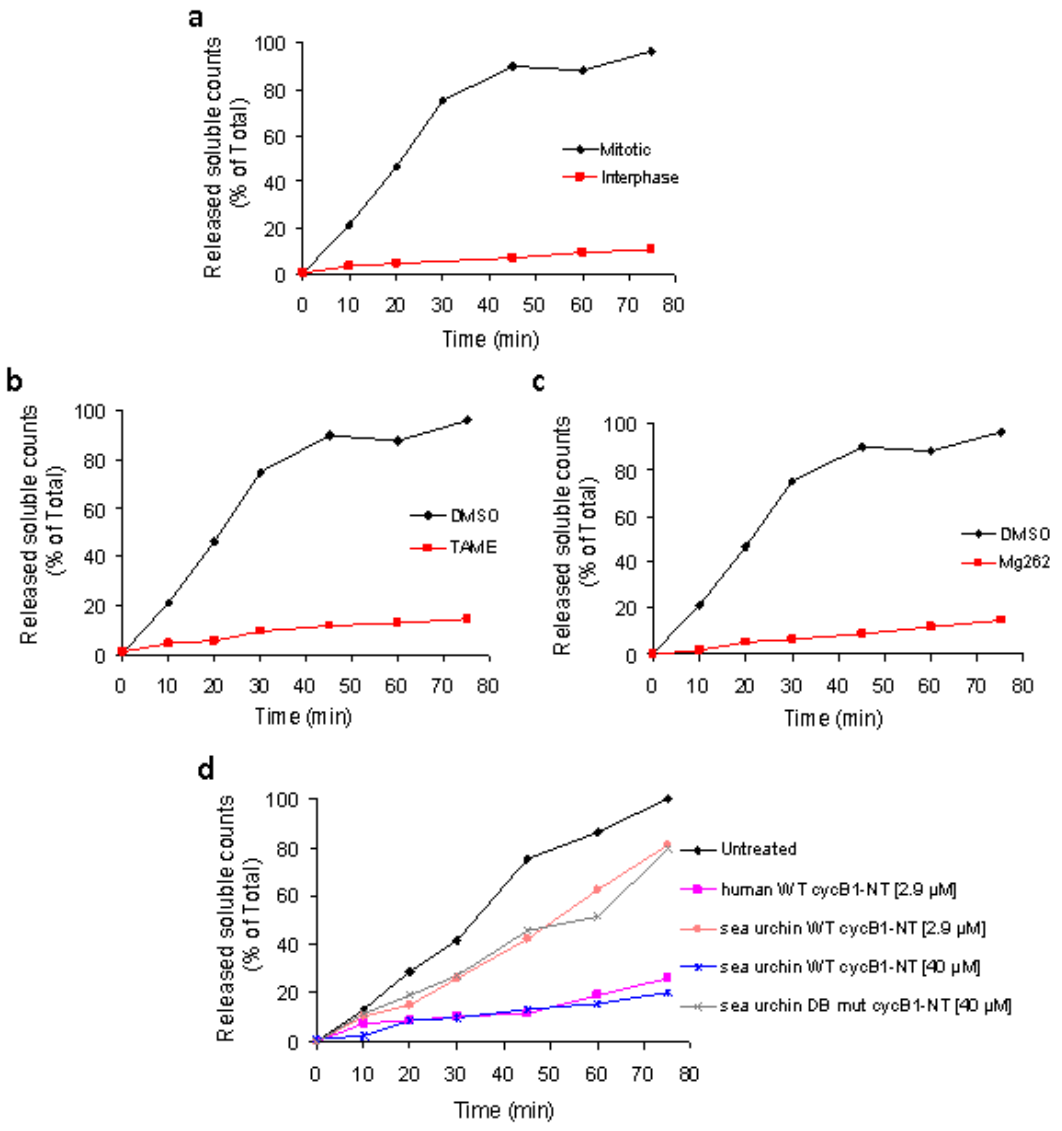

Figure 2.1 N-terminal fragment of cyclin B1 is degraded in *Xenopus* extract in an APC/C- and proteasome-dependent fashion. For all panels, ^{35}S-labeled cycB1-NT (aa 1-88) (~200 nM) was added to extract. Samples were taken at indicated times and subjected to trichloroacetic acid (TCA) precipitation. Proteolysis was measured by release of TCA soluble counts, and is plotted as percentage of input radiolabeled cyclin B1 protein. (**a**) Degradation of ^{35}S-labeled cycB1-NT in interphase and mitotically-arrested *Xenopus* extracts. (**b**) Degradation of ^{35}S-labeled cycB1-NT in mitotic *Xenopus* extract pre-treated with an inhibitor of the APC/C TAME (200 µM) or DMSO. (**c**) Same as **b**, except mitotic *Xenopus* extract was treated with proteasome inhibitor Mg262 (200 µM) or DMSO prior to substrate addition. (**d**) Degradation of ^{35}S-labeled wild-type human cycB1-NT (1-88) in mitotic *Xenopus* extract, supplemented concomitantly with unlabeled WT human cycB1-NT (1-88), WT or D-box mutant sea urchin cyclin B1 NT (13-110), at indicated concentrations.

an interesting possibility that this relative defect in binding to the APC may stem from the lower number of ubiquitination sites neighboring the D-box. Nevertheless, the degradation of both human and sea urchin cycB1-NT in extract was proteasome-dependent, as addition of the proteasome inhibitor MG262 blocked this process (Figure 2.1c; data not shown).

Endogenous ubiquitin levels are limiting for degradation of an N-terminal fragment of cyclin B1 in mitotic *Xenopus* extract

To evaluate the role of different ubiquitin-chain topologies in cyclin degradation in the *Xenopus* system, we first determined the consequences of adding excess wild-type or mutant ubiquitin to mitotic extract. Using ubiquitin-aqua (Ub-AQUA) (Kirkpatrick et al., 2005; Kirkpatrick et al., 2006) measurements, we calculated that free ubiquitin is present at 5-10 μM concentration in *Xenopus* extracts (D. Kirkpatrick and N. Hathaway, unpublished observations). When added at 44 μM final concentration, wild-type ubiquitin substantially accelerated degradation, decreasing the half-life of the substrate from 25 minutes in untreated extract to approximately 15 minutes in the presence of additional ubiquitin (Figure 2.2a). Ubiquitin mutants containing a single lysine-to-arginine substitution at position 48 (Ub^{48R}) or 63 (Ub^{63R}) stimulated degradation almost as well as wild-type ubiquitin, consistent with the idea that these linkages are not essential for degradation. Surprisingly, a ubiquitin containing a lysine-to-arginine mutation at position 11 (Ub^{11R}) also stimulated degradation when added to extract, although the effect was not as dramatic as for wild-type ubiquitin. Similar results were obtained with a ubiquitin variant bearing arginine residues at all three positions, Lys11, 48 and 63 (Ub^{triR}), simultaneously. Similar trends were observed when the amount of ubiquitin was increased approximately 2.5-fold to 116 μM (Figure 2.2b). These results were unexpected, as mass spectrometry analysis indicated that elimination of all three principal sites (Lys11, Lys48 and Lys63) of ubiquitin-ubiquitin linkage by

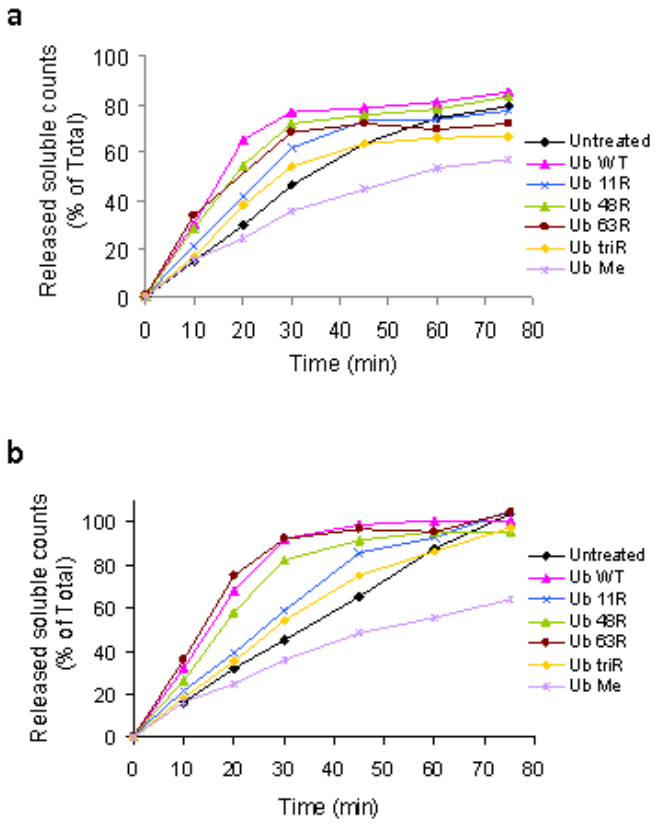

Figure 2.2 Endogenous ubiquitin levels are limiting for degradation of an N-terminal fragment of human cyclin B1 in mitotic *Xenopus* extract. (**a**, **b**) For both panels, ^{35}S-labeled cycB1-NT (amino acids 1-88) (~ 200 nM) was added to mitotically-arrested *Xenopus* extract concomitantly with forms of ubiquitin as indicated or buffer (untreated). Samples were taken at indicated times and subjected to trichloroacetic acid (TCA) precipitation. Proteolysis was measured by release of TCA soluble counts, and is plotted as percentage of input radiolabeled cyclin B1 protein. In **a**, extract was supplemented with 44 µM of exogenous ubiquitin, while in **b**, extract was supplemented with 116 µM of exogenous ubiquitin. Data are representative of at least three independent experiments.

the APC, as in Ub^{triR}, rendered ubiquitin incapable of supporting chain formation in reconstituted reactions (data not shown). In contrast, methylated ubiquitin (Ub^{me}) slowed proteolysis below the rate observed in untreated extract, but even when added at high concentration, the degree to which it suppressed degradation was modest. The capacity of chain-terminating ubiquitin to support robust cyclin proteolysis in mitotic *Xenopus* extract raised the question of whether ubiquitin-chain synthesis is essential in this pathway.

The UbVS system – a novel approach to studying the role of ubiquitin topology in proteasomal targeting

Analysis of ubiquitin-mediated proteolysis in complex systems such as *Xenopus* extracts is hampered by the pool of endogenous ubiquitin which can be incorporated into the ubiquitin signal assembled on a substrate. In *Xenopus* extracts, endogenous ubiquitin levels appeared to be limiting for the proteolysis of cycB1-NT as addition of ubiquitin accelerated this process. To restrict ubiquitin availability further, we sought to suppress ubiquitin-chain disassembly, in essence, locking endogenous ubiquitin into existing conjugates. We reasoned that inhibition of ubiquitin recycling will render the degradative capacity of *Xenopus* extracts dependent on added ubiquitin. To test this idea, we added ubiquitin-vinyl sulfone (UbVS), a general inhibitor of ubiquitin isopeptidases (Borodovsky et al., 2001), to mitotic *Xenopus* extract. Ubiquitin-vinyl sulfone inhibited cyclin proteolysis in a dose-dependent fashion, such that 10 μM suppressed degradation only partially, whereas 20 μM UbVS inhibited degradation by at least 90-95% (Figure 2.3a; data for full-length cyclin B1 not shown). Inhibition of cyclin proteolysis could be fully rescued by addition of wild-type ubiquitin at the end of the pre-incubation, concomitantly with substrate addition (Figure 2.3b). However, while increasing concentrations of UbVS failed to influence appreciably the degree of substrate stabilization, those appeared to slightly dampen

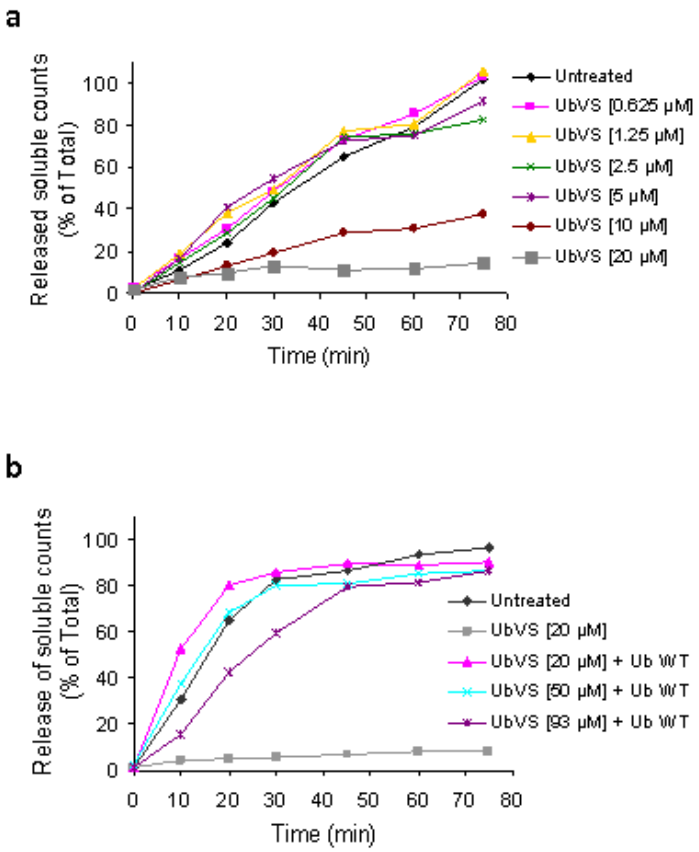

Figure 2.3 Ubiquitin vinyl sulfone (UbVS) inhibits cycB1-NT proteolysis in a dose-dependent fashion. For all panels, mitotically-arrested *Xenopus* extract was pre-treated with indicated concentration of UbVS or buffer (referred to as untreated) for 30 min. ^{35}S-labeled cycB1-NT (~200 nM) was added to extract. Samples were removed at indicated times and subjected to trichloroacetic acid (TCA) precipitation. Proteolysis was measured by release of TCA-soluble counts, and is plotted as percent age of input radiolabeled cyclin B1 protein. (**a**) Degradation of ^{35}S-labeled cycB1-NT was measured in extract that had been pre-treated with UbVS at indicated concentrations. (**b**) Proteolysis of ^{35}S-labeled cycB1-NT in extract pre-treated with increasing concentrations of UbVS and supplemented with wild-type Ub (44 µM) at time of substrate addition. Trends are representative of three or more independent experiments.

the ability of 44 μM of wild-type ubiquitin to restore degradation (Figure 2.3b). The robust stabilization of the N-terminal fragment of human cyclin B1, as well as that of the full-length protein, achieved with 20 μM UbVS prompted us to use this concentration of UbVS for all subsequent experiments where we sought to make the system dependent on exogenous ubiquitin.

We found that the degree of degradation rescue in UbVS-treated extracts depended on the concentration of added ubiquitin (Figure 2.4a). When ubiquitin was supplemented at 20 μM concentration, degradation proceeded at a rapid rate for the first 15 minutes of the reaction, and then plateaued, presumably due to depletion of free ubiquitin. Consistent with this idea, a two-fold increase in the concentration of ubiquitin supported rapid proteolysis for 30 minutes, leading to complete degradation of the substrate (Figure 2.4a). To confirm that the substrate behavior observed under these conditions is consistent with the known properties of the ubiquitin-proteasome system, we examined how mutations in functional surfaces of ubiquitin impacted its capacity to rescue degradation in a UbVS-treated extract. Forms of ubiquitin bearing point mutations in one of the hydrophobic patch residues (L8A, I44A, or V70A) were not capable of supporting proteolysis (Figure 2.4b), as predicted given the importance of the hydrophobic patch in recognition of ubiquitin chains by proteasome-associated ubiquitin receptors (Beal et al., 1996; Beal et al., 1998; Lam et al., 1997). In contrast, mutations that interfere with non-proteolytic functions of ubiquitin (F4A (Shih et al., 2000; Sloper-Mould et al., 2001) or D58A (Lee et al., 2006; Penengo et al., 2006)) supported rapid proteolysis, at rates comparable to wild-type ubiquitin (Figure 2.4b). Importantly, the rate of degradation in UbVS-treated extracts supplemented with wild-type ubiquitin was identical to that observed when adding a similar concentration of ubiquitin to untreated extracts, yielding a half-life of approximately 15 minutes in both cases (Figure 2.2a; Figure 2.4a). These findings suggest that UbVS-sensitive deubiquitinating enzymes are unlikely to present a major kinetic barrier to cyclin B1 degradation and instead suggest that the major role of these deubiquitinating enzymes may be to maintain a pool of free ubiquitin available to the conjugation machinery. Analysis of ubiquitin conjugates

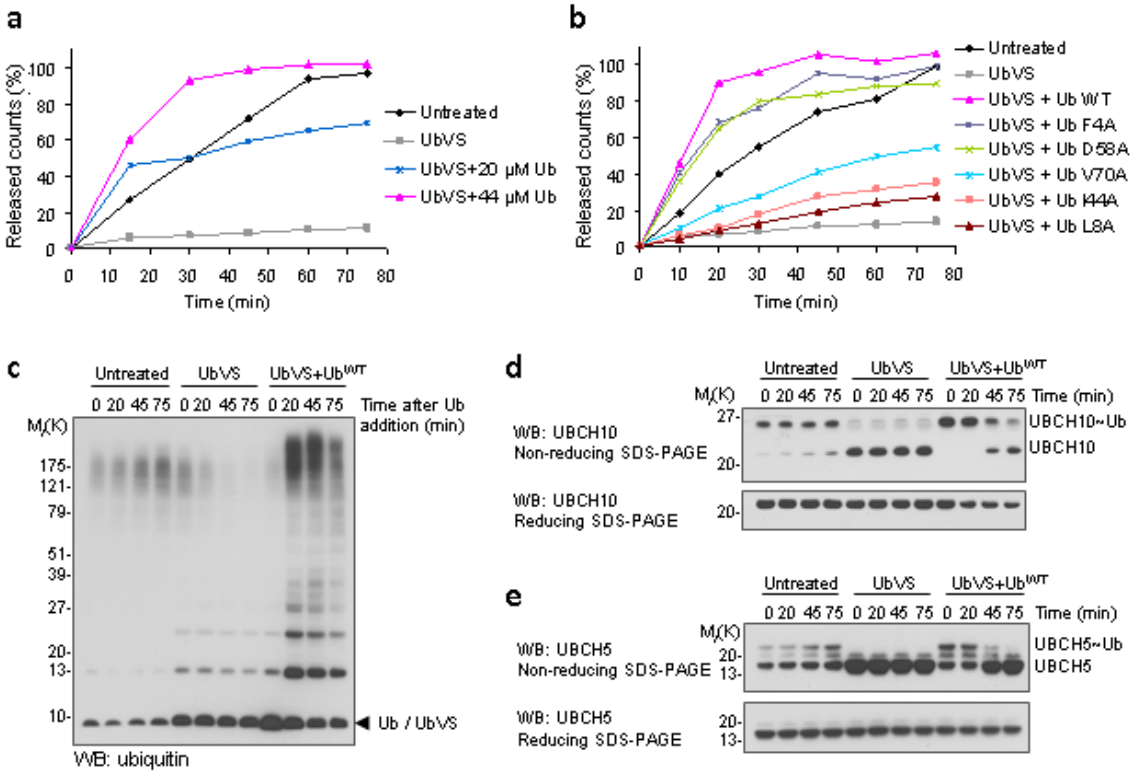

Figure 2.4 Ubiquitin vinyl sulfone (UbVS) inhibits cyclin B1 degradation by depleting available ubiquitin. (**a**) ^{35}S-labeled cycB1-NT and 20 or 44 μM of wild-type (WT) Ub as indicated were introduced into mitotically-arrested *Xenopus* extract that had been pre-treated with UbVS (20 μM) or buffer (referred to as untreated) for 30 min. Proteolysis was measured by release of trichloroacetic acid (TCA) soluble counts, and is plotted as the percentage of input radiolabeled cycB1-NT. Trends are representative of three or more independent experiments. (**b**) Wild-type ubiquitin or forms of ubiquitin (44 μM) bearing single-point mutations in distinct interaction surfaces on ubiquitin, along with radiolabeled substrate, were added to UbVS-treated extract. For panels **c-e** mitotically-arrested *Xenopus* extract was pre-treated with UbVS (20 μM) or buffer (referred to as untreated) for 30 min. Wild-type ubiquitin (44 μM) was added to extract, as indicated. Aliquots were withdrawn at indicated times and analyzed by SDS-PAGE and western blot. (**c**) Ubiquitin status in *Xenopus* extract under the indicated conditions was examined by anti-ubiquitin western blot. (**d**) Levels of Ub-charged endogenous ubch10 (ubch10~Ub) were examined by anti-ubch10 western blot analysis. Aliquots were removed at the indicated times and quenched with either non-reducing sample buffer to examine levels of ubch10~Ub or reducing sample buffer to examine total levels of endogenous ubch10. (**e**) Same as in **d**, but levels of endogenous ubiquitin-charged ubch5 (ubch5~Ub) or total levels of ubch5 were examined by western blotting.

and thioesters in extract under these conditions revealed that inhibition of isopeptidase activity with 20 μM UbVS led to near complete discharge of E2~Ub thioesters ('~' represents a thioester bond between the active-site cysteine of an E2 and the C-terminal glycine of ubiquitin) (Figure 2.4d, e). These trends paralleled the gradual disappearance of ubiquitinated species in the extract (Figure 2.4c). Addition of exogenous ubiquitin restored charging of E2 enzymes and formation of ubiquitin conjugates in the extract. Importantly, addition of wild-type ubiquitin to UbVS-treated extract led to reduction in UBCH10, but not UBCH5, levels (Figure 2.4d, e), suggesting that deubiquitinases may actively oppose UBCH10 degradation in *Xenopus* extracts.

Discussion

In our studies, we sought to evaluate how the nature of the ubiquitin signal constructed on cyclin B1 influences its degradation by the 26S proteasome. The manner in which cyclin B1 is ubiquitinated, however, leads to a heterogeneous mixture of conjugates of different ubiquitin mass which can be difficult to visualize by western analysis. Furthermore, western analysis may not distinguish between ubiquitin intermediates *en route* to the proteasome and those bearing a non-proteolytic ubiquitin tag. Thus, to evaluate the role of different ubiquitin linkages in proteasomal targeting of cyclin B1, we developed a quantitative assay to measure cyclin B1 degradation products. Here, we describe a novel approach where *Xenopus* extracts are made largely dependent on exogenous ubiquitin, allowing analysis of the role of ubiquitin-chain formation in APC-dependent proteolysis of cyclin B1.

Several studies have attempted to examine the role of ubiquitin-chain topology in proteasomal degradation by adding mutant ubiquitin to extracts (Hershko et al., 1991; Jin et al., 2008; Wu et al., 2010) or by injecting the ubiquitin into cells (Jin et al., 2008). Jin and colleagues found that ubiquitin incapable of forming Lys11 linkages (Ub^{11R}) delayed early cell divisions when injected into *Xenopus tropicalis* embryos (Jin et al., 2008). However, the specific mechanism of delay and rates of degradation of APC substrates were not directly addressed. Therefore, it is possible that injection of Ub^{11R} perturbs other processes required for division of early embryos. In contrast, we found that adding such modified forms of ubiquitin typically accelerated degradation, with the exception of methylated ubiquitin. A possible explanation for the lack of effect of chain-terminating ubiquitins, such as Ub^{11R} or Ub^{triR}, is that any added ubiquitin must compete with the endogenous ubiquitin pool. Therefore, dominant-negative effects may be difficult to observe when conducted in a background that contains wild-type ubiquitin. Alternatively, our data suggest that despite their potential effects on chain termination, these ubiquitins are indeed capable of contributing to a signal that can promote degradation.

Intriguingly, the stimulatory effect of ubiquitin addition was more pronounced for an N-terminal fragment of cyclin B1 (cycB1-NT) relative to full-length cyclin B1 (data shown in chapter II and III). One possible explanation for this difference is that the N-terminal fragment binds to APC with lower affinity compared to the full-length protein, imposing a requirement for higher levels of ubiquitin-charged E2 for efficient degradation. Such a phenomenon would be reminiscent of the implicated role of a complex formation with a CDK partner and a Cks protein for cyclin recruitment to the phospho-APC/C and efficient degradation (van Zon et al., 2010; Wolthuis et al., 2008). Also, our work indicates that cyclin B N-termini from different species may have different affinities for the APC/C. An interesting question is whether the lysine profile of these proteins influences the stability of interaction with the E2-E3 complex. Sea urchin cyclin B, having fewer lysines in its N-terminal domain that can be targeted by proximally-acting E2 such as UBCH10, may dissociate from the APC/C more rapidly and therefore require more processive ubiquitination such as catalyzed by the chain-extending Ubc1 (Chen and Pickart, 1990; Rodrigo-Brenni and Morgan, 2007) or UBE2S (Garnett et al., 2009; Williamson et al., 2009; Wu et al., 2010) for its timely destruction. Further experiments will be necessary to better understand these interesting aspects of the behavior of the system.

Our analysis uncovered a strong dependence of the rate of cyclin proteolysis on the levels of free ubiquitin in extract. Addition of exogenous ubiquitin stimulated degradation, whereas inhibition of ubiquitin recycling suppressed degradation. Such a relationship between ubiquitin availability and APC-dependent proteolysis has not been previously appreciated, and it leads to the interesting possibility that control of ubiquitin availability may be a new mechanism by which the rate of APC substrate degradation could be controlled. Future experiments are required to examine whether and how ubiquitin availability may be controlled by cell-cycle regulatory mechanisms. Supplementing UbVS-treated extracts with ubiquitin restores cyclin proteolysis to levels seen in non-treated extract. This finding indicates there may be no requirement for UbVS-sensitive deubiquitination to support cyclin degradation, beyond a role in maintaining levels of

free ubiquitin. Interestingly, as long as ubiquitin is supplied to sufficient levels, the rate of cyclin degradation is no faster in a UbVS-treated extract relative to a non-treated extract. This may indicate that there are few, if any, UbVS-sensitive DUBs that actively antagonize cyclin B1 degradation in mitotic extracts. Alternatively, for deubiquitinating enzymes to be able to antagonize degradation, it may be crucial that the rate of ubiquitination be constrained by restricting availability of free ubiquitin or by rendering ubiquitin transfer less processive.

UbVS-treated extracts provide an opportunity to rigorously examine the degradative function of different ubiquitin-ubiquitin linkages. While the role of UbVS-sensitive DUBs in this process cannot be ascertained using this approach, systematic analysis is likely to provide clues about potential contribution. In the context of cyclin B1, UbVS-sensitive deubiquitination did not appear to appreciably oppose proteasomal targeting. However, APC substrates may be differentially sensitive to the action of such deubiquitinating enzymes and the UbVS approach may allow for this idea to be directly tested. In this regard, the APC was previously suggested to establish temporal order of destruction of its targets based on relative differences in the processivity of ubiquitination (Rape et al., 2006). How deubiquitination may modulate the ubiquitin signal APC builds on various substrates and potentially have an active role in establishing the correct sequence of proteasomal targeting have not been clarified. The UbVS system may provide an avenue to examine how the balance of ubiquitination and deubiquitination influences the temporal order of degradation of APC substrates.

Methods

Antibodies and biochemical reagents

Proteins were separated by SDS-PAGE on NuPAGE 4-12% or 12% Bis-Tris gels (Invitrogen), followed by wet transfer to PVDF. Sources of antibodies for immunoblotting were as follows: anti-cyclin B1 (Ab-2; RB-008-P, Neomarkers), anti-UBCH10 (A-650, Boston Biochem and AB3861, Millipore), anti-UBCH5 (A-615; Boston Biochem), anti-ubiquitin (P4D1; sc-8017; Santa Cruz Biotechnology). Secondary antibodies used include anti-goat IgG-HRP (sc-2020; Santa Cruz Biotechnology), anti-rabbit IgG-HRP (NA934; GE Healthcare), and anti-mouse IgG-HRP (NA931; GE Healthcare). MG262 (I-120), Ub^{me} and ubiquitin mutants except for $Ub^{(11+48)R}$, $Ub^{(11+63)R}$ and Ub^{triR} were purchased from Boston Biochem. TAME (T4626) and ubiquitin (U6253) were purchased from Sigma.

Preparation of recombinant proteins

Ubiquitin mutants $Ub^{(11+48)R}$, $Ub^{(11+63)R}$ and $Ub^{(11+48+63)R}$ (referred to as Ub^{triR}) were generated by introducing arginine codons (AGA and AGG) at the indicated sites through PCR-mediated mutagenesis of the human ubiquitin sequence (cloned in pET3a with ampicillin resistance, the kind gift of C.M. Pickart). Plasmids were verified by sequencing and the purified proteins analyzed by mass spectrometry. To ensure efficient arginine incorporation, BL21 (DE3) cells were co-transformed with pJY2, developed by Pickart lab (You et al., 1999), which carries T7 lysozyme (LysS) and a gene encoding $tRNA_{UCU}^{Arg}$. Cultures were grown at 37 °C to an attenuance (D) of ~ 0.5 at 600 nm, and induced with 100 μM IPTG at $D_{600\ nm} = 0.6$ at 25 ˚C for 5 h. Cells were ruptured by sonication in QA lysis buffer (50 mM HEPES (pH 7.7), 100 mM KCl, protease-inhibitor cocktail, 5 mM 2-mercaptoethanol, 10 μg ml^{-1} DNase). Lysozyme was added to 1 mg ml^{-1} concentration and lysate was incubated with rotation at 4 °C for 15 min. Following sonication, cell lysates were clarified by centrifugation and the resulting supernatants applied to a

Q column. The flow-through containing ubiquitin was concentrated and purified by size-exclusion chromatography. Fractions containing ubiquitin were typically > 95% pure.

To generate full-length cyclin B-CDK1 complex, human cyclin B1 and CDK1 baculoviruses were used as described previously (Kirkpatrick et al., 2006). Baculovirus was added to Sf9 cells and cyclin B1 expression was allowed for 2.5 days. CDK1 was expressed separately in Sf9 cells and then combined with lysate from cells expressing cyclin B1 to allow formation of complex, which was then purified through Ni-NTA affinity and gel filtration chromatography.

CycB1-NT (1-88 amino acids of human cyclin B1) , containing an HA tag at the N terminus and a 6xHis tag at the C terminus was generated using PCR amplification with forward primer (5'-CCA GGA CCA TGG GTT ACC CAT ACG ATG TTC CAG ATT ACG CTG GCT CGA TGG CGC TCC GAG TCA CG-3') and reverse primer (5'-GGG AGC CTC GAG CTA GGG AGC GTG ATG GTG ATG GTG ATG CAT AGG TAC CTT TTC AAG AGG-3'). The resulting PCR product was digested with NcoI and XhoI for subcloning into pET28a. Plasmids were verified by restriction enzyme mapping and sequencing. For ^{35}S labeling in *Escherichia coli*, cultures (50 ml) were grown at 37 ˚C to $D_{600\ nm}$ = 0.8, then collected by centrifugation (3,700*g* for 15 min, at 4 ^{o}C) and resuspended in modified M9 medium (50 ml final volume). After resuspension in modified M9 medium, cells were allowed to grow for additional 15 min at 37 °C before 5 mCi of Easy Tag^{TM} L-[35S]-Methionine (NEG709A005MC; Perkin Elmer) was added. Expression was induced with 0.5 mM IPTG for 2.5 h at 37 ^{o}C. Cells were ruptured in 5 ml g^{-1} of pellet guanidine-HCl lysis buffer (pH 8.0) and lysates rotated at 24 °C until the lysate became slightly translucent; approximately 45 min. Lysates were clarified by centrifugation and cycB1-NT was purified using Ni-NTA affinity chromatography (Qiagen). Eluted protein was desalted into XB buffer (100 mM KCl, 0.1 mM $CaCl_2$, 1 mM $MgCl_2$, 10 mM HEPES, pH 7.8 with KOH), supplemented 2% glycerol, protease inhibitors and phenylmethylsulfonyl fluoride, and stored at – 20 °C.

Preparation of *Xenopus* egg extract

Interphase *Xenopus* egg extract was prepared from eggs laid overnight according to the protocol of Murray (Murray, 1991) with the exception that eggs were activated with 2 μg/ml calcium ionophore (A23187, free acid form, Calbiochem) for 30 min prior to the crushing spin. Extract was frozen in liquid nitrogen and stored at -80 ºC. Interphase extract was induced to enter mitosis by addition of non-degradable cyclin B, which activates CDK1 and stimulates mitotic phosphorylation, resulting in APC/C activation. A fusion of the maltose-binding protein (MBP) to *Xenopus* cyclin B lacking its N-terminal 90 amino acids (MBP-Δ90) (Salic and King, 2005) was expressed in *E. coli* by inducing cultures at an D_{600nm}=0.6 with 300 μM isopropylthiogalactoside (IPTG) for 5 h at room temperature. Purification was carried out following New England BioLabs (NEB) protocol. To make mitotic extract, MBP- Δ90 was added to interphase extract generally at ~ 20 μg ml^{-1} and incubated at 22-24 ºC for 45-60 min.

Cyclin B1 degradation in *Xenopus* egg extract

Degradation assays where non-ubiquitinated cyclin B1 was added to extract were generally performed in 40 μl total volume per reaction condition, with extract constituting 75-80% of that volume. For experiments with TAME and MG262, extracts were pre-treated with relevant compound or dimethyl sulfoxide (DMSO) for 15 min at 24 °C, with agitation (1,250 r.p.m.). For assays containing no UbVS, extracts were supplemented with ubiquitin as indicated or buffer (for untreated sample) concomitantly with ~200-250 nM substrate. For experiments with UbVS, interphase or mitotic extracts were treated with UbVS for 30 min at 24 °C, with agitation (1,250 r.p.m.) before addition of ubiquitin and cyclin B1. Extracts contained 100 μg ml^{-1} cycloheximide to prevent re-incorporation of free labeled amino acid. For competition assays, unlabeled competitor was added concomitantly with radiolabeled cyclin B1 and degradation was initiated. Degradation experiments were performed at 24 °C, with agitation (1,250 r.p.m.), with samples withdrawn at indicated times. Samples for proteolysis of unlabeled full-length cyclin B1-

CDK1 complex were combined with SDS sample buffer and subjected to SDS-PAGE and immunoblot analysis using anti-cyclin B1 polyclonal antibody (Ab-2, Neomarkers). In degradation assays with ^{35}S-labeled cycB1-NT, reactions (3 µl per time point) were quenched with 97 µl of 20% trichloroacetic acid (TCA) (in H_2O), vortexed and incubated on ice ≥ 30 min before centrifugation at 14,000*g*, at 4 °C. A fraction (50%) of sample supernatants was combined with NaOH to neutralize the acid and added to Ultima Gold scintillation fluid (6013327, Perkin Elmer). The radioactivity in the samples was measured by scintillation counting using a Packard scintillation counter. Proteolysis was measured by release of TCA soluble counts and is plotted as the percentage of input radiolabeled cyclin B1 protein.

Ubiquitin dynamics in *Xenopus* extract were examined by anti-ubiquitin western blot analysis. Levels of specific E2s in *Xenopus* extract were examined by western blot analysis. Samples of extract removed at the indicated times were mixed with DTT-containing sample buffer and boiled to examine total endogenous levels of specific E2 enzymes. To analyze levels of ubiquitin-charged endogenous ubch10 (ubch10~Ub) or ubch5 (ubch5~Ub), aliquots were removed at the indicated times and quenched with non-reducing sample buffer.

References

Baboshina, O. V., and Haas, A. L. (1996). Novel multiubiquitin chain linkages catalyzed by the conjugating enzymes E2EPF and RAD6 are recognized by 26 S proteasome subunit 5. J Biol Chem *271*, 2823-2831.

Barford, D. (2011). Structure, function and mechanism of the anaphase promoting complex (APC/C). Q Rev Biophys *44*, 153-190.

Beal, R., Deveraux, Q., Xia, G., Rechsteiner, M., and Pickart, C. (1996). Surface hydrophobic residues of multiubiquitin chains essential for proteolytic targeting. Proc Natl Acad Sci U S A *93*, 861-866.

Beal, R. E., Toscano-Cantaffa, D., Young, P., Rechsteiner, M., and Pickart, C. M. (1998). The hydrophobic effect contributes to polyubiquitin chain recognition. Biochemistry *37*, 2925-2934.

Borodovsky, A., Kessler, B. M., Casagrande, R., Overkleeft, H. S., Wilkinson, K. D., and Ploegh, H. L. (2001). A novel active site-directed probe specific for deubiquitylating enzymes reveals proteasome association of USP14. Embo J *20*, 5187-5196.

Chau, V., Tobias, J. W., Bachmair, A., Marriott, D., Ecker, D. J., Gonda, D. K., and Varshavsky, A. (1989). A multiubiquitin chain is confined to specific lysine in a targeted short-lived protein. Science *243*, 1576-1583.

Chen, Z., and Pickart, C. M. (1990). A 25-kilodalton ubiquitin carrier protein (E2) catalyzes multi-ubiquitin chain synthesis via lysine 48 of ubiquitin. J Biol Chem *265*, 21835-21842.

Ciechanover, A., Finley, D., and Varshavsky, A. (1984). The ubiquitin-mediated proteolytic pathway and mechanisms of energy-dependent intracellular protein degradation. J Cell Biochem *24*, 27-53.

Ciechanover, A., Heller, H., Elias, S., Haas, A. L., and Hershko, A. (1980). ATP-dependent conjugation of reticulocyte proteins with the polypeptide required for protein degradation. Proc Natl Acad Sci U S A *77*, 1365-1368.

Finley, D. (2009). Recognition and processing of ubiquitin-protein conjugates by the proteasome. Annu Rev Biochem *78*, 477-513.

Finley, D., Sadis, S., Monia, B. P., Boucher, P., Ecker, D. J., Crooke, S. T., and Chau, V. (1994). Inhibition of proteolysis and cell cycle progression in a multiubiquitination-deficient yeast mutant. Mol Cell Biol *14*, 5501-5509.

Garnett, M. J., Mansfeld, J., Godwin, C., Matsusaka, T., Wu, J., Russell, P., Pines, J., and Venkitaraman, A. R. (2009). UBE2S elongates ubiquitin chains on APC/C substrates to promote mitotic exit. Nat Cell Biol *11*, 1363-1369. Epub 2009 Oct 1311.

Glotzer, M., Murray, A. W., and Kirschner, M. W. (1991). Cyclin is degraded by the ubiquitin pathway. Nature *349*, 132-138.

Goldknopf, I. L., and Busch, H. (1977). Isopeptide linkage between nonhistone and histone 2A polypeptides of chromosomal conjugate-protein A24. Proc Natl Acad Sci U S A *74*, 864-868.

Hanna, J., Meides, A., Zhang, D. P., and Finley, D. (2007). A ubiquitin stress response induces altered proteasome composition. Cell *129*, 747-759.

Harper, J. W., Burton, J. L., and Solomon, M. J. (2002). The anaphase-promoting complex: it's not just for mitosis any more. Genes Dev *16*, 2179-2206.

Hershko, A., and Ciechanover, A. (1998). The ubiquitin system. Annu Rev Biochem *67*, 425-479.

Hershko, A., Ciechanover, A., and Rose, I. A. (1981). Identification of the active amino acid residue of the polypeptide of ATP-dependent protein breakdown. J Biol Chem *256*, 1525-1528.

Hershko, A., Ganoth, D., Pehrson, J., Palazzo, R. E., and Cohen, L. H. (1991). Methylated ubiquitin inhibits cyclin degradation in clam embryo extracts. J Biol Chem *266*, 16376-16379.

Hunt, L. T., and Dayhoff, M. O. (1977). Amino-terminal sequence identity of ubiquitin and the nonhistone component of nuclear protein A24. Biochem Biophys Res Commun *74*, 650-655.

Jin, L., Williamson, A., Banerjee, S., Philipp, I., and Rape, M. (2008). Mechanism of ubiquitin-chain formation by the human anaphase-promoting complex. Cell *133*, 653-665.

Kirkpatrick, D. S., Gerber, S. A., and Gygi, S. P. (2005). The absolute quantification strategy: a general procedure for the quantification of proteins and post-translational modifications. Methods *35*, 265-273.

Kirkpatrick, D. S., Hathaway, N. A., Hanna, J., Elsasser, S., Rush, J., Finley, D., King, R. W., and Gygi, S. P. (2006). Quantitative analysis of in vitro ubiquitinated cyclin B1 reveals complex chain topology. Nat Cell Biol *8*, 700-710.

Lam, Y. A., DeMartino, G. N., Pickart, C. M., and Cohen, R. E. (1997). Specificity of the ubiquitin isopeptidase in the PA700 regulatory complex of 26 S proteasomes. J Biol Chem *272*, 28438-28446.

Lee, S., Tsai, Y. C., Mattera, R., Smith, W. J., Kostelansky, M. S., Weissman, A. M., Bonifacino, J. S., and Hurley, J. H. (2006). Structural basis for ubiquitin recognition and autoubiquitination by Rabex-5. Nat Struct Mol Biol *13*, 264-271.

Matsumoto, M. L., Wickliffe, K. E., Dong, K. C., Yu, C., Bosanac, I., Bustos, D., Phu, L., Kirkpatrick, D. S., Hymowitz, S. G., Rape, M.*, et al.* (2010). K11-linked polyubiquitination in cell cycle control revealed by a K11 linkage-specific antibody. Mol Cell *39*, 477-484.

Murray, A. W. (1991). Cell cycle extracts. Methods Cell Biol *36*, 581-605.

Newton, K., Matsumoto, M. L., Wertz, I. E., Kirkpatrick, D. S., Lill, J. R., Tan, J., Dugger, D., Gordon, N., Sidhu, S. S., Fellouse, F. A.*, et al.* (2008). Ubiquitin chain editing revealed by polyubiquitin linkage-specific antibodies. Cell *134*, 668-678.

Penengo, L., Mapelli, M., Murachelli, A. G., Confalonieri, S., Magri, L., Musacchio, A., Di Fiore, P. P., Polo, S., and Schneider, T. R. (2006). Crystal structure of the ubiquitin binding domains of rabex-5 reveals two modes of interaction with ubiquitin. Cell *124*, 1183-1195.

Peng, J., Schwartz, D., Elias, J. E., Thoreen, C. C., Cheng, D., Marsischky, G., Roelofs, J., Finley, D., and Gygi, S. P. (2003). A proteomics approach to understanding protein ubiquitination. Nat Biotechnol *21*, 921-926.

Peters, J. M. (2002). The anaphase-promoting complex: proteolysis in mitosis and beyond. Mol Cell *9*, 931-943.

Peters, J. M. (2006). The anaphase promoting complex/cyclosome: a machine designed to destroy. Nat Rev Mol Cell Biol *7*, 644-656.

Pickart, C. M., and Fushman, D. (2004). Polyubiquitin chains: polymeric protein signals. Curr Opin Chem Biol *8*, 610-616.

Rape, M., Reddy, S. K., and Kirschner, M. W. (2006). The processivity of multiubiquitination by the APC determines the order of substrate degradation. Cell *124*, 89-103.

Rodrigo-Brenni, M. C., and Morgan, D. O. (2007). Sequential E2s drive polyubiquitin chain assembly on APC targets. Cell *130*, 127-139.

Salic, A., and King, R. W. (2005). Identifying small molecule inhibitors of the ubiquitin-proteasome pathway in Xenopus egg extracts. Methods Enzymol *399*, 567-585.

Shih, S. C., Sloper-Mould, K. E., and Hicke, L. (2000). Monoubiquitin carries a novel internalization signal that is appended to activated receptors. Embo J *19*, 187-198.
Simon, J. R., Treger, J. M., and McEntee, K. (1999). Multiple independent regulatory pathways control UBI4 expression after heat shock in Saccharomyces cerevisiae. Mol Microbiol *31*, 823-832.

Sloper-Mould, K. E., Jemc, J. C., Pickart, C. M., and Hicke, L. (2001). Distinct functional surface regions on ubiquitin. J Biol Chem *276*, 30483-30489.

Thrower, J. S., Hoffman, L., Rechsteiner, M., and Pickart, C. M. (2000). Recognition of the polyubiquitin proteolytic signal. EMBO J *19*, 94-102.

van Zon, W., Ogink, J., ter Riet, B., Medema, R. H., te Riele, H., and Wolthuis, R. M. (2010). The APC/C recruits cyclin B1-Cdk1-Cks in prometaphase before D box recognition to control mitotic exit. J Cell Biol *190*, 587-602.

Watt, R., and Piper, P. W. (1997). UBI4, the polyubiquitin gene of Saccharomyces cerevisiae, is a heat shock gene that is also subject to catabolite derepression control. Mol Gen Genet *253*, 439-447.

Wickliffe, K. E., Lorenz, S., Wemmer, D. E., Kuriyan, J., and Rape, M. (2011a). The mechanism of linkage-specific ubiquitin chain elongation by a single-subunit E2. Cell *144*, 769-781.

Wickliffe, K. E., Williamson, A., Meyer, H. J., Kelly, A., and Rape, M. (2011b). K11-linked ubiquitin chains as novel regulators of cell division. Trends Cell Biol *21*, 656-663.

Williamson, A., Wickliffe, K. E., Mellone, B. G., Song, L., Karpen, G. H., and Rape, M. (2009). Identification of a physiological E2 module for the human anaphase-promoting complex. Proc Natl Acad Sci U S A *106*, 18213-18218.

Wolthuis, R., Clay-Farrace, L., van Zon, W., Yekezare, M., Koop, L., Ogink, J., Medema, R., and Pines, J. (2008). Cdc20 and Cks direct the spindle checkpoint-independent destruction of cyclin A. Mol Cell *30*, 290-302.

Wu, T., Merbl, Y., Huo, Y., Gallop, J. L., Tzur, A., and Kirschner, M. W. (2010). UBE2S drives elongation of K11-linked ubiquitin chains by the anaphase-promoting complex. Proc Natl Acad Sci U S A *107*, 1355-1360.

Xu, P., Duong, D. M., Seyfried, N. T., Cheng, D., Xie, Y., Robert, J., Rush, J., Hochstrasser, M., Finley, D., and Peng, J. (2009). Quantitative proteomics reveals the function of unconventional ubiquitin chains in proteasomal degradation. Cell *137*, 133-145.

Ye, Y., and Rape, M. (2009). Building ubiquitin chains: E2 enzymes at work. Nat Rev Mol Cell Biol *10*, 755-764.

You, J., Cohen, R. E., and Pickart, C. M. (1999). Construct for high-level expression and low misincorporation of lysine for arginine during expression of pET-encoded eukaryotic proteins in Escherichia coli. Biotechniques *27*, 950-954.

Zeng, X., and King, R. W. (2012). An APC/C inhibitor stabilizes cyclin B1 by prematurely terminating ubiquitination. Nat Chem Biol.

Zeng, X., Sigoillot, F., Gaur, S., Choi, S., Pfaff, K. L., Oh, D. C., Hathaway, N., Dimova, N., Cuny, G. D., and King, R. W. (2010). Pharmacologic inhibition of the anaphase-promoting complex induces a spindle checkpoint-dependent mitotic arrest in the absence of spindle damage. Cancer Cell *18*, 382-395.

Chapter III: APC/C-mediated multiple monoubiquitination provides an alternative degradation signal for cyclin B1

Nevena Dimova, Nathaniel A. Hathaway, Byung-Hoon Lee, Donald S. Kirkpatrick, Marie Lea Berkowitz, Steven P. Gygi, Daniel Finley, Randall W. King

Department of Cell Biology, Harvard Medical School, 240 Longwood Avenue, Boston, Massachusetts 02115, USA

N.D. and R.W.K. designed and interpreted the experiments. N.D. carried out and analyzed all experiments except those outlined below. N.A.H. carried out cyclin B1 ubiquitylation for ubiquitin-AQUA analysis and degradation assays with these species in APC/C-depleted extract. D.S.K. carried out the ubiquitin-AQUA analysis on cyclin B1 ubiquitylated *in vitro* with the E2 UBC4 and different ubiquitin types in the laboratory of S.P.G. B-H.L. provided purified human proteasomes with oversight from D.F. M.L.B. helped with cloning of different cyclin B1 mutants.

Abstract

The Anaphase-Promoting Complex/Cyclosome (APC/C or APC) regulates progression through mitosis by orchestrating the ubiquitination of cell-cycle regulators such as cyclin B1 and securin. Although Lys48-linked ubiquitin chains represent a canonical signal targeting proteins for degradation by the proteasome, they are not required for the degradation of cyclin B1 in a reconstituted system. Recently, Lys11-linked ubiquitin chains have been implicated in degradation of APC/C substrates, but the Lys11-chain forming E2 UBE2S is not essential for mitotic exit. Together these findings raise important questions about the nature of the ubiquitin signal that targets APC/C substrates for degradation. Here, using a reconstituted system and *Xenopus* egg extracts, we demonstrate that multiple monoubiquitination of cyclin B1, catalyzed by UBCH10 or UBC4/5, is sufficient to target cyclin B1 for destruction by the proteasome. However, elaboration of Lys11-linked polymers becomes increasingly important when the number of ubiquitinatable lysines in cyclin B1 is restricted. We therefore define a novel proteolytic signal in the ubiquitin-proteasome pathway that confers flexibility in the requirement for particular E2 enzymes in modulating the rate of ubiquitin-dependent proteolysis.

Introduction

Protein ubiquitination regulates many aspects of cell physiology, including protein degradation. A uniform Lys48-linked ubiquitin polymer was the first signal identified to target substrates for destruction by the 26S proteasome (Chau et al., 1989; Finley et al., 1994; Thrower et al., 2000). Recent work has demonstrated that the repertoire of proteolytic signals encompasses chains of other linkage types, including Lys11-linked ubiquitin chains (Baboshina and Haas, 1996; Garnett et al., 2009; Jin et al., 2008; Matsumoto et al., 2010; Williamson et al., 2009; Wu et al., 2010; Xu et al., 2009) and short chains of mixed linkage types (Kirkpatrick et al., 2006). In contrast, polymers built through Lys63 of ubiquitin have non-proteolytic roles in DNA repair (Hofmann and Pickart, 1999; Spence et al., 1995), kinase activation (Deng et al., 2000), protein trafficking (Pickart and Fushman, 2004; Yang et al., 2009) and translation (Spence et al., 2000). Similarly, the transfer of a single ubiquitin moiety to one (monoubiquitination) or to multiple sites (multiple monoubiquitination) in a substrate has been implicated in mostly non-proteolytic processes (Robzyk et al., 2000; Terrell et al., 1998), although multiple monoubiquitination can target receptor tyrosine kinases (RTKs) to the lysosome (Haglund et al., 2003; Huang et al., 2006; Mosesson et al., 2003). More recently, multiple monoubiquitination has been shown to control proteasomal processing of the p105 NF-kB precursor to the shorter p50 subunit (Kravtsova-Ivantsiv et al., 2009). To date, multiple monoubiquitination has not been coupled with rapid and complete proteolysis of a proteasome substrate.

The E3 ligase activities of the Skp1-Cullin-F-box complex (SCF) family and the Anaphase-Promoting Complex/Cyclosome (APC/C or APC) have long been recognized to be essential for cell-cycle progression (Harper et al., 2002; Peters, 2006; Skaar and Pagano, 2009). Unlike the SCF, which cooperates with the E2 Cdc34 to assemble uniform Lys48-linked ubiquitin polymers on substrates (Petroski and Deshaies, 2005), the APC/C works in conjunction with UBCH10 (also known as E-2C) and enzymes of the UBC4/5 family to catalyze chain formation

through three lysine residues of ubiquitin (Lys11, Lys48 and Lys63) (Kirkpatrick et al., 2006). UBCH10 builds multiple short ubiquitin chains on cyclin B1, which are sufficient to target the protein for degradation by the proteasome (Kirkpatrick et al., 2006). In this context, Lys48-linked ubiquitin polymers are dispensable for binding of modified cyclin B1 to ubiquitin receptors and degradation by the proteasome (Kirkpatrick et al., 2006). More recent work suggests that the assembly of proteolytic signal on APC/C substrates may occur in two stages. In budding yeast, Ubc4 initiates ubiquitin conjugation, whereas Ubc1 elongates ubiquitin chains (Rodrigo-Brenni and Morgan, 2007). Similarly, in metazoans, UBCH10 has been proposed to initiate monoubiquitination of the substrate, followed by UBE2S-dependent extension of Lys11-linked ubiquitin chains (Garnett et al., 2009; Williamson et al., 2009; Wu et al., 2010). Consistent with this idea, depletion of UBE2S from *Drosophila* S2 cells results in a strong delay in a metaphase-like state and stabilization of cyclin B1 at the spindle poles, among other mitotic defects (Williamson et al., 2009). In contrast, UBE2S is not essential for normal mitosis in human HeLa cells and is largely dispensable for timely proteolysis of cyclin B1 in this context (Garnett et al., 2009). These findings imply that UBE2S may not be uniformly required for mitosis, but rather may be important for substrate proteolysis under conditions where APC/C activity is compromised such as during recovery from drug-induced spindle-assembly checkpoint (SAC) activation (Garnett et al., 2009).

The ability of the APC/C, in conjunction with the E2 UBCH10 to extend multiple short ubiquitin chains through lysines 11, 48 and 63 of ubiquitin *in vitro* (Kirkpatrick et al., 2006) raises the question as to whether long homotypic ubiquitin-chain formation is indeed required for proteolysis of APC/C substrates. Even if ubiquitin chains are important, it remains unclear whether this requirement arises from a specific role of UBE2S, or through the chain-forming activity of UBCH10 (Jin et al., 2008; Kirkpatrick et al., 2006). However, it has been challenging to study the role of specific ubiquitin linkages in substrate turnover in cellular extracts due to the presence of endogenous ubiquitin. Using a novel approach in which *Xenopus* extracts are made

largely dependent on exogenous ubiquitin, we sought to understand whether APC/C-catalyzed proteolysis is strictly dependent upon polyubiquitination and whether the proteolytic machinery exerts a requirement for Lys11 or other ubiquitin linkages to efficiently degrade cyclin B1.

Results

Inhibiting ubiquitin-chain formation has only a modest effect in stabilizing cyclin B1 in *Xenopus* extract

We previously showed that by suppressing deubiquitinating activity with ubiquitin-vinyl sulfone (UbVS) we can impose a state of ubiquitin deficiency in *Xenopus* extract that strongly stabilized cyclin B1 (chapter II). Addition of physiologically relevant concentrations of wild-type ubiquitin fully rescued cyclin degradation, as measured by the production of acid-soluble radioactive counts. Using this system, we next tested the ability of chain-terminating ubiquitin mutants to restore proteolysis of ^{35}S-labeled N-terminal fragment of human cyclin B1 (cycB1-NT) in UbVS-treated extracts. Different Ub mutants containing a single lysine-to-arginine substitution at position 11 (Ub^{11R}), 48 (Ub^{48R}), or 63 (Ub^{63R}), or at all three positions simultaneously (Ub^{triR}) restored cycB1-NT proteolysis under these conditions, albeit with different kinetics. Addition of wild-type ubiquitin, Ub^{48R}, and Ub^{63R} rescued degradation most efficiently, showing a half-life of approximately 15 minutes (Figure 3.1a). After 20 minutes, the rate of degradation slowed substantially, likely a consequence of ubiquitin depletion in the UbVS-treated extract, as supplementation with additional ubiquitin restored degradation to the initial rate (Figure 3.1b). Extracts supplemented with Ub^{11R} or Ub^{triR} degraded substrate only somewhat more slowly. These results were unexpected, as mass spectrometric analysis indicated that elimination of all three principal sites of Ub-Ub linkage by the APC/C rendered Ub incapable of forming ubiquitin chains in reconstituted reactions (data not shown). Even addition of Ub^{me} supported degradation, with a half-life of approximately 30 minutes. We next assessed how constraining the topology of ubiquitin chains to a single lysine residue would affect degradation of cycB1-NT (Figure 3.1c). Addition of $Ub^{K11only}$ or $Ub^{K48only}$ to UbVS-treated extract restored cycB1-NT proteolysis, but with slower kinetics compared to wild-type ubiquitin. We were surprised that $Ub^{K11only}$ did not support robust degradation, as previous reports indicated that it

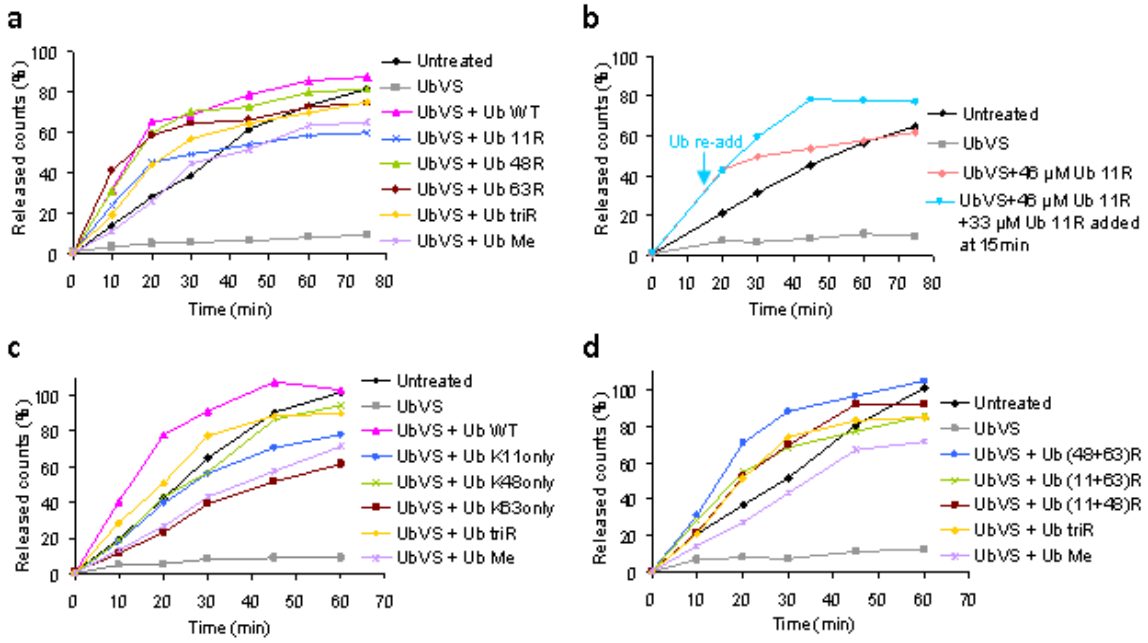

Figure 3.1 Ubiquitin-chain formation is not essential for cyclin B1 degradation in UbVS-treated *Xenopus* extract. ^{35}S-labeled cycB1-NT and different forms of Ub, where indicated, were introduced concomitantly into mitotically-arrested *Xenopus* extract that had been pre-treated with UbVS (20 µM) or buffer (referred to as untreated) for 30 min. Proteolysis was measured by release of trichloroacetic acid (TCA) soluble counts, and is plotted as the percentage of input radiolabeled cycB1-NT. Trends are representative of three or more independent experiments. (**a**) Ubiquitin types (44 µM) with single lysine-to-arginine mutations at indicated positions or at all three positions Lys11, 48 and 63 (Ub^{triR}) simultaneously were added to UbVS-treated extract. (**b**) $Ubiquitin^{11R}$ (46 µM) and substrate were introduced into UbVS-treated extract, and supplemented with Ub^{11R} (33 µM) or buffer control 15 min after initiation of degradation. (**c**) Ubiquitin types (44 µM) used, as indicated. $Ubiquitin^{Konly}$ refers to ubiquitin that has all of its lysines, except for the specified, mutated to arginines. (**d**) Degradation was measured in the presence of different ubiquitin types (44 µM) containing arginine substitutions at two of the three principle sites (Lys11, Lys48, and Lys63) of ubiquitin-ubiquitin conjugation by the APC.

can efficiently support APC/C-dependent ubiquitination (Jin et al., 2008; Williamson et al., 2009; Wu et al., 2010). One possibility is that mutation of Lys6 of ubiquitin may have an inhibitory effect on proteasomal degradation (Shang et al., 2005). We therefore tested the effect of restricting chain formation to one of the three principle sites of ubiquitin-ubiquitin attachment mediated by UBCH10 by mutating the remaining two (data not shown). In these experiments, $Ub^{(48+63)R}$ stimulated degradation efficiently, consistent with the ability of Lys11 linkages to support degradation (Figure 3.1d). Ubiquitin forms supporting Lys48 and Lys63 linkages ($Ub^{(11+63)R}$ and $Ub^{(11+48)R}$, respectively) and Ub^{triR} supported proteolysis with somewhat slower kinetics. Together these findings indicate that even when deubiquitinating enzymes are inhibited, the ability to construct Lys11-linked chains provides a kinetic advantage for degradation, although the advantage is modest. In principle this advantage could arise from the utilization of Lys11 as one of three sites (in addition to Lys48 and Lys63 of ubiquitin) in chain-forming reactions catalyzed by UBCH10, or from a role of UBE2S, which elongates ubiquitin chains exclusively through Lys11 linkages.

Ubiquitin chains are required for cyclin B1 degradation only when the number of available lysine residues in cyclin B1 is restricted

To rule out the possibility that our results thus far were influenced by use of an N-terminal fragment of cyclin B1, we examined proteolysis of full-length wild-type cyclin B1 bound to CDK1 by immunoblotting (Figure 3.2c, left panel). Addition of Ub^{11R} or Ub^{triR} stimulated degradation, albeit at slightly reduced rates relative to wild-type ubiquitin. $Ubiquitin^{me}$ also supported substantial degradation of cyclin B1, although a small fraction of the protein accumulated in a triply-ubiquitinated species. Higher molecular-weight forms were not observed, possibly because they were targeted for degradation by the proteasome.

Figure 3.2 Cyclin B1 proteolysis depends on Lys11-linked ubiquitin-chain formation only when the number of available lysine residues is restricted. (**a**) Sequence comparison of the cyclin B1 N termini from multiple species reveals lysine richness. Lysine residues are colored in blue; the destruction box (D-box) is colored in orange. (**b**) Schematic representation of the N-terminal region (residues 1-88) of human cyclin B1 with lysine residues denoted K in blue and with the D-box motif denoted with an orange rectangle. Cyclin B1 mutants ($cyc^{K64only}$ and $cyc^{K59,63,64,67only}$) were generated by substituting lysine with arginine at all but the specified lysine residues within the first 115 amino acids (residues 89-115 not shown). Cyc^{WT}, wild-type cyclin B1. (**c**) Purified full-length wild-type (cyc^{WT}) or single-lysine ($cyc^{K64only}$) cyclin B1, in complex with CDK1, and forms of Ub (20 μM) as indicated were added to mitotic *Xenopus* egg extract that had been pre-treated with UbVS (20 μM) for 30 min. Stability of the exogenous substrate over time was assessed by SDS-PAGE and cyclin B1 western blot analysis. (**d**) As in **c** , except the behavior of full-length $cyc^{K59,63,64,67only}$, in complex with CDK1, was analyzed.

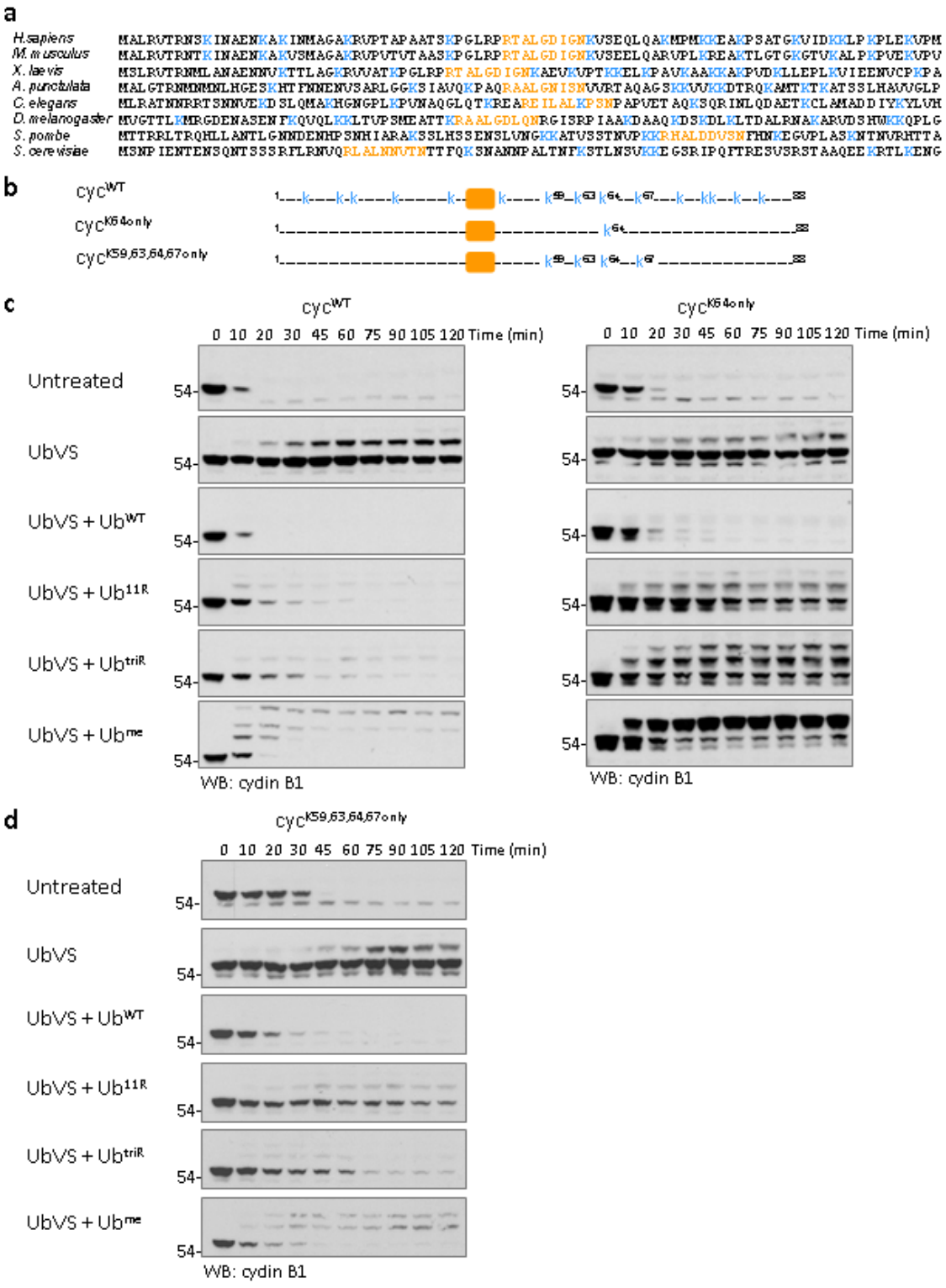

Figure 3.2 (Continued)

Cyclin B1 contains 18 lysine residues in its unstructured N-terminal region upstream of the cyclin box; 15 of these lysine residues are located within the first 88 amino acids close to the destruction box (Figure 3.2a), providing a platform upon which a proteolytic signal consisting of multiple monoubiquitins or short ubiquitin chains can be assembled. To examine whether reducing the number of lysines in cyclin B1 renders its proteolysis dependent on ubiquitin-chain formation, we measured degradation of cyclin B1 mutants that contained either one or four ubiquitinatable lysine residues in the first 115 amino acids at position 64 only ($cyc^{K64only}$) or at positions 59, 63, 64, and 67 ($cyc^{K59,63,64,67only}$) (Figure 3.2b; Figure 3.2c, right panel; Figure 3.2d). We chose these positions as mass spectrometry studies indicated that these lysine residues become ubiquitinated early in the course of reconstituted ubiquitination reactions (D. K., N. H., unpublished observations). $Cyc^{K64only}$ was degraded rapidly in untreated *Xenopus* extract, and was fully stabilized in UbVS-treated extract. However, unlike the case for wild-type cyclin B1, Ub^{11R} was not able to efficiently stimulate the degradation of $cyc^{K64only}$. Similar results were obtained with Ub^{triR}. Interestingly, Ub^{me} did not rescue degradation, but instead caused quantitative accumulation in a monoubiquitinated form. These results contrast strikingly with the behavior of wild-type cyclin B1, where the majority of the protein was degraded upon addition of Ub^{me}.

We next determined whether restoration of a limited number of lysine residues could enable degradation in the presence of chain-terminating ubiquitins (Figure 3.2d). Surprisingly, $cyc^{K59,63,64,67only}$ was degraded somewhat more slowly than $cyc^{K64only}$ in untreated extract, for reasons that remain unclear and may include posttranslational modifications within this lysine cluster that are inhibitory to APC-dependent proteolysis. Addition of Ub^{11R} partially restored degradation of $cyc^{K59,63,64,67only}$ in a UbVS-treated extract. The most striking difference was observed in extracts supplemented with Ub^{me}. Whereas $cyc^{K64only}$ accumulated quantitatively in a monoubiquitinated form, $cyc^{K59,63,64,67only}$ was unstable, although a fraction of the protein accumulated in mono- and di-ubiquitinated species. We conclude that when deubiquitinating enzymes are inhibited, the attachment of single ubiquitin molecules to multiple lysine residues in

cyclin is sufficient to target the substrate for degradation. Strict dependence on elaboration of ubiquitin chains appears to occur only when the number of available substrate lysines is restricted.

Multiple monoubiquitination can target cyclin B1 for efficient degradation in a reconstituted system and in *Xenopus* extract

We next assessed whether the effects of different ubiquitin mutants on proteolysis paralleled their effects on ubiquitin conjugation using a reconstituted system. In APC/C reactions reconstituted with 100 nM UBCH10, we found that elimination of Lys48 or 63 of ubiquitin had no effect on the mass of conjugates generated in 15-minute reactions, consistent with the fact that these mutations had little effect on degradation in UbVS-treated extracts (Figure 3.3a, top panel). Interestingly, elimination of Lys11 reduced the mass of conjugates formed, consistent with the previously reported preference of UBCH10 for synthesizing Lys11 linkages (Jin et al., 2008; Kirkpatrick et al., 2006). These differences became more pronounced in longer ubiquitination reactions (Figure 3.3a, bottom panel). In the presence of ubiquitin types that do not support ubiquitin-polymer assembly (Ub^{triR} and Ub^{me}), the maximal extent of substrate modification (5-6 ubiquitins per cyclin B1 molecule) was observed at early time-points and remained unchanged in longer reactions (Figure 3.3a), implying that there likely is a limited subset of preferred ubiquitination sites in cyclin B1. A time-course of ubiquitination with either wild-type Ub or Ub^{triR} (Figure 3.3b) revealed that, at physiologically relevant E2 concentrations, the conjugation of ubiquitin monomers to distinct lysines in cyclin B1 occurs with rapid kinetics. Furthermore, conjugates bearing 4 or more ubiquitin moieties were capable of binding proteasome-associated ubiquitin-receptors (Deveraux et al., 1994; Elsasser et al., 2004; Elsasser and Finley, 2005; Finley, 2009; Isasa et al., 2010; Matiuhin et al., 2008; Peth et al., 2010; Rao and Sastry, 2002; Riedinger et al., 2010) including Rpn10 (Figure 3.3c, d) and Rad23 (Figure 3.3e, f), in a manner

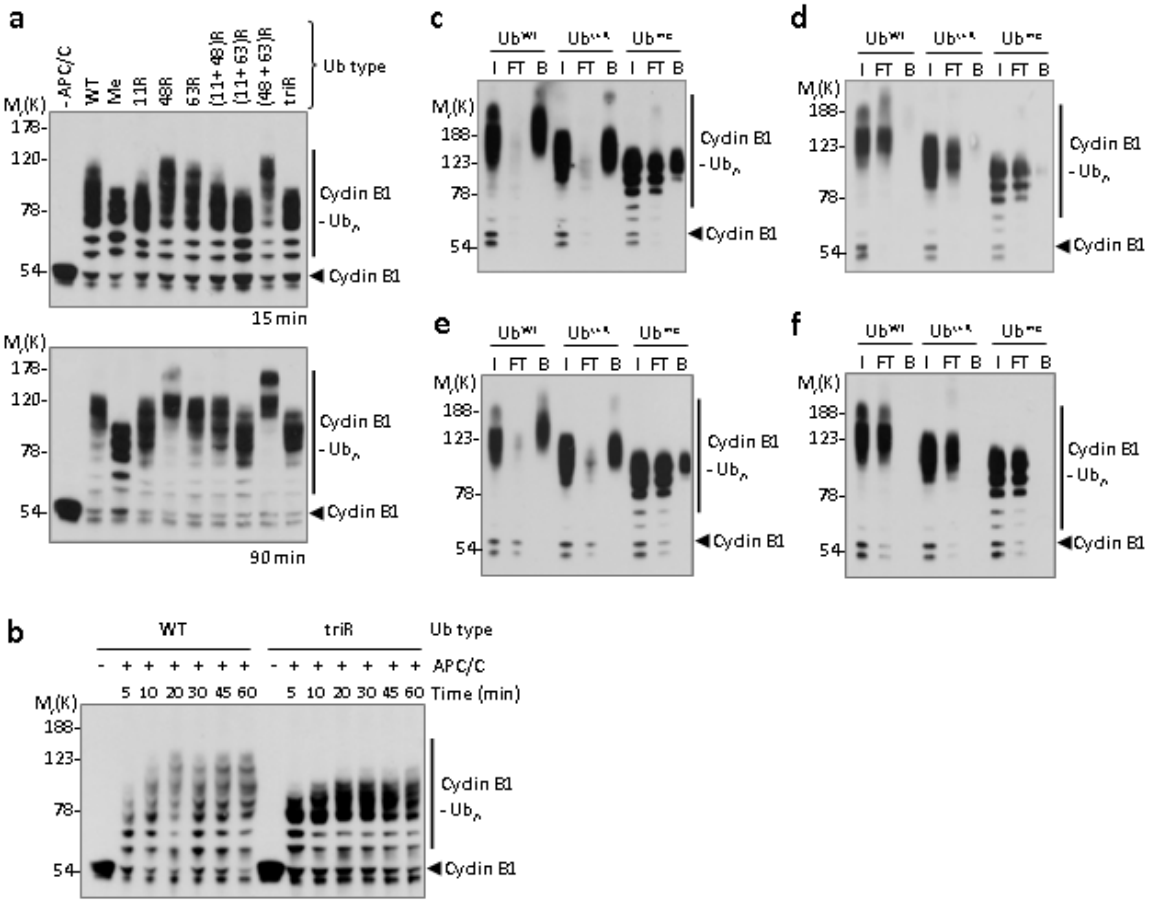

Figure 3.3 UBCH10 and APC/C catalyze rapid multiple monoubiquitination of cyclin B1 that is sufficient for binding ubiquitin receptors. (**a**) Western blot analysis of the *in vitro* ubiquitination reaction containing full-length cyclin B1, APC/C immunopurified from mitotically arrested *Xenopus* extract, recombinant UBCH10 (100 nM), and forms of ubiquitin (118 µM), as indicated. Ubiquitin types with lysine-to-arginine mutations at one , two or all three positions Lys11, 48 and 63 (Ub^{triR}) simultaneously, as well as methylated ubiquitin (Ub^{me}) were used. Control "-APC/C" reactions containing all components except for the E3 ligase were performed in parallel. Reactions were allowed to proceed for 15 or 90 min before analysis by SDS-PAGE and western blotting against cyclin B1. (**b**) Time-course of the *in vitro* ubiquitination of full-length wild-type cyclin B1 with wild-type ubiquitin or Ub^{triR} and remaining components as in **a**. (**c**-**f**) Binding of ubiquitinated cyclin B1 to GST-tagged ubiquitin receptors. Cyclin B1-ubiquitin conjugates were incubated with immobilized receptor proteins for 1 h at 4 °C before reaction products were subjected to SDS-PAGE and western blot analysis against cyclin B1. Equivalent amounts of input (I), flow-through (FT) and bound (B) fractions were loaded in adjacent lanes. Binding experiments with wild-type Rpn10 (**c**) and Rad23 (**e**). Binding with corresponding versions of the receptors lacking the ubiquitin-recognition domains, with engineered block substitution of the UIM domain (LAMAL → NNNNN) of Rpn10 (**d**) or deletion of the ubiquitin-associated domains of Rad 23 (**f**).

that depended on their ubiquitin-interaction domains. For conjugates of a similar molecular mass, substrate ubiquitinated with Ub^{triR} bound to receptors more efficiently than substrate ubiquitinated with Ub^{me}. Given that Ub-AQUA analysis indicates that these forms of ubiquitin suppress ubiquitin-chain formation with similar efficiency, this finding suggests that methylation of ubiquitin may compromise its affinity for ubiquitin receptors. We found similar binding patterns with cyclin B1-ubiquitin conjugates generated with UBC4 as the E2 (discussed in chapter IV). Together these results indicate that multiple monoubiquitination occurs rapidly and can result in a productive signal for binding ubiquitin receptors.

We next sought to determine whether multiple monoubiquitination can target cyclin B1 for degradation in a reconstituted system. To this end, full-length cyclin B1-CDK1 complex was ubiquitinated with UBCH10, in conjunction with wild-type or chain-terminating ubiquitin. The resulting conjugates were incubated with purified human proteasomes that were washed with high salt concentrations to eliminate USP14, a deubiquitinating enzyme that can antagonize cyclin B1 degradation *in vitro* (Hanna et al., 2006; Lee et al., 2010). These proteasomes, which retain the deubiquitinating enzymes RPN11 and UCH37 (Lee et al., 2010), rapidly degraded polyubiquitinated cyclin B1, generated with UBCH10 (Figure 3.4a). While conjugates formed with Ub^{triR} or lysine-less ubiquitin (Ub^{K0}) were efficiently degraded, those generated with methylated ubiquitin were degraded less rapidly, consistent with the defect in the ability of these conjugates to bind ubiquitin receptors (Figure 3.3c, e). Similar trends were observed for cyclin B1 species ubiquitinated with UBC4 as the E2 (discussed in chapter IV). The extent of conjugate proteolysis was quantitated using radiolabeled full-length cyclin B1, in complex with unlabeled CDK1, and was found to closely correlate with the fraction of input cyclin B1 bearing three or more ubiquitin molecules (data not shown). Degradation of cyclin B1 in the reconstituted system was confirmed to be both APC/C- and ubiquitin-dependent (data not shown). Interestingly, analogous experiments performed with radiolabeled cycB1-NT pre-ubiquitinated by UBCH10 (Figure 3.4b) revealed that degradation of multiply monoubiquitinated cyclin B1 was sensitive to

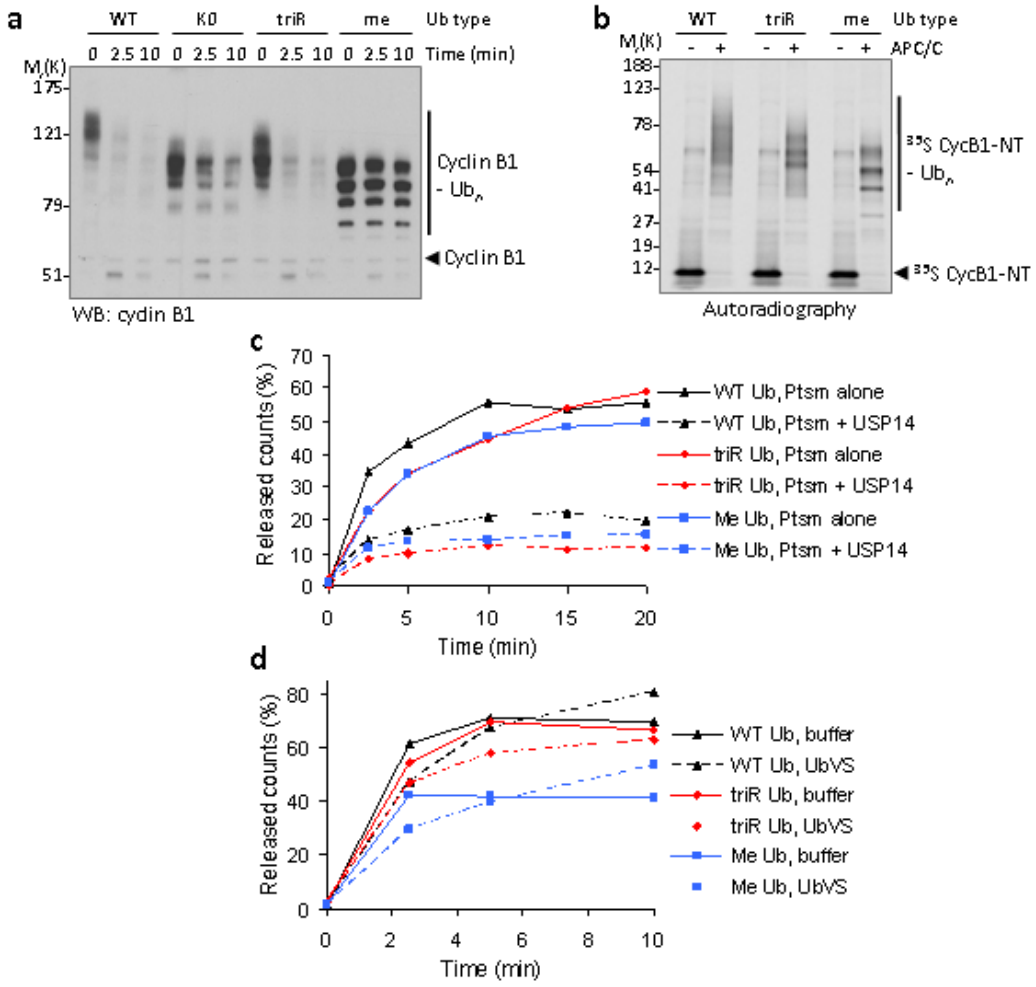

Figure 3.4 Multiply monoubiquitinated cyclin B1 is rapidly degraded by purified proteasomes and in *Xenopus* extract. (**a**) *In vitro* degradation assay with cyclin B1-Ub species generated with immunopurified *Xenopus* APC/C, recombinant UBCH10 (250 nM), and forms of Ub (145 µM), as indicated, and USP14-deficient human proteasomes (20 nM). A ubiquitin type bearing lysine-to-arginine mutations at all three positions Lys11, 48 and 63 simultaneously (Ub^{triR}), methylated (Ub^{me}) or lysine-less (Ub^{KO}) ubiquitin were used as chain-terminating ubiquitins. WT, wild-type. Aliquots were removed at the indicated times and reaction products analyzed by SDS-PAGE and anti-cyclin B1 immunoblotting. (**b**) Autoradiograph of *in vitro* APC/C- and UBCH10-catalyzed ubiquitination of ^{35}S-labeled cycB1-NT (1-88) with immunopurified *Xenopus* APC/C, recombinant UBCH10 (100 nM) and forms of ubiquitin (145 µM) as indicated. Products from a 60-minute ubiquitination assay were separated by SDS-PAGE and analyzed using a phosphorimager. (**c**) CycB1-NT-ubiquitin species from **b** were incubated with purified human proteasomes (Ptsm; 20 nM) reconstituted with or without 20-fold molar excess of GST-tagged wild-type USP14. At indicated times, reactions were terminated by addition of trichloroacetic acid (TCA). Proteolysis was measured by release of TCA soluble counts, and is plotted as the percentage of input radiolabeled cyclin B1 protein. (**d**) CycB1-NT-ubiquitin species from **b** were added to interphase *Xenopus* extract that had been pre-treated with UbVS (15 µM) or buffer control for 30 min. Reactions were terminated by addition of TCA at indicated times. Proteolysis was measured by release of TCA soluble counts, and is plotted as the percentage of input radiolabeled cycB1-NT.

addition of the deubiquitinating enzyme USP14 (Figure 3.4c). This effect was reversed by IU1, an inhibitor of the catalytic activity of USP14 (Lee et al., 2010) (data not shown). Together these results indicate that purified proteasomes can efficiently degrade a multiply monoubiquitinated cyclin B1 and that USP14 can deubiquitinate this substrate to suppress degradation.

To determine whether multiple monoubiquitination could target the protein for degradation under conditions of physiological concentrations of proteasomes and in the presence of relevant DUB activities, we used the same ubiquitinated species from those analyzed in Figure 3.4b and added them to interphase *Xenopus* extract, a state in which the APC/C is inactive (Figure 3.4d). Conjugates generated with Ub^{triR} or Ub^{me} were degraded rapidly with initial rates very similar to that observed for conjugates generated with wild-type ubiquitin. However, a fraction of the conjugates generated with methylated ubiquitin were degraded less efficiently, likely because they were insufficiently ubiquitinated to be recognized by the proteasome. Similar results were obtained when the ubiquitin conjugates were introduced into extracts that were supplemented with excess non-ubiquitinated unlabeled competitor to prevent any potential APC/C-mediated ubiquitination (data not shown) or to extracts that had been immunodepleted of APC/C (data shown in chapter IV). Together these findings further indicate that *Xenopus* extracts can rapidly degrade a cyclin substrate bearing multiple ubiquitin monomers attached to distinct lysine residues.

Pre-treatment of extract with UbVS, at a concentration identical to that used to deplete free ubiquitin, had little ability to accelerate degradation of conjugates generated with wild-type ubiquitin or with Ub^{triR}, but modestly enhanced degradation of species modified with Ub^{me} (Figure 3.4d). Deubiquitination appears to exert little effect on degradation of these pre-ubiquitinated species, perhaps because deubiquitinating enzymes such as USP14 are present at much lower levels in *Xenopus* extracts than in our reconstituted system. Consistent with this idea, addition of an inhibitor of USP14, IU1, failed to accelerate degradation of cyclin B1 in *Xenopus* extracts (data not shown).

Discussion

In this study, we have evaluated the role of ubiquitin-chain topology in targeting cyclin B1 for degradation in a reconstituted system, as well as in mitotic *Xenopus* cell-cycle extracts. Our study was motivated by recent findings suggesting that Lys11 linkages, mediated by the chain-forming E2 enzyme UBE2S, may be important for APC/C-dependent proteolysis. However, our earlier work suggested that APC/C, solely in conjunction with the E2 enzyme UBCH10 or the enzyme UBC4/5, can build a ubiquitin signal that is sufficient for degradation by purified proteasomes (Kirkpatrick et al., 2006). Here we provide a resolution to this paradox, demonstrating that conjugation of ubiquitin to multiple lysine residues of cyclin B1 provides an alternative degradation signal for cyclin B1 that does not require extension of Lys11-linked ubiquitin polymers. Lysine11-linked ubiquitin-chain formation becomes essential only when the number of available lysine residues in cyclin B1 is restricted.

Dominant negative effects of different ubiquitin types may be difficult to observe when examined in a background that contains wild-type ubiquitin. Using UbVS to inhibit deubiquitinases and their capacity to recycle ubiquitin, we were able to impose a state of ubiquitin deficiency in extract that strongly stabilized cyclin B1. Supplementing UbVS-treated extracts with ubiquitin rescues the proteasomal degradation of cyclin. As opposed to addition of excess ubiquitin, this approach allowed us to examine the functional significance of different linkages at physiological concentrations of ubiquitin. Under such conditions, any kinetic advantage specific ubiquitin linkages may confer in protein degradation may be ascertained and more easily uncovered.

The UbVS system enabled us to define the role of different ubiquitin-chain topologies in targeting cyclin B1 for degradation in *Xenopus* extracts. In agreement with earlier work in a reconstituted system (Kirkpatrick et al., 2006), Lys48 ubiquitin-ubiquitin linkages were not required for efficient cyclin proteolysis in UbVS-treated extract. Surprisingly in the light of recent

studies (Jin et al., 2008; Williamson et al., 2009; Wu et al., 2010), ubiquitin incapable of forming Lys11 linkages (Ub^{11R}) also supported very robust degradation of cyclin B1 (Dimova et al., 2012). Importantly, we found that chain-terminating ubiquitins (Ub^{triR} and lysine-less ubiquitin), which greatly diminish chain elongation by UBCH10, UBC4/5, and UBE2S, also support robust rates of cyclin proteolysis. Methylated ubiquitin was somewhat less capable of supporting rapid cyclin degradation, which may reflect less efficient recognition by ubiquitin receptors and the proteasome due to modification of Lys6 of ubiquitin (Shang et al., 2005). However, upon restriction of ubiquitination to a single lysine residue in cyclin as in $cyc^{K64only}$, chain-terminating ubiquitins were no longer able to stimulate substrate degradation and cyclin accumulated as mono- and di-ubiquitinated species. Together these findings suggest that ubiquitin-chain formation is not essential for cyclin proteolysis, unless the number of available ubiquitination sites in the substrate is restricted.

Utilizing a reconstituted system, we demonstrated that UBCH10 can rapidly append mono-ubiquitin to multiple lysines in cyclin. Species bearing 4 or more ubiquitin moieties on distinct lysines were recognized by ubiquitin receptors. Based on these findings, we propose that the presence of multiple lysines in cyclin B1 that are in close proximity to one another has the potential for generating a high density of mono-ubiquitin that promotes receptor binding. In such an arrangement, the hydrophobic patches on distinct ubiquitin units may be available to form contacts with various ubiquitin-binding domains (UBDs). Whether particular spacing of ubiquitinated lysine residues is essential for recognition by ubiquitin receptors remains unknown. In our pull-down experiments, there may be some enhanced avidity resulting from a dimeric GST moiety positioning two ubiquitin-associated domains (UBAs) in close proximity (Sims et al., 2009). However, the rapid destruction of multiply monoubiquitinated species by purified proteasomes and in *Xenopus* extracts implies that this substrate must have sufficient affinity for proteasome-associated ubiquitin receptors.

The capacity of purified proteasomes to rapidly degrade multiply monoubiquitinated cyclin B1 was significantly attenuated by USP14, suggesting that USP14 can efficiently remove monoubiquitin, as well as trim Ub chains. However, such deubiquitinating activity did not appear to strongly antagonize proteasome function in *Xenopus* extract, as treatment of extract with UbVS or the USP14-specific inhibitor IU1 did not appreciably enhance turnover of pre-ubiquitinated cyclin. Although present in *Xenopus* extracts (N.V.D., R.W.K., unpublished data), levels of USP14 associated with proteasomes in extract may be insufficient to impede proteolysis. Together, these findings suggest the proteasome does not impose a requirement for ubiquitin-chain formation for efficient proteolysis of cyclin B1, even when DUBs are not inhibited by UbVS. This study further strengthens the view that the proteasome has the capacity to recognize and degrade substrates bearing ubiquitin modifications distinct from the canonical Lys48-linked polyubiquitin chains (Baboshina and Haas, 1996; Guterman and Glickman, 2004; Hershko and Heller, 1985; Hofmann and Pickart, 2001). The early work of Hershko and Heller demonstrated that methyl-ubiquitin addition to reticulocyte extracts can support the proteolysis of ^{125}I-labeled lysozyme, but overall rates of degradation were slow, with ~12% of input substrate degraded within an hour (Hershko and Heller, 1985). While conjugation of mono-ubiquitin can promote degradation of the model substrate Pax 3 (Boutet et al., 2007), the kinetics of degradation are slow, with a half-life of 3.5 h. In contrast, multiple monoubiquitination of cyclin B1 provides a robust degradation signal.

Previously, we demonstrated that in conjunction with UBCH10 or UBC4/5 enzymes, the APC generates a proteolytic signal on cyclin comprised of Lys11 and Lys63, in addition to Lys48 ubiquitin linkages (Kirkpatrick et al., 2006). In this context where chains are nucleated on multiple substrate lysines, it cannot not be ruled out that distinct chains consisting of a series of identical linkages such as Lys11(Lys11(Lys11))) (Kirkpatrick et al., 2006) are assembled and function as the major degradative signal. This question has become increasingly important in the light of recent studies suggesting that synthesis of Lys11-linked polymers is central to APC-

dependent proteolysis (Williamson et al., 2009; Wu et al., 2010). Such a model is not consistent with our findings where ubiquitin incapable of forming Lys11 linkages (Ub^{11R}) or supporting chain-elongation (Ub^{triR}) allows robust cyclin proteolysis in UbVS-treated extracts. Based on our findings in *Xenopus* extract and in a reconstituted system, we propose that through conjugation of monoubiquitin to multiple lysine residues, and possibly elaboration of some short chains, UBCH10, or possibly members of the UBC4/5 family, cooperates with the APC/C to generate a sufficient proteolytic signal on cyclin B1 (Figure 3.5). Our findings lend strong support to the idea that high local density of ubiquitin, independent of linkage, is sufficient to target a substrate for proteolysis. Upon restriction of available lysine residues, however, such ubiquitin density may not be attainable through the conjugation of monoubiquitin. In this context, ubiquitin moieties will have to be added to the end of a growing chain rather than to a lysine residue in the substrate in order to achieve the threshold necessary for proteolysis. Consistent with this idea, ubiquitin-chain formation becomes essential for proteasomal degradation when the number of available lysine residues in cyclin B1 is restricted. An important question is whether in this context the activity of the inherently less processive UBCH10 is sufficient to promote efficient ubiquitination and targeting to the proteasome, or whether there is a greater dependence on chain-elongation by the Lys11-specific E2 UBE2S (Garnett et al., 2009; Wickliffe et al., 2011; Williamson et al., 2009; Wu et al., 2010).

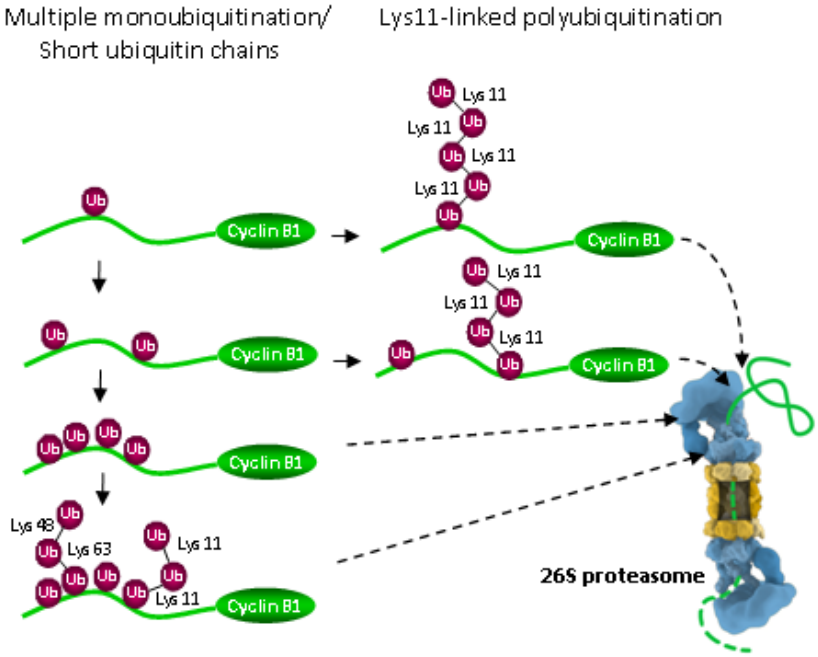

Figure 3.5 Model of cyclin B1 degradation in *Xenopus* cell-cycle extract. The APC/C and the E2 UBCH10 collaborate to transfer ubiquitin monomers to multiple lysine residues on cyclin B1, with subsequent elaboration of short ubiquitin chains containing K63, K48 and K11 linkages, with K11 linkages predominating (Kirkpatrick et al, 2006). On achievement of a threshold of ubiquitin mass, which appears to be 4-5 ubiquitin monomers, multiply monoubiquitinated substrate can associate with proteasome-associated ubiquitin receptors and be degraded efficiently. However, when the number of lysine residues in cyclin B1 is restricted, ubiquitination catalyzed by UBCH10 is insufficient for rapid proteolysis and the activity of another E2 in extending Lys11-linked ubiquitin polymers becomes important for efficient degradation.

Methods

Antibodies and biochemical reagents

Proteins were separated by SDS-PAGE on NuPAGE 4-12% or 12% Bis-Tris gels (Invitrogen), followed by wet transfer to PVDF. Sources of antibodies for immunoblotting were as follows: anti-cyclin B1 (Ab-2; RB-008-P, Neomarkers), anti-Cdc27 (610455, BD Transduction Laboratories), anti-UBCH10 (A-650, Boston Biochem; AB3861, Millipore), anti-UBE2S (N-14; sc-131354, Santa Cruz Biotechnology), anti-UBCH5 (A-615; Boston Biochem), anti-ubiquitin (P4D1; sc-8017; Santa Cruz Biotechnology). Secondary antibodies used include anti-goat IgG-HRP (sc-2020; Santa Cruz Biotechnology), anti-rabbit IgG-HRP (NA934; GE Healthcare), and anti-mouse IgG-HRP (NA931; GE Healthcare). Antibodies for immunoprecipitation or immunodepletion included: anti-Cdc27 (AF3.1; sc-9972) and anti-UBE2S (N-14; sc-131354) from Santa Cruz Biotechnology; anti-UBCH10 (gift from H. Yu, UT Southwestern, USA); and for control depletions, normal rabbit (sc-2027) and normal goat (sc-2028) IgG, both from Santa Cruz Biotechnology. UBE2S antibodies were coupled to UltraLink immobilized protein A/G beads (53132, Pierce). UBCH10 and CDC27 antibodies were coupled to Affiprep protein A beads (156-0006, Bio-Rad). Ubiquitin agarose (U-405), UbVS (U-202), MG262 (I-120), Ub^{me} and ubiquitin mutants except for $Ub^{(11+48)R}$, $Ub^{(11+63)R}$ and Ub^{triR} were purchased from Boston Biochem. TAME (T4626) and ubiquitin (U6253) were purchased from Sigma.

Preparation of recombinant proteins

Ubiquitin mutants $Ub^{(11+48)R}$, $Ub^{(11+63)R}$ and $Ub^{(11+48+63)R}$ (referred to as Ub^{triR}) were generated by introducing arginine codons (AGA and AGG) at the indicated sites through PCR-mediated mutagenesis of the human ubiquitin sequence (cloned in pET3a with ampicillin resistance, the kind gift of C.M. Pickart). Plasmids were verified by sequencing and the purified proteins analyzed by mass spectrometry. To ensure efficient arginine incorporation, BL21 (DE3) cells were co-transformed with pJY2, developed by Pickart lab (You et al., 1999), which carries

T7 lysozyme (LysS) and a gene encoding $tRNA_{UCU}^{Arg}$. Cultures were grown at 37 °C to an attenuance (*D*) of ~ 0.5 at 600 nm, and induced with 100 μM isopropylthiogalactoside (IPTG) at $D_{600\ nm}$ = 0.6 at 25 ˚C for 5 h. Cells were ruptured by sonication in QA lysis buffer (50 mM HEPES (pH 7.7), 100 mM KCl, protease-inhibitor cocktail, 5 mM 2-mercaptoethanol, 10 μg ml^{-1} DNase). Lysozyme was added to 1 mg ml^{-1} concentration and lysate was incubated with rotation at 4 °C for 15 min. Following sonication, cell lysates were clarified by centrifugation and the resulting supernatants applied to a Q column. The flow-through containing ubiquitin was concentrated and purified by size-exclusion chromatography. Fractions containing ubiquitin were typically > 95% pure.

To generate full-length cyclin B-CDK1 complex, human cyclin B1 and CDK1 baculoviruses were used as described previously (Kirkpatrick et al., 2006). To generate mutants of cyclin B1, DNA fragments encoding the N-terminal 124 amino acids of wild-type human cyclin B1 (5'-

AACCGGTCCGAAACCGTCGACATGTCGCATCACCATCACCATCACGGCTC
GATGGCGCTCCGAGTCACGCGTAACTCGAAAATTAATGCTGAAAATAAAGCGAAAA
TCAACATGGCAGGCGCCAAGCGCGTTCCTACGGCACCGGCGGCAACCTCCAAACCCG
GGCTGAGGCCAAGAACAGCTCTTGGGGACATTGGTAACAAAGTCAGTGAACAGCTA
CAGGCCAAAATGCCTATGAAAAAAGAAGCAAAACCTTCAGCTACCGGTAAAGTCAT
TGATAAAAAACTACCAAAACCTCTTGAAAAGGTACCTATGCTGGTGCCAGTGCCAGT
GTCTGAGCCAGTGCCAGAGCCAGAACCTGAGCCAGAACCTGAGCCTGTTAAAGAAG
AAAAACTTTCGCCTGAGCCTATTTTGGTTGATACTGCTAGCAATA-3') or the same region of the protein with arginine substitutions at all lysine residues (cyc^{allR}; 5'-

AACCGGTCCGAAACCGTCGACATGTCGCATCACCATCACCATCACGGCTC
GATGGCGCTCCGAGTCACGCGTAACTCGAGAATTAATGCTGAAAATAGAGCGAGAA
TCAACATGGCAGGCGCCAGGCGCGTTCCTACGGCACCGGCGGCAACCTCCAGACCCG
GGCTGAGGCCAAGAACAGCTCTTGGGGACATTGGTAACAGAGTCAGTGAACAGCTA

CAGGCCAGAATGCCTATGAGAAGAGAAGCAAGACCTTCAGCTACCGGTAGAGTCAT
TGATAGAAGACTACCAAGACCTCTTGAAAGGGTACCTATGCTGGTGCCAGTGCCAGT
GTCTGAGCCAGTGCCAGAGCCAGAACCTGAGCCAGAACCTGAGCCTGTTAGAGAAG
AAAGACTTTCGCCTGAGCCTATTTTGGTTGATACTGCTAGCAATA-3') preceded by 6 x His tag were synthesized (GenScript). Using restriction enzyme digestion with NheI and RsrII, fragments were subcloned into pFASTBac containing the carboxy terminus (125-433 amino acids) of cyclin B1. To generate $cyc^{K64only}$, primers 5'-
TCCAGACCCGGGCTGAGGCCAAGAACAGCTCTTGGGGACATTGGTAACAGAGTCAG
TGAACAGCTACAGGCC-3' and 5' –
AATGACTCTACCGGTAGCTGAAGGTCTTGCTTCTTTTCTCATAGGCATTCTGGCCTGT
AGCTGTTCACTGAC - 3' were used for an extension reaction and the resulting fragments cloned into XmaI and AgeI cleavage sites of pFASTBac carrying full-length cyc^{allR}. Plasmids were verified by restriction enzyme mapping and sequencing. Baculoviruses were generated according to the Bac-to-Bac manual (Invitrogen). Wild-type cyclin B1 was ^{35}S-labeled in Sf9 cultures with resuspending cells (1.5 x 10^6 cells ml^{-1}) in media containing 10% SF-900 II SFM and 90% SF-900 II SFM without methionine or cysteine (both from Invitrogen) to increase radio-label uptake. Baculovirus was added to cells, along with 50 μCi of ^{35}S-labelled methionine and cysteine (NEG772; Perkin Elmer), and cyclin B1 expression was allowed for 2.5 days. CDK1 was expressed separately in Sf9 cells without radiolabeling and then combined with lysate from cells expressing cyclin B1 to allow formation of complex, which was then purified through Ni-NTA affinity and gel filtration chromatography.

CycB1-NT (1-88 amino acids of human cyclin B1) , containing an HA tag at the N terminus and a 6xHis tag at the C terminus was generated using PCR amplification with forward primer (5'-CCA GGA CCA TGG GTT ACC CAT ACG ATG TTC CAG ATT ACG CTG GCT CGA TGG CGC TCC GAG TCA CG-3') and reverse primer (5'-GGG AGC CTC GAG CTA GGG AGC GTG ATG GTG ATG GTG ATG CAT AGG TAC CTT TTC AAG AGG-3'). The

resulting PCR product was digested with NcoI and XhoI for subcloning into pET28a. Plasmids were verified by restriction enzyme mapping and sequencing. For ^{35}S labeling in *Escherichia coli*, cultures (50 ml) were grown at 37 ˚C to $D_{600\ nm}$ = 0.8, then collected by centrifugation (3,700*g* for 15 min, at 4 ^{o}C) and resuspended in modified M9 medium (50 ml final volume). After resuspension in modified M9 medium, cells were allowed to grow for additional 15 min at 37 °C before 5 mCi of Easy Tag™ L-[35S]-Methionine (NEG709A005MC; Perkin Elmer) was added. Expression was induced with 0.5 mM IPTG for 2.5 h at 37 ^{o}C. Cells were ruptured in 5 ml g^{-1} of pellet guanidine-HCl lysis buffer (pH 8.0) and lysates rotated at 24 °C until the lysate became slightly translucent; approximately 45 min. Lysates were clarified by centrifugation and cycB1-NT was purified using Ni-NTA affinity chromatography (Qiagen). Eluted protein was desalted into XB buffer (100 mM KCl, 0.1 mM $CaCl_2$, 1 mM $MgCl_2$, 10 mM HEPES, at pH 7.8 with KOH), supplemented 2% glycerol, protease inhibitors and phenylmethylsulfonyl fluoride, and stored at – 20 °C.

Maltose-binding protein (MBP)-tagged E1 was expressed in *E. coli* inducing cultures at $D_{600\ nm}$ = 0.6 with 300 μM IPTG for 5 h at room temperature. Purification was carried out using a standard MBP purification protocol. For expression of His-tagged UBCH10 and His-tagged UBC4, bacterial cultures were induced at $D_{600\ nm}$ = 0.6 at 37 ˚C with 500 μM IPTG for 4 h. The enzymes were purified through Ni-NTA affinity and gel-filtration chromatography. PET28a expressing human wild-type UBE2S was provided by M. Kirschner (Harvard Medical School, USA). Cultures were grown to $D_{600\ nm}$ = 0.4 and induced with 500 μM IPTG at 37 ˚C for 4 h. His-UBE2S was purified by Ni-NTA purification. Glutathione-*S*-transferase (GST)-fusion proteins for Rpn10 and Rad23, as well as their sub-domains, were purified essentially as reported previously (Elsasser et al., 2004; Elsasser et al., 2002). Recombinant E2-25K (UbcH1) was purchased from Boston Biochem (SP-200).

Preparation of *Xenopus* egg extract

Interphase *Xenopus* egg extract was prepared from eggs laid overnight according to the protocol of Murray (Murray, 1991) with the exception that eggs were activated with 2 μg ml^{-1} calcium ionophore (A23187, free acid form, Calbiochem) for 30 min prior to the crushing spin. Extract was frozen in liquid nitrogen and stored at -80 ºC. Interphase extract was induced to enter mitosis by addition of non-degradable cyclin B, which activates CDK1 and stimulates mitotic phosphorylation, resulting in APC/C activation. A fusion of the maltose-binding protein (MBP) to *Xenopus* cyclin B lacking its N-terminal 90 amino acids (MBP-Δ90) (Salic and King, 2005) was expressed in *E. coli* by inducing cultures at an D_{600nm}=0.6 with 300 μM isopropylthiogalactoside (IPTG) for 5 h at room temperature. Purification was carried out following New England BioLabs (NEB) protocol. To make mitotic extract, MBP- Δ90 was added to interphase extract generally at ~ 20 μg ml^{-1} and incubated at 22-24 ºC for 45-60 min.

Reconstitution of ubiquitination and degradation of cyclin B1

Ubiquitination reactions were carried out essentially as described previously (Kirkpatrick et al., 2006) for the indicated times. Briefly, for each 30 μl reaction, APC/C was immunopurified from 600 μl of mitotic *Xenopus* egg extract by incubation for 1 h at 4 °C with 12 μg of anti-Cdc27 antibodies (AF3.1, Santa Cruz Biotechnology) immobilized onto 30 μl of Affiprep Protein A beads (156-0006, Bio-Rad). Following incubation with extract, beads were washed quickly (to minimize loss of associated APC/C co-activator Cdc20) three times with XB containing 500 mM KCl (10 mM potassium HEPES, pH 7.7, 500 mM KCl, 0.1 mM $CaCl_2$, 1 mM $MgCl_2$), two times with XB same content as above, except with 100 mM KCl), and then three times with reaction buffer (20 mM Tris, pH 7.5, 100 mM KCl, 2.5 mM $MgCl_2$, 2 mM ATP). Ubiquitination reaction were carried out at 24 °C with agitation at 1500 r.p.m and contained APC/C on 30 μl beads, and 30 μl of a mix containing recombinant MBP-human E1 (1.3 μM), His-tagged UBCH10 or UBC4 (100 nM – 4 μM) as the E2 enzyme, wild-type or different forms of ubiquitin (118-145 μM), and 450-500 nM cyclin B1-CDK1 or cycB1-NT. For ubiquitin-receptor binding and degradation

assays, reaction supernatants were combined with the first 20 µl of reaction buffer wash. For analysis of cyclin B1 ubiquitination with different ubiquitins, entire reactions were processed for immunoblotting or autoragiography. Dried gels were analyzed by phosphorimaging (Bio-Rad PMI); quantification was carried out with Quantity One software (Bio-Rad).

For binding experiments with ubiquitin receptors, cyclin B1-CDK1 was pre-ubiquitinated with purified *Xenopus* APC/C, UBCH10 (3 µM), and ubiquitin (118 µM) for 90 min. Approximately 7-8 µg of "bait" protein immobilized onto Glutathione-Sepharose 4B resin (GE Healthcare) was mixed with 4 µl of pre-synthesized ubiquitin-cyclin B1 conjugates and incubated for 1 h at 4 ˚C with agitation in the presence of 100 µg ml^{-1} BSA and 0.1 % Tween 20. Supernatants were collected and mixed with the first wash to make the flow-through fraction. Beads were washed twice and diluted with SDS sample buffer to analyze the bound fraction. Equivalent amounts of input (I), flow-through (FT) and bound (B) fractions were subjected to SDS-PAGE and western blot analysis using anti-cyclin B1 polyclonal antibody (Ab-2, Neomarkers).

For degradation assays with purified proteasomes, human proteasomes (10-20 nM, concentrations as indicated), purified as reported previously (Lee et al., 2010) but non-UbVS treated, were added to cyclin B1-Ub_n in buffer (50 mM Tris-HCl (pH 7.5), 5 mM $MgCl_2$ and 5 mM ATP) (Lee et al., 2010) and incubated at 24 °C. For "0 min" time-point, substrate and proteasome mixtures were individually added to SDS sample buffer to prevent a time-lag from mixing. Aliquots withdrawn at indicated times were combined with SDS sample buffer and subjected to SDS-PAGE/immunoblot analysis using anti-cyclin B1 polyclonal antibody (Ab-2, Neomarkers).

Cyclin B1 degradation in *Xenopus* egg extract

Degradation assays with non-ubiquitinated cyclin B1 were carried out by adding ~ 200-250 nM of cyclin B1 in 40 µl reactions, with extract constituting 75-80% of the total volume. Pre-

treatment of extract with TAME or MG262 was done at 24 °C for 15 min. For assays containing no UbVS, extracts were supplemented with ubiquitin as indicated or buffer (for untreated sample) concomitantly with substrate. UbVS treatment was carried out for 30 min at 24 ˚C, with agitation (1,250 r.p.m.) before addition of ubiquitin and cyclin B1. Extracts contained 100 μg ml^{-1} of cycloheximide to prevent reincorporation of free labeled amino acid. For competition assays, unlabeled competitor was added concomitantly with radiolabelled cyclin B1 and degradation was initiated. Degradation experiments were carried out at 24 °C, with agitation. Samples for proteolysis of unlabeled cyclin B1-CDK1 were processed for anti-cyclin B1 immunoblot using anti-cyclin B1 polyclonal antibody (Ab-2, Neomarkers). In degradation assays with ^{35}S-labelled cycB1-NT, reactions (3 μl per time point) were quenched with 97 μl of 20% TCA (in H_2O), vortexed and incubated on ice ≥ 30 min before centrifugation at 14,000*g*, at 4 °C for 30 min. A fraction (50%) of sample supernatants was combined with NaOH to neutralize the acid and added to Ultima Gold scintillation fluid (6013327, Perkin Elmer). The radioactivity in the supernatant was measured by scintillation counting. Acid-soluble counts were compared to total radioactive counts and results were graphed as percent soluble radioactive counts.

For degradation of pre-ubiquitinated cycB1-NT in extract, interphase extract was pre-treated with UbVS or buffer for 30 min at 24 °C with agitation and supplemented with 100 μg ml^{-1} cycloheximide. In experiments with USP14 inhibitor IU1, IU1 or dimethylsulphoxide (DMSO) was added to extract for 15 min at 24 ˚C before addition of substrate. Where proteolysis was evaluated in the presence of unlabeled cycB1-NT, extract was mixed with unlabeled competitor and ^{35}S cycB1-NT-Ub_n concomitantly. Extract (~14 μl) was added to 4 μl of cycB1-NT-Ub_n conjugates for each time point. Degradation mixtures were incubated at 24 °C, 1250 r.p.m. for indicated times. Reactions were quenched with 107 μl of 20% TCA, vortexed and incubated on ice ≥ 30 min before centrifugation at 14,000*g*, at 4 °C for 30 min. A fraction of supernatants was combined with NaOH and Ultima Gold scintillation fluid (6013327, Perkin Elmer).

To deplete APC/C, 100 µl of interphase extract was mixed 2 µg of anti-Cdc27 antibody coupled to 5 µl of Affiprep Protein A beads and incubated at 4 °C for 3 h. APC/C depletion was confirmed by anti-Cdc27 western blot analysis. Approximately 10 µl of pre-ubiquitinated radiolabelled cyclin B1 was added to 90 µl of APC/C- depleted extract. Reactions were incubated at 22 °C for the indicated times and stopped by the addition of an equal volume of chilled 2% perchloric acid (PCA) (in H_2O) making a new final volume of 200 µl. Reactions were then incubated on ice for ≥30 min and centrifuged at 15,000 r.p.m. for 10 min, at 4 °C. A fraction of supernatants was mixed with Tris Base and Ultima Gold scintillation fluid (6013327, Perkin Elmer) and the radioactivity was measured by scintillation counting.

References

Baboshina, O. V., and Haas, A. L. (1996). Novel multiubiquitin chain linkages catalyzed by the conjugating enzymes E2EPF and RAD6 are recognized by 26 S proteasome subunit 5. J Biol Chem *271*, 2823-2831.

Boutet, S. C., Disatnik, M. H., Chan, L. S., Iori, K., and Rando, T. A. (2007). Regulation of Pax3 by proteasomal degradation of monoubiquitinated protein in skeletal muscle progenitors. Cell *130*, 349-362.

Chau, V., Tobias, J. W., Bachmair, A., Marriott, D., Ecker, D. J., Gonda, D. K., and Varshavsky, A. (1989). A multiubiquitin chain is confined to specific lysine in a targeted short-lived protein. Science *243*, 1576-1583.

Deng, L., Wang, C., Spencer, E., Yang, L., Braun, A., You, J., Slaughter, C., Pickart, C., and Chen, Z. J. (2000). Activation of the IkappaB kinase complex by TRAF6 requires a dimeric ubiquitin-conjugating enzyme complex and a unique polyubiquitin chain. Cell *103*, 351-361.

Deveraux, Q., Ustrell, V., Pickart, C., and Rechsteiner, M. (1994). A 26 S protease subunit that binds ubiquitin conjugates. J Biol Chem *269*, 7059-7061.

Dimova, N. V., Hathaway, N. A., Lee, B. H., Kirkpatrick, D. S., Berkowitz, M. L., Gygi, S. P., Finley, D., and King, R. W. (2012). APC/C-mediated multiple monoubiquitylation provides an alternative degradation signal for cyclin B1. Nat Cell Biol *14*, 168-176.

Elsasser, S., Chandler-Militello, D., Muller, B., Hanna, J., and Finley, D. (2004). Rad23 and Rpn10 serve as alternative ubiquitin receptors for the proteasome. J Biol Chem *279*, 26817-26822.

Elsasser, S., and Finley, D. (2005). Delivery of ubiquitinated substrates to protein-unfolding machines. Nat Cell Biol *7*, 742-749.

Elsasser, S., Gali, R. R., Schwickart, M., Larsen, C. N., Leggett, D. S., Muller, B., Feng, M. T., Tubing, F., Dittmar, G. A., and Finley, D. (2002). Proteasome subunit Rpn1 binds ubiquitin-like protein domains. Nat Cell Biol *4*, 725-730.

Finley, D. (2009). Recognition and processing of ubiquitin-protein conjugates by the proteasome. Annu Rev Biochem *78*, 477-513.

Finley, D., Sadis, S., Monia, B. P., Boucher, P., Ecker, D. J., Crooke, S. T., and Chau, V. (1994). Inhibition of proteolysis and cell cycle progression in a multiubiquitination-deficient yeast mutant. Mol Cell Biol *14*, 5501-5509.

Garnett, M. J., Mansfeld, J., Godwin, C., Matsusaka, T., Wu, J., Russell, P., Pines, J., and Venkitaraman, A. R. (2009). UBE2S elongates ubiquitin chains on APC/C substrates to promote mitotic exit. Nat Cell Biol *11*, 1363-1369. Epub 2009 Oct 1311.

Guterman, A., and Glickman, M. H. (2004). Complementary roles for Rpn11 and Ubp6 in deubiquitination and proteolysis by the proteasome. J Biol Chem *279*, 1729-1738.

Haglund, K., Sigismund, S., Polo, S., Szymkiewicz, I., Di Fiore, P. P., and Dikic, I. (2003). Multiple monoubiquitination of RTKs is sufficient for their endocytosis and degradation. Nat Cell Biol *5*, 461-466.

Hanna, J., Hathaway, N. A., Tone, Y., Crosas, B., Elsasser, S., Kirkpatrick, D. S., Leggett, D. S., Gygi, S. P., King, R. W., and Finley, D. (2006). Deubiquitinating enzyme Ubp6 functions noncatalytically to delay proteasomal degradation. Cell *127*, 99-111.

Harper, J. W., Burton, J. L., and Solomon, M. J. (2002). The anaphase-promoting complex: it's not just for mitosis any more. Genes Dev *16*, 2179-2206.

Hershko, A., and Heller, H. (1985). Occurrence of a polyubiquitin structure in ubiquitin-protein conjugates. Biochem Biophys Res Commun *128*, 1079-1086.

Hofmann, R. M., and Pickart, C. M. (1999). Noncanonical MMS2-encoded ubiquitin-conjugating enzyme functions in assembly of novel polyubiquitin chains for DNA repair. Cell *96*, 645-653.

Hofmann, R. M., and Pickart, C. M. (2001). In vitro assembly and recognition of Lys-63 polyubiquitin chains. J Biol Chem *276*, 27936-27943.

Huang, F., Kirkpatrick, D., Jiang, X., Gygi, S., and Sorkin, A. (2006). Differential regulation of EGF receptor internalization and degradation by multiubiquitination within the kinase domain. Mol Cell *21*, 737-748.

Isasa, M., Katz, E. J., Kim, W., Yugo, V., Gonzalez, S., Kirkpatrick, D. S., Thomson, T. M., Finley, D., Gygi, S. P., and Crosas, B. (2010). Monoubiquitination of RPN10 regulates substrate recruitment to the proteasome. Mol Cell *38*, 733-745.

Jin, L., Williamson, A., Banerjee, S., Philipp, I., and Rape, M. (2008). Mechanism of ubiquitin-chain formation by the human anaphase-promoting complex. Cell *133*, 653-665.

Kirkpatrick, D. S., Hathaway, N. A., Hanna, J., Elsasser, S., Rush, J., Finley, D., King, R. W., and Gygi, S. P. (2006). Quantitative analysis of in vitro ubiquitinated cyclin B1 reveals complex chain topology. Nat Cell Biol *8*, 700-710.

Kravtsova-Ivantsiv, Y., Cohen, S., and Ciechanover, A. (2009). Modification by single ubiquitin moieties rather than polyubiquitination is sufficient for proteasomal processing of the p105 NF-kappaB precursor. Mol Cell *33*, 496-504.

Lee, B. H., Lee, M. J., Park, S., Oh, D. C., Elsasser, S., Chen, P. C., Gartner, C., Dimova, N., Hanna, J., Gygi, S. P.*, et al.* (2010). Enhancement of proteasome activity by a small-molecule inhibitor of USP14. Nature *467*, 179-184.

Matiuhin, Y., Kirkpatrick, D. S., Ziv, I., Kim, W., Dakshinamurthy, A., Kleifeld, O., Gygi, S. P., Reis, N., and Glickman, M. H. (2008). Extraproteasomal Rpn10 restricts access of the polyubiquitin-binding protein Dsk2 to proteasome. Mol Cell *32*, 415-425.

Matsumoto, M. L., Wickliffe, K. E., Dong, K. C., Yu, C., Bosanac, I., Bustos, D., Phu, L., Kirkpatrick, D. S., Hymowitz, S. G., Rape, M.*, et al.* (2010). K11-linked polyubiquitination in cell cycle control revealed by a K11 linkage-specific antibody. Mol Cell *39*, 477-484.

Mosesson, Y., Shtiegman, K., Katz, M., Zwang, Y., Vereb, G., Szollosi, J., and Yarden, Y. (2003). Endocytosis of receptor tyrosine kinases is driven by monoubiquitylation, not polyubiquitylation. J Biol Chem *278*, 21323-21326.

Murray, A. W. (1991). Cell cycle extracts. Methods Cell Biol *36*, 581-605.

Peters, J. M. (2006). The anaphase promoting complex/cyclosome: a machine designed to destroy. Nat Rev Mol Cell Biol *7*, 644-656.

Peth, A., Uchiki, T., and Goldberg, A. L. (2010). ATP-dependent steps in the binding of ubiquitin conjugates to the 26S proteasome that commit to degradation. Mol Cell *40*, 671-681.

Petroski, M. D., and Deshaies, R. J. (2005). Mechanism of lysine 48-linked ubiquitin-chain synthesis by the cullin-RING ubiquitin-ligase complex SCF-Cdc34. Cell *123*, 1107-1120.

Pickart, C. M., and Fushman, D. (2004). Polyubiquitin chains: polymeric protein signals. Curr Opin Chem Biol *8*, 610-616.

Rao, H., and Sastry, A. (2002). Recognition of specific ubiquitin conjugates is important for the proteolytic functions of the ubiquitin-associated domain proteins Dsk2 and Rad23. J Biol Chem *277*, 11691-11695.

Riedinger, C., Boehringer, J., Trempe, J. F., Lowe, E. D., Brown, N. R., Gehring, K., Noble, M. E., Gordon, C., and Endicott, J. A. (2010). Structure of Rpn10 and its interactions with polyubiquitin chains and the proteasome subunit Rpn12. J Biol Chem *285*, 33992-34003.

Robzyk, K., Recht, J., and Osley, M. A. (2000). Rad6-dependent ubiquitination of histone H2B in yeast. Science *287*, 501-504.

Rodrigo-Brenni, M. C., and Morgan, D. O. (2007). Sequential E2s drive polyubiquitin chain assembly on APC targets. Cell *130*, 127-139.

Salic, A., and King, R. W. (2005). Identifying small molecule inhibitors of the ubiquitin-proteasome pathway in Xenopus egg extracts. Methods Enzymol *399*, 567-585.

Shang, F., Deng, G., Liu, Q., Guo, W., Haas, A. L., Crosas, B., Finley, D., and Taylor, A. (2005). Lys6-modified ubiquitin inhibits ubiquitin-dependent protein degradation. J Biol Chem *280*, 20365-20374.

Sims, J. J., Haririnia, A., Dickinson, B. C., Fushman, D., and Cohen, R. E. (2009). Avid interactions underlie the Lys63-linked polyubiquitin binding specificities observed for UBA domains. Nat Struct Mol Biol *16*, 883-889.

Skaar, J. R., and Pagano, M. (2009). Control of cell growth by the SCF and APC/C ubiquitin ligases. Curr Opin Cell Biol *21*, 816-824.

Spence, J., Gali, R. R., Dittmar, G., Sherman, F., Karin, M., and Finley, D. (2000). Cell cycle-regulated modification of the ribosome by a variant multiubiquitin chain. Cell *102*, 67-76.

Spence, J., Sadis, S., Haas, A. L., and Finley, D. (1995). A ubiquitin mutant with specific defects in DNA repair and multiubiquitination. Mol Cell Biol *15*, 1265-1273.

Terrell, J., Shih, S., Dunn, R., and Hicke, L. (1998). A function for monoubiquitination in the internalization of a G protein-coupled receptor. Mol Cell *1*, 193-202.

Thrower, J. S., Hoffman, L., Rechsteiner, M., and Pickart, C. M. (2000). Recognition of the polyubiquitin proteolytic signal. EMBO J *19*, 94-102.

Wickliffe, K. E., Lorenz, S., Wemmer, D. E., Kuriyan, J., and Rape, M. (2011). The mechanism of linkage-specific ubiquitin chain elongation by a single-subunit E2. Cell *144*, 769-781.

Williamson, A., Wickliffe, K. E., Mellone, B. G., Song, L., Karpen, G. H., and Rape, M. (2009). Identification of a physiological E2 module for the human anaphase-promoting complex. Proc Natl Acad Sci U S A *106*, 18213-18218.

Wu, T., Merbl, Y., Huo, Y., Gallop, J. L., Tzur, A., and Kirschner, M. W. (2010). UBE2S drives elongation of K11-linked ubiquitin chains by the anaphase-promoting complex. Proc Natl Acad Sci U S A *107*, 1355-1360.

Xu, P., Duong, D. M., Seyfried, N. T., Cheng, D., Xie, Y., Robert, J., Rush, J., Hochstrasser, M., Finley, D., and Peng, J. (2009). Quantitative proteomics reveals the function of unconventional ubiquitin chains in proteasomal degradation. Cell *137*, 133-145.

Yang, W. L., Wang, J., Chan, C. H., Lee, S. W., Campos, A. D., Lamothe, B., Hur, L., Grabiner, B. C., Lin, X., Darnay, B. G., and Lin, H. K. (2009). The E3 ligase TRAF6 regulates Akt ubiquitination and activation. Science *325*, 1134-1138.

You, J., Cohen, R. E., and Pickart, C. M. (1999). Construct for high-level expression and low misincorporation of lysine for arginine during expression of pET-encoded eukaryotic proteins in Escherichia coli. Biotechniques *27*, 950-954.

Chapter IV: Role of E2 enzymes in APC/C-dependent proteolysis

Nevena Dimova

Abstract

The Anaphase-Promoting Complex/Cyclosome (APC/C or APC) regulates progression through mitosis by orchestrating the ubiquitination of cell-cycle regulators such as cyclin B1 and securin. Recent reports have implicated Lys11-linked ubiquitin chains in degradation of APC/C substrates, but the Lys11 chain-forming E2 UBE2S is not essential for mitotic exit. In *Xenopus* cell-cycle extracts, conjugation of ubiquitin to multiple lysine residues of cyclin B1 provides an alternative degradation signal for cyclin B1 that does not require chain extension. Here, we evaluate the relative contribution of different E2 enzymes to APC activity and demonstrate that the chain-elongating activity of UBE2S is dispensable for cyclin degradation unless the number of ubiquitinatable lysines in cyclin B1 is restricted.

Introduction

Covalent attachment of ubiquitin to proteins controls the stability, localization or activation status of myriad cellular proteins and thereby constitutes a powerful mechanism for regulating almost all aspects of cell physiology (Behrends and Harper, 2011; Kerscher et al., 2006). Ubiquitination of substrates requires the concerted actions of an ubiquitin-activating enzyme (E1), a ubiquitin-conjugating enzyme (E2) and a ubiquitin ligase (E3) (Hershko and Ciechanover, 1998; Kerscher et al., 2006). A view emerging from recent structural and mechanistic studies invokes E2 enzymes to play an active role in determining the length and topology of ubiquitin assemblies, as well as the processivity of ubiquitination, thereby influencing the downstream fate of the substrate (Behrends and Harper, 2011; Chen and Pickart, 1990; Eddins et al., 2006; Garnett et al., 2009; Hofmann and Pickart, 1999; Petroski et al., 2007; Rodrigo-Brenni and Morgan, 2007; Wickliffe et al., 2011a; Williamson et al., 2009; Ye and Rape, 2009).

The Anaphase-Promoting Complex/Cyclosome (APC/C or APC) is a multi-subunit E3 ubiquitin ligase that initiates anaphase and mitotic exit by ubiquitinating regulatory proteins, including cyclin B1 and securin, to target them for destruction by the 26S proteasome (Barford, 2011; Harper et al., 2002; Peters, 2002; Peters, 2006). Biochemical studies in frog and clam oocytes originally showed that two different E2 enzymes, Ubc4 and UbcX, or E-2C, can independently support APC activity (Aristarkhov et al., 1996; Yu et al., 1996). In conjunction with either E2, *X. laevis* APC was found to modify cyclin B1 with ubiquitin chains linked through multiple lysine residues of ubiquitin (Lys11 and Lys63, in addition to Lys48) (Kirkpatrick et al., 2006). In this context, uniform Lys48-linked ubiquitin chains were found dispensable for binding of ubiquitinated cyclin B1 to ubiquitin-receptor proteins and robust degradation by the 26S proteasome (Kirkpatrick et al., 2006). A model emerging from more recent work challenges the view that a single E2 enzyme is sufficient to support the assembly of proteolytic tag on APC substrates and instead suggests that this process requires the sequential

action of two distinct E2 enzymes (Rodrigo-Brenni and Morgan, 2007). In metazoans, the conjugating enzyme UBE2S promotes processive Lys11-linked chain-extension after the initial monoubiquitination or short-chain formation by UBCH10 (Barford, 2011; Behrends and Harper, 2011; Garnett et al., 2009; Wickliffe et al., 2011a; Wickliffe et al., 2011b; Williamson et al., 2009; Wu et al., 2010; Ye and Rape, 2009). Consistent with this model, depletion of both UBCH10 and UBE2S causes mitotic arrest and stabilization of APC substrates (Williamson et al., 2009). While important for APC activity in *Drosophila* S2 cells (Williamson et al., 2009), UBE2S was not found to be essential for normal mitosis in human HeLa cells and is largely dispensable for timely proteolysis of cyclin B1 in this context (Garnett et al., 2009). Together these findings imply that the contribution of UBE2S and long polyubiquitin chains in the degradation of APC substrates may be organism- and condition-specific, and that there may not be a uniform requirement for UBE2S in all systems or circumstances.

Our recent study revealed that conjugation of ubiquitin to multiple lysine residues of cyclin B1 provides an alternative degradation signal for cyclin B1 that does not require chain elongation (discussed in chapter III). However, chain formation becomes essential for substrate proteolysis when the number of ubiquitination sites in cyclin B1 is restricted. Here we sought to examine whether this requirement for chain formation arises from a specific role of UBE2S or through the chain-forming activity of UBCH10.

Results

Analysis of the role of chain-elongating E2 UBE2S in cyclin B1 degradation

The ability of Ub^{11R} and chain-terminating ubiquitins to support reasonably efficient proteolysis of cyclin B1 in *Xenopus* extract raised a question as to whether the E2 enzyme UBE2S is important for APC activity in this context. To assess the role of UBE2S in cyclin B1 proteolysis, we immunodepleted the protein and measured how this affected the kinetics of cyclin degradation. Antibodies efficiently depleted the UBE2S protein, as observed by the absence of signal following 25-fold enrichment of E2 enzymes on Ub agarose (Figure 4.1a, lanes 4-6), without affecting levels of the APC/C or the E2 UBCH10. UBE2S depletion caused only a modest increase in the half-life of cycB1-NT as compared to control-depleted extract (Figure 4.1b). This effect was reversed by adding back 10 nM of the recombinant enzyme, implying that the delay was specifically due to loss of UBE2S activity.

We hypothesized that perhaps UBE2S is not essential for rapid degradation of cyclin B1 because this substrate contains multiple lysine residues that can serve as sites of attachment of short ubiquitin chains generated by UBCH10. If this hypothesis is correct, then restricting the number of available lysine residues should make degradation more dependent on UBE2S. We therefore examined the effect of UBE2S depletion on the rates of degradation of $cyc^{K64only}$ compared to that of wild-type cyclin B1 (Figure 4.1c). As we observed for cycB1-NT, the degradation of full-length wild-type cyclin B1 was largely unaffected by depletion of UBE2S (Figure 4.1c, top and bottom left panels). In contrast, the proteolysis of $cyc^{K64only}$ was highly sensitive to the depletion of UBE2S (Figure 4.1c, top and bottom right panels), and addition of recombinant UBE2S fully restored degradation. Supplementing control-depleted mitotic extract with 10 nM of recombinant UBE2S had little effect on the turnover of wild-type cyclin B1 (Figure 4.1b and 4.1c top left panel), but slightly stimulated degradation of $cyc^{K64only}$ (Figure 4.1c,

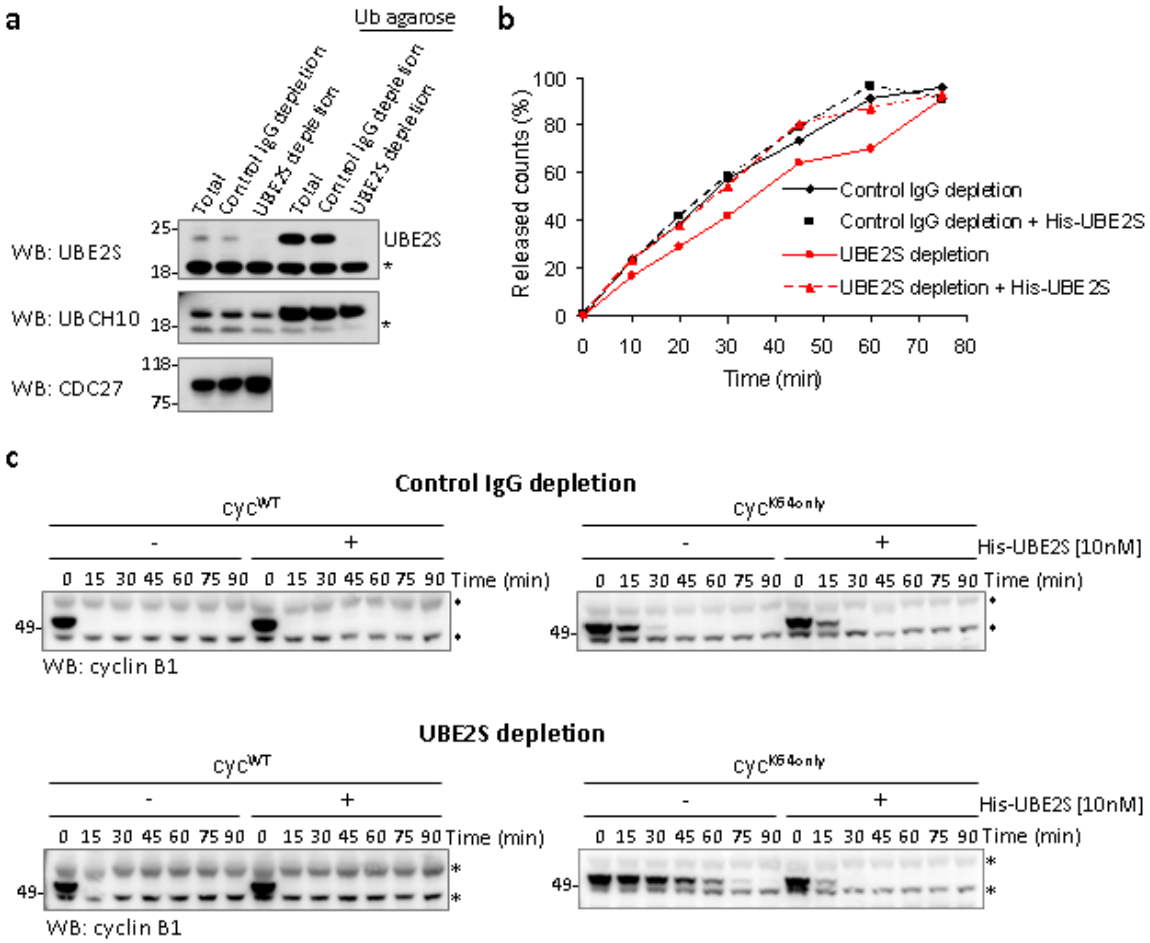

Figure 4.1 UBE2S is required for cyclin B1 proteolysis only when ubiquitination is constrained to a single lysine. (**a**) Mitotically arrested *Xenopus* extract was immunodepleted with UBE2S antibody or control IgG. Samples were further incubated with ubiquitin agarose (10:1 ratio of extract to resin) to enrich for E2 enzymes, and bound proteins were analyzed by SDS-PAGE and immunoblotting. Lanes 4-6 represent 25-fold enrichment of E2 enzymes on ubiquitin agarose. Levels of UBE2S, UBCH10 and APC/C subunit CDC27 were examined by immunoblotting. Asterisks, nonspecific signal. (**b**) Rate of degradation of ^{35}S-labeled cycB1-NT in UBE2S- or control-depleted mitotic *Xenopus* extract from **a**. Recombinant His-UBE2S (10 nM), where indicated, was added to reactions concomitantly with substrate. Proteolysis was measured by release of trichloroacetic-acid-soluble counts, and is plotted as the percentage of input radiolabeled cycB1-NT. (**c**) Time course of degradation of full-length cyclin B1 (cyc^{WT}) or single-lysine-containing mutant (cyc^{K64only}), each in complex with CDK1, in control- or UBE2S-depleted mitotic *Xenopus* extract. Recombinant His-UBE2S (10 nM), where indicated, was added to reactions concomitantly with substrate. Cyclin B1 proteolysis was analyzed by SDS-PAGE and immunoblotting. Asterisks, nonspecific signal.

top right panel). Together these findings indicate that UBE2S is indeed present in *Xenopus* extract at sufficient levels to support cyclin proteolysis, but becomes essential only when the number of ubiquitinatable lysine residues in cyclin B1 is restricted.

Role of chain-extending enzyme E2-25K in APC-mediated ubiquitination

Similarly to UBE2S, in budding yeast another ubiquitin-conjugating enzyme Ubc1 has been shown to stimulate processive ubiquitin-chain extension on APC substrates carrying pre-attached ubiquitins (Rodrigo-Brenni and Morgan, 2007). The human homolog of Ubc1, E2-25K was also found to promote higher extent of polyubiquitination when added to assays containing human APC and UBCH10. Motivated by these findings, we sought to examine whether E2-25K has any effect on the extent or pattern of cyclin ubiquitination catalyzed by *Xenopus* APC using reconstituted ubiquitination assays. Consistent with studies showing that this E2 cannot initiate conjugation, but rather elongates nascent ubiquitin chains (Rodrigo-Brenni and Morgan, 2007; Wu et al., 2010), E2-25K did not catalyze cyclin ubiquitination on its own (Figure 4.2). Unexpectedly, when E2-25K was added to the assay together with UBC4, the number of conjugated Ub molecules per cyclin remained largely unaffected (Figure 4.2; data not shown). Similarly, we found no effect of the chain-elongating activity of E2-25K when combined with UBCH10 (Figure 4.2). To rule out the possibility that the apparent lack of contribution of E2-25K resulted from competition for ubiquitin charging or binding to the APC/C, we added the proximally-acting E2s UBCH10 and UBC4 at nanomolar concentrations concomitantly with increasing the E2-25K concentration approximately tenfold to 10 μM. Under these conditions, the catalytically active E2-25K had no appreciable effect on cyclin B1 ubiquitination (data not shown).

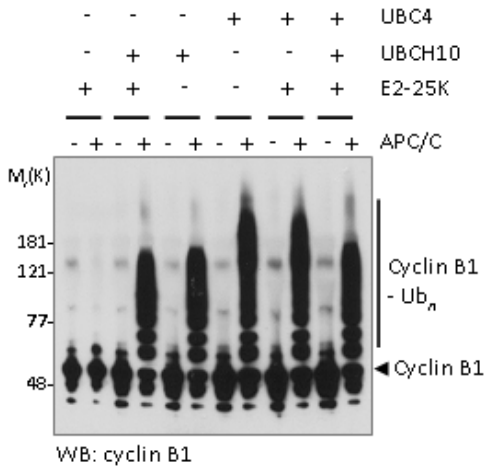

Figure 4.2 Chain-elongating enzyme E2-25K does not enhance cyclin B1 ubiquitination catalyzed by *Xenopus* APC. Western analysis of an *in vitro* ubiquitination reaction containing full-length cyclin B1, in complex with CDK1, APC/C immunopurified from mitotically arrested *Xenopus* extract, recombinant UBC4 or UBCH10 (100 nM), E2-25K (1 µM) , and wild-type ubiquitin (118 µM), as indicated. Ubiquitination was allowed to proceed for 90 min before samples were processed for SDS-PAGE and cyclin B1 western blot analysis.

Analysis of the role of UBCH10 in APC activity in *Xenopus* extract

The lack of requirement for UBE2S activity and ubiquitin-chain formation for efficient proteolysis of cyclin B1 in *Xenopus* extract suggest that UBCH10, or perhaps enzymes of the UBC4/5 family, are sufficient to support APC/C-dependent degradation in this context. We next examined how recruitment of the E2 UBCH10 contributes to the function of mitotically activated APC. To quantitatively evaluate a requirement for UBCH10-mediated ubiquitination in targeting cyclin to the proteasome, we immunodepleted the protein and measured how this affected levels of ^{35}S-labeled cycB1-NT. Antibodies efficiently depleted the UBCH10 protein, as observed by the absence of signal following 20-fold enrichment of E2 enzymes on ubiquitin agarose (Figure 4.3a). UBCH10 depletion with two different antibodies (Figure 4.3a; data not shown) caused a modest increase in the half-life of cycB1-NT as compared to control-depleted extract (Figure 4.3b), but failed to stabilize the substrate which would be expected if UBCH10 were required for substrate degradation in this context. The delay in degradation was rescued by addition of 50 nM of recombinant UBCH10. In analogous experiments, proteolysis of full-length cyclin B1-CDK1 complex was largely unaffected by depletion of UBCH10 (Figure 4.3c). In contrast with wild-type cyclin B1, depletion of UBCH10 more significantly delayed turnover of the single-lysine ($cyc^{K64only}$) cyclin B1 (Figure 4.3c), an effect reversed by the addition of 50 nM of recombinant UBCH10. The lack of requirement for UBCH10 in cyclin B1 degradation indicates that other E2 enzymes in the extract may be sufficient to prime APC molecules for substrate ubiquitination. Members of the UBC4/5 family, which have been demonstrated to cooperate with the APC *in vitro* (Garnett et al., 2009; Kirkpatrick et al., 2006; Mathe et al., 2004; Summers et al., 2008; Yu et al., 1996; Zeng et al., 2010), are the best candidates for such a role. We therefore sought to examine the role of this class of E2s in cyclin B1 destruction.

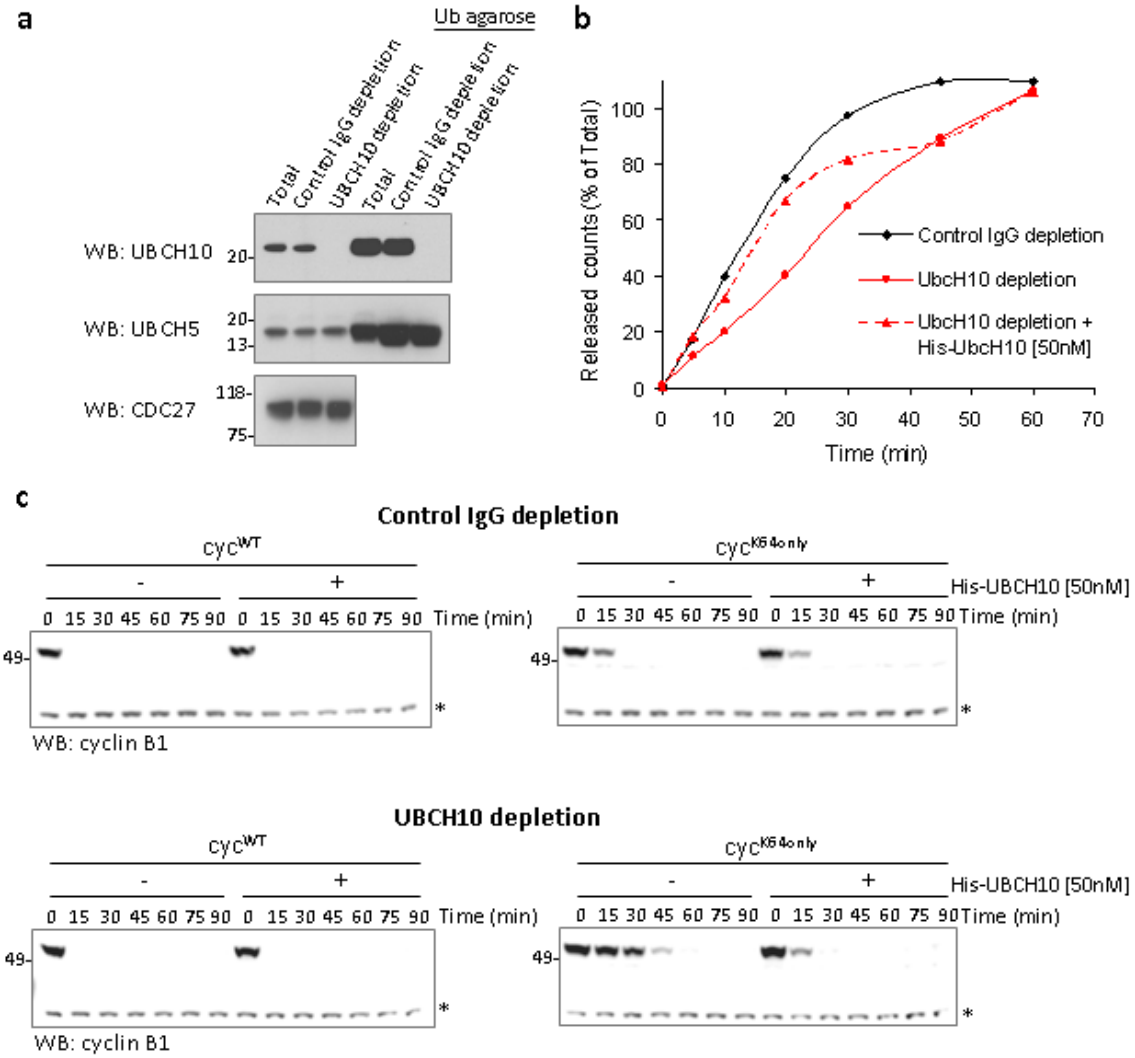

Figure 4.3 Depletion of UBCH10 more significantly delays cyclin B1 degradation when ubiquitination is limited to a single lysine residue. (**a**) Mitotically arrested *Xenopus* extract was immunodepleted with UBCH10 antibody or control IgG. Samples were further incubated with Ub agarose to enrich for E2 enzymes. Samples were separated by SDS-PAGE and analyzed by western blot against UBCH10, UBCH5 and the APC/C subunit CDC27. Lanes 4-6 represent 20-fold enrichment of E2 enzymes on Ub agarose. (**b**) Rate of degradation of ^{35}S-labeled cycB1-NT in UBCH10- or control-depleted mitotic *Xenopus* extract from **a**. Recombinant His-UBCH10 (50 nM), where indicated, was added to reactions concomitantly with substrate. Proteolysis was measured by release of TCA soluble counts, and is plotted as percentage of input radiolabeled cycB1-NT. (**c**) Time-course of degradation of full-length wild-type cyclin B1 (cyc^{WT}) or single lysine-containing mutant (cyc^{K64only}), each in complex with CDK1, in control- or UBCH10-depleted mitotically-arrested *Xenopus* extract. Recombinant His-UBCH10 (50 nM), where indicated, was added to reactions concomitantly with substrate. Cyclin B1 proteolysis was analyzed by SDS-PAGE and cyclin B1 immunoblotting. Asterisks, nonspecific signal.

UBC4 cooperates with the APC to assemble an efficient proteolytic signal on cyclin B1

To evaluate a potential role for enzymes from the UBC4/5 class in cyclin B1 degradation, we assessed whether effects of different ubiquitin mutants on proteolysis in *Xenopus* extract (discussed in chapter III) paralleled their effects on UBC4-catalyzed conjugation in a reconstituted system. Elimination of Lys11 or 63 of ubiquitin had no effect on the overall pattern or extent of substrate ubiquitination, whereas elimination of Lys48 slightly reduced the mass of conjugates, consistent with the preference of UBC4 for forming Lys48 linkages (Kirkpatrick et al., 2006) (Figure 4.4a). In the presence of chain-terminating ubiquitin types such as methylated ubiquitin and Ub^{triR} (ubiquitin containing lysine-to-arginine substitutions at all three sites Lys11, 48 and 63 simultaneously), UBC4, similarly to UBCH10 (discussed in chapter III), was capable of appending ubiquitin monomers to distinct lysine residues on cyclin. The maximal extent of ubiquitination achieved with UBC4 under these conditions appeared higher relative to that seen with UBCH10 (Figure 4.4a; data shown in chapter III). Together these findings indicate that UBC4 can facilitate ubiquitination on more cyclin B1 lysine residues than UBCH10, consistent with previous work (Garnett et al., 2009; Kirkpatrick et al., 2006).

Ubiquitin assemblies elaborated by UBC4 in the presence of wild-type ubiquitin were recognized by proteasome-associated ubiquitin receptors (Deveraux et al., 1994; Elsasser et al., 2004; Elsasser and Finley, 2005; Finley, 2009; Isasa et al., 2010; Matiuhin et al., 2008; Peth et al., 2010; Rao and Sastry, 2002; Riedinger et al., 2010) including Rpn10 (Figure 4.4b) and Rad23 (Figure 4.4d), consistent with previous findings (Kirkpatrick et al., 2006). Importantly, multiply monoubiquitinated substrate was also capable of binding to both receptors. For conjugates of a similar molecular mass, substrate ubiquitinated with Ub^{triR} bound to receptors more efficiently than substrate ubiquitinated with Ub^{me}, a difference more pronounced in binding to Rad23. In contrast to species bearing a higher number of ubiquitin groups, unmodified and oligoubiquitinated cyclin B1 had much lower affinity for ubiquitin receptors. As observed

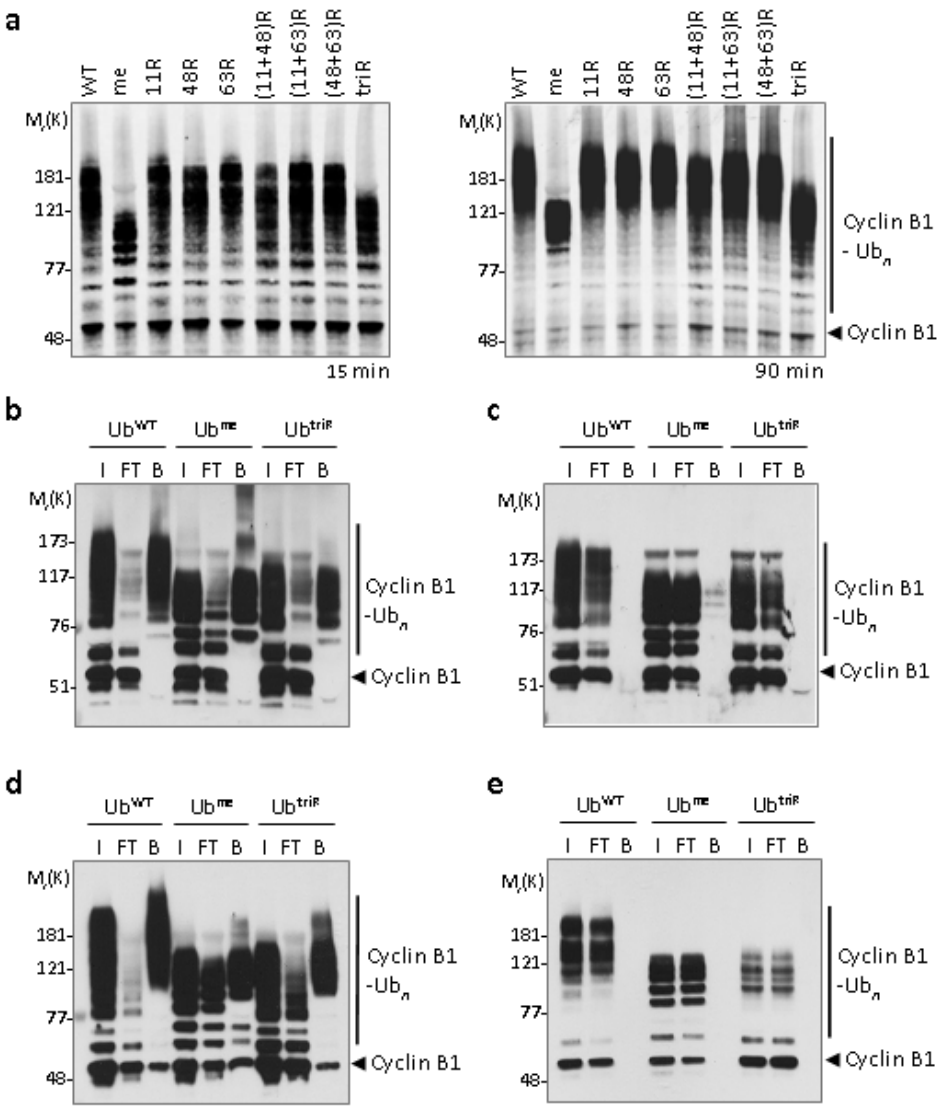

Figure 4.4 UBC4 and APC/C catalyze multiple monoubiquitination of cyclin B1 that is sufficient for binding ubiquitin receptors. (**a**) Western blot analysis of an *in vitro* ubiquitination reaction containing full-length cyclin B1, APC/C immunopurified from mitotically arrested *Xenopus* extract, recombinant UBC4 (66 μg ml^{-1}), and forms of ubiquitin (118 μM), as indicated. Ubiquitin types with lysine-to-arginine mutations at indicated one, two or at all three positions simultaneously Lys11, 48 and 63 (Ub^{triR}), as well as methylated ubiquitin (Ub^{me}) were used. Reactions were allowed to proceed for 15 or 90 min before analysis by SDS-PAGE and western blotting against cyclin B1. (**b-e**) Binding of ubiquitinated cyclin B1 to GST-tagged ubiquitin receptors. Cyclin B1-ubiquitin conjugates were incubated with immobilized receptor proteins for 1 h at 4 °C before reaction products were subjected to SDS-PAGE and western blot analysis against cyclin B1. Equivalent amounts of input (I), flow-through (FT) and bound (B) fractions were loaded in adjacent lanes. Binding experiments with wild-type Rpn10 (**b**) and Rad23 (**d**). Binding with corresponding versions of the receptors lacking the ubiquitin-recognition domains, with engineered block substitution of the UIM domain (LAMAL → NNNNN) of Rpn10 (**c**) or deletion of the ubiquitin-associated domains of Rad 23 (**e**).

previously (data shown in chapter III) (Kirkpatrick et al., 2006), all binding was dependent on the integrity of the receptor domains recognizing ubiquitin (Figure 4.4c, e).

Since UBC4 mediated transfer of monoubiquitin to multiple substrate residues and generated a ubiquitin signal that was recognized by ubiquitin receptors, we sought to determine whether multiple monoubiquitination catalyzed by UBC4 can target cyclin B1 for degradation. To this end, full-length cyclin B1-CDK1 complex was ubiquitinated with UBC4, in conjunction with wild-type or chain-terminating ubiquitin. The resulting species were incubated with human proteasomes, purified as reported previously (Lee et al., 2010) and containing the deubiquitinating enzymes RPN11 and UCH37, but no USP14. The deubiquitinase USP14 was previously shown to attenuate the capacity of the proteasome to rapidly degrade cyclin-ubiquitin species *in vitro*, presumably by trimming poly-ubiquitin chains assembled on substrate residues (Hanna et al., 2006; Lee et al., 2010). In agreement with previous findings (Crosas et al., 2006; Hanna et al., 2006; Lee et al., 2010), these USP14-deficient proteasomes rapidly degraded cyclin B1 that was polyubiquitinated by UBC4-APC (Figure 4.5a). While conjugates formed with Ub^{triR} or lysine-less ubiquitin (Ub^{K0}) were also degraded rapidly, those generated with methylated ubiquitin (Ub^{me}) were degraded more slowly. This observation parallels the effects of these mutant ubiquitins in *Xenopus* extract (discussed in chapter III) and is consistent with the defect in the ability of cyclin B1-Ub^{me} to bind ubiquitin receptors (Figure 4.4b, d). We previously quantitated the extent of substrate proteolysis using ^{35}S-labeled full-length cyclin B1 and found that it closely correlated with the percentage of cyclin B1 modified with three or more ubiquitin moieties (data not shown). Together these results indicate that purified proteasomes do not impose a requirement for long ubiquitin polymers and can efficiently degrade multiply monoubiquitinated cyclin B1.

We extended the analysis of these multiply monoubiquitinated species by measuring their degradation under conditions where different ubiquitin receptors, deubiquitinating enzymes and the proteolytic machinery are present at physiological concentrations. To this end, we added

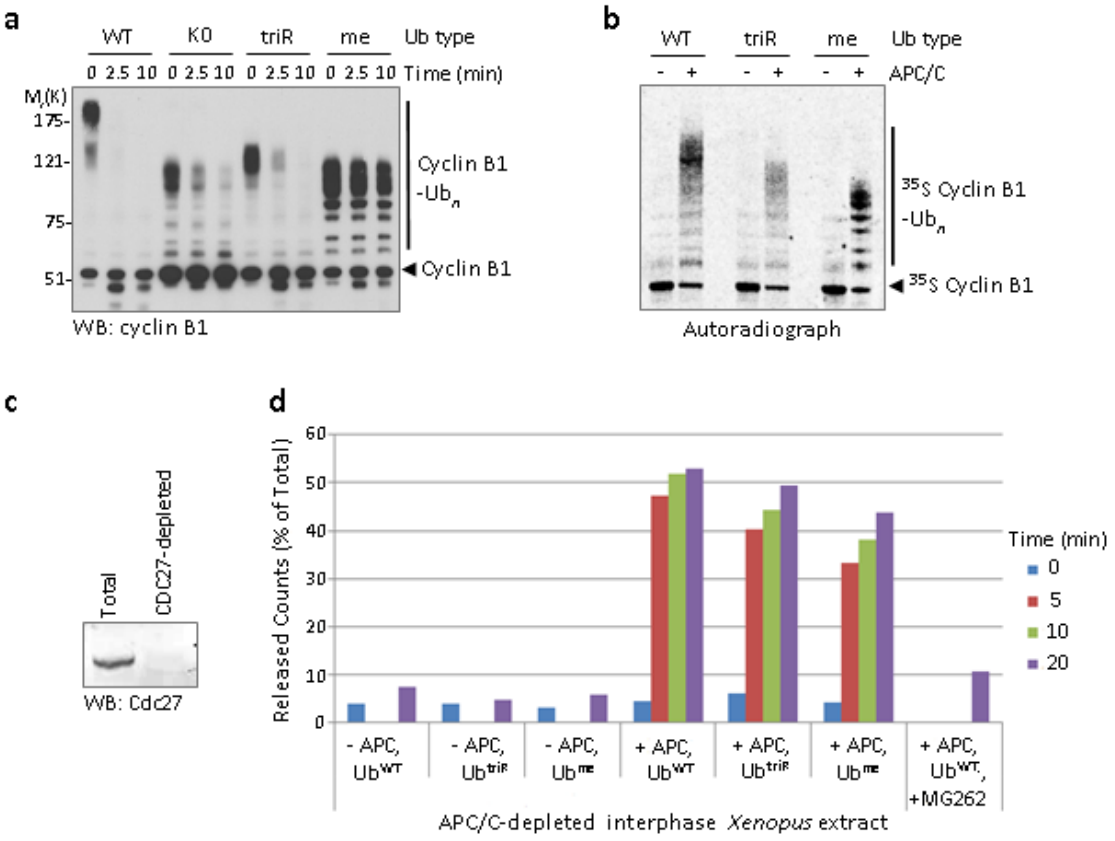

Figure 4.5 Cyclin B1 multiply monoubiquitinated by UBC4 and APC/C is rapidly degraded by purified proteasomes and in *Xenopus* extract. (**a**) *In vitro* degradation assay with cyclin B1-ubiquitin species generated with *Xenopus* APC/C immunopurified from mitotically arrested extract, recombinant UBC4 (250 nM) and forms of ubiquitin (145 µM), as indicated, and USP14-deficient human proteasomes (20 nM). WT, wild-type; K0, lysine-less; triR, lysine-to-arginine mutations at all three positions Lys 11, 48 and 63; me, methylated ubiquitin. Aliquots were removed at the indicated times and reaction products analyzed by SDS-PAGE and anti-cyclin B1 western blot analysis. (**b**) Autoradiograph of *in vitro* APC/C- and UBC4-catalyzed ubiquitination of ^{35}S-labeled full-length cyclin B1 with immunopurified *Xenopus* APC/C, recombinant UBC4 (4 µM), and forms of ubiquitin (145 µM) as indicated. Products from a 90-min ubiquitination assay were separated by SDS-PAGE and analyzed using a phosphorimager. (**c**) Interphase *Xenopus* extract was depleted of APC/C, as seen by western blot against the APC/C subunit CDC27, before cyclin B1-ubiquitin conjugates were introduced. (**d**) Samples from **b** were introduced into APC/C-depleted interphase *Xenopus* extract for the indicated times, following which a perchloric acid (PCA) precipitation was done. Pre-treatment of extract with proteasome inhibitor MG262 (200 µM) was used as control at the 20 min time-point. Proteolysis was measured by release of PCA soluble counts, and is plotted as percentage of input radiolabeled cyclin B1 protein.

radiolabeled full-length cyclin B1 pre-ubiquitinated by UBC4 (Figure 4.5b) to interphase *Xenopus* extract that had been immunodepleted of the APC (Figure 4.5c). The extent and kinetics of degradation of species formed with Ub^{triR} were very similar to those for conjugates formed with wild-type ubiquitin. Conjugates generated with Ub^{me} were degraded slightly less efficiently. Together these results further support the view that *Xenopus* extracts can rapidly degrade a cyclin substrate bearing multiple ubiquitin groups attached to distinct lysine residues even when deubiquitination is not inhibited.

Role of UBC4/5 enzymes in cyclin B1 degradation in *Xenopus* extract

The modest stabilization of cyclin B1 observed in UBCH10-depleted extracts (Figure 4.3b) raises the possibility that additional E2 enzymes may support APC catalysis in this context. Based on this and previous work (Hanna et al., 2006; Kirkpatrick et al., 2006; Lee et al., 2010), members of the UBC4/5 class appear to be the best candidates for such a role. We sought to deplete the extract of these enzymes and assess the effect on cyclin degradation. To this end, we screened five different commercially available antibodies against UBC4/5. Despite extensive optimization of assay conditions, we were unable to achieve significant depletion of UBC4/5 in order to evaluate their role in cyclin proteolysis. We therefore took an alternative approach in addressing this question. Using ubiquitin covalently coupled to agarose beads via primary amines allowing for a fully functional C-terminus, we attempted to deplete the extract of proteins that have an affinity for ubiquitin, including ubiquitin-activating enzyme (E1), ubiquitin-conjugating enzymes (E2s), ubiquitin ligases (E3s) and ubiquitin C-terminal hydrolases (UCHs). Unlike immunodepletion experiments which address necessity, ubiquitin-agarose depletions have the potential to reveal sufficiency of particular E2 enzymes in cyclin degradation.

To quantitatively assess the effect of depleting the enzymatic machinery that targets cyclin B1 for degradation in mitotic *Xenopus* extracts, we measured the proteolysis of a purified, ^{35}S-labeled cycB1-NT. In parallel, we examined the levels of UBC4/5, UBCH10 and UBE2S enzymes, as well as the APC, by western analysis. Interestingly, even trace levels of different E2 enzymes known to work in conjunction with the APC (Aristarkhov et al., 1996; Jin et al., 2008; King et al., 1995; Mathe et al., 2004; Rodrigo-Brenni and Morgan, 2007; Townsley et al., 1997; Williamson et al., 2009; Yu et al., 1996) were sufficient to support cyclin proteolysis. We found that while four rounds of incubation with ubiquitin agarose led to significant depletion of UBC4/5 and UBCH10, as observed by western blotting (Figure 4.6a), cycB1-NT degradation remained largely unaffected (data not shown). Increasing the rounds of ubiquitin-agarose depletion to six rendered the extract incapable of promoting cyclin degradation (Figure 4.6b), consistent with complete depletion of E2 enzymes (Figure 4.6a). To rescue proteolysis in depleted extracts, recombinant E1, ubiquitin, ATP and the E2 enzyme of interest were added back. Addition of ubiquitin-activating enzyme (E1) and ubiquitin alone did not restore degradation, indicating that the relevant E2 machinery had been depleted below the threshold required to support proteolysis (Figure 4.6b). We found that supplementing the depleted extract with 100 nM (data not shown) or 250 nM (Figure 4.6b) of recombinant UBC4 partially rescued proteolysis. Similar trends were observed even when the concentration of recombinant UBC4 was increased to 3 μM (data not shown). In contrast, under these conditions, addition of 250 nM of recombinant UBCH10 restored degradation to levels observed in undepleted extract (Figure 4.6b). Together these findings imply that another member of the UBC4/5 family may be a preferred E2 partner of the APC in *Xenopus* egg extract. Future experiments are required to determine whether other members of the UBC4/5 family may be more efficient at priming APC substrates for proteasomal degradation.

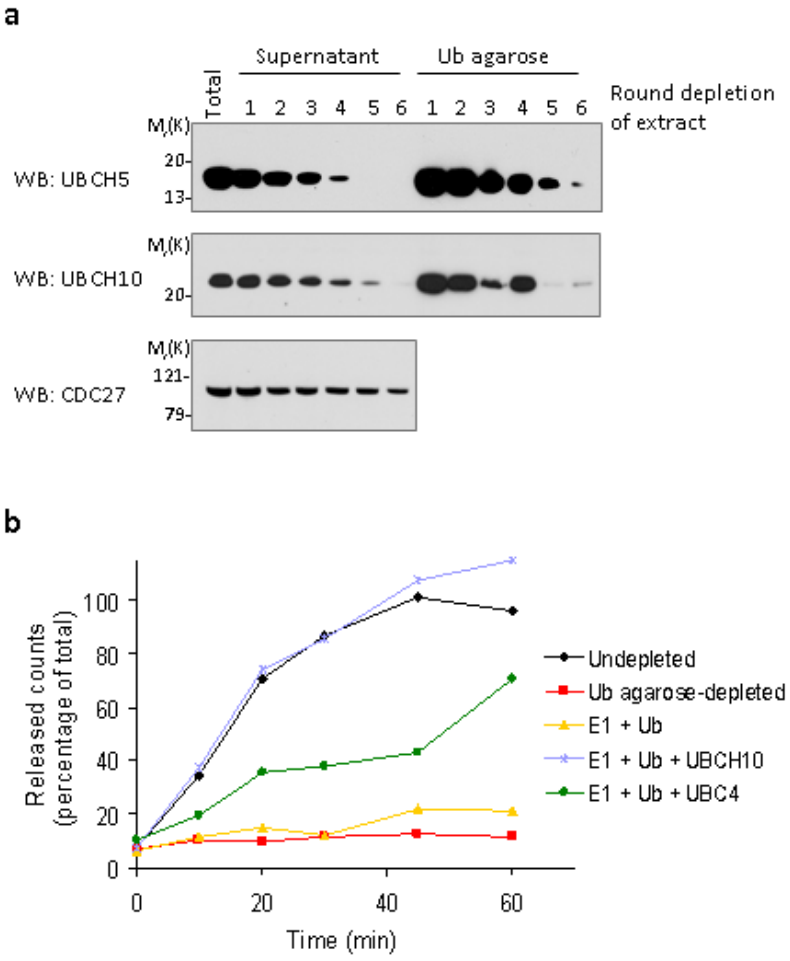

Figure 4.6 UBC4 partially rescues cyclin B1 degradation in *Xenopus* extract that is depleted of E2 enzymes. (**a**) Mitotically-arrested *Xenopus* extract was incubated with ubiquitin that is covalently coupled to agarose beads (Ub agarose) for number of rounds as indicated to allow depletion of E2 enzymes promoting cyclin B1 ubiquitination and degradation. Aliquots were removed after the indicated number of rounds of depletion and levels of UBCH5, UBCH10 and the APC/C subunit CDC27 analyzed by SDS-PAGE and immunoblotting. Factors bound to Ub agarose were eluted by boiling in SDS sample buffer and analyzed in parallel. (**b**) Rate of degradation of ^{35}S-labeled cycB1-NT in mitotic *Xenopus* extract , that is undepleted or subjected to six rounds of E2 depletion with Ub agarose prior to substrate addition. Recombinant E1, wild-type ubiquitin, ATP and E2 enzymes, as indicated, were added back to Ub agarose-depleted extract, concomitantly with substrate. Proteolysis was measured by release of TCA soluble counts, and is plotted as percentage of input radiolabeled cycB1-NT.

Discussion

Here we have evaluated the role of E2 enzymes in supporting APC activity in *Xenopus* cell-cycle extracts. Our study was motivated by recent reports suggesting that the assembly of Lys11-linked ubiquitin chains, mediated by the E2 enzyme UBE2S, may be essential for APC-dependent proteolysis. However, we found that the proteolytic machinery in *Xenopus* extract and in the reconstituted system does not impose a requirement for chain formation to efficiently degrade ubiquitinated cyclin and that the elaboration of Lys11-linked chains becomes essential only when the number of ubiquitinatable residues in cyclin B1 is restricted. Here we provide evidence that the chain-forming E2 UBE2S is dispensable for cyclin proteolysis, unless the number of available lysine residues in cyclin B1 is restricted, and evaluate how proximally-acting E2s UBCH10 and UBC4 may promote substrate degradation.

Our previous work revealed that chain-terminating ubiquitins support efficient proteolysis of cyclin B1 in *Xenopus* extracts (discussed in chapter III). Utilizing a reconstituted system, we demonstrated that multiply monoubiquitinated species generated with either UBCH10 or UBC4 are efficiently degraded by purified proteasomes. These findings raise the possibility that through conjugation of monoubiquitin to distinct lysines in cyclin, and possibly the elaboration of short chains, either of these E2 may promote APC-dependent proteolysis of cyclin B1 in *Xenopus* extracts. Consistent with such a model, UBCH10 supported robust APC catalysis when added to ubiquitin-agarose depleted extract. Interestingly, the importance of UBCH10 in substrate degradation appears to increase with elimination of available ubiquitin-acceptor sites in cyclin B1. Nevertheless, the effects seen upon UBCH10 depletion were not very dramatic. These findings were surprising in the light of a previous report showing that an N-terminal fragment of human cyclin B1 is stabilized upon UBCH10 depletion, arguing that UBCH10 is required for cyclin proteolysis in *Xenopus* extract (Tang et al., 2001). An important question the authors did not address, which may provide an explanation for these findings, was whether the antibody

efficiently and specifically depleted the UBCH10 protein, without affecting the levels of E2 enzymes from the UBC4/5 family. As the core ubiquitin-conjugating (UBC) domains of these E2s share a high degree of sequence homology (Osaka et al., 1997; Summers et al., 2008; Ye and Rape, 2009), it may be non-trivial to avoid unintended co-depletion.

Evidence from simpler model organisms indicates that E-2C family members are most likely to be biologically relevant as E2 partners of the APC (Mathe et al., 2004; Osaka et al., 1997). These models do not rule out the possibility that members of the UBC4/5 family, or possibly other E2s, influence APC -dependent proteolysis in *Xenopus* extracts. Our earlier work suggested that APC, solely in conjunction with the E2 UBC4, can generate polyubiquitinated cyclin B1 that is rapidly degraded by purified proteasomes (Crosas et al., 2006; Hanna et al., 2006; Kirkpatrick et al., 2006; Lee et al., 2010). These findings, together with the lack of substrate stabilization in UBCH10-depleted extract, led us to investigate a potential contribution of UBC4/5 to cyclin proteolysis in this system. Furthermore, we sought to determine whether UBCH10 and UBC4/5 enzymes are functionally redundant in creating multiple monoubiquitination sufficient for cyclin proteolysis.

Utilizing a reconstituted system, we demonstrated that UBC4 can catalyze transfer of ubiquitin monomers to multiple lysine residues in cyclin, consistent with previous studies (Garnett et al., 2009; Kirkpatrick et al., 2005). Experiments with chain-terminating ubiquitin revealed higher number of substrate monoubiquitination sites in reactions catalyzed by UBC4, as compared to UBCH10 (discussed in chapter III). An interesting question is whether this more extensive multiple monoubiquitination and the apparent lower threshold of modification required for binding at least some ubiquitin receptors translates into more efficient degradation of UBC4-generated cyclin B1-Ub_n by the proteasome. Quantitative analysis of degradation with purified proteasomes (discussed in chapter III) revealed no such enhanced rate, or extent, of degradation of UBC4-generated conjugates. The capacity of purified proteasomes to rapidly degrade multiply monoubiquitinated species generated with either UBC4 or UBCH10 (data shown in chapter III)

further strengthens our proposition that the proteasome does not impose a requirement for ubiquitin-chain formation for efficient proteolysis of cyclin B1.

Unlike the E-2C enzymes, members of the UBC4/5 class have been regarded as promiscuous E2s (Summers et al., 2008; Ye and Rape, 2009) with no essential role in APC - mediated catalysis. Consistent with this view, Summers and colleagues found that addition of UBCH10, but not UBCH5 (a member of the UBC4/5 family), to extracts from nocodaloze-arrested HeLa cells was required and sufficient to activate the APC and mediate destruction of securin and cyclin B1 (Summers et al., 2008). However, the simultaneous addition of excess ubiquitin allowed UBCH5 to catalyze destruction of APC substrates in this context, presumably by increasing the levels of ubiquitin-charged UBCH5 above the threshold required to stimulate APC activity (Summers et al., 2008). Due to technical limitations, we were unable to immunodeplete UBC4/5 and investigate potential functional redundancy between UBCH10 and UBC4/5 enzymes, explaining the partial effects in UBCH10-depleted extracts. Utilizing the ubiquitin-agarose depletion strategy, we examined whether UBC4/5 enzymatic activity supports cyclin proteolysis. Strikingly, E2s from the UBC4/5 and E-2C families had to be completely depleted in order to abolish substrate turnover in *Xenopus* extract. The incomplete rescue achieved with UBC4 under these conditions may imply that another member of the UBC4/5 class is a preferred APC partner. A limitation of the ubiquitin-agarose depletion approach is that multiple factors, which may impact substrate proteolysis directly or indirectly, become depleted (as revealed by mass spectrometry analysis) making it difficult to ascertain the contribution of UBC4/5 enzymes. It is possible that following multiple rounds of depletion, the extracts become deficient of components, such as ubiquitin receptors, which may be important for UBC4/5-driven pathways.

Recent studies have proposed that the Lys11-specific chain-elongating E2 UBE2S has a critical role in the efficient ubiquitination and degradation of APC substrates in *Xenopus*, *Drosophila*, and humans (Williamson et al., 2009; Wu et al., 2010). We found that UBE2S

depletion of *Xenopus* egg extract had no impact on degradation of wild-type cyclin B1, but significantly slowed substrate proteolysis when ubiquitination was restricted to a single site. These trends closely paralleled the effects of adding chain-terminating ubiquitins to UbVS-treated *Xenopus* extract (discussed in chapter III). Our findings are consistent with a report suggesting that UBE2S is largely dispensable for cyclin B1 degradation in normal mitosis in human HeLa cells (Garnett et al., 2009). In contrast, UBE2S was found to be more important for substrate degradation when APC activity is compromised as upon activation of the spindle assembly-checkpoint (Garnett et al., 2009). The lack of requirement for UBE2S activity and long Lys11-linked ubiquitin chains for robust degradation of cyclin B1 in *Xenopus* extracts may be a consequence of higher levels of active UBCH10 and APC than seen in other biological contexts (Garnett et al., 2009; Williamson et al., 2009), as well as the availability of multiple lysine residues in cyclin B1 that can serve as ubiquitin acceptor sites. Our observations favor the idea that the increased importance of UBE2S seen with limiting the number of ubiquitination sites reflects the ability of this E2 to extend long polymers with high processivity rather than a major degradative role of Lys11 linkages it forms. In this context, UBCH10 or UBC4/5 enzymes appear to be less efficient in rapidly elongating individual ubiquitin chains that would facilitate proteasomal recognition and substrate breakdown. We anticipate that the relative contribution of UBCH10 and UBE2S in degradation of different APC substrates may vary. Human cyclin B1 is lysine-rich in its N-terminal domain, containing 18 lysine residues, whereas cyclin A2 has 12 lysine residues in the same region, which may make the latter protein more dependent on the chain-elongating enzyme UBE2S for degradation. Similarly, *S. cerevisiae* Clb2 is relatively lysine-poor in its N-terminal domain, containing only 6 lysine residues, potentially explaining the importance of a chain-elongating E2 in this system (Rodrigo-Brenni and Morgan, 2007). A greater dependence on chain-elongating E2s may impact the sensitivity of different substrates to deubiquitination. In this regard, cyclin A2 degradation during interphase is specifically impeded by the deubiquitinating enzyme USP37 (Huang et al., 2011), but this enzyme does not appear to

antagonize cyclin B1 degradation. An interesting future question is how the balance between multiple monoubiquitination and ubiquitin-chain formation affects sensitivity of degradation to deubiquitinating enzymes. Finally, our work raises the interesting possibility that the degree of dependence on UBE2S could be regulated by post-translational modification of the substrate. For example, acetylation is known to affect degradation of the spindle-checkpoint protein BubR1 (Choi et al., 2009). By restricting the number of ubiquitinatable lysine residues, acetylation could increase the dependence of degradation pathways on UBE2S-catalyzed chain formation.

Methods

Antibodies and biochemical reagents

Proteins were separated by SDS-PAGE on NuPAGE 4-12% or 12% Bis-Tris gels (Invitrogen), followed by wet transfer to PVDF. Sources of antibodies for immunoblotting were as follows: anti-cyclin B1 (Ab-2; RB-008-P, Neomarkers), anti-Cdc27 (610455, BD Transduction Laboratories), anti-UBCH10 (A-650, Boston Biochem; AB3861, Millipore), anti-UBE2S (N-14; sc-131354, Santa Cruz Biotechnology), anti-UBCH5 (A-615; Boston Biochem), anti-ubiquitin (P4D1; sc-8017; Santa Cruz Biotechnology). Secondary antibodies used include anti-goat IgG-HRP (sc-2020; Santa Cruz Biotechnology), anti-rabbit IgG-HRP (NA934; GE Healthcare), and anti-mouse IgG-HRP (NA931; GE Healthcare). Antibodies for immunoprecipitation or immunodepletion included: anti-Cdc27 (AF3.1; sc-9972, Santa Cruz Biotechnology), anti-UBE2S (N-14; sc-131354, Santa Cruz Biotechnology), anti-UBCH10 (gift from H. Yu, UT Southwestern, USA); and for control depletions, normal rabbit IgG (sc-2027, Santa Cruz Biotechnology) and normal goat IgG (sc-2028, Santa Cruz Biotechnology) were used. UBE2S antibodies were coupled to UltraLink immobilized protein A/G beads (53132, Pierce). UBCH10 and CDC27 antibodies were coupled to Affiprep protein A beads (156-0006, Bio-Rad). Ubiquitin agarose (U-405), MG262 (I-120), Ub^{me} and ubiquitin mutants except for $Ub^{(11+48)R}$, $Ub^{(11+63)R}$ and Ub^{triR} were purchased from Boston Biochem. Ubiquitin (U6253) were purchased from Sigma.

Preparation of recombinant proteins

Ubiquitin mutants $Ub^{(11+48)R}$, $Ub^{(11+63)R}$ and $Ub^{(11+48+63)R}$ (referred to as Ub^{triR}) were generated by introducing arginine codons (AGA, AGG) at the indicated sites through PCR-mediated mutagenesis of the human ubiquitin sequence (cloned in pET3a with ampicillin resistance, the kind gift of C.M. Pickart). Plasmids were verified by sequencing and the purified proteins analyzed by mass spectrometry. To ensure efficient arginine incorporation, BL21 (DE3) cells were co-transformed with pJY2, developed by Pickart lab (You et al., 1999), which carries

T7 lysozyme (LysS) and a gene encoding $tRNA_{UCU}^{Arg}$. Cultures were grown at 37 °C to an attenuance (*D*) of ~ 0.5 at 600 nm, and induced with 100 μM isopropylthiogalactoside (IPTG) at $D_{600\,nm}$ = 0.6 at 25 ˚C for 5 h. Cells were ruptured by sonication in QA lysis buffer (50 mM HEPES (pH 7.7), 100 mM KCl, protease-inhibitor cocktail, 5 mM 2-mercaptoethanol, 10 μg ml^{-1} DNase). Lysozyme was added to 1 mg ml^{-1} concentration and lysate was incubated with rotation at 4 °C for 15 min. Following sonication, cell lysates were clarified by centrifugation and the resulting supernatants applied to a Q column. The flow-through containing ubiquitin was concentrated and purified by size-exclusion chromatography. Fractions containing ubiquitin were typically > 95% pure.

To generate full-length cyclin B1-CDK1 complex, human cyclin B1 and CDK1 baculoviruses were used as described previously (Kirkpatrick et al., 2006). To generate mutants of cyclin B1, DNA fragments encoding the N-terminal 124 amino acids of wild-type human cyclin B1 (5′-

AACCGGTCCGAAACCGTCGACATGTCGCATCACCATCACCATCACGGCTC

GATGGCGCTCCGAGTCACGCGTAACTCGAAAATTAATGCTGAAAATAAAGCGAAAA

TCAACATGGCAGGCGCCAAGCGCGTTCCTACGGCACCGGCGGCAACCTCCAAACCCG

GGCTGAGGCCAAGAACAGCTCTTGGGGACATTGGTAACAAAGTCAGTGAACAGCTA

CAGGCCAAAATGCCTATGAAAAAAGAAGCAAAACCTTCAGCTACCGGTAAAGTCAT

TGATAAAAAACTACCAAAACCTCTTGAAAAGGTACCTATGCTGGTGCCAGTGCCAGT

GTCTGAGCCAGTGCCAGAGCCAGAACCTGAGCCAGAACCTGAGCCTGTTAAAGAAG

AAAAACTTTCGCCTGAGCCTATTTTGGTTGATACTGCTAGCAATA-3′) or the same region of the protein with arginine substitutions at all lysine residues (cyc^{allR}; 5′-

AACCGGTCCGAAACCGTCGACATGTCGCATCACCATCACCATCACGGCTC

GATGGCGCTCCGAGTCACGCGTAACTCGAGAATTAATGCTGAAAATAGAGCGAGAA

TCAACATGGCAGGCGCCAGGCGCGTTCCTACGGCACCGGCGGCAACCTCCAGACCCG

GGCTGAGGCCAAGAACAGCTCTTGGGGACATTGGTAACAGAGTCAGTGAACAGCTA
CAGGCCAGAATGCCTATGAGAAGAGAAGCAAGACCTTCAGCTACCGGTAGAGTCAT
TGATAGAAGACTACCAAGACCTCTTGAAAGGGTACCTATGCTGGTGCCAGTGCCAGT
GTCTGAGCCAGTGCCAGAGCCAGAACCTGAGCCAGAACCTGAGCCTGTTAGAGAAG
AAAGACTTTCGCCTGAGCCTATTTTGGTTGATACTGCTAGCAATA-3′) preceded by 6 x His tag were synthesized (GenScript). Using restriction enzyme digestion with NheI and RsrII, fragments were subcloned into pFASTBac containing the carboxy terminus (125-433 amino acids) of cyclin B1. To generate $cyc^{K64only}$, primers 5'-TCCAGACCCGGGCTGAGGCCAAGAACAGCTCTTGGGGACATTGGTAACAGAGTCAG TGAACAGCTACAGGCC-3' and 5'-AATGACTCTACCGGTAGCTGAAGGTCTTGCTTCTTTTCTCATAGGCATTCTGGCCTGT AGCTGTTCACTGAC- 3' were used for an extension reaction and the resulting fragments cloned into XmaI and AgeI cleavage sites of pFASTBac carrying full-length cyc^{allR}. Plasmids were verified by restriction enzyme mapping and sequencing. Baculoviruses were generated according to the Bac-to-Bac manual (Invitrogen). Wild-type cyclin B1 was ^{35}S-labeled in Sf9 cultures with resuspending cells (1.5 x 10^6 cells ml^{-1}) in media containing 10% SF-900 II SFM and 90% SF-900 II SFM without methionine or cysteine (both from Invitrogen) to increase radio-label uptake. Baculovirus was added to cells, along with 50 μCi of ^{35}S-labeled methionine and cysteine (NEG772; Perkin Elmer), and cyclin B1 expression was allowed for 2.5 days. CDK1 was expressed separately in Sf9 cells without radiolabeling and then combined with lysate from cells expressing cyclin B1 to allow formation of complex, which was then purified through Ni-NTA affinity and gel filtration chromatography.

CycB1-NT (1-88 amino acids of human cyclin B1) , containing an HA tag at the N terminus and a 6xHis tag at the C terminus was generated using PCR amplification with forward primer (5′-CCA GGA CCA TGG GTT ACC CAT ACG ATG TTC CAG ATT ACG CTG GCT

CGA TGG CGC TCC GAG TCA CG-3′) and reverse primer (5′-GGG AGC CTC GAG CTA GGG AGC GTG ATG GTG ATG GTG ATG CAT AGG TAC CTT TTC AAG AGG-3′). The resulting PCR product was digested with NcoI and XhoI for subcloning into pET28a. Plasmids were verified by restriction enzyme mapping and sequencing. For ^{35}S labeling in *Escherichia coli*, cultures (50 ml) were grown at 37 ˚C to $D_{600\,nm}$ = 0.8, then collected by centrifugation (3,700*g* for 15 min, at 4 ^{o}C) and resuspended in modified M9 medium (50 ml final volume). After resuspension in modified M9 medium, cells were allowed to grow for additional 15 min at 37 °C before 5 mCi of Easy Tag^{TM} L-[35S]-Methionine (NEG709A005MC; Perkin Elmer) was added. Expression was induced with 0.5 mM IPTG for 2.5 h at 37 ^{o}C. Cells were ruptured in 5 ml g^{-1} of pellet guanidine-HCl lysis buffer (pH 8.0) and lysates rotated at 24 °C until the lysate became slightly translucent; approximately 45 min. Lysates were clarified by centrifugation and cycB1-NT was purified using Ni-NTA affinity chromatography (Qiagen). Eluted protein was desalted into XB buffer (100 mM KCl, 0.1 mM $CaCl_2$, 1 mM $MgCl_2$, 10 mM HEPES, at pH 7.8 with KOH), supplemented 2% glycerol, protease inhibitors and phenylmethylsulfonyl fluoride, and stored at – 20 °C.

Maltose-binding protein (MBP)-tagged E1 was expressed in *E. coli* inducing cultures at $D_{600\,nm}$ = 0.6 with 300 μM IPTG for 5 h at room temperature. Purification was carried out using a standard MBP purification protocol. For expression of His-tagged UBCH10 and His-tagged UBC4, bacterial cultures were induced at $D_{600\,nm}$ = 0.6 at 37 ˚C with 500 μM IPTG for 4 h. The enzymes were purified through Ni-NTA affinity and gel-filtration chromatography. Glutathione-*S*-transferase (GST)-fusion proteins for Rpn10 and Rad23, as well as their sub-domains, were purified essentially as reported previously (Elsasser et al., 2004; Elsasser et al., 2002). Recombinant E2-25K (UbcH1) was purchased from Boston Biochem (SP-200).

Preparation of *Xenopus* egg extract

Interphase *Xenopus* egg extract was prepared from eggs laid overnight according to the protocol of Murray (Murray, 1991) with the exception that eggs were activated with 2 μg ml^{-1} calcium ionophore (A23187, free acid form, Calbiochem) for 30 min prior to the crushing spin. Extract was frozen in liquid nitrogen and stored at -80 ºC. Interphase extract was induced to enter mitosis by addition of non-degradable cyclin B, which activates CDK1 and stimulates mitotic phosphorylation, resulting in APC activation. A fusion of the maltose-binding protein (MBP) to *Xenopus* cyclin B lacking its N-terminal 90 amino acids (MBP-Δ90) (Salic and King, 2005) was expressed in *E. coli* by inducing cultures at an D_{600nm}=0.6 with 300 μM IPTG for 5 h at room temperature. Purification was carried out following New England BioLabs (NEB) protocol. To make mitotic extract, MBP-Δ90 was added to interphase extract generally at ~ 20 μg ml^{-1} and incubated at 22-24 ºC for 45-60 min.

Reconstitution of ubiquitination and degradation of cyclin B1

Ubiquitination reactions were carried out essentially as described previously (Kirkpatrick et al., 2006) for the indicated times. Briefly, for each 30 μl reaction, APC was immunopurified from 600 μl of mitotic *Xenopus* egg extract by incubation for 1 h at 4 °C with 12 μg of anti-Cdc27 antibodies (AF3.1, Santa Cruz Biotechnology) immobilized onto 30 μl of Affiprep Protein A beads (156-0006, Bio-Rad). Following incubation with extract, beads were washed quickly (to minimize loss of associated APC co-activator Cdc20) three times with XB containing 500 mM KCl (10 mM potassium HEPES, pH 7.7, 500 mM KCl, 0.1 mM $CaCl_2$, 1 mM $MgCl_2$), two times with XB (same content as above, except with 100 mM KCl), and then three times with reaction buffer (20 mM Tris, pH 7.5, 100 mM KCl, 2.5 mM $MgCl_2$, 2 mM ATP). Ubiquitination reaction were carried out at 24 °C with agitation at 1500 r.p.m and contained APC on 30 μl beads, and 30 μl of a mix containing recombinant MBP-human E1 (1.3 μM), His-tagged UBCH10 or UBC4 (100 nM – 4 μM), and E2-25K (concentration as indicated) as the E2 enzyme, wild-type or different forms of ubiquitin (118-145 μM), and 450-500 nM cyclin B1-CDK1 or cycB1-NT. For

ubiquitin-receptor binding and degradation assays, reaction supernatants were combined with the first 20 µl of reaction buffer wash. For analysis of cyclin B1 ubiquitination with different ubiquitins, entire reactions were processed for immunoblotting or autoradiography. Dried gels were analyzed by phosphorimaging (Bio-Rad PMI); quantification was carried out with Quantity One software (Bio-Rad).

For binding experiments with ubiquitin receptors, cyclin B1-CDK1 was pre-ubiquitinated with purified *Xenopus* APC, UBC4 (3 µM), and ubiquitin (118 µM) for 90 min. Approximately 7-8 µg of "bait" protein immobilized onto Glutathione-Sepharose 4B resin (GE Healthcare) was mixed with 4 µl of pre-synthesized ubiquitin-cyclin B1 conjugates and incubated for 1 h at 4 ˚C with agitation in the presence of 100 µg ml^{-1} BSA and 0.1 % Tween 20. Supernatants were collected and mixed with the first wash to make the flow-through fraction. Beads were washed twice and diluted with SDS sample buffer to analyze the bound fraction. Equivalent amounts of input (I), flow-through (FT) and bound (B) fractions were subjected to SDS-PAGE and western blot analysis using anti-cyclin B1 polyclonal antibody (Ab-2, Neomarkers).

For degradation assays with purified proteasomes, human proteasomes (10-20 nM, concentrations as indicated), purified as reported previously (Lee et al., 2010) but non-UbVS treated, were added to cyclin B1-Ub_n in buffer (50 mM Tris-HCl (pH 7.5), 5 mM $MgCl_2$ and 5 mM ATP) (Lee et al., 2010) and incubated at 24 °C. For 0 min time-point, substrate and proteasome mixtures were individually added to SDS sample buffer to prevent a time-lag from mixing. Aliquots withdrawn at indicated times were combined with SDS sample buffer and subjected to SDS-PAGE and immunoblot analysis using anti-cyclin B1 polyclonal antibody (Ab-2, Neomarkers).

Cyclin B1 degradation in *Xenopus* egg extract

To deplete APC, 100 µl of interphase extract was mixed 2 µg of anti-Cdc27 antibody coupled to 5 µl of Affiprep Protein A beads and incubated at 4 ˚C for 3 h. APC depletion was

confirmed by anti-Cdc27 western blot analysis. Approximately 10 µl of pre-ubiquitinated radiolabeled cyclin B1 was added to 90 µl of APC-depleted extract. Reactions were incubated at 22 °C for the indicated times and stopped by the addition of an equal volume of chilled 2% perchloric acid (PCA) (in H_2O) making a new final volume of 200 µl. Reactions were then incubated on ice for ≥30 min and centrifuged at 15,000 r.p.m. for 10 min, at 4 °C. A fraction of supernatants was mixed with Tris Base and Ultima Gold scintillation fluid (6013327, Perkin Elmer) and the radioactivity was measured by scintillation counting.

Immunodepletion of E2 enzymes

For UBE2S immunodepletion, 10 µg of anti-UBE2S antibody (N-14, Santa Cruz Biotechnology) or control goat IgG antibody (Santa Cruz Biotechnology) was bound to 25 µl UltraLink Immobilized Protein A/G (Pierce) and incubated with 250 µl extract at 4 °C for ~ 1 h. For UBCH10 immunodepletion, 100 µl of anti-UbcX antibody or an equivalent amount of control rabbit IgG coupled to Affiprep protein A support was used to deplete 170 µl extract. Following incubation, samples were briefly centrifuged and supernatants constituting E2- or control-depleted extracts removed carefully without disturbing resin. Samples of depleted extract were centrifuged again to ensure no resin was present. Cyclin B1-CDK1 (~200 nM) was added to E2- or control-depleted extract and analysis of the time course of degradation was carried out at 24 ˚C (1,250 r.p.m.). The equivalent of 1 µl of extract was analyzed by SDS-PAGE and anti-cyclin B1 immunoblot analysis. Depletion of UBE2S and UBCH10 was confirmed by western blotting using anti-UBE2S and anti-UBCH10, respectively. To confirm the efficiency of E2 depletion, extract was incubated with ubiquitin agarose, at a ratio of ~10:1 (extract/ resin). Ubiquitin agarose was pre-washed four times with 1x energy mix (for 20x stock: 150 mM creatine phosphate, 20 mM ATP, 2 mM EGTA and 20 mM $MgCl_2$, at pH 7.7) in XB buffer (100 mM KCl). Extract and 2x energy mix were added to ubiquitin agarose and incubated with agitation at 24 ˚C for 45 min. Samples were centrifuged, extract was removed and ubiquitin agarose was washed once with a

tenfold volume of 1x energy mix in XB. Bound proteins were eluted by boiling in SDS sample buffer and analyzed by immunoblotting.

Ubiquitin-agarose depletion of *Xenopus* extract

Ubiquitin (Ub) agarose (concentration of Ub was 10 mg ml^{-1} or 1.2 mM) was pre-washed four times with 1x energy mix (for 20x stock: 150 mM creatine phosphate, 20 mM ATP, 2 mM EGTA and 20 mM $MgCl_2$, at pH 7.7) in XB buffer (100 mM KCl). To pre-washed Ub agarose, added mitotically arrested *Xenopus* extract and 2x energy mix (20x stock) at a ratio of ~2:1 (extract/ resin), and incubated with agitation (1,250 r.p.m) at 24 °C for 7 min. Following incubation, centrifuged sample at 2,000 r.p.m. for 30 sec to return resin to bottom of the tube. The resulting supernatant is transferred to a new tube containing Ub agarose, repeating the steps described above for a total of 7 rounds of depletion. Samples of supernatant following each round of depletion were combined with SDS sample buffer and levels of proteins analyzed by immunoblotting. Proteins bound to Ub agarose were eluted by boiling in SDS sample buffer and analyzed by immunoblotting.

Ub agarose-depleted extracts were supplemented with 0.9 μM human or *Xenopus laevis* E1 enzyme (kind gift of Brenda Schulman), ~120 μM wild-type ubiquitin, E2 enzymes (100 nM – 3 μM), as indicated, and 1x energy mix. ^{35}S-labeled cycB1-NT (~200-250 nM) was added to Ub agarose-depleted or undepleted extract and analysis of the time course of degradation was carried out at 24 ˚C (1,250 r.p.m.). At indicated times, reactions (3 μl per time point) were quenched with 97 μl of 20 % TCA, vortexed and incubated on ice (≥ 30 min) before centrifugation at 14,000*g* for 30 min at 4 °C. The radioactivity in the supernatant was measured by scintillation counting.

References

Aristarkhov, A., Eytan, E., Moghe, A., Admon, A., Hershko, A., and Ruderman, J. V. (1996). E2-C, a cyclin-selective ubiquitin carrier protein required for the destruction of mitotic cyclins. Proc Natl Acad Sci U S A *93*, 4294-4299.

Barford, D. (2011). Structure, function and mechanism of the anaphase promoting complex (APC/C). Q Rev Biophys *44*, 153-190.

Behrends, C., and Harper, J. W. (2011). Constructing and decoding unconventional ubiquitin chains. Nat Struct Mol Biol *18*, 520-528.

Chen, Z., and Pickart, C. M. (1990). A 25-kilodalton ubiquitin carrier protein (E2) catalyzes multi-ubiquitin chain synthesis via lysine 48 of ubiquitin. J Biol Chem *265*, 21835-21842.

Choi, E., Choe, H., Min, J., Choi, J. Y., Kim, J., and Lee, H. (2009). BubR1 acetylation at prometaphase is required for modulating APC/C activity and timing of mitosis. Embo J *28*, 2077-2089.

Crosas, B., Hanna, J., Kirkpatrick, D. S., Zhang, D. P., Tone, Y., Hathaway, N. A., Buecker, C., Leggett, D. S., Schmidt, M., King, R. W*., et al.* (2006). Ubiquitin chains are remodeled at the proteasome by opposing ubiquitin ligase and deubiquitinating activities. Cell *127*, 1401-1413.

Deveraux, Q., Ustrell, V., Pickart, C., and Rechsteiner, M. (1994). A 26 S protease subunit that binds ubiquitin conjugates. J Biol Chem *269*, 7059-7061.

Eddins, M. J., Carlile, C. M., Gomez, K. M., Pickart, C. M., and Wolberger, C. (2006). Mms2-Ubc13 covalently bound to ubiquitin reveals the structural basis of linkage-specific polyubiquitin chain formation. Nat Struct Mol Biol *13*, 915-920.

Elsasser, S., Chandler-Militello, D., Muller, B., Hanna, J., and Finley, D. (2004). Rad23 and Rpn10 serve as alternative ubiquitin receptors for the proteasome. J Biol Chem *279*, 26817-26822.

Elsasser, S., and Finley, D. (2005). Delivery of ubiquitinated substrates to protein-unfolding machines. Nat Cell Biol *7*, 742-749.

Elsasser, S., Gali, R. R., Schwickart, M., Larsen, C. N., Leggett, D. S., Muller, B., Feng, M. T., Tubing, F., Dittmar, G. A., and Finley, D. (2002). Proteasome subunit Rpn1 binds ubiquitin-like protein domains. Nat Cell Biol *4*, 725-730.

Finley, D. (2009). Recognition and processing of ubiquitin-protein conjugates by the proteasome. Annu Rev Biochem *78*, 477-513.

Garnett, M. J., Mansfeld, J., Godwin, C., Matsusaka, T., Wu, J., Russell, P., Pines, J., and Venkitaraman, A. R. (2009). UBE2S elongates ubiquitin chains on APC/C substrates to promote mitotic exit. Nat Cell Biol *11*, 1363-1369. Epub 2009 Oct 1311.

Hanna, J., Hathaway, N. A., Tone, Y., Crosas, B., Elsasser, S., Kirkpatrick, D. S., Leggett, D. S., Gygi, S. P., King, R. W., and Finley, D. (2006). Deubiquitinating enzyme Ubp6 functions noncatalytically to delay proteasomal degradation. Cell *127*, 99-111.

Harper, J. W., Burton, J. L., and Solomon, M. J. (2002). The anaphase-promoting complex: it's not just for mitosis any more. Genes Dev *16*, 2179-2206.

Hershko, A., and Ciechanover, A. (1998). The ubiquitin system. Annu Rev Biochem *67*, 425-479.

Hofmann, R. M., and Pickart, C. M. (1999). Noncanonical MMS2-encoded ubiquitin-conjugating enzyme functions in assembly of novel polyubiquitin chains for DNA repair. Cell *96*, 645-653.

Huang, X., Summers, M. K., Pham, V., Lill, J. R., Liu, J., Lee, G., Kirkpatrick, D. S., Jackson, P. K., Fang, G., and Dixit, V. M. (2011). Deubiquitinase USP37 Is Activated by CDK2 to Antagonize APC(CDH1) and Promote S Phase Entry. Mol Cell *42*, 511-523.

Isasa, M., Katz, E. J., Kim, W., Yugo, V., Gonzalez, S., Kirkpatrick, D. S., Thomson, T. M., Finley, D., Gygi, S. P., and Crosas, B. (2010). Monoubiquitination of RPN10 regulates substrate recruitment to the proteasome. Mol Cell *38*, 733-745.

Jin, L., Williamson, A., Banerjee, S., Philipp, I., and Rape, M. (2008). Mechanism of ubiquitin-chain formation by the human anaphase-promoting complex. Cell *133*, 653-665.

Kerscher, O., Felberbaum, R., and Hochstrasser, M. (2006). Modification of proteins by ubiquitin and ubiquitin-like proteins. Annu Rev Cell Dev Biol *22*, 159-180.

King, R. W., Peters, J. M., Tugendreich, S., Rolfe, M., Hieter, P., and Kirschner, M. W. (1995). A 20S complex containing CDC27 and CDC16 catalyzes the mitosis-specific conjugation of ubiquitin to cyclin B. Cell *81*, 279-288.

Kirkpatrick, D. S., Gerber, S. A., and Gygi, S. P. (2005). The absolute quantification strategy: a general procedure for the quantification of proteins and post-translational modifications. Methods *35*, 265-273.

Kirkpatrick, D. S., Hathaway, N. A., Hanna, J., Elsasser, S., Rush, J., Finley, D., King, R. W., and Gygi, S. P. (2006). Quantitative analysis of in vitro ubiquitinated cyclin B1 reveals complex chain topology. Nat Cell Biol *8*, 700-710.

Lee, B. H., Lee, M. J., Park, S., Oh, D. C., Elsasser, S., Chen, P. C., Gartner, C., Dimova, N., Hanna, J., Gygi, S. P.*, et al.* (2010). Enhancement of proteasome activity by a small-molecule inhibitor of USP14. Nature *467*, 179-184.

Mathe, E., Kraft, C., Giet, R., Deak, P., Peters, J. M., and Glover, D. M. (2004). The E2-C vihar is required for the correct spatiotemporal proteolysis of cyclin B and itself undergoes cyclical degradation. Curr Biol *14*, 1723-1733.

Matiuhin, Y., Kirkpatrick, D. S., Ziv, I., Kim, W., Dakshinamurthy, A., Kleifeld, O., Gygi, S. P., Reis, N., and Glickman, M. H. (2008). Extraproteasomal Rpn10 restricts access of the polyubiquitin-binding protein Dsk2 to proteasome. Mol Cell *32*, 415-425.

Murray, A. W. (1991). Cell cycle extracts. Methods Cell Biol *36*, 581-605.

Osaka, F., Seino, H., Seno, T., and Yamao, F. (1997). A ubiquitin-conjugating enzyme in fission yeast that is essential for the onset of anaphase in mitosis. Mol Cell Biol *17*, 3388-3397.

Peters, J. M. (2002). The anaphase-promoting complex: proteolysis in mitosis and beyond. Mol Cell *9*, 931-943.

Peters, J. M. (2006). The anaphase promoting complex/cyclosome: a machine designed to destroy. Nat Rev Mol Cell Biol *7*, 644-656.

Peth, A., Uchiki, T., and Goldberg, A. L. (2010). ATP-dependent steps in the binding of ubiquitin conjugates to the 26S proteasome that commit to degradation. Mol Cell *40*, 671-681.

Petroski, M. D., Zhou, X., Dong, G., Daniel-Issakani, S., Payan, D. G., and Huang, J. (2007). Substrate modification with lysine 63-linked ubiquitin chains through the UBC13-UEV1A ubiquitin-conjugating enzyme. J Biol Chem *282*, 29936-29945.

Rao, H., and Sastry, A. (2002). Recognition of specific ubiquitin conjugates is important for the proteolytic functions of the ubiquitin-associated domain proteins Dsk2 and Rad23. J Biol Chem *277*, 11691-11695.

Riedinger, C., Boehringer, J., Trempe, J. F., Lowe, E. D., Brown, N. R., Gehring, K., Noble, M. E., Gordon, C., and Endicott, J. A. (2010). Structure of Rpn10 and its interactions with polyubiquitin chains and the proteasome subunit Rpn12. J Biol Chem *285*, 33992-34003.

Rodrigo-Brenni, M. C., and Morgan, D. O. (2007). Sequential E2s drive polyubiquitin chain assembly on APC targets. Cell *130*, 127-139.

Salic, A., and King, R. W. (2005). Identifying small molecule inhibitors of the ubiquitin-proteasome pathway in Xenopus egg extracts. Methods Enzymol *399*, 567-585.

Summers, M. K., Pan, B., Mukhyala, K., and Jackson, P. K. (2008). The unique N terminus of the UbcH10 E2 enzyme controls the threshold for APC activation and enhances checkpoint regulation of the APC. Mol Cell *31*, 544-556.

Tang, Z., Li, B., Bharadwaj, R., Zhu, H., Ozkan, E., Hakala, K., Deisenhofer, J., and Yu, H. (2001). APC2 Cullin protein and APC11 RING protein comprise the minimal ubiquitin ligase module of the anaphase-promoting complex. Mol Biol Cell *12*, 3839-3851.

Townsley, F. M., Aristarkhov, A., Beck, S., Hershko, A., and Ruderman, J. V. (1997). Dominant-negative cyclin-selective ubiquitin carrier protein E2-C/UbcH10 blocks cells in metaphase. Proc Natl Acad Sci U S A *94*, 2362-2367.

Wickliffe, K. E., Lorenz, S., Wemmer, D. E., Kuriyan, J., and Rape, M. (2011a). The mechanism of linkage-specific ubiquitin chain elongation by a single-subunit E2. Cell *144*, 769-781.

Wickliffe, K. E., Williamson, A., Meyer, H. J., Kelly, A., and Rape, M. (2011b). K11-linked ubiquitin chains as novel regulators of cell division. Trends Cell Biol *21*, 656-663.

Williamson, A., Wickliffe, K. E., Mellone, B. G., Song, L., Karpen, G. H., and Rape, M. (2009). Identification of a physiological E2 module for the human anaphase-promoting complex. Proc Natl Acad Sci U S A *106*, 18213-18218.

Wu, T., Merbl, Y., Huo, Y., Gallop, J. L., Tzur, A., and Kirschner, M. W. (2010). UBE2S drives elongation of K11-linked ubiquitin chains by the anaphase-promoting complex. Proc Natl Acad Sci U S A *107*, 1355-1360.

Ye, Y., and Rape, M. (2009). Building ubiquitin chains: E2 enzymes at work. Nat Rev Mol Cell Biol *10*, 755-764.

You, J., Cohen, R. E., and Pickart, C. M. (1999). Construct for high-level expression and low misincorporation of lysine for arginine during expression of pET-encoded eukaryotic proteins in Escherichia coli. Biotechniques *27*, 950-954.

Yu, H., King, R. W., Peters, J. M., and Kirschner, M. W. (1996). Identification of a novel ubiquitin-conjugating enzyme involved in mitotic cyclin degradation. Curr Biol *6*, 455-466.

Zeng, X., Sigoillot, F., Gaur, S., Choi, S., Pfaff, K. L., Oh, D. C., Hathaway, N., Dimova, N., Cuny, G. D., and King, R. W. (2010). Pharmacologic inhibition of the anaphase-promoting complex induces a spindle checkpoint-dependent mitotic arrest in the absence of spindle damage. Cancer Cell *18*, 382-395.

Chapter V: Conclusions and Future Directions

Nevena Dimova

The Anaphase-Promoting Complex/Cyclosome (APC/C or APC) is a multi-subunit ligase complex that initiates anaphase and mitotic exit by ubiquitinating cell-cycle regulators, including cyclin B1. Here, we sought to understand the role of ubiquitin-chain formation in APC catalysis and proteasomal targeting. Our work provides strong evidence that the proteolytic machinery does not exert a requirement for Lys11 or other ubiquitin-ubiquitin linkages for efficient degradation of ubiquitinated cyclin B1. Utilizing a reconstituted system and *Xenopus* cell-cycle extracts, we demonstrate that multiple monoubiquitination can indeed be coupled to robust proteolysis, at least in the context of cyclin B1. Upon restriction of the ubiquitin-acceptor sites in cyclin B1, Lys11-linked ubiquitin polymers elaborated by the E2 UBE2S become increasingly important for substrate proteolysis. The existence of two distinct degradative pathways driven by multiple monoubiquitination vs. ubiquitin-chain formation has important implications for how APC activity may be coupled to, and regulated by, distinct E2 enzymes. Our findings explain how the presence of multiple ubiquitin-acceptor sites confers flexibility in the requirement for particular E2 enzymes in modulating the rate of ubiquitin-dependent proteolysis.

Development of a system to study the role of ubiquitin linkage in proteasomal targeting

Chapter II of this dissertation presents a novel approach we developed to gain better understanding of the importance of different ubiquitin-chain topologies in promoting substrate degradation by the 26S proteasome. To investigate the nature of the ubiquitin signal targeting cyclin B1 for proteolysis, a system for the expression and purification of radiolabeled N-terminal fragment of the protein was established, which was critical to our ability to examine cyclin degradation in a rigorous and quantitative manner. Analysis of APC -mediated ubiquitination and degradation with purified proteasomes provided us with strong confidence that the behavior of

the N-terminal fragment of human cyclin B1 (amino acids 1-88) (referred to as cycB1-NT) closely resembled that of the full-length protein.

The problem of ubiquitin-chain formation and function has been challenging to study in physiologically relevant systems due to the presence of endogenous ubiquitin. Development of strategies for effective blockade of the regulatory pathways maintaining ubiquitin levels is a non-trivial task and for that reason manipulation of the endogenous ubiquitin pool in any model system is difficult. One experimental approach to studying the role of specific ubiquitin-ubiquitin linkages, or lack thereof, in proteasomal targeting has been the addition of mutant ubiquitin in excess to endogenous ubiquitin (Hershko et al., 1991; Jin et al., 2008; Wu et al., 2010). However, the contribution of specific ubiquitin-chain topologies in proteasomal degradation may be difficult to ascertain when conducted in a background that contains wild-type ubiquitin. Importantly, alteration of ubiquitin levels as upon adding exogenous ubiquitin may influence pairing of a specific E3 ubiquitin ligase with ubiquitin-conjugating enzymes, potentially impacting different aspects of substrate ubiquitination and/or the downstream fate of modified proteins. In this regard, excess added ubiquitin was found to increase the fraction of ubiquitin-charged UBCH5, thereby promoting a functional interaction of this promiscuous E2 with APC in mitotic cell extracts (Summers et al., 2008). These findings emphasize the need for methods where no gross fluctuations in the available ubiquitin pool are introduced. In the UbVS system, recycling of endogenous ubiquitin from existing conjugates is inhibited and wild-type ubiquitin is supplemented at levels just sufficient to restore degradation. Thereby we were able to examine the functional significance of distinct ubiquitin linkages in APC catalysis and proteasomal degradation at more physiologically relevant ubiquitin concentrations.

Our analysis revealed that the availability of free ubiquitin in *Xenopus* extract has a strong effect on the kinetics of cyclin degradation. One future direction would be to extend our analysis and examine the possibility that control of ubiquitin availability may be a mechanism by which the rate of APC-substrate degradation can be controlled. Utilizing this system, we can

quantitatively evaluate how proteasomal targeting of different APC substrates may be differentially sensitive to levels of free ubiquitin. Less processive substrates of the APC such as cyclin A and UBCH10, which require multiple binding cycles to obtain their proteolytic tags (Rape et al., 2006), may exhibit higher sensitivity to ubiquitin levels. Such sensitivity would be potentially amplified if proteasomal targeting of a substrate is actively opposed by the activity of deubiquitinating enzymes. An exciting finding from our work suggests that proteolysis of endogenous UBCH10 in *Xenopus* extracts may be actively antagonized through the disassembly or editing of its ubiquitin signal. Levels of UBCH10 are reduced upon supplementing UbVS-treated mitotic extract with wild-type ubiquitin. In this context, an interesting question to address will be how the balance of ubiquitination and deubiquitination of UBCH10 modulates the levels of active E2, thereby providing a mechanism for regulating APC activity. Tools including immunodepletion and the APC-specific inhibitor TAME (Zeng and King, 2012; Zeng et al., 2010) would allow us to test whether the reduction in UBCH10 levels in this context is APC-dependent and how levels of APC activity influence stability of the E2. Furthermore, the deubiqutinating activity that potentially antagonizes UBCH10 degradation can be identified and characterized.

In contrast to our findings about UBCH10, UbVS-sensitive isopeptidases are unlikely to present a major kinetic barrier to cyclin B1 proteolysis in mitotic extract. Importantly, this may not hold true for interphase extracts. We found that inhibiting the catalytic activity of deubiquitinases with UbVS in the presence of wild-type ubiquitin stimulated cyclin proteolysis (data presented in appendix). These findings suggest that the activity of interphase APC can support cyclin degradation, but is effectively overwhelmed by deubiquitination which prevents dysregulated substrate proteolysis. We are currently pursuing identification of such deubiquitinating activity which may specifically oppose the activity of interphase APC, thereby preventing untimely substrate degradation.

Role of ubiquitin linkage and E2 enzymes in APC/C-mediated degradation

There have been significant efforts dedicated to understanding the mechanistic and architectural complexities underlying APC activity. Structural studies comprise one aspect of these efforts and recent work has shed important insight into how subunit organization of the APC and conformational rearrangements may be coupled with proper substrate recognition and efficient ubiquitin transfer to substrate residues (Buschhorn et al., 2011; da Fonseca et al., 2011). These studies have advanced our understanding of this complex ubiquitin ligase and complement work examining the mechanism of ubiquitin-chain formation by the APC. In this context, recent findings have suggested that Lys11-linked ubiquitin polymers, assembled by the chain-elongating E2 UBE2S, may be important in APC-dependent proteolysis. While important for normal mitotic progression in *Drosophila* S2 cells (Williamson et al., 2009), UBE2S was found to be dispensable for this process in human cells (Garnett et al., 2009). The lack of a uniform requirement for UBE2S, together with the capacity of the proteasome to rapidly degrade cyclin bearing multiple short chains (Kirkpatrick et al., 2006), motivated us to examine whether APC-mediated proteolysis is strictly dependent upon polyubiquitination and whether the proteasome exerts a requirement for specific ubiquitin-ubiquitin linkages to efficiently degrade cyclin B1. To address this question, we utilized the UbVS system. Neither Lys48, nor Lys11, ubiquitin-ubiquitin linkages were essential for robust rates of cyclin proteolysis. Furthermore, our analysis revealed that ubiquitin-chain formation is dispensable for cyclin proteolysis in *Xenopus* extracts, unless the number of available lysine residues is limited. In agreement with the effects of chain-terminating ubiquitin in *Xenopus* extract, purified proteasomes degraded multiply monoubiquitinated cyclin B1 with fast kinetics, comparable to those for substrate bearing ubiquitin chains. Based on our findings, we propose that the presence of multiple lysines in cyclin B1 that are in close proximity to one another has the potential for generating a high local density of monoubiquitin that

promotes receptor binding and proteasomal degradation. Perhaps similar to how linkage of ubiquitin units into a polymer structure may determine its potential as a degradative element, particular spacing of monoubiquitins along the substrate may be differentially conducive to productive engagement with the proteolytic machinery. Previously, Hershko and Heller found that while in the presence of methylated ubiquitin lysozyme is conjugated with up to 7 monoubiquitins, it is degraded with slow kinetics (Hershko and Heller, 1985). An interesting possibility is that, unlike in the context of cyclin B1, the distribution of modified lysines in lysozyme cannot generate sufficient local density of ubiquitin to facilitate ubiquitin receptor and proteasome binding. It may be of interest in the future to examine how the distribution of available ubiquitin-acceptor sites in cyclin B1 influences the capacity of multiple monoubiquitination to serve as a robust proteolytic signal. These efforts would be particularly important as we develop strategies to understanding steps subsequent to dissociation of ubiquitinated cyclin B1 from the ligase, including how conjugates are delivered to the proteasome, and how those events may be coupled to different aspects of cyclin ubiquitination.

An important aspect of our work has been understanding how the architecture of a ubiquitin tag is decoded by the proteolytic machinery. Our analysis indicates that multiple monoubiquitination can promote rapid and complete degradation of a physiological proteasome substrate. Importantly, we define a novel proteolytic signal that confers flexibility in the requirement for particular E2 enzymes in modulating the rate of ubiquitin-dependent proteolysis. In *Xenopus* cell-cycle extracts, we found that the chain-elongating E2 UBE2S is dispensable for APC/C-mediated degradation of cyclin. Our findings are consistent with a model where UBCH10, or possibly UBC4/5 enzymes, catalyzes the conjugation of monoubiquitin to multiple lysine residues and possibly the elaboration of some short chains, generating degradation-competent cyclin. These E2 enzymes are recruited to the ligase through the RING domain of APC11 (Peters, 2006; Tang et al., 2001; Yu et al., 1998) without impeding the recruitment of UBE2S, which interacts at least in part through the substrate-adaptor proteins Cdc20 and Cdh1

(Behrends and Harper, 2011; Wickliffe et al., 2011; Williamson et al., 2009). Such a mode of recruitment of multiple ubiquitin-conjugating enzymes would potentially overcome the separation of ubiquitin-chain initiation and elongation steps, favoring the processive assembly of long polymers. Although UBE2S appears to be present in *Xenopus* extract at sufficient levels to support cyclin proteolysis, it does not appear to be an active component of the conjugation machinery and becomes essential only when the number of ubiquitinatable lysine residues in cyclin B1 is restricted. This raises questions as to whether UBE2S is tightly associated with the APC/C and how its activity is regulated. An intriguing possibility is that levels of free ubiquitin regulate activity of UBE2S. Perhaps under conditions of ubiquitin limitation as may be the case in *Xenopus* extract, there are mechanisms in place to conserve ubiquitin, restricting extent of ubiquitination to what is sufficient for timely destruction and preventing the formation of multiple long chains. Future work will be needed to address these questions.

While our work provides strong evidence that multiple monoubiquitination can serve as an efficient proteolytic signal in the context of cyclin B1, further studies are required to determine if such mode of ubiquitination targets additional APC substrates to the proteasome or if it is a degradative pathway uniquely pertaining to cyclin B1. The UbVS system, described earlier, provides an exciting opportunity to extend our analysis to other APC substrates and better understand how the lysine profile of a substrate may influence the balance between multiple monoubiquitination and ubiquitin-chain extension. Perhaps robust APC-mediated proteolysis of securin, which like cyclin B1 has 18 lysines, may show little or no dependence on ubiquitin-chain formation and catalysis by the E2 UBE2S. For other substrates such as cyclin A2 and UBCH10, each of which has 12 lysines, degradation may be more dependent on the chain-elongating enzyme UBE2S. Currently, we are investigating whether the blockage of lysines by other post-translational modifications or a crosstalk between neighboring post-translational modifications may limit the availability of ubiquitin-acceptor sites in cyclin B1, enforcing a requirement for synthesis of long ubiquitin chains for efficient turnover. Work carried out in collaboration with

the Gygi lab has uncovered residues within the N-terminal domain of cyclin B1 that are modified with acetyl groups. Current and future efforts may be dedicated to identifying a physiological setting most conducive to studying effects of acetylation on APC-mediated catalysis and ubiquitin-dependent proteolysis.

It was surprising to find that in *Xenopus* cell-cycle extracts multiple monoubiquitination can signal robust proteasomal turnover. Our findings in a purified system and in *Xenopus* extract suggest that the proteasome does not impose a requirement for ubiquitin-chain formation for cyclin B1 destruction. One could envision that degradation of a substrate conjugated with 5 or 6 monoubiquitins, as appears to be the case for cyclin B1, may be more sensitive to deubiquitinases, as compared to a heavily ubiquitinated protein. We found that one such DUB able to remove monoubiquitins attached to cyclin is the proteasome-associated enzyme USP14. Unlike in an *in vitro* system, USP14 did not appear to antagonize cyclin B1 degradation in *Xenopus* extracts (data also shown in appendix). APC-dependent proteolysis of cyclin B1, at least in mitotic *Xenopus* extracts, was not appreciably impeded by UbVS-sensitive DUBs. These findings do not rule out the possibility that multiply monoubiquitinated species of cyclin B1 are effectively "shielded" by the activity of deubiquitinating enzymes through binding to proteins such as ubiquitin receptors. There is minimal knowledge of what factors may recognize and decode a signal specifically comprised of multiple monoubiquitins or Lys11-linked ubiquitin polymers. With reports demonstrating that several DUBs, including the OTU-domain containing Cezanne protein, have a preference for Lys11-linked chains (Bremm et al., 2010), we are only beginning to understand how the ubiquitin code is read. Development of tools to identify factors interacting with ubiquitin conjugates downstream of different E2-E3 complexes will provide us with an opportunity to examine how distinct ubiquitin-ubiquitin linkages are assigned independent functions in the pathway leading to the proteasome.

References

Behrends, C., and Harper, J. W. (2011). Constructing and decoding unconventional ubiquitin chains. Nat Struct Mol Biol *18*, 520-528.

Bremm, A., Freund, S. M., and Komander, D. (2010). Lys11-linked ubiquitin chains adopt compact conformations and are preferentially hydrolyzed by the deubiquitinase Cezanne. Nat Struct Mol Biol *17*, 939-947.

Buschhorn, B. A., Petzold, G., Galova, M., Dube, P., Kraft, C., Herzog, F., Stark, H., and Peters, J. M. (2011). Substrate binding on the APC/C occurs between the coactivator Cdh1 and the processivity factor Doc1. Nat Struct Mol Biol *18*, 6-13.

da Fonseca, P. C., Kong, E. H., Zhang, Z., Schreiber, A., Williams, M. A., Morris, E. P., and Barford, D. (2011). Structures of APC/C(Cdh1) with substrates identify Cdh1 and Apc10 as the D-box co-receptor. Nature *470*, 274-278.

Garnett, M. J., Mansfeld, J., Godwin, C., Matsusaka, T., Wu, J., Russell, P., Pines, J., and Venkitaraman, A. R. (2009). UBE2S elongates ubiquitin chains on APC/C substrates to promote mitotic exit. Nat Cell Biol *11*, 1363-1369. Epub 2009 Oct 1311.

Hershko, A., Ganoth, D., Pehrson, J., Palazzo, R. E., and Cohen, L. H. (1991). Methylated ubiquitin inhibits cyclin degradation in clam embryo extracts. J Biol Chem *266*, 16376-16379.

Hershko, A., and Heller, H. (1985). Occurrence of a polyubiquitin structure in ubiquitin-protein conjugates. Biochem Biophys Res Commun *128*, 1079-1086.

Jin, L., Williamson, A., Banerjee, S., Philipp, I., and Rape, M. (2008). Mechanism of ubiquitin-chain formation by the human anaphase-promoting complex. Cell *133*, 653-665.

Kirkpatrick, D. S., Hathaway, N. A., Hanna, J., Elsasser, S., Rush, J., Finley, D., King, R. W., and Gygi, S. P. (2006). Quantitative analysis of in vitro ubiquitinated cyclin B1 reveals complex chain topology. Nat Cell Biol *8*, 700-710.

Peters, J. M. (2006). The anaphase promoting complex/cyclosome: a machine designed to destroy. Nat Rev Mol Cell Biol *7*, 644-656.

Rape, M., Reddy, S. K., and Kirschner, M. W. (2006). The processivity of multiubiquitination by the APC determines the order of substrate degradation. Cell *124*, 89-103.

Summers, M. K., Pan, B., Mukhyala, K., and Jackson, P. K. (2008). The unique N terminus of the UbcH10 E2 enzyme controls the threshold for APC activation and enhances checkpoint regulation of the APC. Mol Cell *31*, 544-556.

Tang, Z., Li, B., Bharadwaj, R., Zhu, H., Ozkan, E., Hakala, K., Deisenhofer, J., and Yu, H. (2001). APC2 Cullin protein and APC11 RING protein comprise the minimal ubiquitin ligase module of the anaphase-promoting complex. Mol Biol Cell *12*, 3839-3851.

Wickliffe, K. E., Lorenz, S., Wemmer, D. E., Kuriyan, J., and Rape, M. (2011). The mechanism of linkage-specific ubiquitin chain elongation by a single-subunit E2. Cell *144*, 769-781.

Williamson, A., Wickliffe, K. E., Mellone, B. G., Song, L., Karpen, G. H., and Rape, M. (2009). Identification of a physiological E2 module for the human anaphase-promoting complex. Proc Natl Acad Sci U S A *106*, 18213-18218.

Wu, T., Merbl, Y., Huo, Y., Gallop, J. L., Tzur, A., and Kirschner, M. W. (2010). UBE2S drives elongation of K11-linked ubiquitin chains by the anaphase-promoting complex. Proc Natl Acad Sci U S A *107*, 1355-1360.

Yu, H., Peters, J. M., King, R. W., Page, A. M., Hieter, P., and Kirschner, M. W. (1998). Identification of a cullin homology region in a subunit of the anaphase-promoting complex. Science *279*, 1219-1222.

Zeng, X., and King, R. W. (2012). An APC/C inhibitor stabilizes cyclin B1 by prematurely terminating ubiquitination. Nat Chem Biol.

Zeng, X., Sigoillot, F., Gaur, S., Choi, S., Pfaff, K. L., Oh, D. C., Hathaway, N., Dimova, N., Cuny, G. D., and King, R. W. (2010). Pharmacologic inhibition of the anaphase-promoting complex induces a spindle checkpoint-dependent mitotic arrest in the absence of spindle damage. Cancer Cell *18*, 382-395.

Chapter VI: Appendix

A. Dimova NV, Hathaway NA, Lee BH, Kirkpatrick DS, Berkowitz ML, Gygi SP, Finley D, King RW (2012) APC/C-mediated multiple monoubiquitylation provides an alternative degradation signal for cyclin B1. *Nat Cell Biol* **14**:168-76.

N.D. and R.W.K. designed and interpreted the experiments. N. D. carried out and analyzed all experiments except those outlined below. N.A.H. carried out cyclin B1 ubiquitylation for ubiquitin-AQUA analysis and degradation assays with these species in APC/C-depleted extract. D.S.K. carried out the ubiquitin-AQUA analysis on cyclin B1 ubiquitylated *in vitro* with the E2 UBC4 and different ubiquitin types in the laboratory of S.P.G. B-H.L. provided purified human proteasomes with oversight from D.F. M.L.B. helped with cloning of different cyclin B1 mutants. The manuscript was written by N.D. and R.W.K. with input from all authors.

B. Analysis of the role of USP14 in cyclin B1 proteolysis in *Xenopus* extract

Nevena Dimova designed and carried out all experiments. Nevena Dimova wrote this chapter.

C. Lee BH, Lee MJ, Park S, Oh DC, Elsasser S, Chen PC, Gartner C, Dimova N, Hanna J, Gygi SP, Wilson SM, King RW and Finley D (2010) Enhancement of proteasome activity by a small-molecule inhibitor of USP14. *Nature* **467**:179-84.

Nevena Dimova designed and carried out *in vitro* ubiquitination of cyclin B1 for degradation assays, part of the manuscript.

D. Zeng X, Sigoillot F, Gaur S, Choi S, Pfaff KL, Oh DC, Hathaway N, Dimova N, Cuny GD and King RW (2010) Pharmacologic inhibition of the anaphase-promoting complex induces a spindle checkpoint-dependent mitotic arrest in the absence of spindle damage. *Cancer Cell* **18**:382-95.

Nevena Dimova carried out degradation assays with pre-ubiquitinated cyclin B1 and critically read this manuscript.

nature cell biology

APC/C-mediated multiple monoubiquitylation provides an alternative degradation signal for cyclin B1

Nevena V. Dimova[1], Nathaniel A. Hathaway[1,2], Byung-Hoon Lee[1], Donald S. Kirkpatrick[1,2], Marie Lea Berkowitz[1], Steven P. Gygi[1], Daniel Finley[1] and Randall W. King[1,3]

The anaphase-promoting complex or cyclosome (APC/C) initiates mitotic exit by ubiquitylating cell-cycle regulators such as cyclin B1 and securin. Lys 48-linked ubiquitin chains represent the canonical signal targeting proteins for degradation by the proteasome, but they are not required for the degradation of cyclin B1. Lys 11-linked ubiquitin chains have been implicated in degradation of APC/C substrates, but the Lys 11-chain-forming E2 UBE2S is not essential for mitotic exit, raising questions about the nature of the ubiquitin signal that targets APC/C substrates for degradation. Here we demonstrate that multiple monoubiquitylation of cyclin B1, catalysed by UBCH10 or UBC4/5, is sufficient to target cyclin B1 for destruction by the proteasome. When the number of ubiquitylatable lysines in cyclin B1 is restricted, Lys 11-linked ubiquitin polymers elaborated by UBE2S become increasingly important. We therefore explain how a substrate that contains multiple ubiquitin acceptor sites confers flexibility in the requirement for particular E2 enzymes in modulating the rate of ubiquitin-dependent proteolysis.

A uniform Lys 48-linked ubiquitin polymer was the first signal identified to target substrates for destruction by the 26S proteasome[1–3]. Recent work has demonstrated that the repertoire of proteolytic signals encompasses chains of other linkage types, including Lys 11-linked ubiquitin chains[4–10] and short chains of mixed linkage types[11]. In contrast, Lys 63-linked chains have non-proteolytic roles in DNA repair[12,13], kinase activation[14], protein trafficking[15,16] and translation[17]. Similarly, the transfer of a single ubiquitin moiety to one (monoubiquitylation) or to multiple sites (multiple monoubiquitylation) in a substrate has been implicated in mostly non-proteolytic processes[18,19], although multiple monoubiquitylation can target receptor tyrosine kinases to the lysosome[20–22]. More recently, multiple monoubiquitylation has been shown to control proteasomal processing of the p105 NF-κB precursor to the shorter p50 subunit[23]. So far, multiple monoubiquitylation has not been coupled with rapid and complete proteolysis of a proteasome substrate.

The E3 ligase activities of the Skp1–Cullin–F-box complex (SCF) family and the APC/C are essential for cell-cycle progression[24,25]. The SCF cooperates with the E2 Cdc34 to assemble uniform Lys 48-linked ubiquitin polymers on substrates[26], and the APC/C works in conjunction with UBCH10 (also known as UBE2C) and enzymes of the UBC4/5 family to catalyse chain formation through three lysine residues of ubiquitin (Lys 11, Lys 48 and Lys 63; ref. 11). UBCH10 builds multiple short ubiquitin chains on cyclin B1, which are sufficient to target the protein for degradation by the proteasome[11]. In this context, Lys 48-linked ubiquitin polymers are dispensable for binding of modified cyclin B1 to ubiquitin receptors and degradation by the proteasome[11]. More recent work indicates that the assembly of a proteolytic signal on APC/C substrates may occur in two stages. In budding yeast, Ubc4 initiates ubiquitin conjugation, whereas Ubc1 elongates ubiquitin chains[27]. Similarly, in metazoans, UBCH10 has been proposed to initiate monoubiquitylation of the substrate, followed by UBE2S-dependent extension of Lys 11-linked ubiquitin chains[7,8,10]. Consistent with this idea, depletion of UBE2S from *Drosophila* S2 cells prolongs metaphase and stabilizes cyclin B1 at the spindle poles[7]. In contrast, UBE2S is not essential for normal mitosis in human HeLa cells, but rather may be important for proteolysis under conditions where APC/C activity is compromised, such as during recovery from drug-induced spindle-assembly checkpoint activation[8]. Using an approach in which *Xenopus* extracts are made dependent on exogenous ubiquitin, we sought to understand whether APC/C-catalysed proteolysis requires Lys 11 or other ubiquitin linkages to efficiently degrade cyclin B1.

RESULTS

Inhibiting ubiquitin-chain formation has only a modest effect in stabilizing cyclin B1 in *Xenopus* extract

To quantitatively evaluate the role of different ubiquitin-chain linkages in targeting cyclin B1 for degradation in mitotic *Xenopus*

[1]Department of Cell Biology, Harvard Medical School, 240 Longwood Avenue, Boston, Massachusetts 02115, USA. [2]Present addresses: Howard Hughes Medical Institute, Department of Pathology, Stanford University, Stanford, California 94305, USA (N.A.H.); Department of Protein Chemistry, Genetech Inc., 1 DNA Way, South San Francisco, California 94080, USA (D.S.K.).
[3]Correspondence should be addressed to R.W.K. (e-mail: randy_king@hms.harvard.edu)

Received 22 June 2011; accepted 20 December 2011; published online 29 January 2012; DOI: 10.1038/ncb2425

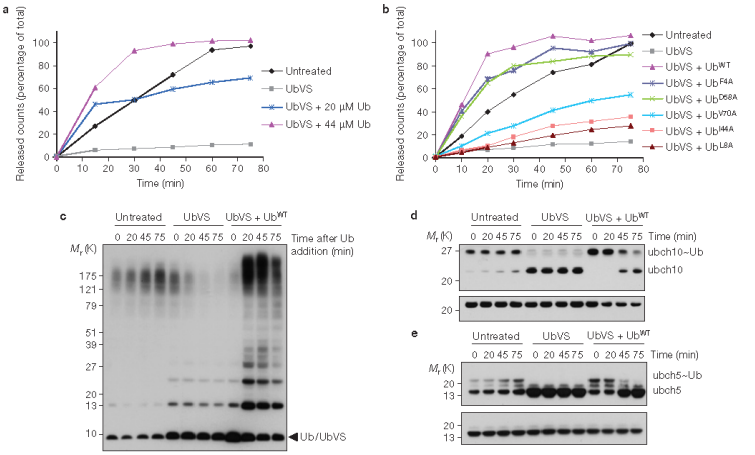

Figure 1 UbVS inhibits cyclin B1 degradation by depleting the amount of available ubiquitin. (**a**) ^{35}S-labelled cycB1-NT and 20 or 44 μM wild-type ubiquitin were introduced into mitotically arrested *Xenopus* extract that had been pre-treated with UbVS (20 μM) or buffer (untreated) for 30 min. Proteolysis was measured by release of trichloroacetic-acid-soluble counts, and is plotted as the percentage of input radiolabelled cycB1-NT. Trends are representative of three or more independent experiments. (**b**) Wild-type ubiquitin (Ub^{WT}) or forms of ubiquitin (44 μM) bearing single-point mutations in distinct interaction surfaces, along with radiolabelled substrate, were added to UbVS-treated extract. For **c**–**e**, mitotically arrested *Xenopus* extract was pre-treated with UbVS (20 μM) or buffer (untreated) for 30 min. Wild-type ubiquitin (44 μM) was added to extract, as indicated. Aliquots were withdrawn at indicated times and analysed by SDS–PAGE and western blotting. (**c**) Ubiquitin status in *Xenopus* extract was examined by anti-ubiquitin western blot analysis. (**d**) Levels of ubiquitin-charged endogenous ubch10 (ubch10~Ub) were examined by anti-ubch10 western blot analysis. Aliquots were removed at the indicated times and quenched with either non-reducing sample buffer to examine levels of ubch10~ubiquitin (top immunoblot) or reducing sample buffer to examine total levels of ubch10 (bottom immunoblot). (**e**) Levels of endogenous ubiquitin-charged ubch5 (ubch5~Ub) were examined by western blotting (non-reducing buffer, top; reducing buffer, bottom). Uncropped images of immunoblots are presented in Supplementary Fig. S9.

extracts, we measured the degradation of a purified, ^{35}S-labelled amino-terminal fragment of human cyclin B1 (cycB1-NT), which was degraded in an APC/C- and proteasome-dependent manner (Supplementary Fig. S1a–d). Using ubiquitin absolute quantification (AQUA) measurements[11,28], we calculated that free ubiquitin is present at 5–10 μM concentration in *Xenopus* extracts (D.K. and N.H., unpublished observations). When added at 44 μM or 116 μM final concentration, wild-type ubiquitin and different ubiquitin mutants containing a single lysine-to-arginine substitution at position 11, 48 or 63, or at all three positions simultaneously (Ub^{triR}), stimulated cycB1-NT proteolysis, albeit with different kinetics (Supplementary Fig. S1e,f). These results were unexpected, as mass spectrometric analysis indicated that elimination of all three principal sites of ubiquitin–ubiquitin linkage by the APC/C rendered ubiquitin incapable of forming ubiquitin chains in reconstituted reactions (Supplementary Fig. S2). In contrast, addition of methylated ubiquitin (Ub^{me}) was slightly inhibitory. These findings indicate that ubiquitin levels are limiting for proteolysis, and raise the question of whether ubiquitin chains are essential for cyclin B1 degradation in *Xenopus* extract.

We next sought to make *Xenopus* extracts dependent on exogenous ubiquitin by inhibiting ubiquitin recycling. Pre-treatment of extracts with ubiquitin vinyl sulfone (UbVS), a general inhibitor of ubiquitin isopeptidases[29], inhibited cyclin proteolysis in a dose-dependent manner, such that 20 μM UbVS inhibited degradation by 90–95% (Supplementary Fig. S3a). Degradation was fully restored by addition of 44 μM wild-type ubiquitin with partial rescue observed at lower concentrations (Fig. 1a). Concentrations of UbVS greater than 20 μM dampened the ability of 44 μM wild-type ubiquitin to restore degradation (Supplementary Fig. S3b). Mutations that interfere with recognition of ubiquitin by proteasome receptors (L8A, I44A or V70A; refs 30–32) hampered its ability to support proteolysis (Fig. 1b). In contrast, mutations that interfere with the non-proteolytic functions of ubiquitin (F4A (refs 33,34) or D58A (refs 35,36)) had no effect on its ability to stimulate degradation (Fig. 1b). UbVS treatment led to loss of ubiquitylated species in the extract (Fig. 1c) and near complete discharge of E2 ~ ubiquitin thioesters (Fig. 1d,e); both effects were reversed following addition of exogenous ubiquitin.

We next examined the ability of chain-terminating ubiquitin mutants to rescue degradation in UbVS-treated extracts. Addition of wild-type ubiquitin, Ub^{48R} and Ub^{63R} rescued degradation efficiently, showing a half-life of approximately 15 min (Fig. 2a). After 20 min, the rate of degradation slowed, probably a consequence of ubiquitin depletion in

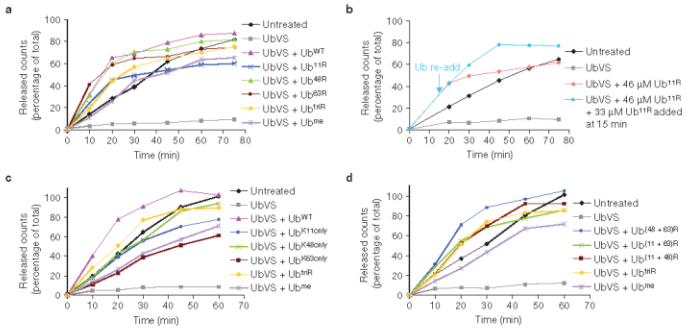

Figure 2 Ubiquitin-chain formation is not essential for cyclin B1 degradation in UbVS-treated *Xenopus* extract. ^{35}S-labelled cycB1-NT and different forms of ubiquitin, where indicated, were introduced concomitantly into mitotically arrested *Xenopus* extract that had been pre-treated with UbVS (20 μM) or buffer (untreated) for 30 min. Proteolysis was measured by release of trichloroacetic-acid-soluble counts, and is plotted as the percentage of input radiolabelled cycB1-NT. Trends are representative of three or more independent experiments. Ub^{WT}, wild-type ubiquitin; Ub^{me}, methylated ubiquitin. (**a**) Ubiquitin types (44 μM) with single lysine-to-arginine mutations at indicated positions or at all three positions Lys 11, 48 and 63 (Ub^{triR}) were added to UbVS-treated extract. (**b**) Ub^{11R} and substrate were introduced into UbVS-treated extract, and supplemented with Ub^{11R} or buffer control 15 min after initiation of degradation. (**c**) Ubiquitin types (44 μM), as indicated. Ub^{KXOnly} refers to ubiquitin that has all of its lysines, except for those specified, mutated to arginines. (**d**) Degradation was measured in the presence of different ubiquitin types (44 μM) containing arginine substitutions at two of the three principal sites of ubiquitin–ubiquitin conjugation by the APC/C.

the UbVS-treated extract, as supplementation with additional ubiquitin restored degradation to the initial rate (Fig. 2b). Extracts supplemented with Ub^{11R} or Ub^{triR} degraded substrate with surprisingly fast kinetics. Even addition of Ub^{me} (Fig. 2c) or a lysine-less ubiquitin (Ub^{E0}; Supplementary Fig. S3c) supported degradation, with a half-life of approximately 30 min. We next assessed how constraining the topology of ubiquitin chains to a single lysine residue affected degradation of cycB1-NT (Fig. 2c). Addition of $Ub^{K11only}$ or $Ub^{K48only}$ to UbVS-treated extract restored cycB1-NT proteolysis, but with slower kinetics when compared with wild-type ubiquitin. As mutation of Lys 6 of ubiquitin may have an inhibitory effect on proteasomal degradation[37], we examined the effect of restricting chain formation to one of the three principal sites of ubiquitin–ubiquitin attachment mediated by UBCH10 by mutating the remaining two (Supplementary Fig. S2). $Ub^{(48+63)R}$ stimulated degradation efficiently, consistent with the ability of Lys 11 linkages to support degradation (Fig. 2d). Ubiquitin forms supporting Lys 48 and Lys 63 linkages ($Ub^{(11+63)R}$ and $Ub^{(11+48)R}$, respectively) and Ub^{triR} supported proteolysis with slightly slower kinetics. Together these findings indicate that the ability to construct Lys 11-linked chains provides a kinetic advantage for degradation, but the advantage is modest. In principle this advantage could arise from the utilization of Lys 11 in chain-forming reactions catalysed by UBCH10, or from a role of UBE2S, which elongates ubiquitin chains exclusively through Lys 11 linkages.

Ubiquitin chains are required for cyclin B1 degradation only when the number of available lysine residues in cyclin B1 is restricted

Cyclin B1 contains 18 lysine residues in its unstructured N-terminal region upstream of the cyclin box; 15 of these lysine residues are located within the first 88 amino acids close to the destruction box (Fig. 3a). To rule out the possibility that our results were influenced by use of an N-terminal fragment of cyclin B1, we first examined proteolysis of full-length wild-type cyclin B1 in UbVS-treated extracts (Fig. 3c). Addition of Ub^{11R} or Ub^{triR} stimulated degradation, albeit at slightly reduced rates relative to wild-type ubiquitin. Ub^{me} also supported degradation of cyclin B1, although a small fraction of the protein accumulated in a triply ubiquitylated species. To examine whether reducing the number of lysines in cyclin B1 renders its proteolysis dependent on ubiquitin-chain formation, we measured degradation of cyclin B1 mutants that contained either one or four lysine residues in the first 115 amino acids only at position 64 ($cyc^{K64only}$) or at positions 59, 63, 64 and 67 ($cyc^{K59,63,64,67only}$). We chose these positions as mass spectrometry studies indicated that these lysine residues become ubiquitylated early in the course of reconstituted ubiquitylation reactions (D.K. and N.H., unpublished observations). $Cyc^{K64only}$ was degraded rapidly in untreated *Xenopus* extract, and was fully stabilized in UbVS-treated extract (Fig. 3c). However, unlike the case for wild-type cyclin B1, Ub^{11R} did not support efficient degradation of $cyc^{K64only}$. Similar results were obtained with Ub^{triR} and Ub^{me}, with the latter causing quantitative accumulation of cyclin B1 in a monoubiquitylated form. Restoration of three additional lysine residues in cyclin B1 ($cyc^{K59,63,64,67only}$) partially rescued its degradation in UbVS-treated extracts supplemented with Ub^{me} (Fig. 3d). We conclude that when deubiquitylating enzymes are inhibited, the attachment of single ubiquitin molecules to multiple lysine residues in cyclin is sufficient to target the substrate for degradation. Strict dependence on elaboration of ubiquitin chains seems to occur only when the number of available substrate lysines is restricted.

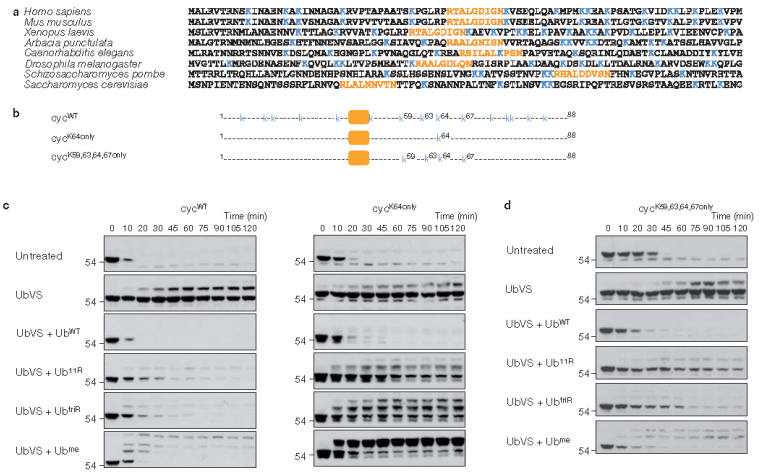

Figure 3 Cyclin B1 proteolysis depends on Lys 11-linked ubiquitin-chain formation only when the number of available lysine residues is restricted. (**a**) Sequence comparison of the cyclin B1 N termini from multiple species. Lysine residues are coloured in blue; the destruction box (D-box) is coloured in orange. (**b**) Schematic representation of the N-terminal region (residues 1–88) of human cyclin B1 with lysine residues denoted K in blue and with the D-box motif denoted with an orange rectangle. Cyclin B1 mutants ($cyc^{K64only}$ and $cyc^{K59,63,64,67only}$) were generated by substituting lysine with arginine at all but the specified lysine residues within the first 115 amino acids (residues 89–115 not shown). cyc^{WT}, wild-type cyclin B1. (**c**) Purified full-length wild-type or single-lysine cyclin B1, in complex with CDK1, and forms of ubiquitin (20 μM) as indicated were added to mitotic *Xenopus* egg extract that had been pre-treated with UbVS (20 μM) for 30 min. Ub^{WT}, wild-type ubiquitin; Ub^{me}, methylated ubiquitin. Stability of the exogenous substrate over time was assessed by SDS–PAGE and cyclin B1 western blot analysis. (**d**) As in **c**, except the behaviour of full-length $cyc^{K59,63,64,67only}$, in complex with CDK1, was analysed. Uncropped images of immunoblots are shown in Supplementary Fig. S9.

Multiple monoubiquitylation can target cyclin B1 for efficient degradation in a reconstituted system and in *Xenopus* extract

We next assessed whether the effects of ubiquitin mutants on proteolysis paralleled effects on ubiquitin conjugation in reconstituted ubiquitylation reactions. Elimination of Lys 48 or 63 of ubiquitin had no effect on the mass of conjugates generated by UBCH10, whereas elimination of Lys 11 reduced the mass of conjugates, consistent with the previously reported preference of UBCH10 for synthesizing Lys 11 ubiquitin–ubiquitin linkages[6,11] (Fig. 4a). In the presence of ubiquitin types that do not support ubiquitin polymer assembly (Ub^{trR} and Ub^{me}), the maximal extent of substrate modification (5–6 ubiquitins per cyclin B1 molecule) was observed at early time points and remained unchanged in longer reactions (Fig. 4a), implying that only a subset of the 18 lysine residues in the cyclin B1 N-terminal domain become ubiquitylated. A time course analysis of ubiquitylation with either wild-type ubiquitin or Ub^{trR} (Fig. 4b) revealed that the conjugation of ubiquitin monomers to distinct lysines in cyclin B1 occurs with rapid kinetics. Furthermore, conjugates bearing 4 or more ubiquitin moieties were capable of binding proteasome-associated ubiquitin-receptors[38–46] including Rpn10 (Fig. 4c,d) and Rad23 (Fig. 4e,f). For conjugates of a similar molecular mass, substrate ubiquitylated with Ub^{trR} bound to receptors more efficiently than substrate ubiquitylated with Ub^{me}, indicating that methylation of ubiquitin may compromise its affinity for ubiquitin receptors. We found similar binding patterns with cyclin B1–ubiquitin conjugates generated with UBC4 as the E2 (data not shown). Together these results indicate that multiple monoubiquitylation occurs rapidly and can result in a productive signal for binding ubiquitin receptors.

We next sought to determine whether multiple monoubiquitylation can target cyclin B1 for degradation in a reconstituted system. Full-length cyclin B1 in complex with CDK1 was ubiquitylated with either UBCH10 or UBC4, in conjunction with wild-type or mutant ubiquitin. The resulting conjugates were incubated with purified human proteasomes that were washed with high salt concentrations to eliminate USP14, a deubiquitylating enzyme that can antagonize cyclin B1 degradation *in vitro*[47,48]. These proteasomes, which retain the deubiquitylating enzymes RPN11 and UCH37 (ref. 47), rapidly degraded polyubiquitylated cyclin B1 generated with UBCH10 (Fig. 5a) or UBC4 (Fig. 5b). Conjugates formed with Ub^{trR} or Ub^{Rb} were efficiently degraded, whereas those generated with Ub^{me} were degraded less rapidly, consistent with the defect in the ability of these conjugates to bind ubiquitin receptors (Fig. 4c,e). Similar results were obtained in a quantitative assay using radiolabelled full-length cyclin B1

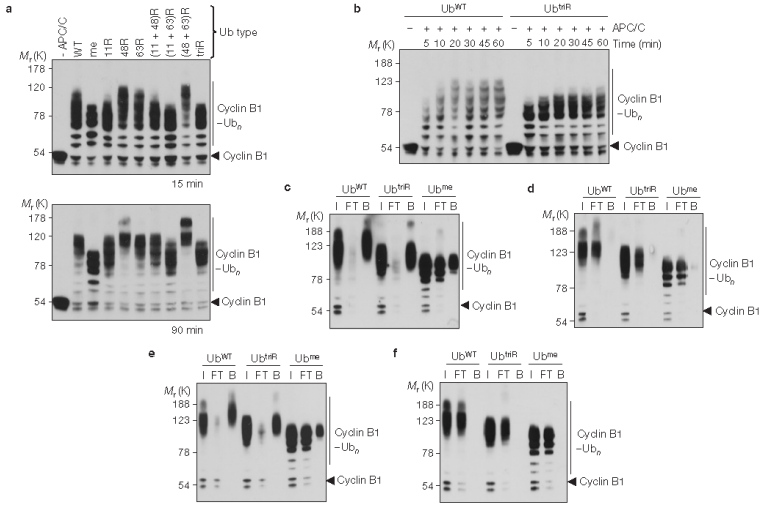

Figure 4 UBCH10 and APC/C catalyse rapid multiple monoubiquitylation of cyclin B1 that is sufficient for binding ubiquitin receptors. (**a**) Western blot analysis of the *in vitro* ubiquitylation reaction containing full-length cyclin B1, APC/C immunopurified from mitotically arrested *Xenopus* extract, recombinant UBCH10 (100 nM) and forms of ubiquitin (118 μM), as indicated. Ubiquitin types with lysine-to-arginine mutations at one, two or all three positions Lys 11, 48 and 63 (Ub^{trR}), as well as Ub^{me} (methylated ubiquitin) were used. Control '-APC/C' reactions containing all components except for the E3 ligase were carried out in parallel. Reactions were allowed to proceed for 15 or 90 min before analysis by SDS–PAGE and western blotting against cyclin B1. (**b**) Time course of the *in vitro* ubiquitylation of full-length wild-type cyclin B1 with wild-type ubiquitin or Ub^{trR} and remaining components as in **a**. (**c**–**f**) Binding of ubiquitylated cyclin B1 to GST-tagged ubiquitin receptors. Ub^{WT}, wild-type ubiquitin. Cyclin B1–ubiquitin conjugates were incubated with immobilized receptor proteins for 1 h at 4 °C before reaction products were subjected to SDS–PAGE and western blot analysis against cyclin B1. Equivalent amounts of input (I), flow-through (FT) and bound (B) fractions were loaded in adjacent lanes. Binding experiments with wild-type Rpn10 (**c**) and Rad23 (**e**). Binding with corresponding versions of the receptors lacking the ubiquitin-recognition domains, with engineered block substitution of the UIM domain (LAMAL → NNNNN) of Rpn10 (**d**) or deletion of the ubiquitin-associated domains of Rad 23 (**f**).

(Supplementary Fig. S4). Degradation of cyclin B1 in the reconstituted system was confirmed to be both APC/C and ubiquitin dependent (Supplementary Figs S4 and S5c). Similar experiments with radiolabelled cycB1-NT pre-ubiquitylated by UBCH10 (Fig. 5c) revealed that that degradation of multiply monoubiquitylated cyclin B1 was sensitive to addition of the deubiquitylating enzyme USP14 (Fig. 5d). This effect was reversed by IU1, an inhibitor of the catalytic activity of USP14 (Supplementary Fig. S5; ref. 47). Together these results indicate that purified proteasomes can efficiently degrade multiply monoubiquitylated cyclin B1 and that USP14 can deubiquitylate this substrate to suppress degradation.

To determine whether multiple monoubiquitylation can target cyclin B1 for degradation under physiological conditions in the presence of active deubiquitylating enzymes, we added the ubiquitylated species analysed in Fig. 5c to interphase *Xenopus* extract, a state in which the APC/C is inactive (Fig. 5e). Conjugates generated with wild-type ubiquitin or Ub^{trR} were efficiently degraded, whereas conjugates generated with Ub^{me} were degraded less efficiently. Similar results were obtained when the ubiquitin conjugates were introduced into extracts supplemented with excess non-ubiquitylated unlabelled competitor to prevent additional APC/C-mediated ubiquitylation (Supplementary Fig. S6b,c) or to extracts that had been immunodepleted of APC/C (Supplementary Fig. S6f). Pre-treatment with UbVS, at a concentration identical to that used to deplete free ubiquitin, did not accelerate degradation of conjugates (Fig. 5e). Similarly, addition of an inhibitor of USP14, IU1, failed to accelerate degradation of cyclin B1 in *Xenopus* extracts (Supplementary Fig. S7). Together these findings indicate that *Xenopus* extracts can rapidly degrade cyclin B1 bearing multiple ubiquitin monomers attached to distinct lysine residues.

Analysis of the role of UBE2S in cyclin B1 degradation

The ability of Ub^{11R} and chain-terminating ubiquitins to support proteolysis raised a question as to whether the E2 enzyme UBE2S is required for cyclin B1 degradation in *Xenopus* extract. We therefore

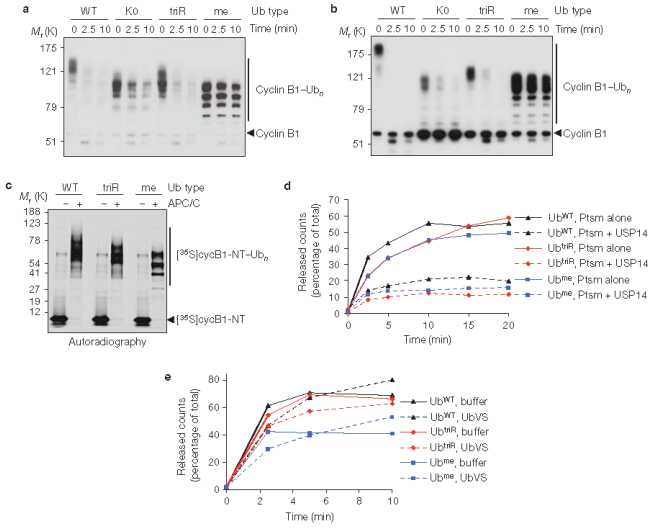

Figure 5 Multiple monoubiquitylated cyclin B1 is rapidly degraded by purified proteasomes and in *Xenopus* extract. (**a**) *In vitro* degradation assay with cyclin B1–ubiquitin species generated with immunopurified *Xenopus* APC/C, recombinant UBCH10 (250 nM) and forms of ubiquitin (145 μM), as indicated, and USP14-deficient human proteasomes (20 nM). WT, wild type; K0, lysine-less; triR, lysine-to-arginine mutations at one, two or all three positions Lys 11, 48 and 63; me, methylated. Aliquots were removed at the indicated times and reaction products analysed by SDS–PAGE and anti-cyclin B1 western blot analysis. **b** The same as in **a**, but conjugates were generated with UBC4 as the E2 enzyme. (**c**) Autoradiograph of *in vitro* APC/C- and UBCH10-catalysed ubiquitylation of ^{35}S-labelled cycB1-NT (1–88) with immunopurified *Xenopus* APC/C, recombinant UBCH10 (100 nM) and forms of ubiquitin (145 μM) as indicated. Products from a 60-min ubiquitylation assay were separated by SDS–PAGE and analysed using a phosphorimager. (**d**) cycB1-NT–ubiquitin species from **c** were incubated with purified human proteasomes (Ptsm; 20 nM) reconstituted with or without a 20-fold molar excess of GST-tagged wild-type USP14. Ub^{WT}, wild-type ubiquitin. At indicated times, reactions were terminated by addition of trichloroacetic acid. Proteolysis was measured by release of trichloroacetic-acid-soluble counts, and is plotted as the percentage of input radiolabelled cyclin B1 protein. See Supplementary Fig. S5c for additional controls. (**e**) cycB1-NT–ubiquitin species from **c** were added to interphase *Xenopus* extract that had been pre-treated with UbVS (15 μM) or buffer control for 30 min. Reactions were terminated by addition of trichloroacetic acid at indicated times. Proteolysis was measured by release of trichloroacetic-acid-soluble counts, and is plotted as the percentage of input radiolabelled cycB1-NT.

immunodepleted the protein and measured how this affected cyclin degradation. Antibodies efficiently depleted the UBE2S protein, as observed by the absence of signal following 25-fold enrichment of E2 enzymes on ubiquitin agarose (Fig. 6a), without affecting levels of the APC/C or the E2 UBCH10 (Fig. 6a). UBE2S depletion caused only a slight increase in the half-life of cycB1-NT as compared with control-depleted extract (Fig. 6b), which was reversed by adding back 10 nM of the recombinant enzyme. We reasoned that UBE2S is not essential for rapid degradation of cyclin B1 because the substrate contains multiple lysine residues that can serve as sites of attachment of short ubiquitin chains. We therefore examined the effect of UBE2S depletion on the rate of degradation of cyc^{K64only} compared with that of wild-type cyclin B1 (Fig. 6c). Degradation of full-length wild-type cyclin B1 was unaffected by depletion of UBE2S, but proteolysis of cyc^{K64only} was highly sensitive to the depletion of UBE2S, and addition of recombinant UBE2S fully restored degradation (Fig. 6c). Together these findings indicate that UBE2S is present in *Xenopus* extract at sufficient levels to support cyclin proteolysis, but becomes essential only when the number of ubiquitylatable lysine residues in cyclin B1 is restricted. Similarly, we found that immunodepletion of UBCH10 (Supplementary Fig. S8a) had a modest effect on degradation of wild-type cyclin B1, but more significantly delayed turnover of cyc^{K64only} (Supplementary Fig. S8b). The delay in degradation of cyc^{K64only} was rescued by addition of 50 nM of recombinant UBCH10. These findings indicate that other E2 enzymes in the extract may be sufficient to support APC/C-dependent degradation of cyclin B1 in *Xenopus* extracts. Enzymes of the UBC4/5 class are the best candidates for such a role, but we were unable to identify an antibody that could efficiently deplete endogenous UBC4/5 and thus could not evaluate their role in cyclin B1 degradation.

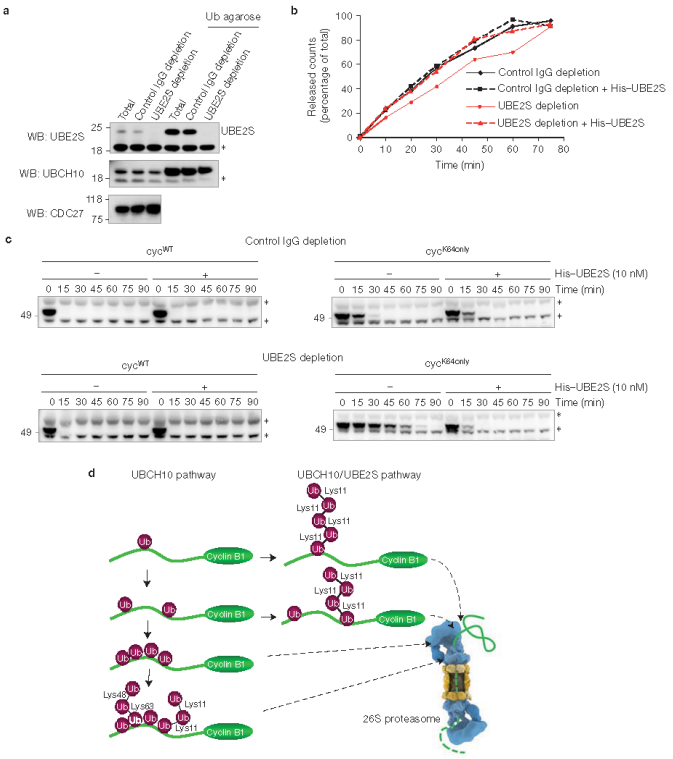

Figure 6 UBE2S is required for cyclin B1 proteolysis only when ubiquitylation is constrained to a single lysine. (**a**) Mitotically arrested *Xenopus* extract was immunodepleted with UBE2S antibody or control IgG. Samples were further incubated with ubiquitin agarose (10:1 ratio of extract to resin) to enrich for E2 enzymes, and bound proteins were analysed by SDS–PAGE and immunoblotting. Lanes 4–6 represent 25-fold enrichment of E2 enzymes on ubiquitin agarose. Levels of UBE2S, UBCH10 and APC/C subunit CDC27 were examined by immunoblotting. Asterisks, nonspecific signal. Uncropped images of immunoblots are shown in Supplementary Fig. S9. (**b**) Rate of degradation of ^{35}S-labelled cycB1-NT in UBE2S- or control-depleted mitotic *Xenopus* extract from **a**. Recombinant His–UBE2S (10 nM), where indicated, was added to reactions concomitantly with substrate. Proteolysis was measured by release of trichloroacetic-acid-soluble counts, and is plotted as the percentage of input radiolabelled cycB1-NT. (**c**) Time course of degradation of full-length cyclin B1 (cyc^{WT}) or single-lysine-containing mutant, each in complex with CDK1, in control- or UBE2S-depleted mitotic *Xenopus* extract. Recombinant His–UBE2S (10 nM), where indicated, was added to reactions concomitantly with substrate. Cyclin B1 proteolysis was analysed by SDS–PAGE and immunoblotting. Asterisks, nonspecific signal. Uncropped images of immunoblots are shown in Supplementary Fig. S9. (**d**) Model of cyclin B1 degradation in *Xenopus* cell-cycle extract. The APC/C and the E2 UBCH10 collaborate to transfer ubiquitin monomers to multiple lysine residues on cyclin B1, with subsequent elaboration of short ubiquitin chains containing Lys 63, Lys 48 and Lys 11 linkages, with Lys 11 linkages predominating[11]. On achievement of a threshold of ubiquitin mass, which seems to be 4–5 ubiquitin monomers, multiply monoubiquitylated substrate can associate with proteasome-associated ubiquitin receptors and be degraded efficiently. However, when the number of lysine residues in cyclin B1 is restricted, ubiquitylation catalysed by UBCH10 is insufficient for rapid proteolysis and the activity of UBE2S in extending Lys 11-linked ubiquitin polymers becomes important for efficient degradation.

DISCUSSION

Here we have evaluated the role of ubiquitin-chain topology in targeting cyclin B1 for degradation. Our study was motivated by recent findings indicating that Lys 11 linkages, mediated by the chain-forming E2 enzyme UBE2S, may be important for APC/C-dependent proteolysis. However, our earlier work indicated that APC/C, solely in conjunction with the E2 enzyme UBCH10 or the enzyme UBC4/5, can build a ubiquitin signal that is sufficient for degradation by purified proteasomes[11]. Here we provide a resolution to this paradox, demonstrating that conjugation of ubiquitin to multiple lysine residues of cyclin B1 provides an alternative degradation signal for cyclin B1 that does not require chain extension by the Lys 11-specific E2 UBE2S. Lys 11-linked ubiquitin-chain formation becomes essential only when the number of available lysine residues in cyclin B1 is restricted.

Dominant-negative effects of different ubiquitin types may be difficult to observe when examined in a background that contains wild-type ubiquitin. By inhibiting ubiquitin recycling, we were able to impose a state of ubiquitin deficiency in extract sufficient to stabilize cyclin B1. The strong dependence of cyclin proteolysis on ubiquitin availability has not been previously appreciated, and supports the possibility that control of ubiquitin availability could regulate the rate of APC/C substrate degradation. Addition of ubiquitin fully rescues cyclin degradation in UbVS-treated extracts, but the rate of cyclin degradation is no faster in a UbVS-treated extract relative to a non-treated extract. This finding indicates that for deubiquitylating enzymes to be able to antagonize degradation, it may be crucial that the rate of ubiquitylation be constrained by limiting the availability of free ubiquitin.

The UbVS system enabled us to define the role of different chain linkages in targeting substrates for degradation by the proteasome. In agreement with earlier work in a reconstituted system[11], Lys 48 ubiquitin linkages were not required for efficient cyclin proteolysis in UbVS-treated extract. Surprisingly, in the light of recent studies[6,7,10], ubiquitin incapable of forming Lys 11 linkages (Ub^{11R}) also supported efficient degradation of cyclin B1. Importantly, we found that chain-terminating ubiquitins (Ub^{tri} and lysine-less ubiquitin) also supported robust rates of cyclin proteolysis. Ub^{mi} was less capable of supporting rapid degradation, which may reflect less efficient recognition by ubiquitin receptors and the proteasome due to modification of Lys 6 of ubiquitin[37]. However, on restriction of ubiquitylation to a single lysine residue in cyclin as in $cyc^{R64only}$, chain-terminating ubiquitins were no longer able to support substrate degradation. Together these findings indicate that ubiquitin-chain formation may not be essential for cyclin proteolysis unless the number of available lysine residues is restricted.

We propose that attachment of monoubiquitin to multiple lysines in cyclin B1 has the potential for generating a high density of ubiquitin that promotes receptor binding (Fig. 6d). In such an arrangement, the hydrophobic patches on distinct ubiquitin units may be able to engage multiple ubiquitin receptors. Multiply monoubiquitylated cyclin B1 thus resembles a ubiquitin chain, except that the cyclin B1 polypeptide chain is used as a backbone to link one ubiquitin molecule to another. Whether particular spacing of ubiquitylated lysine residues is essential for recognition by ubiquitin receptors remains unknown. In our pulldown experiments, there may be some enhanced avidity resulting from a dimeric glutathione-*S*-transferase (GST) moiety positioning two ubiquitin-associated domains in close proximity[49]. However, the ability of the multiply monoubiquitylated protein to be degraded by purified proteasomes and in *Xenopus* extracts indicates that this substrate must have sufficient affinity for proteasome-associated ubiquitin receptors to support proteolysis.

The capacity of purified proteasomes to rapidly degrade multiply monoubiquitylated cyclin B1 was significantly suppressed by USP14, indicating that USP14 can efficiently remove monoubiquitin, as well as trim ubiquitin chains. However, USP14 does not seem to strongly antagonize proteasome function in *Xenopus* extract, as treatment of extract with UbVS or the USP14-specific inhibitor IU1 did not appreciably enhance turnover of pre-ubiquitylated cyclin. Although present in *Xenopus* extracts (N.V.D. and R.W.K., unpublished data), levels of USP14 associated with proteasomes in extract may be insufficient to impede proteolysis. Together, these findings indicate that the proteasome does not impose a requirement for ubiquitin-chain formation for efficient proteolysis of cyclin B1 in *Xenopus* extract. Our study further strengthens the view that the proteasome has the capacity to recognize and degrade substrates bearing ubiquitin modifications distinct from the canonical Lys 48-linked polyubiquitin chains[4,50–53].

Although UBE2S is sufficient to elongate Lys 11-linked ubiquitin chains to promote the degradation of APC/C substrates[7–10], we found that UBE2S depletion of *Xenopus* egg extract had no impact on degradation of wild-type cyclin B1. Our findings are consistent with the report that UBE2S is largely dispensable for cyclin B1 degradation in unperturbed mitosis in human cells[8]. The lack of requirement for UBE2S and Lys 11-linked ubiquitin chains for robust degradation of cyclin B1 in the *Xenopus* system may be a consequence of higher levels of UBCH10 than seen in other biological contexts[7,8]. Furthermore, the relative importance of UBCH10 and UBE2S in degradation of different APC/C substrates may vary. Human cyclin B1 is lysine rich in its N-terminal domain, containing 18 lysine residues, whereas cyclin A2 has 12 lysine residues in the same region, which may make the latter protein more dependent on the chain-elongating enzyme UBE2S for degradation. Similarly, *Saccharomyces cerevisiae* Clb2 is relatively lysine poor in its N-terminal domain, containing only 6 lysine residues, potentially explaining the importance of a chain-elongating E2 in this system[27]. A greater dependence on chain-elongating E2s may impact the sensitivity of different substrates to deubiquitylation. In this regard, cyclin A2 degradation during interphase is specifically impeded by the deubiquitylating enzyme USP37 (ref. 54), but this enzyme does not seem to antagonize cyclin B1 degradation. An interesting future question is how the balance between multiple monoubiquitylation and ubiquitin-chain formation affects sensitivity of degradation to deubiquitylating enzymes. Finally, our work raises the possibility that the degree of dependence on UBE2S could be regulated by post-translational modification of the substrate. For example, acetylation is known to affect degradation of the spindle-checkpoint protein BubR1 (ref. 55). By restricting the number of ubiquitylatable lysine residues, acetylation could increase the dependence of degradation pathways on UBE2S-catalysed chain formation. □

METHODS

Methods and any associated references are available in the online version of the paper at http://www.nature.com/naturecellbiology

Note: Supplementary Information is available on the Nature Cell Biology website

ACKNOWLEDGEMENTS

We thank D. Morgan (UCSF, USA) for baculoviruses encoding human cyclin B1 and CDK1. Human ubiquitin cloned in pET3a was a gift from C. M. Pickart (Johns Hopkins University, USA). Antibody for UBCH10 immunodepletion was a gift from H. Yu (UT Southwestern, USA). We thank M. Aguilar (Gygi laboratory, Harvard Medical School, USA) for carrying out mass spectrometry to confirm the presence of UBE2S and USP14 in *Xenopus* egg extract, and H. Besche and S. Elsasser (Harvard Medical School, USA), as well as K. Sackton and F. Sigoillot and the remaining members of the King laboratory, for helpful discussions. This work was financially supported by NIH GM66492 to R.W.K. and GM095526 to D.F.

AUTHOR CONTRIBUTIONS

N.V.D. and R.W.K. designed and interpreted the experiments. N.V.D. carried out and analysed all experiments except those outlined below. N.A.H. carried out cyclin B1 ubiquitylation for ubiquitin-AQUA analysis and degradation assays with these species in APC/C-depleted extract. D.S.K. carried out the ubiquitin-AQUA analysis on cyclin B1 ubiquitylated *in vitro* with the E2 UBC4 and different ubiquitin types in the laboratory of S.P.G. B-H.L. provided purified human proteasomes with oversight from D.F. M.L.B. helped with cloning of different cyclin B1 mutants. The manuscript was written by N.V.D. and R.W.K. with input from all authors.

COMPETING FINANCIAL INTERESTS

The authors declare no competing financial interests.

Published online at http://www.nature.com/naturecellbiology
Reprints and permissions information is available online at http://www.nature.com/reprints

1. Thrower, J. S., Hoffman, L., Rechsteiner, M. & Pickart, C. M. Recognition of the polyubiquitin proteolytic signal. *EMBO J.* **19,** 94–102 (2000).
2. Finley, D. *et al.* Inhibition of proteolysis and cell cycle progression in a multiubiquitination-deficient yeast mutant. *Mol. Cell. Biol.* **14,** 5501–5509 (1994).
3. Chau, V. *et al.* A multiubiquitin chain is confined to specific lysine in a targeted short-lived protein. *Science* **243,** 1576–1583 (1989).
4. Baboshina, O. V. & Haas, A. L. Novel multiubiquitin chain linkages catalyzed by the conjugating enzymes E2EPF and RAD6 are recognized by 26S proteasome subunit 5. *J. Biol. Chem.* **271,** 2823–2831 (1996).
5. Xu, P. *et al.* Quantitative proteomics reveals the function of unconventional ubiquitin chains in proteasomal degradation. *Cell* **137,** 133–145 (2009).
6. Jin, L., Williamson, A., Banerjee, S., Philipp, I. & Rape, M. Mechanism of ubiquitin-chain formation by the human anaphase-promoting complex. *Cell* **133,** 653–665 (2008).
7. Williamson, A. *et al.* Identification of a physiological E2 module for the human anaphase-promoting complex. *Proc. Natl Acad. Sci. USA* **106,** 18213–18218 (2009).
8. Garnett, M. J. *et al.* UBE2S elongates ubiquitin chains on APC/C substrates to promote mitotic exit. *Nat. Cell Biol.* **11,** 1363–1369 (2009).
9. Matsumoto, M. L. *et al.* K11-linked polyubiquitination in cell cycle control revealed by a K11 linkage-specific antibody. *Mol. Cell* **39,** 477–484 (2010).
10. Wu, T. *et al.* UBE2S drives elongation of K11-linked ubiquitin chains by the anaphase-promoting complex. *Proc. Natl Acad. Sci. USA* **107,** 1355–1360 (2010).
11. Kirkpatrick, D. S. *et al.* Quantitative analysis of *in vitro* ubiquitinated cyclin B1 reveals complex chain topology. *Nat. Cell Biol.* **8,** 700–710 (2006).
12. Spence, J., Sadis, S., Haas, A. L. & Finley, D. A ubiquitin mutant with specific defects in DNA repair and multiubiquitination. *Mol. Cell. Biol.* **15,** 1265–1273 (1995).
13. Hofmann, R. M. & Pickart, C. M. Noncanonical MMS2-encoded ubiquitin-conjugating enzyme functions in assembly of novel polyubiquitin chains for DNA repair. *Cell* **96,** 645–653 (1999).
14. Deng, L. *et al.* Activation of the IκB kinase complex by TRAF6 requires a dimeric ubiquitin-conjugating enzyme complex and a unique polyubiquitin chain. *Cell* **103,** 351–361 (2000).
15. Pickart, C. M. & Fushman, D. Polyubiquitin chains: polymeric protein signals. *Curr. Opin. Chem. Biol.* **8,** 610–616 (2004).
16. Yang, W. L. *et al.* The E3 ligase TRAF6 regulates Akt ubiquitination and activation. *Science* **325,** 1134–1138 (2009).
17. Spence, J. *et al.* Cell cycle-regulated modification of the ribosome by a variant multiubiquitin chain. *Cell* **102,** 67–76 (2000).
18. Robzyk, K., Recht, J. & Osley, M. A. Rad6-dependent ubiquitination of histone H2B in yeast. *Science* **287,** 501–504 (2000).
19. Terrell, J., Shih, S., Dunn, R. & Hicke, L. A function for monoubiquitination in the internalization of a G protein-coupled receptor. *Mol. Cell* **1,** 193–202 (1998).
20. Haglund, K. *et al.* Multiple monoubiquitination of RTKs is sufficient for their endocytosis and degradation. *Nat. Cell Biol.* **5,** 461–466 (2003).
21. Mosesson, Y. *et al.* Endocytosis of receptor tyrosine kinases is driven by monoubiquitylation, not polyubiquitylation. *J. Biol. Chem.* **278,** 21323–21326 (2003).
22. Huang, F., Kirkpatrick, D., Jiang, X., Gygi, S. & Sorkin, A. Differential regulation of EGF receptor internalization and degradation by multiubiquitination within the kinase domain. *Mol. Cell* **21,** 737–748 (2006).
23. Kravtsova-Ivantsiv, Y., Cohen, S. & Ciechanover, A. Modification by single ubiquitin moieties rather than polyubiquitination is sufficient for proteasomal processing of the p105 NF-κB precursor. *Mol. Cell* **33,** 496–504 (2009).
24. Peters, J. M. The anaphase promoting complex/cyclosome: a machine designed to destroy. *Nat. Rev. Mol. Cell Biol.* **7,** 644–656 (2006).
25. Skaar, J. R. & Pagano, M. Control of cell growth by the SCF and APC/C ubiquitin ligases. *Curr. Opin. Cell Biol.* **21,** 816–824 (2009).
26. Petroski, M. D. & Deshaies, R. J. Mechanism of lysine 48-linked ubiquitin-chain synthesis by the cullin-RING ubiquitin-ligase complex SCF-Cdc34. *Cell* **123,** 1107–1120 (2005).
27. Rodrigo-Brenni, M. C. & Morgan, D. O. Sequential E2s drive polyubiquitin chain assembly on APC targets. *Cell* **130,** 127–139 (2007).
28. Kirkpatrick, D. S., Gerber, S. A. & Gygi, S. P. The absolute quantification strategy: a general procedure for the quantification of proteins and post-translational modifications. *Methods* **35,** 265–273 (2005).
29. Borodovsky, A. *et al.* A novel active site-directed probe specific for deubiquitylating enzymes reveals proteasome association of USP14. *EMBO J.* **20,** 5187–5196 (2001).
30. Beal, R., Deveraux, Q., Xia, G., Rechsteiner, M. & Pickart, C. Surface hydrophobic residues of multiubiquitin chains essential for proteolytic targeting. *Proc. Natl Acad. Sci. USA* **93,** 861–866 (1996).
31. Beal, R. E., Toscano-Cantaffa, D., Young, P., Rechsteiner, M. & Pickart, C. M. The hydrophobic effect contributes to polyubiquitin chain recognition. *Biochemistry* **37,** 2925–2934 (1998).
32. Lam, Y. A., DeMartino, G. N., Pickart, C. M. & Cohen, R. E. Specificity of the ubiquitin isopeptidase in the PA700 regulatory complex of 26S proteasomes. *J. Biol. Chem.* **272,** 28438–28446 (1997).
33. Shih, S. C., Sloper-Mould, K. E. & Hicke, L. Monoubiquitin carries a novel internalization signal that is appended to activated receptors. *EMBO J.* **19,** 187–198 (2000).
34. Sloper-Mould, K. E., Jemc, J. C., Pickart, C. M. & Hicke, L. Distinct functional surface regions on ubiquitin. *J. Biol. Chem.* **276,** 30483–30489 (2001).
35. Penengo, L. *et al.* Crystal structure of the ubiquitin binding domains of rabex-5 reveals two modes of interaction with ubiquitin. *Cell* **124,** 1183–1195 (2006).
36. Lee, S. *et al.* Structural basis for ubiquitin recognition and autoubiquitination by Rabex-5. *Nat. Struct. Mol. Biol.* **13,** 264–271 (2006).
37. Shang, F. *et al.* Lys6-modified ubiquitin inhibits ubiquitin-dependent protein degradation. *J. Biol. Chem.* **280,** 20365–20374 (2005).
38. Deveraux, Q., Ustrell, V., Pickart, C. & Rechsteiner, M. A 26S protease subunit that binds ubiquitin conjugates. *J. Biol. Chem.* **269,** 7059–7061 (1994).
39. Elsasser, S., Chandler-Militello, D., Muller, B., Hanna, J. & Finley, D. Rad23 and Rpn10 serve as alternative ubiquitin receptors for the proteasome. *J. Biol. Chem.* **279,** 26817–26822 (2004).
40. Elsasser, S. & Finley, D. Delivery of ubiquitinated substrates to protein-unfolding machines. *Nat. Cell Biol.* **7,** 742–749 (2005).
41. Rao, H. & Sastry, A. Recognition of specific ubiquitin conjugates is important for the proteolytic functions of the ubiquitin-associated domain proteins Dsk2 and Rad23. *J. Biol. Chem.* **277,** 11691–11695 (2002).
42. Matiuhin, Y. *et al.* Extraproteasomal Rpn10 restricts access of the polyubiquitin-binding protein Dsk2 to proteasome. *Mol. Cell* **32,** 415–425 (2008).
43. Finley, D. Recognition and processing of ubiquitin-protein conjugates by the proteasome. *Annu. Rev Biochem.* **78,** 477–513 (2009).
44. Isasa, M. *et al.* Monoubiquitination of RPN10 regulates substrate recruitment to the proteasome. *Mol. Cell* **38,** 733–745 (2010).
45. Peth, A., Uchiki, T. & Goldberg, A. L. ATP-dependent steps in the binding of ubiquitin conjugates to the 26S proteasome that commit to degradation. *Mol. Cell* **40,** 671–681 (2010).
46. Riedinger, C. *et al.* Structure of Rpn10 and its interactions with polyubiquitin chains and the proteasome subunit Rpn12. *J. Biol. Chem.* **285,** 33992–34003 (2010).
47. Lee, B. H. *et al.* Enhancement of proteasome activity by a small-molecule inhibitor of USP14. *Nature* **467,** 179–184 (2010).
48. Hanna, J. *et al.* Deubiquitinating enzyme Ubp6 functions noncatalytically to delay proteasomal degradation. *Cell* **127,** 99–111 (2006).
49. Sims, J. J., Haririnia, A., Dickinson, B. C., Fushman, D. & Cohen, R. E. Avid interactions underlie the Lys63-linked polyubiquitin binding specificities observed for UBA domains. *Nat. Struct. Mol. Biol.* **16,** 883–889 (2009).
50. Guterman, A. & Glickman, M. H. Complementary roles for Rpn11 and Ubp6 in deubiquitination and proteolysis by the proteasome. *J. Biol. Chem.* **279,** 1729–1738 (2004).
51. Hershko, A. & Heller, H. Occurrence of a polyubiquitin structure in ubiquitin-protein conjugates. *Biochem. Biophys. Res. Commun.* **128,** 1079–1086 (1985).
52. Hofmann, R. M. & Pickart, C. M. *In vitro* assembly and recognition of Lys-63 polyubiquitin chains. *J. Biol. Chem.* **276,** 27936–27943 (2001).
53. Boutet, S. C., Disatnik, M. H., Chan, L. S., Iori, K. & Rando, T. A. Regulation of Pax3 by proteasomal degradation of monoubiquitinated protein in skeletal muscle progenitors. *Cell* **130,** 349–362 (2007).
54. Huang, X. *et al.* Deubiquitinase USP37 is activated by CDK2 to antagonize APC(CDH1) and promote S phase entry. *Mol. Cell* **42,** 511–523 (2011).
55. Choi, E. *et al.* BubR1 acetylation at prometaphase is required for modulating APC/C activity and timing of mitosis. *EMBO J.* **28,** 2077–2089 (2009).

METHODS

Antibodies and reagents. Proteins were separated by SDS–PAGE on NuPAGE 4–12% or 12% Bis–Tris gels (Invitrogen), followed by wet transfer to PVDF. Sources of antibodies for immunoblotting were as follows: anti-cyclin B1 (Ab-2; RB-008-P, Neomarkers), anti-Cdc27 (610455, BD Transduction Laboratories), anti-UBCH10 (A-650, Boston Biochem; AB3861, Millipore), anti-UBE2S (N-14; sc-131354, Santa Cruz Biotechnology), anti-UBCH5 (A-615; Boston Biochem), anti-ubiquitin (P4D1; sc-8017; Santa Cruz Biotechnology). Secondary antibodies included anti-goat IgG–HRP (sc-2020; Santa Cruz Biotechnology); anti-rabbit IgG–HRP (NA934) and anti-mouse IgG–HRP (NA931) were from GE Healthcare. Antibodies for immunoprecipitation or immunodepletion included: anti-Cdc27 (AF3.1; sc-9972) and anti-UBE2S (N-14; sc-131354) from Santa Cruz Biotechnology; anti-UBCH10 (gift from H. Yu, UT Southwestern, USA); and for control depletions, normal rabbit (sc-2027) and normal goat (sc-2028) IgG, both from Santa Cruz Biotechnology. UBE2S antibodies were coupled to UltraLink immobilized protein A/G beads (53132, Pierce). UBCH10 and CDC27 antibodies were coupled to Affiprep protein A beads (156-0006, Bio-Rad). Ubiquitin agarose (U-405), UbVS (U-202), MG262 (I-120), Ub^{aa} and ubiquitin mutants except for $Ub^{(1-74)R}$, $Ub^{(1-76)R}$ and Ub^{noR} were purchased from Boston Biochem. TAME (T4626) and ubiquitin (U6253) were purchased from Sigma.

Preparation of recombinant proteins. Ubiquitin mutants $Ub^{(1-74)R}$, $Ub^{(1-76)R}$ and Ub^{noR} were generated by introducing arginine codons (AGA, AGG) through PCR-mediated mutagenesis of the human ubiquitin sequence (cloned in pET3a). Plasmids were verified by sequencing and the purified proteins analysed by mass spectrometry. To ensure efficient arginine incorporation, BL21(DE3) cells were co-transformed with pJY2 (refs 56), which carries T7 lysozyme (LysS) and a gene encoding $tRNA^{Arg}_{CCU}$. Cultures were grown at 37°C to an attenuance (D) of ~0.5 at 600 nm, and induced with 100 μM IPTG at $D_{600\,nm} = 0.6$ at 25°C for 5 h. Cells were ruptured by sonication in QA lysis buffer (50 mM HEPES (pH 7.7), 100 mM KCl, protease-inhibitor cocktail, 5 mM 2-mercaptoethanol and 10 μg ml^{-1} DNase), lysozyme was added to 1 mg ml^{-1} concentration, and incubated with rotation at 4°C for 15 min. Following sonication, cell lysates were clarified by centrifugation and the resulting supernatants applied to a Q column. The flow-through containing ubiquitin was concentrated and purified by size-exclusion chromatography. Fractions containing ubiquitin were typically >95% pure.

To generate full-length cyclin B1–CDK1 complex, human cyclin B1 and CDK1 baculoviruses were used as described previously[11]. To generate mutants of cyclin B1, DNA fragments encoding the N-terminal 124 amino acids of wild-type human cyclin B1 (5′-AACCGGTCGAAACCGTCGACATGTCGCATCACCAT-CACCATCACGGCTCGATGGCGCTCGAGTCACGGGTAACTCGAAAATTAA-TGCTGAAAATAAAGCGAAAATCAACATGGCAGGCGGCAAGGCGGTTCCTA-CGGCACCGGCGGCAACCTCCAAACCCGGGCTGAGGCAAGAACAGCTCT-TGGGGACATTGGTAACAAAGTCAGTGAACAGCTACAGGCCAAAATGCCTA-TGAAAAAAGAAGCAAAACCTTCAGCTACCGGTAAAGTCATTGATAAAAAA-CTACCAAAACCTCTTGAAAAGGTACCTATGCTGGTGCCAGTGCCAGTGTC-TGAGCCAGTGCCAGAGCCAGAACCTGAGCCAGAACCTGAGCCTGTTAAA-GAAGAAAAACTTTCGCCTGAGCCTATTTTGGTTGATACTGCTAGCAATA-3′) or the same region of the protein with arginine substitutions at all lysine residues (cyc^{nlR}; 5′-AACCGGTCCGAAACCGTCGACATGTCGCATC-ACCATCACCATCACGGCTCGATGGCGCTCCGAGTCACGCGTAACTCGAGA-ATTAATGCTGAAAATAGAGCGAGAATCAACATGGCAGGCGGCAGGCGCG-TTCCTACGGCACCGGCGGCAACCTCCAGACCCGGGCTGAGGCCAAGAAC-AGCTCTTGGGGACATTGGTAACAGAGTCAGTGAACAGCTACAGGCCAGA-ATGCCTATGAGAAGAGAAGCAAGACCTTCAGCTACCGGTAGAGTCATTG-ATAGAAGACTACCAAGACCTCTTGAAAGGGTACCTATGCTGGTGCCAGT-GCCAGTGTCTGAGCCAGTGCCAGAGCCAGAACCTGAGCCAGAACCTGA-GCCTGTTAGAGAAGAAAGACTTTCGCCTGAGCCTATTTTGGTTGATACT-GCTAGCAATA-3′) preceded by 6×His tag were synthesized (GenScript). Using restriction enzyme digestion with NheI and RsrII, fragments were subcloned into pFASTBac containing the carboxy terminus (125–433 amino acids) of cyclin B1. To generate $cyc^{R64A/R67A}$, primers 5′-TCCAGACCCGGGCTGAGGCCAAGAACAGC-TCTTGGGGACATTGGTAACAGAGTCAGTGAACAGCTACAGGCC-3′ and 5′-AATGACTCTACCGGTAGCTGAAGGTCTTGCTTCTTTTCTCATAGGCATTC-TGGCCTGTAGCTGTTCACTGAC-3′ were used for an extension reaction and the resulting fragments cloned into XmaI and AgeI cleavage sites of pFASTBac carrying full-length cyc^{nlR}. Plasmids were verified by restriction enzyme mapping and sequencing. Baculoviruses were generated according to the Bac-to-Bac manual (Invitrogen). Wild-type cyclin B1 was ^{35}S-labelled in Sf9 cultures by resuspending cells (1.5×10^6 cells ml^{-1}) in media containing 10% SF-900 II SFM and 90% SF-900 II SFM without methionine or cysteine (both from Invitrogen). Baculovirus was added to cells, along with 50 μCi of ^{35}S-labelled methionine and cysteine (NEG772; Perkin Elmer), and cyclin B1 expression was allowed for 2.5 days. CDK1 was expressed separately in Sf9 cells without radiolabelling and then combined with lysate from cells expressing cyclin B1 to allow formation of complex, which was then purified through Ni-NTA affinity and gel filtration chromatography.

cycB1-NT (1–88) containing an HA tag at the N terminus and a 6×His tag at the C terminus was generated using PCR amplification with forward primer (5′-CCAGGACCATGGGTTACCCATACGA-TGTTCCAGATTACGCTGGCTCGATGGCGCTCCGAGTCACG-3′) and reverse primer (5′-GGGAGCCTCGAGCTAGGGAGCGTGATGGTGATGGTGATGC-ATAGGTACCTTTTCAAGAGG-3′). The resulting PCR product was digested with NcoI and XhoI for subcloning into pET28a. Plasmids were verified by restriction enzyme mapping and sequencing. For ^{35}S labelling in *Escherichia coli*, cultures (50 ml) were grown at 37°C to $D_{600\,nm} = 0.8$, then collected by centrifugation (3,700*g* for 15 min, at 4°C) and resuspended in modified M9 medium (50 ml final volume). Cells were allowed to grow for 15 min at 37°C before 5 mCi of Easy Tag L-[^{35}S]methionine (NEG709A005MC; Perkin Elmer) was added. Expression was induced with 0.5 mM IPTG for 2.5 h at 37°C. Cells were ruptured in 5 ml g^{-1} of pellet guanidine-HCl lysis buffer (pH 8.0) and lysates rotated at 24°C until the lysate became slightly translucent; approximately 45 min. Lysates were cleared by centrifugation and cycB1-NT was purified using Ni-NTA affinity chromatography (Qiagen). Eluted protein was desalted into XB buffer (100 mM KCl, 0.1 mM $CaCl_2$, 1 mM $MgCl_2$ and 10 mM HEPES, at pH 7.8 with KOH), supplemented with 2% glycerol, protease inhibitors and phenylmethylsulfonyl fluoride, and stored at −20°C.

Maltose-binding protein (MBP)-tagged E1 was expressed in *E. coli* inducing cultures at $D_{600\,nm} = 0.6$ with 300 μM IPTG for 5 h at room temperature. Purification was carried out using a standard MBP purification protocol. For expression of His-tagged UBCH10 and His-tagged UBC4, bacterial cultures were induced at $D_{600\,nm} = 0.6$ at 37°C with 500 μM IPTG for 4 h. The enzymes were purified through Ni-NTA affinity and gel filtration chromatography. PET28a expressing human wild-type UBE2S was provided by M. Kirschner (Harvard Medical School, USA). Cultures were grown to $D_{600\,nm} = 0.4$ and induced with 500 μM IPTG at 37°C for 4 h. His–UBE2S was purified by Ni-NTA purification. GST-fusion proteins for Rpn10 and Rad23 were purified as reported previously[28,58].

Preparation of *Xenopus* egg extract. Interphase extract was prepared as described previously[57] but using 2 μg ml^{-1} calcium ionophore (A23187, Calbiochem) for egg activation. Interphase extract was induced to enter mitosis by addition of non-degradable cyclin B (MBP-Δ90; ref. 59) as described previously[60] except that extracts were treated for 45–60 min before assay.

Reconstitution of ubiquitylation and degradation of cyclin B1. Ubiquitylation reactions were carried out as described previously[11], but to minimize loss of Cdc20, immunoprecipitated APC/C was washed quickly three times with XB containing 500 mM KCl, two times with XB and then three times with reaction buffer. Ubiquitylation reactions were carried out at 24°C with agitation at 1,500 r.p.m. and contained APC/C on 30 μl beads, and 30 μl of a mix containing recombinant MBP–human E1 (1.3 μM), His-tagged UBCH10 or UBC4 (100 nM–4 μM), ubiquitin (118–145 μM) and 450–500 nM cyclin B1–CDK1 or cycB1-NT. For ubiquitin-receptor binding and degradation assays, reaction supernatants were combined with the first 20 μl of reaction buffer wash. For analysis of cyclin B1 ubiquitylation with different ubiquitins, entire reactions were processed for immunoblotting or autoradiography. Dried gels were analysed by phosphorimaging (Bio-Rad PMI); quantification was carried out with Quantity One software (Bio-Rad).

For binding experiments with ubiquitin receptors, cyclin B1–CDK1 was pre-ubiquitylated with purified *Xenopus* APC/C, UBCH10 (3 μM) and ubiquitin (118 μM) for 90 min. Binding was carried out essentially as described previously[11] in the presence of 0.1% Tween 20. Supernatants were collected and mixed with the first wash to make the flow-through fraction. Beads were washed twice and diluted with SDS sample buffer to analyse the bound fraction.

For degradation assays with purified proteasomes, human proteasomes (10–20 nM), purified as reported previously[47] but non-UbVS treated, were incubated with cyclin B1–Ub_R in buffer (50 mM Tris–HCl (pH 7.5), 5 mM $MgCl_2$ and 5 mM ATP; ref. 47) and incubated at 24°C. Recombinant GST–USP14 (ref. 47) was incubated with proteasome for ~5–10 min before initiating degradation. In experiments with USP14 inhibitor IU1 (ref. 47), GST–USP14 was pre-incubated with IU1 or dimethylsulphoxide for 5 min at 24°C before adding proteasomes. For degradation of cycB1-NT, reactions (20 μl proteasome mix and 4 μl cycB1-NT–Ub_R for each time point) were quenched with 81 μl of 32% trichloroacetic acid (TCA) and 20 μl bovine serum albumin (BSA; 10 mg ml^{-1} stock). For degradation of full-length cyclin B1, 90 μl proteasome mix was added to 10 μl cyclin B1–Ub_R for each time point, and the reaction quenched with 112 μl pre-chilled 2% perchloric acid (PCA) and 12 μl of BSA (10 mg ml^{-1} stock). For 0 min time point, substrate and proteasome mixtures were individually added to acid. Following acid addition, samples were incubated on ice ≥30 min and centrifuged at 14,000*g*, at 4°C. A fraction (50–80%) of supernatants and NaOH to neutralize TCA (or Tris Base to neutralize PCA) were added to Ultima Gold scintillation fluid (6013327, Perkin Elmer). A Packard

DOI: 10.1038/ncb2425

scintillation counter was used to take measurements. Proteolysis was measured by release of TCA-soluble counts, and plotted as the percentage of input radiolabelled substrate. For degradation assays with unlabelled full-length cyclin B1, samples were analysed by anti-cyclin B1 immunoblot.

Cyclin B1 degradation in *Xenopus* extract. Degradation assays with non-ubiquitylated cyclin B1 were carried out by adding ~200–250 nM of cyclin B1 in 40 µl reactions, with extract constituting 75–80% of the total volume. Pre-treatment of extract with TAME or MG262 was done at 24 °C for 15 min. UbVS treatment was carried out for 30 min at 24 °C, with agitation. Extracts contained 100 µg ml^{-1} cycloheximide to prevent re-incorporation of free labelled amino acid. Degradation experiments were carried out at 24 °C, with agitation. Samples for proteolysis of unlabelled cyclin B1–CDK1 were processed for anti-cyclin B1 immunoblot. In degradation assays with ^{35}S-labelled cycB1-NT, reactions (3 µl per time point) were quenched with 97 µl of 20% TCA, vortexed and incubated on ice before centrifugation at 14,000*g*, at 4 °C. The radioactivity in the supernatant was measured by scintillation counting.

For degradation of pre-ubiquitylated cycB1-NT, interphase extract was pre-treated with UbVS or buffer for 30 min at 24 °C with agitation and supplemented with 100 µg ml^{-1} cycloheximide. In experiments with IU1, IU1 or dimethylsulphoxide was added to extract for 15 min at 24 °C before addition of substrate. Extract (~14 µl) was added to 4 µl of cycB1-NT–Ub_n conjugates for each time point. Reactions were quenched with 107 µl of 20% TCA, vortexed and incubated on ice before centrifugation at 14,000*g*, at 4 °C for 30 min. A fraction of supernatants was combined with NaOH and scintillation fluid.

To deplete APC/C, 100 µl of interphase extract was mixed with 2 µg of anti-Cdc27 antibody coupled to 5 µl of Affiprep protein A beads and incubated at 4 °C for 3 h. Approximately 10 µl of pre-ubiquitylated radiolabelled cyclin B1 was added to 90 µl of APC/C-depleted extract. Reactions were incubated at 22 °C for the indicated times and stopped by the addition of an equal volume of chilled 2% PCA. Reactions were then incubated on ice for ≥30 min and centrifuged at 15,000 r.p.m. for 10 min, at 4 °C and radioactivity in the supernatant was measured by scintillation counting.

Immunodepletion of E2 enzymes. For UBE2S immunodepletion, 10 µg of anti-UBE2S antibody or control goat IgG antibody was bound to 25 µl UltraLink immobilized protein A/G and incubated with 250 µl extract at 4 °C for ~1 h. For UBCH10 immunodepletion, 100 µl of anti-UbcX antibody or an equivalent amount of control rabbit IgG coupled to Affiprep protein A support was used to deplete 170 µl extract. Cyclin B1–CDK1 (~200 nM) was added to E2- or control-depleted extract and analysis of the time course of degradation was carried out at 24 °C (1,250 r.p.m.) and the equivalent of 1 µl of extract was analysed by SDS–PAGE and anti-cyclin B1 immunoblot analysis. Depletion of UBE2S and UBCH10 was confirmed by western blotting using anti-UBE2S and anti-UBCH10, respectively. To confirm the efficiency of E2 depletion, extract was incubated with ubiquitin agarose, at a ratio of ~10:1 (extract/resin). Ubiquitin agarose was pre-washed four times with 1× energy mix (for 20× stock: 150 mM creatine phosphate, 20 mM ATP, 2 mM EGTA and 20 mM $MgCl_2$, at pH 7.7) in XB buffer (100 mM KCl). Extract and 2× energy mix were added to ubiquitin agarose and incubated with agitation at 24 °C for 45 min. Samples were centrifuged, extract was removed and ubiquitin agarose was washed once with a tenfold volume of 1× energy mix. Bound proteins were eluted by boiling in SDS sample buffer and analysed by immunoblotting.

56. You, J., Cohen, R. E. & Pickart, C. M. Construct for high-level expression and low misincorporation of lysine for arginine during expression of pET-encoded eukaryotic proteins in *Escherichia coli*. *Biotechnques* **27,** 950–954 (1999).
57. Murray, A. W. Cell cycle extracts. *Methods Cell Biol.* **36,** 581–605 (1991).
58. Elsasser, S. *et al.* Proteasome subunit Rpn1 binds ubiquitin-like protein domains. *Nat. Cell Biol.* **4,** 725–730 (2002).
59. Salic, A. & King, R. W. Identifying small molecule inhibitors of the ubiquitin-proteasome pathway in Xenopus egg extracts. *Methods Enzymol.* **399,** 567–585 (2005).
60. Zeng, X. *et al.* Pharmacologic inhibition of the anaphase-promoting complex induces a spindle checkpoint-dependent mitotic arrest in the absence of spindle damage. *Cancer Cell* **18,** 382–395 (2010).

DOI: 10.1038/ncb2425

nature cell biology

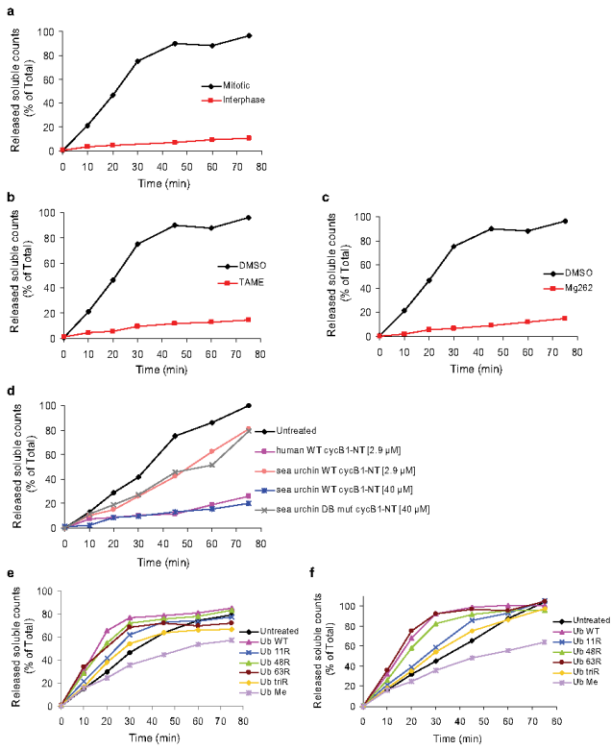

Figure S1 Endogenous ubiquitin levels are limiting for degradation of an N-terminal fragment of human cyclin B1 in mitotic *Xenopus* extract. For all panels, ^{35}S-labeled cycB1-NT (aa 1-88) (~200 nM) was added to extract. Samples were taken at indicated times and subjected to trichloroacetic acid (TCA) precipitation. Proteolysis was measured by release of TCA soluble counts, and plotted as percent of input radiolabeled cyclin B1 protein. (**a**) Degradation of ^{35}S-labeled cycB1-NT in interphase and mitotically-arrested *Xenopus* extracts. (**b**) Degradation of ^{35}S-labeled cycB1-NT in mitotic *Xenopus* extract pre-treated with an inhibitor of the APC/C, TAME (Zeng et al, *Cancer Cell* 18, 382-395 (2010)) (200 μM) or DMSO. (**c**) Same as **b**, except mitotic *Xenopus* extract was treated with proteasome inhibitor Mg262 (200 μM) or DMSO prior to substrate addition. (**d**) Degradation of ^{35}S-labeled wild-type human cycB1-NT (1-88) in mitotic *Xenopus* extract supplemented concomitantly with unlabeled WT human cycB1-NT (1-88), WT or D-box mutant sea urchin cyclin B1 NT (13-110), at indicated concentrations. (**e-f**) ^{35}S-labeled cycB1-NT (amino acids 1-88) was added to mitotically-arrested *Xenopus* extract concomitantly with forms of ubiquitin as indicated or buffer (untreated). In **e**, extract was supplemented with 44 μM of exogenous ubiquitin, while in **f**, extract was supplemented with 116 μM of exogenous ubiquitin. Data are representative of at least three independent experiments.

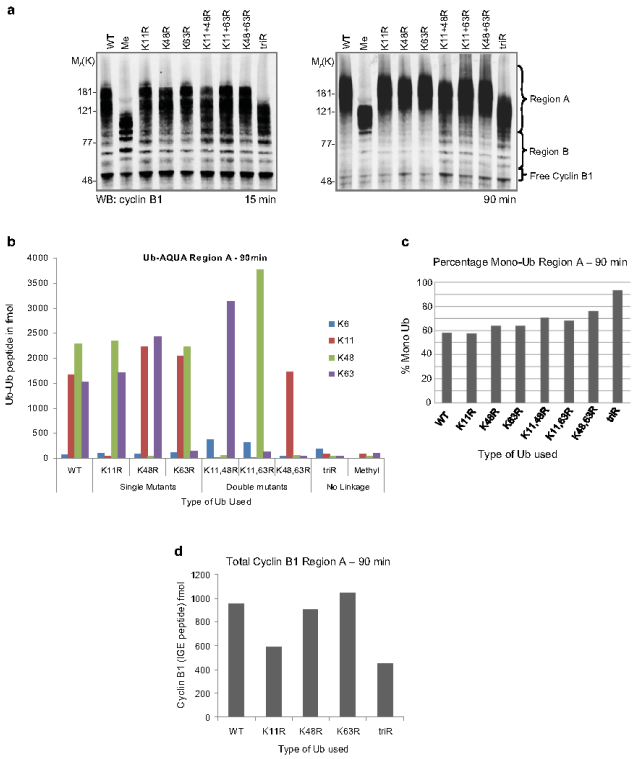

Figure S2 Ub-AQUA analysis of UBC4-APC/C-mediated ubiquitination of cyclin B1 reveals topology of conjugates formed with lysine mutants of ubiquitin. (**a**) Cyclin B1 western blots of an *in vitro* APC/C activity assay containing E1 (1.3 μM), UBC4 (66 μg ml^{-1}), APC/C purified from mitotic *Xenopus* extract and indicated Ub combined to ubiquitinate cyclin B1. Reactions were performed at 22 °C for 15 or 90 min. Ub-AQUA analysis (Kirkpatrick et al, *Nat Cell Biol* 8, 700-710 (2006)) was carried out using a Coomassie stained gel that was run under the same conditions used for the western blots. The results of high molecular weight region A from the 90-minute reaction are shown. (**b**) Total amount of each individual ubiquitin-ubiquitin linkage (fmol) for the corresponding reaction in **a**. (**c**) Percent of ubiquitin in conjugates that lacks linkage through lysines, defined by ubiquitin that is attached to cyclin B1 or ubiquitin terminating a poly-ubiquitin chain without itself containing a ubiquitin chain linkage. (**d**) Total amount of cyclin B1 (fmol) as measured by quantitative mass spectrometry using a standard peptide derived from cyclin B.

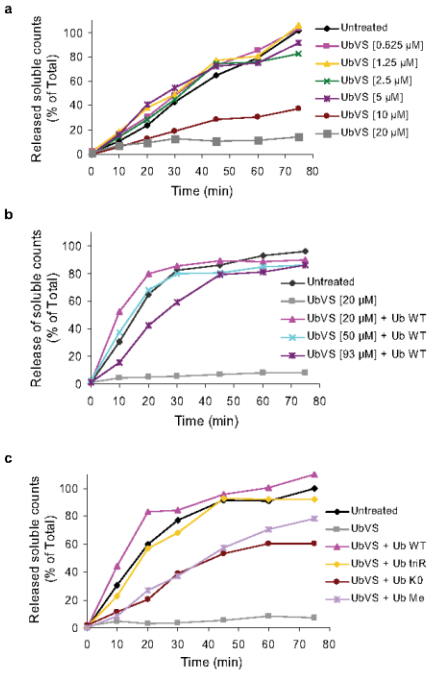

Figure S3 Ubiquitin chain formation is not essential for cycB1-NT proteolysis in UbVS-treated *Xenopus* extract. For all panels, mitotically-arrested *Xenopus* extract was pre-treated with indicated concentration of UbVS or buffer (referred to as untreated) for 30 min. ^{35}S-labeled cycB1-NT (aa 1-88) (~200 nM) was added to extract. Samples were taken at indicated times and subjected to trichloroacetic acid (TCA) precipitation. Proteolysis was measured by release of TCA soluble counts, and plotted as percent of input radiolabeled cyclin B1 protein. (**a**) Degradation of ^{35}S-labeled cycB1-NT was measured in extract that had been pre-treated with UbVS at indicated concentrations. (**b**) Proteolysis of ^{35}S-labeled cycB1-NT in extract pre-treated with increasing concentrations of UbVS and supplemented with wild-type Ub (44 μM) at time of substrate addition. (**c**) Radiolabeled cycB1-NT and 44 μM of different forms of Ub, as indicated, were introduced concomitantly into mitotically-arrested *Xenopus* extract that had been pre-treated with UbVS (20 μM) for 30 min. Ubiquitin^{triR} refers to ubiquitin mutant bearing lysine-to-arginine substitutions at positions Lys11, 48 and 63, whereas Ub^{K0} refers to lysine-less ubiquitin. Ub^{Me} is reductively methylated ubiquitin. Trends are representative of three or more independent experiments.

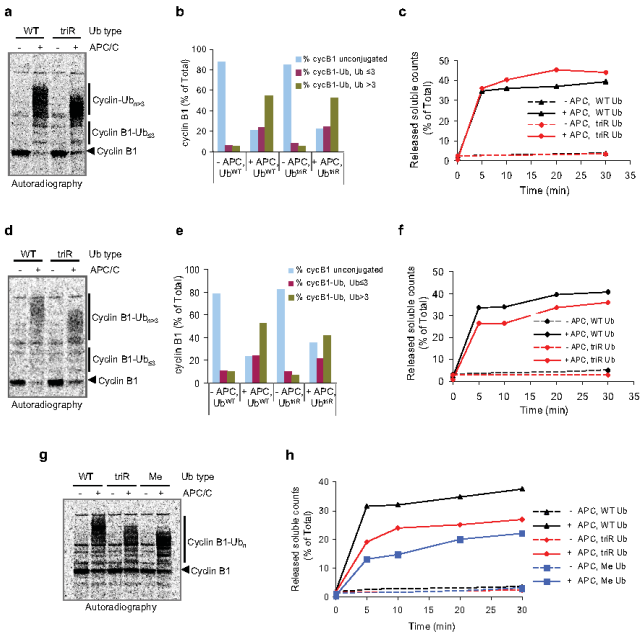

Figure S4 Multiply monoubiquitinated cyclin B1 is rapidly degraded by purified proteasomes. (**a**) Autoradiograph of an *in vitro* APC/C activity assay. Recombinant E1 (1.3 μM), UBCH10 (3 μM), APC/C immunopurified from *Xenopus* extract, forms of ubiquitin (118 μM) as indicated and radiolabeled cyclin B1-CDK1 complex were combined to allow substrate ubiquitination. Control reactions containing all components except for the APC/C ("-APC/C") were performed in parallel. Reaction proceeded for 90 min before analysis by SDS-PAGE/ phosphorimaging. (**b**) Quantification of cyclin B1 ubiquitination shown in **a**. Data were normalized to the total amount of cyclin B1 in the sample. (**c**) *In vitro* degradation assay with cyclin B1-Ub species from **a** and USP14-deficient human proteasomes (10 nM). At indicated times, samples were subjected to perchloric acid (PCA) precipitation and proteolysis measured by release of PCA soluble counts. Results were plotted as percent of input radiolabeled cyclin B1 protein. (**d**) Same as in **a**, but UBC4 (3 μM) was used as the E2. (**e**),(**f**), Same as **b** and **c**, respectively, for UBC4-generated cyclin B1-Ub species. (**g**) Same as UBC4-catalyzed ubiquitination shown in **d**, but using methylated (Ub^{me}) in addition to wild-type (Ub^{WT}) and Ub with lysine-to-arginine substitutions at Lys11, 48 and 63 (Ub^{triR}). (**h**) *In vitro* degradation assay with cyclin B1-Ub species from **g** and USP14-deficient human proteasomes (10 nM) as in **f**.

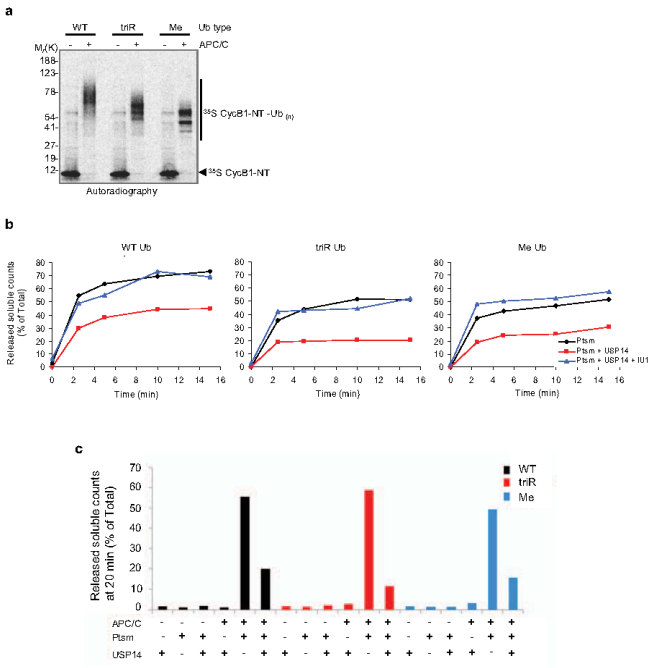

Figure S5 USP14-mediated inhibition of proteolysis is dependent on the catalytic activity of USP14 and is reversed by USP14 inhibitor IU1. (**a**) Autoradiograph of an *in vitro* APC/C-UBCH10 ubiquitination of cycB1-NT, same as in Fig. 5c. (**b**) GST-USP14 (400 nM or 20-fold molar excess over proteasome) was pre-incubated with IU1 (150 μM) or DMSO control prior to allowing association with proteasomes. CycB1-NT-Ub species from **a** were incubated with proteasome mixtures. Reactions were allowed to proceed for indicated times before addition of trichloroacetic acid (TCA). Proteolysis was measured by release of TCA soluble counts, and plotted as percent of input radiolabeled cyclin B1 protein. (**c**) Radiolabeled unmodified and ubiquitinated cycB1-NT from *in vitro* ubiquitination assay shown in autoradiograph in Fig. 5c were incubated with GST-USP14 (400 nM) alone, or with purified human proteasomes (20 nM) reconstituted with or without GST-USP14 (400 nM) for 20 min at 24 °C before reactions were terminated by the addition of trichloroacetic acid (TCA). Proteolysis was measured by release of TCA soluble counts, and plotted as percent of input radiolabeled cyclin B1 protein.

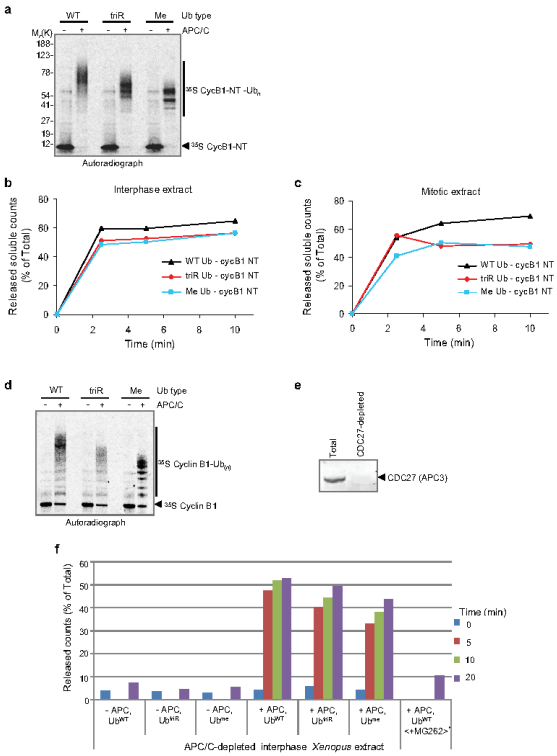

Figure S6 Degradation of pre-ubiquitinated cyclin B1 in *Xenopus* extract does not require ubiquitination by endogenous APC/C. (**a**) Autoradiograph of an *in vitro* APC/C-UBCH10 ubiquitination of ^{35}S cycB1-NT performed as in Fig. 5c. (**b**) CycB1-NT-Ub conjugates from **a** were introduced into interphase *Xenopus* extract concomitantly with excess unlabeled non-ubiquitinated cycB1-NT (10 μM). Timecourse of degradation was performed at 24 °C and reactions were terminated at indicated times by addition of trichloroacetic acid (TCA). Proteolysis was measured by release of TCA soluble counts, and plotted as percent of input radiolabeled cyclin B1 protein. (**c**) As **b**, except that cycB1-NT-Ub species from **a** were introduced into mitotically-arrested *Xenopus* extract. (**d**) Autoradiograph of an *in vitro* APC/C-UBC4 ubiquitination of full-length cyclin B1. Recombinant E1 (1.3 μM), UBC4 (4 μM), APC/C purified from mitotic *Xenopus* extract, forms of ubiquitin (145 μM) as indicated and cyclin B1-CDK1 complex were combined to allow substrate ubiquitination. Reactions were performed for 90 min before separation by SDS-PAGE and analysis using a phosphorimager. (**e**) Interphase *Xenopus* extract was depleted of APC/C, as seen by western blot against the APC/C subunit CDC27, before cyclin B1-Ub conjugates were introduced. (**f**) Samples from **d** were introduced into APC/C-depleted interphase *Xenopus* extract for the indicated times, following which a perchloric acid (PCA) precipitation was done. Pre-treatment of extract with proteasome inhibitor Mg262 (200 μM) was used as control at the 20 min time-point. Proteolysis was measured by release of PCA soluble counts, and plotted as percent of input radiolabeled cyclin B1 protein.

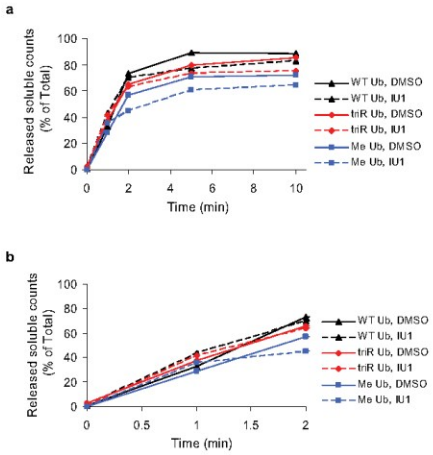

Figure S7 IU1 does not accelerate degradation of cyclin B1-Ub conjugates added to *Xenopus* extract. (**a**, **b**) ^{35}S-labeled cycB1-NT was pre-ubiquitinated with Ub^{WT}, Ub^{triR} or Ub^{me} and APC/C-UBCH10 as in Fig. 5c. CycB1-NT-Ub species were introduced into interphase *Xenopus* extract that had been pre-treated with USP14-inhibitor IU1 (100 μM) or DMSO control for 15 min at 24 °C. Degradation was performed at 24 °C with reactions terminated at indicated times by the addition of trichloroacetic acid (TCA). Proteolysis was measured by release of TCA soluble counts, and plotted as percent of input radiolabeled cyclin B1 protein. Bottom panel (**b**) is an enlargement of the graph for 0-2 min of the time-course shown in (**a**).

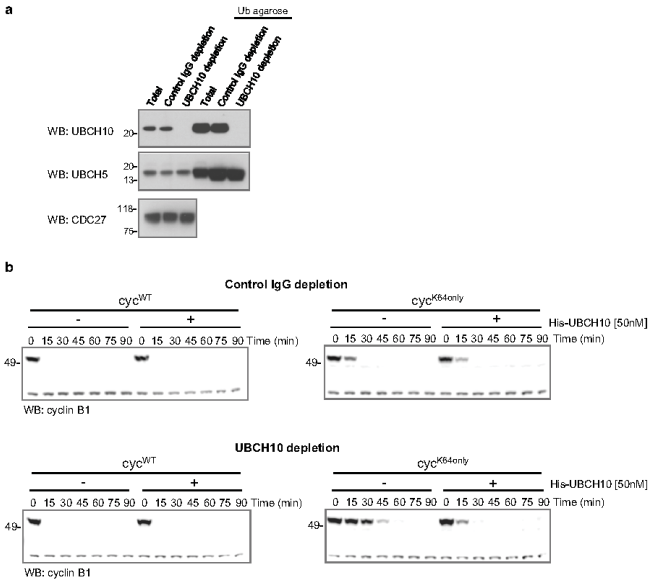

Figure S8 Depletion of UBCH10 more significantly delays cyclin B1 degradation when ubiquitination is limited to a single lysine residue. (**a**) Samples from complete, control- and UBCH10-depleted extracts were processed for SDS-PAGE and western analysis. Equal volumes of these extracts were incubated with Ub agarose to enrich for E2 enzymes. Samples were separated by SDS-PAGE and analyzed by western blot against UBCH10, UBCH5 and the APC/C subunit CDC27. Lanes 4-6 represent 20-fold enrichment of E2 enzymes on Ub agarose. (**b**) Time-course of degradation of full-length wild-type cyclin B1 (cyc^{WT}) or single lysine-containing mutant ($cyc^{K64only}$), each in complex with CDK1, in control- or UBCH10-depleted mitotically-arrested *Xenopus* extract. Recombinant His-UBCH10 (50 nM), where indicated, was added to reactions concomitantly with substrate. Cyclin B1 proteolysis was analyzed by SDS-PAGE/cyclin B1 immunoblotting.

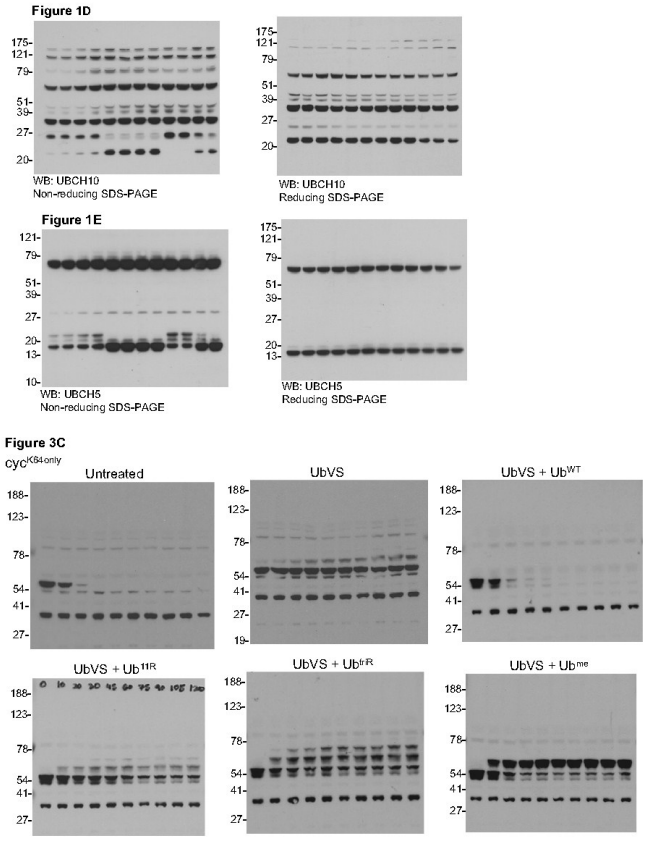

Figure S9 Uncropped scans of immunublots.

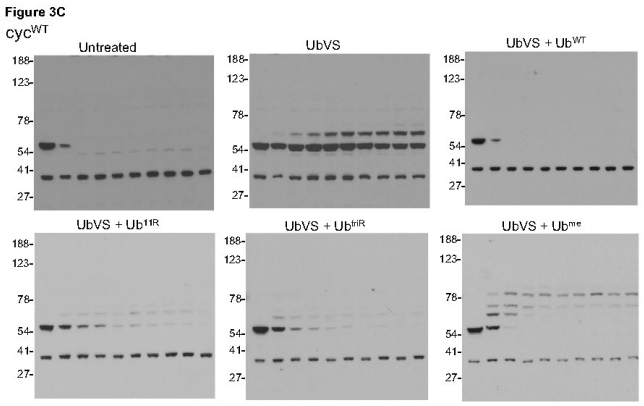

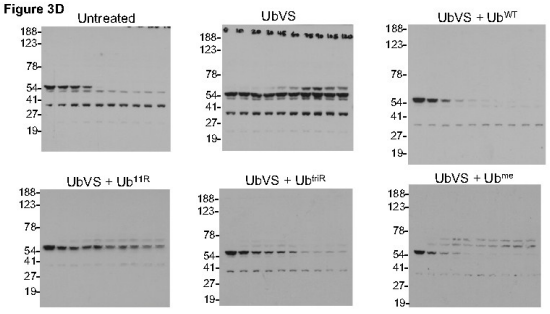

Figure S9 continued

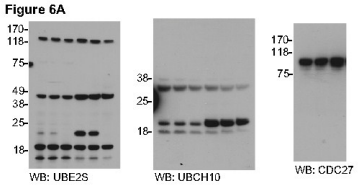

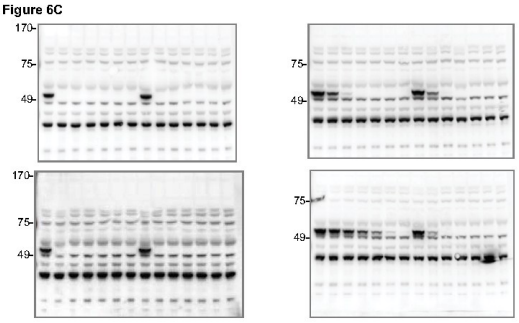

Figure S9 continued

Supplementary Figure 8A

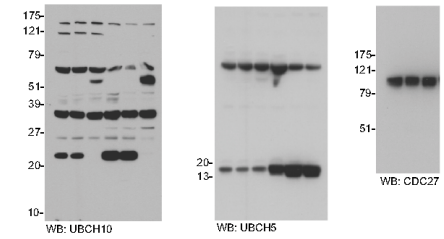

Supplementary Figure 8B

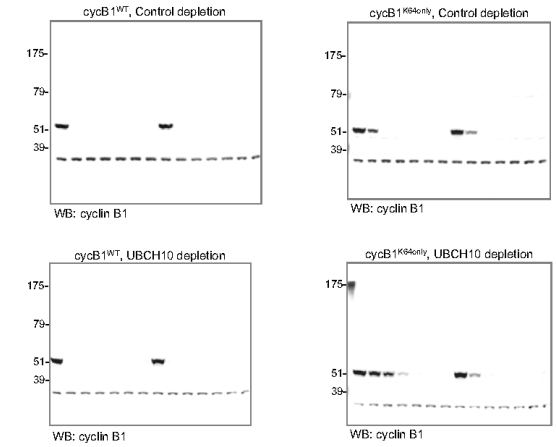

Figure S9 continued

Analysis of the role of USP14 in cyclin B1 degradation in *Xenopus* extract

Results

Analysis of the role of USP14 in cyclin B1 degradation in *Xenopus* extracts

Our previous findings indicated that as long as ubiquitin (Ub) availability is high enough, deubiquitination mediated by UbVS-sensitive DUBs is unlikely to present a major kinetic barrier to cyclin B1 degradation in mitotic *Xenopus* extract (Dimova et al., 2012). While the analysis we carried out could not ascertain a role for DUBs, which are not inhibited by UbVS, our findings suggested that there are few, if any, UbVS-senstitive deubiquitinases that actively antagonize proteasomal targeting of cyclin B1 in mitotic extracts. Alternatively, our findings suggested that for such activity to oppose degradation, it may be crucial that the rate of ubiquitination be constrained by limiting activity of the ubiquitination machinery or by limiting availability of free ubiquitin.

Activity of the APC in mitotic *Xenopus* extracts is dependent on the reversible association with the activator Cdc20, which helps recruit substrates to the APC and may also directly stimulate the catalytic activity of the ligase (Kimata et al., 2008). Surprisingly, work from our lab uncovered that in *Xenopus* extracts Cdc20 also interacted with interphase APC, albeit with different dynamics relative to the mitotically phosphorylated ligase (Xing Zeng, unpublished observations). We hypothesized that the catalytic capacity of interphase APC^{Cdc20}, while sufficient to promote ubiquitin-dependent proteolysis, is strongly opposed by the activity of deubiquitinases. To test this idea, we took advantage of the UbVS system (described in chapter II) (Dimova et al., 2012) and a purified ^{35}S-labeled N-terminal fragment (1-88 amino acid residues) of human cyclin B1 (referred to as cycB1-NT). When added to interphase extract, cycB1-NT, which is incapable of binding endogenous CDK1 and phosphorylating the APC, remained largely stable for the duration of the experiment. Low levels of degradation, observed at later times, were presumably resulting from partial activation of the ubiquitination machinery.

Addition of 110 μM of wild-type ubiquitin, which accelerates substrate degradation in mitotic extracts (Dimova et al., 2012), had no appreciable impact on cyclin stability in interphase extract. Upon pre-treatment with 20 μM UbVS, basal proteolysis was slightly inhibited in extracts, likely due to ubiquitin deficiency. Surprisingly, wild-type ubiquitin stimulated cyclin B1degradation in UbVS-treated extract (Figure S1b). The degree of stimulation depended on the concentration of added ubiquitin (data not shown). Under these conditions, no phosphorylation of Cdc27 was observed by western blotting (Figure S1a), suggesting that the observed degradation was unlikely due to mitotic entry. These findings indicate that UbVS-sensitive deubiquitination may oppose proteasomal targeting of cyclin B1 in interphase extract.

Previous work, carried out in collaboration with the Finley lab, revealed that in a reconstituted system, the proteasome-associated DUB USP14 strongly attenuated the capacity of proteasomes to rapidly degrade polyubiquitinated cyclin B1 (Hanna et al., 2006; Lee et al., 2010b), presumably by trimming ubiquitin chains. Unexpectedly, USP14 was comparably efficient at removing substrate-linked ubiquitin, suppressing the turnover of multiply monoubiquitinated cyclin B1 (Dimova et al., 2012). These findings motivated us to examine a potential role of USP14 in cyclin proteolysis in *Xenopus* extract. To this end, we first wanted test whether USP14 was required for cyclin turnover. USP14 levels in total extracts were hard to detect by western analysis (Figure S2a). To confirm its presence in this physiological context, we sought to enrich for USP14 by isolating endogenous proteasomes from *Xenopus* extract using the UBl-domain of ubiquitin receptor Rad23 (Figure S2a). Mass spectrometry (Mike Aguiar, Gygi lab) and western blot analyses of isolated proteasomes indicated that levels of proteasome-bound USP14 in interphase extracts are comparable to those in mitotic extracts. Importantly, species in both extracts were similarly UbVS-reactive (Borodovsky et al., 2001), suggesting proper proteasomal association and activation of USP14 (Figure S2a).

We next examined how inhibiting the activity of USP14 will impact cyclin B1 degradation in *Xenopus* extract. Pre-treatment of mitotically arrested *Xenopus* extract with IU1

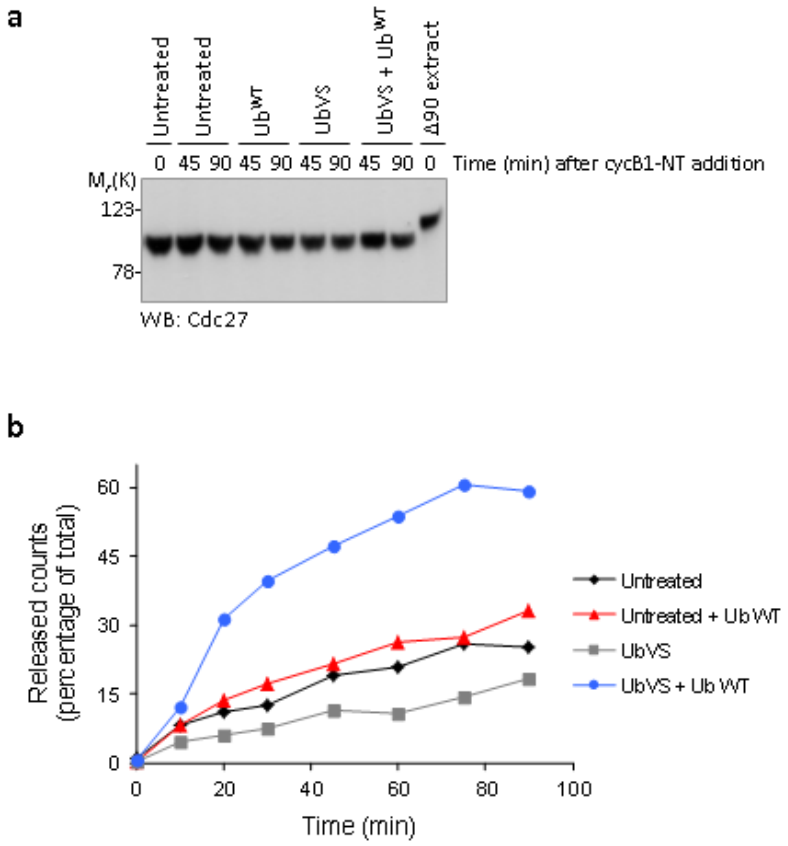

Figure S1 Ubiquitin vinyl sulfone (UbVS) stimulates cyclin proteolysis in interphase *Xenopus* extract in a ubiquitin-dependent manner. (**a**) Aliquots were removed from interphase *Xenopus* extract before or after treatment with UbVS (20µM) or buffer for 30 min, as well as during the time course of cycB1-NT degradation. Phosphorylation of APC subunit Cdc27 was examined by immunoblotting. Last lane represent phosphorylation of Cdc27 in mitotically arrested *Xenopus* extract. (**b**) ^{35} S-labeled cycB1-NT and 110 µM of wild-type ubiquitin, where indicated, were introduced concomitantly into interphase *Xenopus* extract that had been pre-treated with UbVS (20 µM) or buffer (untreated) for 30 min. Proteolysis was measured by release of TCA soluble counts and is plotted as percentage of input radiolabeled cycB1-NT.

Figure S2 USP14-specific inhibitors, IU1 and IU2, do not impact cyclin B1 proteolysis in *Xenopus* extract. (**a**) Proteasomes, affinity purified from interphase or mitotically arrested *Xenopus* extract, were incubated with ubiquitin vinyl sulfone, (UbVS) where indicated. Levels of USP14, unmodified or as covalent-adduct form with UbVS , were examined by western blot against USP14. In parallel, USP14 levels in total extract were analyzed. (**b**) Mitotically arrested *Xenopus* extract was pre-treated with USP14-specific inhibitors, IU1 or IU2 (200 µM), for 20 min at 24 °C before cycB1-NT (~ 200 nM) and wild-type ubiquitin (44 µM) were added concomitantly, as indicated. Proteolysis was measured by release of TCA soluble counts and is plotted as percentage of input radiolabeled cycB1-NT. (**c**) Mitotically arrested *Xenopus* extract was treated with APC inhibitor TAME (200 µM), prior to addition of USP14 inhibitors, IU1 or IU2 (200 µM) for 20 min at 24 °C. CycB1-NT (200 nM) was added to extract. Proteolysis was measured by release of TCA soluble counts and is plotted as percentage of input radiolabeled cycB1-NT. (**d**) Mitotically arrested *Xenopus* extract was treated with proteasome inhibitor MG262 or DMSO, as indicated, prior to addition of USP14 inhibitor IU1 (100 µM). CycB1-NT (200 nM) and wild-type ubiquitin (44 µM), where indicated, were added concomitantly. Proteolysis was measured by release of TCA soluble counts and is plotted as percentage of input radiolabeled cycB1-NT.

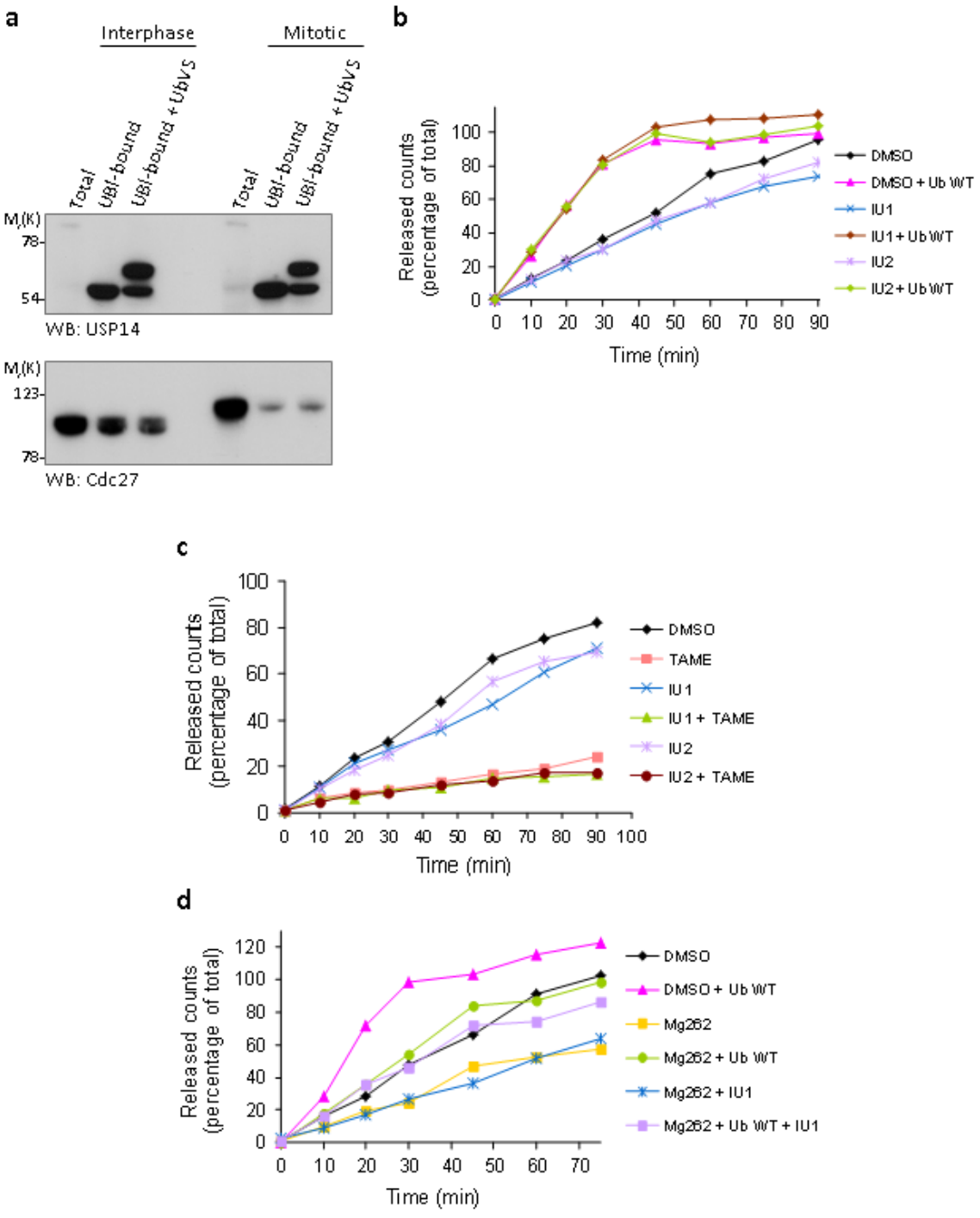

Figure S2 (Continued)

(Lee et al., 2010a) or IU2, two different small-molecule inhibitors of the catalytic activity of USP14, had a slightly inhibitory effect on cycB1-NT degradation (Figure S2b). To compensate for the ubiquitin deficiency potentially imposed by USP14 inhibition, we supplemented extracts with wild-type ubiquitin. In the presence of 44 μM of added ubiquitin, the rate of cyclin degradation was no faster in IU1- or IU2-treated extract relative to a non-treated extract. Similar trends were observed in interphase *Xenopus* extracts (data not shown). The failure of the USP14 inhibitors to stimulate cyclin turnover could result from inefficiency of USP14 in opposing the processive ubiquitination and proteasomal targeting, mediated by the APC. We therefore sought to examine whether partial inhibition of APC activity may reveal an effect of USP14 on cyclin degradation. To this end, we used TAME which was suggested to stabilize APC substrates by terminating ubiquitination prior to assembly of an efficient proteolytic signal, favoring deubiquitination rather than degradation (Zeng and King, 2012). We hypothesized that if USP14 acts on such under-ubiquitinated species, then attenuating its isopeptidase activity with IU1 or IU2 may rescue substrate degradation in TAME-treated extracts. As expected, the proteolysis of cycB1-NT was highly sensitive to TAME addition (Zeng and King, 2012; Zeng et al., 2010) (Figure S2c). Concomitant treatment of extract with USP14 inhibitors, IU1 or IU2, failed to rescue the TAME effect on substrate stability. These findings suggest that USP14 may not actively oppose APC-mediated proteolysis by deubiquitinating modified intermediates.

We next sought to determine whether a partial inhibition of the 26S proteasome may better reveal an effect of USP14 on cyclin degradation. When the catalytic activity of the proteasome is attenuated, ubiquitin conjugates may remain associated with the 19S sub-complex longer, allowing potentially for more extensive deubiquitination by USP14. At final concentrations higher than 100 μM, the proteasome inhibitor MG262 largely blocked cyclin turnover (data not shown). In contrast, pre-treatment of extract with 25 μM MG262 delayed degradation, extending substrate half-life from 30 minutes in untreated extract to 55 minutes (Figure S2d). Following treatment with the proteasome inhibitor, extract was incubated with IU1

for 15 minutes prior to substrate addition. The kinetics of cyclin degradation observed in MG262-treated extracts were largely unaffected by the addition of the USP14 inhibitor IU1. A possible explanation for the lack of effect of IU1 is that the catalytic activity of USP14 does not modulate the rate of cyclin degradation in a major way. Alternatively, our data indicate that in spite of the sequence conservation between the human and frog USP14, IU1 fails to efficiently inhibit the activity of the enzyme in *Xenopus* extract.

We next attempted to rule out the possibility that our results thus far were influenced by failure of the small-molecule inhibitors to bind *Xenopus* USP14. To this end, we examined the ability of IU1to interact with the enzyme's catalytic site, preventing labeling with UbVS. When isolated *Xenopus* proteasomes were briefly incubated with UbVS, a significant fraction of the present USP14 was found as a covalent adduct with the ubiquitin derivative (Figure S3a). At 20 μM final concentration, IU1 was not capable of inhibiting the formation of USP14-UbVS adducts, as compared to untreated or negative-control IU1C-treated proteasomes (Figure S3a). When the concentration of IU1 was increased 5-fold to 100 μM, labeling with UbVS was partially diminished, as suggested by reduced levels of the slower migrating form of USP14. IU1-47 exhibited higher affinity for the *Xenopus* USP14 than the parental compound. Even at 20 μM final concentration, IU1-47 significantly reduced extent of UbVS labeling, whereas at 100 μM, it completely abolished this interaction (Figure S3a). Surprisingly, this more potent inhibitor IU1-47 had no appreciable effect on the kinetics of cyclin degradation in mitotic *Xenopus* extracts, supplemented with 44 μM of wild-type ubiquitin (Figure S3b). Similar results were obtained in interphase extracts (data not shown).

Degradation of cyclin conjugates generated with wild-type or chain-terminating ubiquitin was largely unaffected by pre-treatment of interphase *Xenopus* extract with the USP14-specific inhibitor IU1-47 (Figure S3c). This is very similar to what we observed in analogous experiments performed with IU1 (Dimova et al., 2012). The efficiency of cyclin degradation in *Xenopus* extracts suggested, surprisingly, that USP14 activity is unlike to strongly impact the proteasomal

Figure S3 USP14-specific inhibitor IU1-47 has no effect on cyclin B1 proteolysis in *Xenopus* extract. (**a**) *Xenopus* proteasomes, affinity purified from mitotically arrested *Xenopus* extract, were incubated with USP14-specific inhibitor IU1 or IU1-47, or a specificity control IU1-C, at the indicated concentrations, for 15 min at 24 °C prior to chase with 2 µM ubiquitin vinyl sulfone (UbVS). Reaction species were processed for SDS-PAGE and anti-USP14 western analysis. (**b**) Degradation of ^{35}S-labeled cycB1-NT in mitotically arrested *Xenopus* extract pre-treated with an USP14-inhibitor IU1-47, concentrations as indicated. CycB1-NT (~200 nM) was added to extract. Proteolysis was measured by release of TCA soluble counts and is plotted as percentage of input radiolabeled cycB1-NT. (**c**) ^{35}S-labeled cycB1-NT was preubiquitinated with Ub^{WT}, Ub^{triR} or Ub^{me} and UBCH10. Resulting cycB1-NT-ubiquitin species were introduced into interphase *Xenopus* extract that had been pre-treated with USP14-inhibitor IU1-47 (200 µM) or DMSO control for 15 min at 24 °C. Degradation was performed at 24 °C with reactions terminated at indicated times by the addition of trichloroacetic acid (TCA). Proteolysis was measured by release of TCA soluble counts, and is plotted as percentage of input radiolabeled cyclin B1 protein. Bottom panel is an enlargement of the graph for 0-5 min of the time-course shown in top panel.

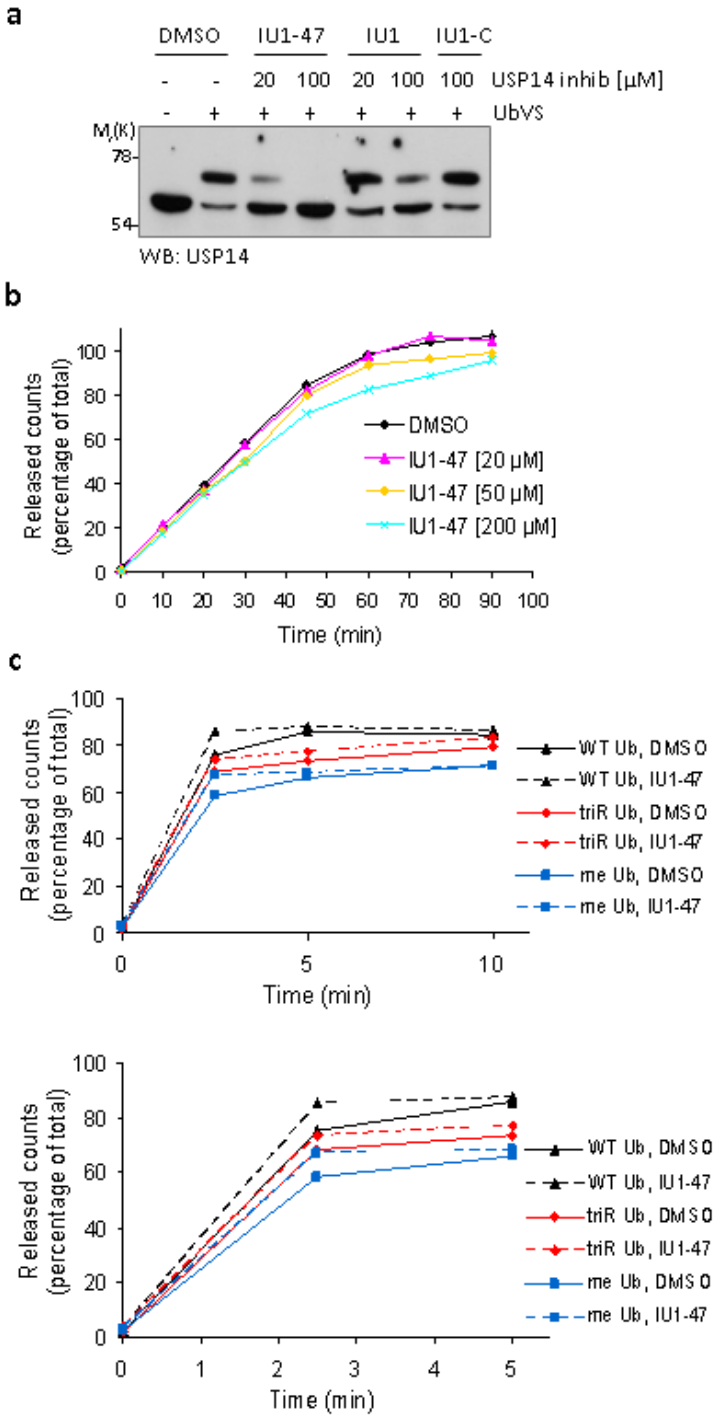

Figure S3 (Continued)

targeting of cyclin B1. A possible explanation for these observations is that deubiquitinating enzymes such as USP14 are present at much lower levels in *Xenopus* extracts than in our *in vitro* reconstituted reactions (Dimova et al., 2012).

The Ub-AMC hydrolyzing activity of USP14 was reported to increase 800-fold upon association with the proteasome over that of isolated protein (Lee et al., 2010a). Thus, the deubiquitinating activity of USP14 is strongly enhanced by proteasomes (Borodovsky et al., 2001; Lee et al., 2010a; Leggett et al., 2002). Our findings raised the possibility that levels of USP14 associated with proteasomes in extracts may be insufficient to impede cyclin turnover. To test this idea, we sought to increase loading of proteasomes with USP14 by adding recombinant protein to extracts. Based on previous reports (Borodovsky et al., 2001; Lee et al., 2010a; Leggett et al., 2002), we reasoned that exogenous USP14 would be specifically activated in the context of the proteasome and perhaps render kinetics of substrate turnover comparable to those in a purified system reconstituted with the deubiquitinase (Crosas et al., 2006; Dimova et al., 2012; Hanna et al., 2006; Lee et al., 2010a). When added to mitotically arrested extract, GST-tagged human USP14, but not GST alone, delayed cyclin proteolysis in a dose-dependent fashion (Figure S4a; data not shown). Surprisingly, we found that co-treatment of these extracts with 200 μM IU1-47 failed to accelerate degradation (Figure S4b).

Previous work demonstrated that USP14 delays the breakdown of conjugates by the proteasome and that a major component of its inhibitory effect is non-catalytic in nature (Hanna et al., 2006). These findings prompted us to examine the possibility that in *Xenopus* extracts USP14 utilizes mostly non-catalytic functions to modulate the activity of the proteasome. We found that an active-site mutant of USP14, USP14 (C114A), inhibited cyclin degradation, albeit to a lesser degree than the wild-type protein (Figure S4b). The kinetics of degradation in extracts supplemented with USP14 (C114A) were not altered by the addition of IU1-47, consistent with resistance of USP14 non-catalytic functions to IU1 treatment (Lee et al., 2010a). Thus, our analysis may indicate a contribution of USP14, independent of its catalytic function, even though

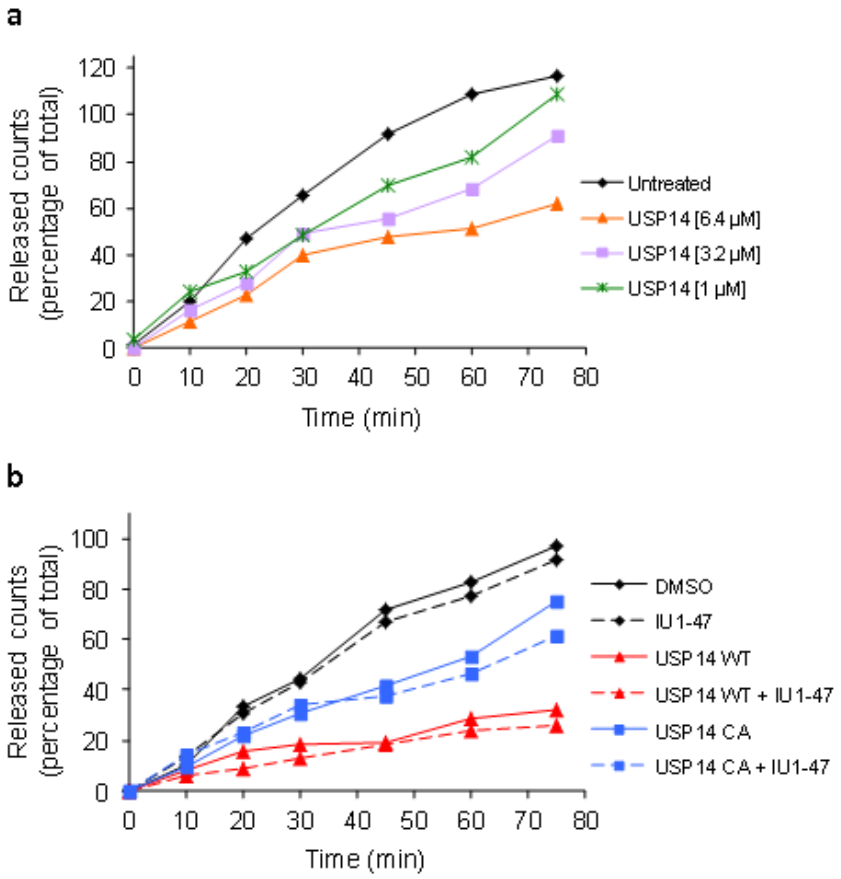

Figure S4 Exogenous USP14 delays proteolysis of cyclin B1 in *Xenopus* extract. (**a**) Mitotically arrested *Xenopus* extract was incubated with recombinant GST-tagged USP14 at concentrations, as indicated for 15 min prior to addition of ^{35}S-labeled cycB1-NT. Time course of degradation was carried at 24 ° and reactions terminated at indicated times by the addition of trichloroacetic (TCA) acid. Proteolysis was measured by release of TCA soluble counts and is plotted as percentage of input radiolabeled cycB1-NT. (**b**) Recombinant GST-tagged wild-type (WT) or catalytically inactive variant (CA) (C114A) of USP14 (6 µM) were added to mitotically arrested *Xenopus* extract for 15 min, prior to treatment with USP14-specific inhibitor IU1-47 (200 µM) or DMSO for 15 min. Time course of degradation was initiated with substrate addition (200 nM). Proteolysis of radiolabeled cycB1-NT was measured as in **a.**

further work will be required to address this possibility. Together our findings suggest that the abundance of proteasomes containing USP14 in *Xenopus* extract may be below levels necessary to influence cyclin proteolysis. Alternatively, the ubiquitin signal assembled on cyclin B1 may be primarily modulated by activities upstream of the proteasome. Even following a recent identification of USP37 as a DUB antagonizing ubiquitination of cyclin A2 by APC^{Cdh1} (Huang et al., 2011), it remains to be determined if there is a ubiquitin isopeptidase specific for cyclin B1. We set out, therefore, to search for such activity that may influence the rate of cyclin B1 proteolysis and perhaps that of other APC substrates.

Deubiquitinating activity antagonizing APC-dependent proteolysis in *Xenopus* extracts

We sought to broaden our approach and look for APC-associating DUBs which could potentially influence APC-mediated proteolysis. Based on our findings in interphase extract, we initially examined potential association of the ligase with UbVS-sensitive isopeptidases. We immunopurified interphase or mitotic APC from *Xenopus* egg extract and treated the isolated material with hemagglutinin (HA)-tagged UbVS to label any co-purifying deubiquitinases. Following incubation with HA-UbVS, covalently labeled species were analyzed by western blotting against the HA epitope tag. When material isolated on anti-Cdc27 resin was subjected to less stringent washes, multiple HA immunoreactive species were evident (Figure S5a). We reasoned that any deubiquitinase that may specifically modulate the ubiquitin signal built on substrates by the APC is likely to be recruited to the ligase module in the presence of substrate. Thus, extract was supplemented with 10 μM N-terminal fragment of sea urchin cyclin B1 (13-110 amino acid residues) during immunoprecipitation. Isolated APC was washed with excess low-salt buffer and incubated with 10 μM HA-UbVS for 30 minutes. We found that the patterns of HA-reactive species for the Cdc27- and control IgG-immunopurification were largely identical.

Interestingly, one band in the high M_r region of the gel appeared specific for the Cdc27 immunopurifcation (Figure S5b). The intensity of the band remained largely unaffected by the addition of excess substrate (Figure S5b; data not shown).

To examine the pattern of isopeptidase activities co-purifying with interphase *Xenopus* APC in an independent manner, we carried out labeling with a different active-site probe. To this end, we utilized ubiquitin-vinyl methylester (Ub-VME) where vinyl methylester is used as the thiol-reactive functional group at the carboxy terminus. As the vinyl sulfone substitution may hinder interaction or not be reactive with the active sites of some deubiquitinases, such proteins will be refractory to labeling. Thus, a ubiquitin probe in which the vinyl sulfone moiety is replaced with a different group such as vinyl methylester can potentially allow for additional DUBs to be visualized. Consistent with this idea, we found the overall pattern of labeling with Ub-VME to be different from that in assays containing UbVS (data not shown). Intriguingly, far fewer species form covalent adducts with Ub-VME, suggesting differential affinity for the ubiquitin probe (data not shown). Interestingly, we found a Ub-VME-reactive species that migrated similarly to the APC-IP specific band seen in UbVS experiments. Using this approach, we were unable to detect any DUB/DUBs associating with mitotic APC (data not shown). We found no evidence of differential labeling with UbVS even when extracts were supplemented with cyclin B1 and wild-type ubiquitin (data not shown).

We next tested whether the UbVS labeling we observed was indeed reflecting specific association of particular deubiquitinases with the APC. To this end, we immunopurified APC from interphase extract that had been pre-depleted with either a control IgG or an antibody against the APC subunit Cdc27 and incubated the resulting material with HA-UbVS. Surprisingly, western analysis revealed that the appearance of labeled species remained unchanged in extracts pre-depleted of the APC, as compared to control-depleted extracts (Figure S5b). These results suggest that the UbVS-reactive species may not be specifically binding to the

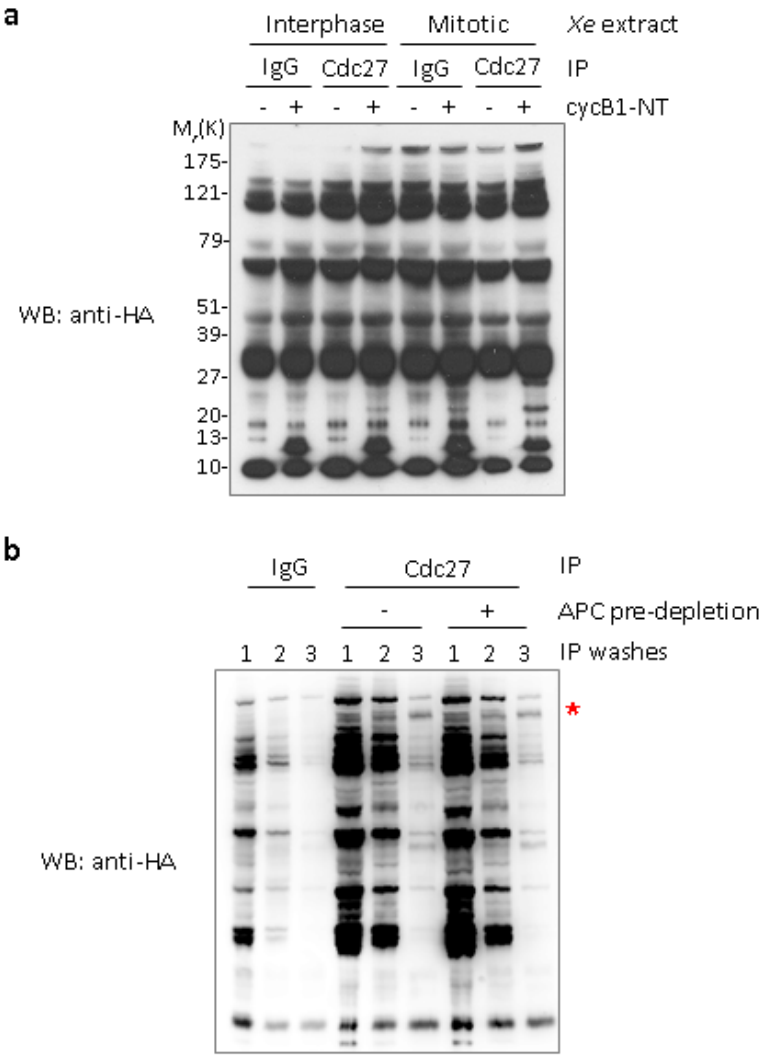

Figure S5. UbVS-labeling of deubiquitinases co-purifying with *Xenopus* APC. (**a**) *Xenopus* APC was immunopurified from interphase or mitotic extract, as indicated, for ~ 1 h before material bound to resin was washed and incubated with 15 µM HA-tagged UbVS at 24˚C for 20 min. Entire reactions were mixed with sample buffer and samples were analyzed by SDS-PAGE/anti-HA western blotting. Cdc27, an APC subunit. (**b**) *Xenopus* APC was immunopurified from interphase extract that had been supplemented with 10 µM of sea urchin N-terminal fragment of cyclin B1 (cycB1-NT) and pre-depleted with Cdc 27 or control IgG. Following incubation for ~1 h at 4 ˚C, immunopurified material was subjected to quick washes with low-salt buffer and incubated with 10 µM of HA-UbVS at 24 ˚C for 30 min. Entire reactions were mixed with sample buffer and reactions species were analyzed by SDS-PAGE/anti-HA western blotting. Red asterisk denotes band specific for immunopurification with CDC27 IgG.

ubiquitin ligase. Together our findings may indicate that there are few, if any, UbVS-reactive DUBs that form a stable association with the APC in *Xenopus* extract.

Discussion

Here we have evaluated a potential role of USP14 in proteasomal targeting of cyclin B1 in *Xenopus* cell-cycle extracts. Our study was motivated by previous work (Dimova et al., 2012; Hanna et al., 2006; Lee et al., 2010a) indicating that that the proteasome-associated deubiquitinase USP14 or its yeast orthologue Ubp6 strongly reduces the efficiency of cyclin B1 degradation by purified proteasomes. Although, USP14 has been found to modulate the stability of a number of cellular proteins *in vivo* (Hanna et al., 2006; Lee et al., 2010a), to date, its activity has not been linked to APC-mediated proteolysis. In the context of *Xenopus* egg extracts, we conclude that USP14 is unlikely to regulate the magnitude of proteasome activity against ubiquitinated cyclin B1.

Our previous work showed that in a reconstituted system USP14 can antagonize the degradation of cyclin B1-Ub_n species (Dimova et al., 2012; Lee et al., 2010a). At the basis of this inhibition was the capacity of USP14 to trim polyubiquitin assemblies (Dimova et al., 2012; Lee et al., 2010b), as well as remove substrate-attached monoubiquitins (Dimova et al., 2012). Cyclin turnover *in vitro* was markedly stimulated by USP14-specific inhibitor IU1, whereas degradation of pre-ubiquitinated cyclin B1 in *Xenopus* extract was largely insensitive to IU1 treatment (Dimova et al., 2012). We sought to resolve this paradox by examining a potential role of USP14 in the context of *Xenopus* proteasomes. Although USP14 is present in the *Xenopus* system and associates with the proteasome in both interphase and mitotic extract, our analysis suggested that it may be of low abundance. This raises an interesting possibility that the limited ubiquitin availability in extracts may be accounted, at least in part, by lower levels of proteasome-bound USP14. Consistent with this idea, treatment with the USP14-specific inhibitor IU1caused a slight delay in cyclin proteolysis, an effect rescued by exogenous ubiquitin.

The magnitude of proteasome inhibition by USP14 that has been observed in a reconstituted system (Dimova et al., 2012; Hanna et al., 2006; Lee et al., 2010a) and in some

physiological contexts (Hanna et al., 2006; Lee et al., 2010a) does not appear to parallel that in *Xenopus* egg extracts. Perhaps this reflects that the deubiquitinating enzyme USP14 is present at much lower levels on *Xenopus* proteasomes than in our *in vitro* reconstituted reactions. Consistent with this idea, upon increasing the levels of USP14 by adding recombinant protein, we observed a significant delay in cyclin turnover. Interestingly, in *Xenopus* extracts a major component of this inhibitory effect may be noncatalytic in nature. Similar observations have been reported for the yeast orthologue Ubp6 (Hanna et al., 2006). This may provide a possible explanation for the lack of effect of USP14-specific inhibitors, IU1 and IU2, on the kinetics of degradation of cyclin-ubiquitin conjugates introduced in extract. It is unlikely that these findings reflect some artifact of *in vitro* ubiquitination, rendering conjugates insensitive to deubiquitinating activity in extract. When allowed to be ubiquitinated by the endogenous machinery, cyclin was efficiently degraded in IU1- or IU2-treated extracts, with rates largely identical to those in untreated extract. These findings are in agreement with our previous work indicating that few, if any, UbVS-sensitive DUBs such as USP14 may be strongly modulating cyclin degradation in mitotic *Xenopus* extracts.

Importantly, exogenous ubiquitin was found to stimulate cyclin proteolysis in interphase extracts in a manner dependent on DUB inhibition with UbVS. Under these conditions, there is no detectable phosphorylation of Cdc27 that would indicate mitotic entry of extracts. Intriguingly, both interphase and mitotic APC appear to associate with proteasomes in *Xenopus* extract. Future work will be required to elucidate the functional significance of such interactions. Such an association, however, raises an important question as to how ubiquitination and degradation may be coupled, and how this may influence sensitivity to deubiquitination. Our analysis thus far has not yielded any UbVS-sensitive deubiquitinases that form stable interaction with the APC. These findings do not rule out the possibility that there are isopeptidases antagonizing APC activity or modulating the ubiquitin signal it assembles on target proteins. Such deubiquitinating enzymes would not necessarily associate with the E3 ligase to exert their effect.

Methods

Antibodies and biochemical reagents

Protein samples were resolved by SDS-PAGE on NuPAGE 4-12% Bis-Tris or 12% Bis-Tris gels (Invitrogen), followed by wet transfer to PVDF and immunoblotting against the indicated proteins. Sources of commercial antibodies used for western analysis are as follows: anti-cyclin B1 (Ab-2; RB-008-P, Neomarkers), anti-Cdc27 (610455, BD Transduction Laboratories^{TM}), Secondary antibodies used include anti-goat IgG-HRP (sc2020; Santa Cruz Biotechnology), anti-rabbit IgG-HRP (NA934; GE Healthcare), and anti-mouse IgG-HRP (NA931; GE Healthcare). For APC/C immunopurification from *Xenopus* extract, anti-Cdc27 (AF3.1; sc-9972, Santa Cruz Biotechnology) was used. Other reagents utilized include ubiquitin vinyl sulfone (UbVS) (U-202, Boston Biochem), TAME (T4626, Sigma), Mg262 (I-120, Boston Biochem), methylated ubiquitin (U-502, Boston Biochem), ubiquitin mutants except for $Ub^{11,48R}$, $Ub^{11,63R}$, and Ub^{triR} were purchased from Boston Biochem. Wild-type ubiquitin was purchased from Sigma-Aldrich (U6253-25MG) and Boston Biochem.

Preparation of recombinant proteins

CycB1-NT (1-88 amino acids of human cyclin B1) , containing an HA tag at the N terminus and a 6xHis tag at the C terminus was generated using PCR amplification with forward primer (5′-CCA GGA CCA TGG GTT ACC CAT ACG ATG TTC CAG ATT ACG CTG GCT CGA TGG CGC TCC GAG TCA CG-3′) and reverse primer (5′-GGG AGC CTC GAG CTA GGG AGC GTG ATG GTG ATG GTG ATG CAT AGG TAC CTT TTC AAG AGG-3′). The resulting PCR product was digested with NcoI and XhoI for subcloning into pET28a. Plasmids were verified by restriction enzyme mapping and sequencing. For ^{35}S labeling in *Escherichia coli*, cultures (50 ml) were grown at 37 ˚C to $D_{600\ nm}$ = 0.8, then collected by centrifugation (3,700*g* for 15 min, at 4 ^{o}C) and resuspended in modified M9 medium (50 ml final volume). After

resuspension in modified M9 medium, cells were allowed to grow for additional 15 min at 37 °C before 5 mCi of Easy Tag^{TM} L-[35S]-Methionine (NEG709A005MC; Perkin Elmer) was added. Expression was induced with 0.5 mM IPTG for 2.5 h at 37 ^{o}C. Cells were ruptured in 5 ml g^{-1} of pellet guanidine-HCl lysis buffer (pH 8.0) and lysates rotated at 24 °C until the lysate became slightly translucent; approximately 45 min. Lysates were clarified by centrifugation and cycB1-NT was purified using Ni-NTA affinity chromatography (Qiagen). Eluted protein was desalted into XB buffer (100 mM KCl, 0.1 mM $CaCl_2$, 1 mM $MgCl_2$, 10 mM HEPES, at pH 7.8 with KOH), supplemented 2% glycerol, protease inhibitors and phenylmethylsulfonyl fluoride, and stored at – 20 °C.

Maltose-binding protein (MBP)-tagged E1 was expressed in *E. coli* inducing cultures at $D_{600\,nm}$ = 0.6 with 300 μM IPTG for 5 h at room temperature. Purification was carried out using a standard MBP purification protocol. For expression of His-tagged UBCH10 and His-tagged UBC4, bacterial cultures were induced at $D_{600\,nm}$ = 0.6 at 37 ˚C with 500 μM IPTG for 4 h. The enzymes were purified through Ni-NTA affinity and gel-filtration chromatography. Glutathione *S*-transferase (GST)-tagged USP14, wild-type or catalytically inactive variant C114A, were expressed and purified as reported previously (Lee et al., 2010a).

Preparation of *Xenopus* egg extract

Interphase *Xenopus* egg extract was prepared from eggs laid overnight according to the protocol of Murray (Murray, 1991) with the exception that eggs were activated with 2 μg ml^{-1} calcium ionophore (A23187, free acid form, Calbiochem) for 30 min prior to the crushing spin. Extract was frozen in liquid nitrogen and stored at -80 ºC. Interphase extract was induced to enter mitosis by addition of non-degradable cyclin B, which activates CDK1 and stimulates mitotic phosphorylation, resulting in APC/C activation. A fusion of the maltose-binding protein (MBP) to *Xenopus* cyclin B lacking its N-terminal 90 amino acids (MBP-Δ90) (Salic and King, 2005) was expressed in *E. coli* by inducing cultures at an D_{600nm}=0.6 with 300 μM

isopropylthiogalactoside (IPTG) for 5 h at room temperature. Purification was carried out following New England BioLabs (NEB) protocol. To make mitotic extract, MBP- Δ90 was added to interphase extract generally at ~ 20 μg ml^{-1} and incubated at 22-24 ºC for 45-60 min.

APC/C purification and reconstituted ubiquitination of cyclin B1

Reactions were performed essentially as described previously (Kirkpatrick et al., 2006) for the indicated times. Briefly, for each 30 μl reaction, APC/C was immunopurified from 600 μl of mitotic *Xenopus* egg extract by incubation for 1 h at 4 °C with 12 μg of anti-Cdc27 antibodies (AF3.1, Santa Cruz Biotechnology) immobilized onto 30 μl of Affiprep Protein A beads (156-0006, Bio-Rad). Following incubation with extract, beads were washed very quickly to minimize loss of associated APC/C co-activator Cdc20 three times with XB high salt (10 mM potassium HEPES, pH 7.7, 500 mM KCl, 0.1 mM $CaCl_2$, 1 mM $MgCl_2$), two times with XB (the same content as XB high salt, except with 100 mM KCl), and then three times with the reaction buffer (20 mM Tris, pH 7.5, 100 mM KCl, 2.5 mM $MgCl_2$, 2 mM ATP). Ubiquitination reactions were typically performed at 24 °C with agitation on a shaker at 1500 r.p.m.. Ubiquitination reactions contained immunoprecipitated APC/C on 30 μl beads, and 30 μl of a mix containing recombinant MBP-human E1 (1.3 μM), His-tagged UBCH10 (100 nM – 4 μM, concentrations as indicated) as the E2 enzyme, wild-type or different forms of ubiquitin (118-145 μM, concentrations as indicated), and 450-500 nM of HA-cyclin B1 NT(1-88)-His.

Cyclin B1 degradation in *Xenopus* egg extract

Degradation assays where nonubiquitinated cyclin B1 was added to extract were generally performed in 40 μl total volume per reaction condition with extract constituting 75-80% of that volume. For experiments with TAME and Mg262, extracts were pre-treated with relevant compound or DMSO control for 15 min at 24 °C, 1250 r.p.m.. Extracts contained 100 μg ml^{-1} cycloheximide to prevent re-incorporation of free labeled amino acid. Degradation experiments

were performed at 24 °C, 1250 r.p.m., with samples taken at indicated times. In degradation assays with ^{35}S-labeled cyclin B1 NT, reactions (3 μl per time-point) were terminated by addition of 97 μl of 20% TCA (in H_2O), vortexed and incubated on ice ≥ 30 min before centrifugation at 14,000*g*, 4 °C. A fraction (50%) of sample supernatants was combined with NaOH to neutralize the acid and added to Ultima Gold scintillation fluid (6013327, Perkin Elmer). A Packard scintillation counter was used to take all measurements. Acid-soluble counts were compared to total radioactive counts and results were graphed as percent soluble radioactive counts.

For degradation of preubiquitinated cycB1-NT in extract, interphase extract was pre-treated with USP14 inhibitor, as indicated, or DMSO for 15 min at 24 °C, 1250 r.p.m. and supplemented with 100 μg ml^{-1} cycloheximide prior to substrate addition. For degradation of ^{5}S cyclin B1 NT-Ub conjugates, extract (14 μl) was added to 4 μl of cyclin B1 NT-Ub_n conjugates for each time-point. Degradation mixtures were incubated at 24 °C, 1250 r.p.m. for indicated times. Reactions were quenched by addition of 107 μl of 20% TCA (in H_2O), vortexed and incubated on ice ≥ 30 min before centrifugation at 14,000*g*, at 4 °C for 30 min. A fraction of supernatants was combined with NaOH and added to Ultima Gold scintillation fluid (6013327, Perkin Elmer).

References

Borodovsky, A., Kessler, B. M., Casagrande, R., Overkleeft, H. S., Wilkinson, K. D., and Ploegh, H. L. (2001). A novel active site-directed probe specific for deubiquitylating enzymes reveals proteasome association of USP14. Embo J *20*, 5187-5196.

Crosas, B., Hanna, J., Kirkpatrick, D. S., Zhang, D. P., Tone, Y., Hathaway, N. A., Buecker, C., Leggett, D. S., Schmidt, M., King, R. W.*, et al.* (2006). Ubiquitin chains are remodeled at the proteasome by opposing ubiquitin ligase and deubiquitinating activities. Cell *127*, 1401-1413.

Dimova, N. V., Hathaway, N. A., Lee, B. H., Kirkpatrick, D. S., Berkowitz, M. L., Gygi, S. P., Finley, D., and King, R. W. (2012). APC/C-mediated multiple monoubiquitylation provides an alternative degradation signal for cyclin B1. Nat Cell Biol *14*, 168-176.

Hanna, J., Hathaway, N. A., Tone, Y., Crosas, B., Elsasser, S., Kirkpatrick, D. S., Leggett, D. S., Gygi, S. P., King, R. W., and Finley, D. (2006). Deubiquitinating enzyme Ubp6 functions noncatalytically to delay proteasomal degradation. Cell *127*, 99-111.

Huang, X., Summers, M. K., Pham, V., Lill, J. R., Liu, J., Lee, G., Kirkpatrick, D. S., Jackson, P. K., Fang, G., and Dixit, V. M. (2011). Deubiquitinase USP37 Is Activated by CDK2 to Antagonize APC(CDH1) and Promote S Phase Entry. Mol Cell *42*, 511-523.

Kimata, Y., Baxter, J. E., Fry, A. M., and Yamano, H. (2008). A role for the Fizzy/Cdc20 family of proteins in activation of the APC/C distinct from substrate recruitment. Mol Cell *32*, 576-583.

Kirkpatrick, D. S., Hathaway, N. A., Hanna, J., Elsasser, S., Rush, J., Finley, D., King, R. W., and Gygi, S. P. (2006). Quantitative analysis of in vitro ubiquitinated cyclin B1 reveals complex chain topology. Nat Cell Biol *8*, 700-710.

Lee, B. H., Lee, M. J., Park, S., Oh, D. C., Elsasser, S., Chen, P. C., Gartner, C., Dimova, N., Hanna, J., Gygi, S. P.*, et al.* (2010a). Enhancement of proteasome activity by a small-molecule inhibitor of USP14. Nature *467*, 179-184.

Lee, M. J., Lee, B. H., Hanna, J., King, R. W., and Finley, D. (2010b). Trimming of ubiquitin chains by proteasome-associated deubiquitinating enzymes. Mol Cell Proteomics *10*, R110 003871.

Leggett, D. S., Hanna, J., Borodovsky, A., Crosas, B., Schmidt, M., Baker, R. T., Walz, T., Ploegh, H., and Finley, D. (2002). Multiple associated proteins regulate proteasome structure and function. Mol Cell *10*, 495-507.

Murray, A. W. (1991). Cell cycle extracts. Methods Cell Biol *36*, 581-605.

Salic, A., and King, R. W. (2005). Identifying small molecule inhibitors of the ubiquitin-proteasome pathway in Xenopus egg extracts. Methods Enzymol *399*, 567-585.

Zeng, X., and King, R. W. (2012). An APC/C inhibitor stabilizes cyclin B1 by prematurely terminating ubiquitination. Nat Chem Biol.

Zeng, X., Sigoillot, F., Gaur, S., Choi, S., Pfaff, K. L., Oh, D. C., Hathaway, N., Dimova, N., Cuny, G. D., and King, R. W. (2010). Pharmacologic inhibition of the anaphase-promoting

complex induces a spindle checkpoint-dependent mitotic arrest in the absence of spindle damage. Cancer Cell *18*, 382-395.

Vol 467|9 September 2010|doi:10.1038/nature09299 nature

ARTICLES

Enhancement of proteasome activity by a small-molecule inhibitor of USP14

Byung-Hoon Lee[1]*, Min Jae Lee[1]*, Soyeon Park[1], Dong-Chan Oh[2,3], Suzanne Elsasser[1], Ping-Chung Chen[4], Carlos Gartner[1]†, Nevena Dimova[1], John Hanna[1]†, Steven P. Gygi[1], Scott M. Wilson[4], Randall W. King[1] & Daniel Finley[1]

Proteasomes, the primary mediators of ubiquitin–protein conjugate degradation, are regulated through complex and poorly understood mechanisms. Here we show that USP14, a proteasome-associated deubiquitinating enzyme, can inhibit the degradation of ubiquitin–protein conjugates both *in vitro* and in cells. A catalytically inactive variant of USP14 has reduced inhibitory activity, indicating that inhibition is mediated by trimming of the ubiquitin chain on the substrate. A high-throughput screen identified a selective small-molecule inhibitor of the deubiquitinating activity of human USP14. Treatment of cultured cells with this compound enhanced degradation of several proteasome substrates that have been implicated in neurodegenerative disease. USP14 inhibition accelerated the degradation of oxidized proteins and enhanced resistance to oxidative stress. Enhancement of proteasome activity through inhibition of USP14 may offer a strategy to reduce the levels of aberrant proteins in cells under proteotoxic stress.

The proteasome is essential for life in eukaryotes and regulates many aspects of cell physiology[1,2]. Substrates are targeted to the proteasome most often by means of ubiquitination. The proteasome holoenzyme is composed of a 19-subunit regulatory particle (known as the RP, 19S complex, or PA700) and a 28-subunit core particle (known as the CP or 20S complex). Substrate first binds the RP, and is then actively translocated to the CP, where it is degraded. The mechanisms regulating proteasome activity remain poorly understood, but involve numerous proteins that reversibly associate with it. Some bind the RP and deliver ubiquitin conjugates to the proteasome, whereas others open the axial channel into the CP. A third class of associated proteins, composed of ubiquitin ligases and deubiquitinating enzymes (DUBs), modifies proteasome-bound ubiquitin chains. Ubiquitin chains vary in their linkage type and length, and longer variants interact more strongly with the proteasome[3]. The extension and disassembly of chains at the proteasome may alter substrate degradation rates by changing substrate affinity for the proteasome.

Mammalian proteasomes are associated with three DUBs: RPN11, UCH37 and USP14 (refs 4–22). UCH37 and USP14 associate reversibly with the proteasome, whereas RPN11 is a stoichiometric subunit[2]. These enzymes reside on the RP and remove ubiquitin from the substrate before substrate degradation. The release of ubiquitin spares it from degradation, minimizing fluctuations in ubiquitin pools. The activity of RPN11 on the substrate's ubiquitin chain is thought to be delayed until the proteasome is committed to degrading the substrate[4,5]. RPN11 then cuts at the base of a ubiquitin chain, freeing substrate[5]. Thus, removal of the ubiquitin chain by RPN11 can promote substrate translocation into the CP to be hydrolysed[4,5]. However, deubiquitination before commitment might inhibit substrate degradation, as ubiquitin targets the protein for degradation[6].

In contrast to RPN11, USP14 and UCH37 can attack ubiquitin chains independently of commitment to substrate degradation. UCH37, and perhaps USP14, disassemble the chain from its substrate-distal tip[6,15,16], thus shortening chains rather than removing them en bloc. Little is known about such 'chain-trimming' reactions[6–8]. One model is that chain trimming increases the ability of proteasomes to discriminate between long and short multiubiquitin chains[6]. Here we show that a small-molecule inhibitor of deubiquitination by USP14 stimulates protein degradation *in vitro* and in cells. These findings reveal that, for those substrates tested, proteasome function is limited by USP14-dependent chain trimming. Thus, otherwise competent substrates of the proteasome can be rejected when chain trimming is faster than competing steps leading to substrate degradation.

USP14 inhibits the proteasome *in vitro*

We have previously shown that Ubp6, the yeast orthologue of USP14, is a potent inhibitor of the proteasome[16]. To test whether this is also true of USP14 from humans, we first developed a purification procedure that results in proteasomes lacking detectable USP14 (modified from ref. 23). Such proteasomes retain high levels of ubiquitin-7-amido-4-methylcoumarin (Ub–AMC) hydrolysing activity (data not shown), which is presumably UCH37-dependent (Supplementary Fig. 1). This activity can be inhibited irreversibly using ubiquitin–vinylsulphone (Ub–VS)[24], which forms an adduct with the active site Cys in DUBs of the thiol protease class. When such 'VS-proteasomes' were reconstituted with recombinant USP14 (Supplementary Fig. 2), Ub–AMC hydrolysing activity was increased 800-fold over that of isolated USP14 (Fig. 1a). Thus, the deubiquitinating activity of USP14 is activated by proteasomes (see also refs 10, 11, 15, 18, 22). Using the Ub–AMC assay, the affinity of USP14 for the proteasome was found to be 4 nM (Supplementary Fig. 3).

Proteasomes reconstituted with a saturating amount of USP14 were challenged with a model proteasome substrate, ubiquitinated

[1]Department of Cell Biology, Harvard Medical School, 240 Longwood Avenue, Boston, Massachusetts 02115, USA. [2]Department of Biological Chemistry and Molecular Pharmacology, Harvard Medical School, 240 Longwood Avenue, Boston, Massachusetts 02115, USA. [3]Natural Products Research Institute, College of Pharmacy, Seoul National University, San 56-1, Sillim, Seoul 151-742, Republic of Korea. [4]Department of Neurobiology, Evelyn F. McKnight Brain Institute, Civitan International Research Center, University of Alabama at Birmingham, Birmingham, Alabama 35294, USA. †Present addresses: Department of Biological Sciences, 193 Galvin Life Sciences Center, Notre Dame, Indiana 46556, USA (C.G.); Department of Pathology, Brigham and Women's Hospital, 75 Francis Street, Boston, Massachusetts 02115, USA (J.H.).
*These authors contributed equally to this work.

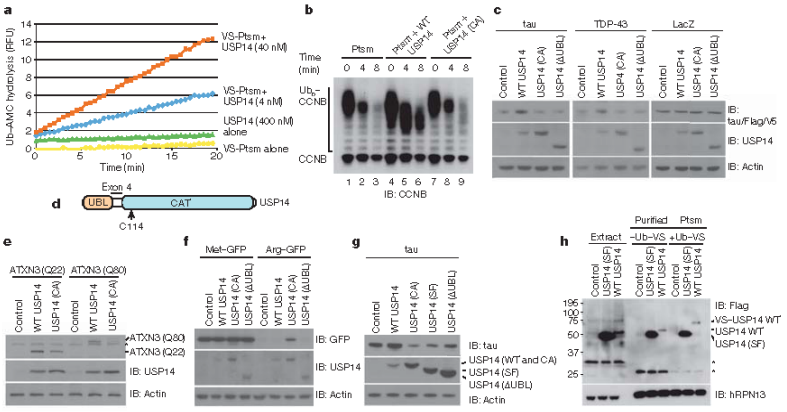

Figure 1 | USP14 is an inhibitor of the proteasome. **a**, Ub–AMC hydrolysis assay of USP14 activity in the presence or absence of Ub–VS-treated human proteasome (VS-proteasome; 1 nM). RFU, relative fluorescence units. Ptsm, 26S proteasome. **b**, *In vitro* degradation assay with polyubiquitinated CCNB (Ub_n–CCNB), human proteasome (4 nM), and wild-type (WT) USP14 (USP14) or mutant USP14(C114A) (USP14(CA); 60 nM). Samples in **b**, **c** and **e**–**h** were analysed by SDS–PAGE/immunoblotting (IB). **c**, Plasmids expressing tau, Flag–TDP-43, or V5–LacZ were co-transfected into *Usp14*$^{-/-}$ MEFs with variants of Flag–USP14 as indicated. Samples were collected 2 days after transfection. Actin, loading control. **d**, Diagram of human USP14, showing ubiquitin-like (UBL) and catalytic (CAT) domains. C114, active site cysteine. Splice variant USP14(SF) is produced from an mRNA lacking exon 4 (ref. 12). **e**, Flag-tagged ATXN3(Q22) or ATXN3(Q80) was co-expressed with USP14 variants in *Usp14*$^{-/-}$ MEFs and detected with anti-Flag antibodies. **f**, Arg–GFP or control Met–GFP co-expressed with USP14 variants in *Usp14*$^{-/-}$ MEFs. **g**, As **c** except HEK293 cells were used. **h**, USP14(SF) associates with but is not activated by proteasomes. Each variant of Flag–USP14 was expressed in HEK293T cells containing tagged hRPN11, and proteasomes were affinity purified. Where indicated, Ub–VS was incubated with lysate before proteasome purification. Extract samples represent 5% of total. Asterisks indicate nonspecific signals. Proteasome subunit hRPN13, loading control. Control samples, empty vector. Equal cell numbers were used for each lane.

cyclin B (Ub–CCNB). Like Ubp6, USP14 inhibited the degradation of Ub–CCNB (Fig. 1b). An active site mutant of USP14, USP14(C114A), showed little inhibitory effect, indicating that chain trimming is the basis for inhibition. Indeed, extensive trimming of ubiquitin from CCNB, as indicated by the shift of Ub–CCNB bands to a lower molecular mass, was evident in the presence of USP14 but not USP14(C114A) (Fig. 1b). Apparently, complete deubiquitination of CCNB is not required to suppress degradation, because USP14 rapidly removed only a portion of the ubiquitin from CCNB, even upon longer incubation (Fig. 1b). The strong dependence of chain trimming on USP14 was unexpected because active UCH37 was present in these proteasomes (Supplementary Fig. 1). When Ub–AMC is used as a substrate, UCH37 activity predominates over that of USP14 (refs 7, 8), but a true ubiquitin–protein conjugate, Ub–CCNB, shows the inverse effect. The lack of significant inhibition of degradation seen with USP14(C114A) was also surprising because Ubp6 exhibits a non-catalytic mechanism of proteasome inhibition[16]. As described below, a non-catalytic effect is seen with USP14, although it is not well visualized in this assay.

USP14 inhibits protein turnover in cells

To verify that USP14 inhibits the proteasome in cells, we expressed USP14 variants in *Usp14*$^{-/-}$ murine embryonic fibroblasts (MEFs), together with proteasome substrates. As substrates we initially chose two proteins that are critical in neurodegenerative diseases: tau and TDP-43 (refs 25, 26). Tau is thought to undergo proteasomal degradation[27,28]. Tau and TDP-43 showed increased levels when co-expressed with wild-type USP14 in *Usp14*$^{-/-}$ MEFs, indicating proteasome inhibition by USP14 (Fig. 1c). No effect was seen at the mRNA level (Supplementary Fig. 4). As seen *in vitro*, USP14(C114A) showed little or no activity in the assay. Thus, the ability of the proteasome to degrade tau and TDP-43 in MEFs seems to be suppressed by trimming of ubiquitin from these substrates. The amino-terminal ubiquitin-like (UBL) domain of USP14 (Fig. 1d) is its principal proteasome-binding site[15], and accordingly deletion of the UBL domain abrogated the USP14 effect (Fig. 1c). The effects on tau levels reflected accelerated degradation: tau disappeared more slowly from cells expressing USP14 in a chase experiment (Supplementary Fig. 5). USP14 did not affect the levels of two proteins that are thought to be stable: LacZ and actin (Fig. 1c). In MEFs and other cell types, wild-type USP14 was usually expressed at lower levels than USP14(C114A) (Fig. 1), indicating that USP14 may be subject to autoregulation.

Another protein linked to neurodegeneration and thought to be a substrate of the proteasome is ataxin-3 (ATXN3)[29]. Polyglutamine-expanded forms of ATXN3 give rise to spinocerebellar ataxia 3. Both wild-type (22 glutamines; Q22) and expanded forms of ATXN3(Q80) were stabilized by expression of USP14 in *Usp14*$^{-/-}$ MEFs (Fig. 1e). Expression of wild-type USP14 engendered stronger accumulation of ATXN3 than expression of USP14(C114A). However, in contrast to tau and TDP-43, the stabilizing effect of catalytically inactive USP14 was substantial for ATXN3(Q22) and ATXN3(Q80). Stabilization of ATXN3 by USP14(C114A) presumably represents the same non-catalytic effect as described for Ubp6 in *Saccharomyces cerevisiae*[16]. Thus, the non-catalytic inhibitory effect is apparently conserved in evolution. A non-catalytic effect was also observed for a model substrate of the proteasome[30,31], Arg–GFP (Fig. 1f). Wild-type USP14 was

ineffective in Arg–GFP stabilization in comparison to USP14(C114A) (Fig. 1f), the non-catalytic effect being dominant. Met–GFP, a stable protein, was unaffected by USP14. It will be interesting to determine what substrate features underlie the differing sensitivities of these substrates to catalytic and non-catalytic inhibition of degradation.

The effect of USP14 on tau degradation was confirmed in HEK293 cells. As in MEFs, USP14 overexpression stabilized tau (Fig. 1g). Results obtained with USP14 mutants differed from those obtained using MEFs, as expected, given that HEK293 cells express endogenous USP14; the expression of USP14(C114A) in *Usp14*$^{-/-}$ MEFs had no effect on tau, whereas in HEK293 cells the USP14(C114A) mutant produced accelerated tau degradation (Fig. 1g). This result presumably reflects displacement of endogenous USP14 from the proteasome. As expected, deletion of the UBL domain attenuated the dominant-negative effect (Fig. 1g). In contrast to USP14(ΔUBL), the short form (SF) of USP14—expressed from a developmentally regulated[18] mRNA that lacks a 33-codon junctional exon (exon 4) between the UBL domain and the catalytic domain[13,18] (Fig. 1d)—did exhibit a dominant-negative effect (Fig. 1g). This result indicated that USP14(SF) might bind proteasomes and counter the action of full-length USP14. Thus, USP14(SF) may be an endogenous inhibitor of USP14 activity. Consistent with this possibility, USP14(SF) binds proteasomes, but is not activated enzymatically by proteasome binding, as shown by its inability to react with Ub–VS (Fig. 1h). USP14(SF) also seems to lack non-catalytic proteasome-inhibitory capacity, because its expression in *Usp14*$^{-/-}$ MEFs did not stabilize Arg–GFP (Supplementary Fig. 6).

A selective small-molecule inhibitor of USP14

The results above suggested that chain trimming at the proteasome antagonizes the degradation of multiple substrates. Therefore, a small-molecule inhibitor of USP14 might enhance proteasome activity. We screened 63,052 compounds for the ability to inhibit USP14, using VS-proteasomes reconstituted with USP14 and assayed with Ub–AMC, identifying 215 as true USP14 inhibitors (details in Methods, Supplementary Table and Supplementary Fig. 7). When the hits were counter-screened against a panel of DUBs, only three of the strong hits showed selectivity for USP14. We proceeded with more detailed studies of the strongest hit, 1-[1-(4-fluorophenyl)-2,5-dimethylpyrrol-3-yl]-2-pyrrolidin-1-ylethanone, referred to hereafter as IU1 (Fig. 2a). Its structure is suggestive of an active-site-directed thiol protease inhibitor. The half-maximal inhibitory concentration (IC_{50}) of IU1 for USP14 is 4–5 μM (Fig. 2b and Supplementary Fig. 8). IU1 failed to significantly inhibit eight DUBs of human origin (Fig. 2b, c and Supplementary Figs 9 and 10), as well as Ub–AMC hydrolysis by proteasomes lacking USP14, which is attributable to UCH37 (Supplementary Fig. 8). We also identified a compound that is closely related to IU1 but does not inhibit USP14 (IU1C; Fig. 2a and Supplementary Fig. 11), and used this as a specificity control in subsequent assays. In the absence of proteasomes, USP14 was insensitive to IU1 (Supplementary Fig. 8), indicating that IU1 binds specifically to the activated form of USP14. IU1 could potentially inhibit USP14 by preventing its docking on the proteasome, but direct tests of this scenario proved negative (Supplementary Fig. 12). USP14 inhibition was rapidly established upon addition of IU1 and rapidly reversed upon its removal (Fig. 2d and Supplementary Fig. 13).

We used Ub–CCNB to test whether IU1 could inhibit the trimming of ubiquitin chains by the proteasome. To separate chain trimming from substrate degradation, these assays were done in the presence of proteasome inhibitors[4]. When proteasomes lacking USP14 were tested, IU1 had no effect on ubiquitin chain trimming (Fig. 3a). Chain trimming was strongly enhanced by USP14, as apparent from the increased electrophoretic mobility of Ub–CCNB species. Addition of IU1 to the assay reversed this effect (Fig. 3a; see also Supplementary Fig. 14).

We next tested whether IU1 could enhance degradation. Proteasomal degradation of Ub–CCNB was indeed markedly stimulated

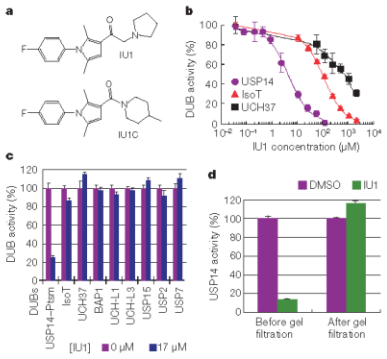

Figure 2 | IU1 inhibits human USP14 specifically and reversibly. **a**, Chemical structures of IU1 and IU1C. Analytical data shown in Supplementary Fig. 16. **b**, IC_{50} determination for IU1 inhibition of Ub–AMC hydrolysis by proteasome-bound USP14 (4.7 + 0.7 μM), IsoT (100 + 0.4 μM) and UCH37 (700 + 300 μM). **c**, Ub–AMC (1 μM) hydrolysis assays showing specificity of IU1 for USP14 in comparison to eight other DUB enzymes. **d**, Reversibility of USP14 inhibition. 60 nM USP14 and 5 nM human proteasome were treated with vehicle (DMSO) or 100 μM IU1 for 2 h. After rapid spin gel-filtration, proteins were assayed for Ub–AMC hydrolysis. All values are presented as mean + s.d. ($n = 3$).

by IU1 (Fig. 3b). Proteasomes lacking USP14 were insensitive to IU1 (Fig. 3b), and CCNB degradation was unaffected by IU1 when proteasomes were reconstituted with USP14(C114A) (Supplementary Fig. 15). Thus, suppression of chain trimming by IU1 may account for its enhancement of degradation. IU1 also promoted degradation of Sic1, a CDK inhibitor from *S. cerevisiae* (Fig. 3c). These assays used a modified form of Sic1 in which the PY element signals ubiquitination[32]. Both substrates used in these *in vitro* assays, Ub–CCNB and Sic1, carry mixed ubiquitin chains, including linkages via K48, K63 and K11 residues[32,33]. Whether chains of different topologies vary in their susceptibility to USP14-dependent regulation is an important issue for future study.

A USP14 inhibitor accelerates proteolysis in cells

To determine whether IU1 is cell permeable, it was added to cultures and cell-associated IU1 was quantified by liquid chromatography-mass spectrometry (LC-MS) or ultraviolet absorption. When added at 50 μM, IU1 reached an apparent intracellular concentration of ~13 μM within 1 h, which remained constant over the course of the experiment (Supplementary Figs 17–19). Effects of IU1 on the viability of MEFs only became apparent at 250 μM (Supplementary Figs 20 and 21). Moreover, IU1 did not noticeably induce apoptosis (Supplementary Fig. 22). When cell proliferation was measured in real time, slight inhibition became apparent at 120 μM (Supplementary Fig. 21). In the case of both cell viability and proliferation assays, *Usp14*$^{-/-}$ MEFs were no less sensitive than wild type, indicating that IU1 toxicity at high concentrations was independent of USP14 inhibition.

To determine whether IU1 could enhance proteasome function in cells, we expressed tau in MEFs treated with sub-cytotoxic doses of IU1. IU1 induced dose-dependent reduction in tau levels, with a strong effect seen at 50 μM (Fig. 4a and Supplementary Fig. 23). Thus, IU1 treatment affected tau similarly to USP14(C114A) (Fig. 1c), consistent with active site inhibition. No effect was seen on tau mRNA (Supplementary Fig. 24). When *Usp14*$^{-/-}$ MEFs were

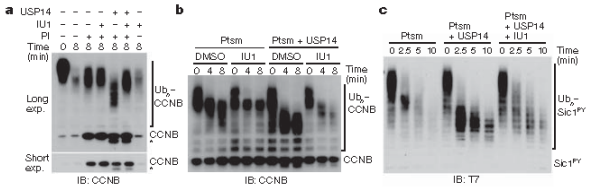

Figure 3 | IU1 inhibits chain trimming and stimulates substrate degradation *in vitro*. **a**, Chain-trimming assays. Samples contained 4 nM proteasome, and USP14 was added at 15-fold molar excess over proteasome. IU1 was added at 50 μM and proteasome inhibitors (PI) at 5 μM (PS-341, epoxomicin). Asterisk indicates CCNB species derived from residual thrombin from USP14 preparation[36]. All panels, SDS–PAGE/immunoblot analysis. **b**, *In vitro* Ub_n–CCNB degradation assay (IU1 at 34 μM). **c**, *In vitro* degradation assay with polyubiquitinated, T7-tagged $Sic1^{PY}$, human proteasome (5 nM) and wild-type USP14 (75 nM) in the absence or presence of IU1 (75 μM).

treated with IU1, no effect on tau was observed, indicating that IU1 enhances tau degradation through inhibiting USP14 (Fig. 4b). On the basis of these and previous experiments (Fig. 2c), nonspecific inhibition of other DUBs by IU1 does not affect proteasome function at this dose. The effect of IU1 on tau degradation was independent of autophagy (Supplementary Fig. 25). Several other proteins implicated in proteotoxic mechanisms—TDP-43, ATXN3, and glial fibrillary acidic protein (GFAP)—were similarly depleted from MEFs by IU1 (Fig. 4d, e and Supplementary Fig. 26). The effectiveness of IU1 in neurons, where proteotoxic mechanisms are commonly observed, has not been examined.

IU1 enhanced the extent of ubiquitin modification of TDP-43 in cells, perhaps accounting for its accelerated degradation (Fig. 4f). In contrast, little change was seen in bulk cellular ubiquitin conjugates (Fig. 4g and Supplementary Fig. 27). Free ubiquitin was reduced after IU1 addition, and, as the dose of IU1 increased, the level of free ubiquitin in wild-type MEFs approached that of untreated *Usp14*$^{-/-}$ MEFs (Fig. 4g). Previous work showed that USP14 and Ubp6 assist in the maintenance of cellular ubiquitin pools by suppressing proteasomal degradation of ubiquitin[11,13,14,17,34,35]. The conjugated rather than free form of ubiquitin is most subject to degradation[36]. By separating ubiquitin from its conjugative target, USP14 antagonizes this pathway of ubiquitin degradation.

Enhanced protein degradation in cells treated with IU1 could result from increased synthesis of proteasomes; however, no significant changes in proteasome composition were seen after IU1 treatment (Supplementary Fig. 28). USP14 is known to regulate gating of the proteasome[21], but this does not seem to be critical in the mode of action of IU1 (B.-H.L. and D.F., unpublished data). The detailed similarities observed between the effects of mutational inactivation

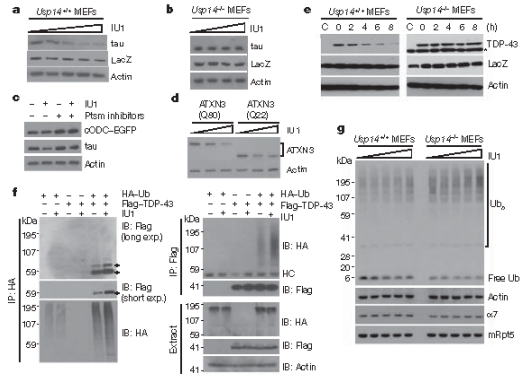

Figure 4 | IU1 enhances proteasomal degradation in cells. All panels show SDS–PAGE/immunoblot data. **a**, Thirty-six hours after co-transfecting wild-type MEFs with plasmids expressing tau and V5–LacZ, cells were incubated with 0, 25, 50, 75, or 100 μM of IU1 for 6 h. LacZ, transfection control. Actin, loading control. **b**, As in **a** except that MEFs were *Usp14*$^{-/-}$ and IU1 was at 0, 10, 50, or 100 μM. **c**, Tau and Ub-independent proteasome substrate cODC–EGFP were co-expressed in wild-type MEFs and incubated with 50 μM IU1 for 6 h. Proteasome inhibitors were MG132 (30 μM) and PS-341 (10 μM). **d**, As **b** except with ATXN3(Q80) and ATXN3(Q22), and IU1 at 0, 50 and 100 μM. **e**, Flag–TDP-43 was co-transfected with a LacZ-expressing plasmid into either wild-type or *Usp14*$^{-/-}$ MEFs, then treated with IU1 (75 μM) for the indicated time. Asterisk, nonspecific signal. **f**, HA-tagged Ub and/or Flag-tagged TDP-43 were transiently overexpressed in wild-type MEFs with 50 μM IU1 incubation for 6 h. Proteasome inhibitors (20 μM MG132, 10 μM PS-341) were added 4 h before lysis. Lysates were subjected to immunoprecipitation with anti-HA or anti-Flag. Arrows indicate likely ubiquitinated TDP-43 species. HC, heavy chain. **g**, Wild-type MEFs and *Usp14*$^{-/-}$ MEFs were treated with IU1 (0, 25, 50, 75, or 100 μM) for 6 h, followed by analysis for ubiquitin, actin, CP subunit α7 and RP subunit mRpt5.

of USP14's catalytic site and IU1 treatment, as well as the observation that USP14 is required for IU1 to affect protein degradation, provide strong evidence for the importance of chain trimming by USP14. In addition, IU1 had little or no effect in a cell-based assay on the degradation of a ubiquitin-independent substrate[37] of the proteasome, C-terminal ornithine decarboxylase-EGFP (cODC–EGFP) (Fig. 4c). Similar results were obtained *in vitro* with antizyme-promoted ODC degradation (data not shown). The effects of IU1 are probably restricted to ubiquitin-dependent proteasome substrates, based on its mode of action, but further characterization is required to establish this. Finally, Arg–GFP levels did not change upon treatment with IU1, when assayed in cells expressing USP14(C114A), indicating that IU1 does not influence USP14's non-catalytic inhibitory effect (Supplementary Fig. 26).

Oxidized proteins form a class of misfolded proteasome substrates that increase with age and are apparently toxic when they accumulate[38,39]. We induced protein oxidation by treating cells with menadione, and visualized oxidized species via their carbonyl groups. IU1 treatment strongly reduced the accumulation of oxidized proteins (Fig. 5a). When proteasome inhibitor was added, the effect of IU1 was attenuated, indicating that IU1 does not prevent the oxidation reaction itself. IU1 treatment reduced menadione toxicity substantially in HEK293 cells (Fig. 5b), strongly supporting the hypothesis that proteins are critical targets of oxidative damage. IU1 also reduced the toxicity of an unrelated oxidizing agent, hydrogen peroxide (data not shown). IU1C, the IU1 variant that is inactive against USP14, failed to reduce menadione cytotoxicity (Supplementary Fig. 29). These experiments suggest that IU1 can promote cell survival during proteotoxic stress.

Ubiquitin chain trimming antagonizes proteasome function

We report here that a small molecule selected for its capacity to inhibit the proteasome-associated deubiquitinating enzyme USP14 strongly enhances substrate degradation by the proteasome in cells. This is the first evidence that chain trimming by USP14 or its yeast orthologue Ubp6 inhibits proteasome activity through deubiquitination. The trimming of substrate-bound ubiquitin chains on the proteasome seems to govern the degradation rates of many ubiquitin–protein conjugates. Under normal growth conditions, the proteasome may be subject to tonic inhibition through this mechanism.

The scope of proteasome inhibition by chain trimming is not limited to substrates bearing only one or a few ubiquitin groups[5], as shown by studies of cyclin B and $Sic1^{PY}$ degradation. Also, suppression of degradation by chain trimming does not seem to be restricted to proteins that are not proper substrates of the proteasome. Chain trimming may be a more general, although not universal, mechanism for regulating protein turnover rates, suppressing the degradation of some substrates but not others. Further work will be required to determine what fraction of proteasome substrates can be regulated through this pathway, and what distinguishing features they share.

We also report that USP14 can inhibit proteasome function non-catalytically, as previously observed for its yeast orthologue Ubp6 (ref. 16). The capacity of USP14 to inhibit proteasomes via two distinct pathways has important implications. Briefly, the non-catalytic effect, in slowing substrate degradation at the proteasome, may allow individual substrates to be docked at the proteasome for a longer time, thus resulting in more extensive trimming of ubiquitin chains. However, the two modes of proteasome inhibition are not obligatorily coupled, because proteasome substrates exhibited differing relative sensitivities to catalytic and non-catalytic inhibition by USP14 (Fig. 1c–f). It will be important to identify the mechanistic basis of these differences.

Both USP14 and UCH37 exhibit chain-trimming activity, but the effectiveness of IU1 in reducing chain trimming and stimulating proteasome activity suggests that the redundancy between these two proteasome-bound enzymes may be less than expected. UCH37 does not readily substitute for USP14. Proteasomes are associated with multiple ubiquitin receptors, and the relative susceptibility of substrates to chain trimming by USP14 and UCH37 may depend on which receptors are engaged with a given substrate and the positioning of these receptors with respect to USP14 and UCH37. For example, UCH37 binds proteasomes via a ubiquitin receptor, RPN13 (refs 24, 40–42). Whether chain trimming by UCH37 can suppress proteasome activity as powerfully as USP14 will require further study.

Although eukaryotic cells require proteasome function, proteasome inhibitors have proven highly effective in the treatment of multiple myeloma[43], and may have additional applications[44]. In other contexts, however, enhancement of proteasome activity might be beneficial[45,46]. For example, enhanced proteasome function could have applications in disorders that result from partial loss-of-function mutations in ubiquitin pathway components[47]. More generally, many diseases, including major neurodegenerative diseases, are thought to be caused by the accumulation of misfolded proteins[48–50]. Misfolding, which renders these proteins toxic, can also mark them as substrates of the ubiquitin-proteasome and autophagy pathways[50]. Enhanced proteasome function, as induced by inhibitors of chain trimming, could therefore potentially be used to eliminate such toxic proteins more effectively.

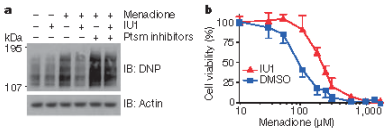

Figure 5 | IU1 alleviates cytotoxicity induced by oxidative stress. **a**, HEK293 cells were pre-incubated with IU1 (75 μM) or proteasome inhibitors (20 μM MG132, 10 μM PS-341) for 4 h, then treated with menadione (300 μM) for 60 min. Lysates were treated with DNPH and immunoblotted with anti-DNP antibody to assay oxidized proteins. **b**, Cell survival under oxidative stress measured using the MTT assay. HEK293 cells were pre-treated with 50 μM IU1 for 2 h. Menadione was added, followed by 4 h incubation. IU1 effects comparable to those of panels **a** and **b** were obtained in wild-type but not *Usp14*$^{-/-}$ MEFs (data not shown). Values are represented as mean ± s.d. ($n = 3$).

METHODS SUMMARY

For expression in mammalian cells we used full length USP14 (wild type USP14) and its splice variant lacking exon 4 (USP14(SF)) subcloned into pcDNA3.1 (Invitrogen) as previously described[16]. The USP14(C114A) and USP14(ΔUBL) constructs were generated in the same vector by PCR mediated mutagenesis and confirmed by sequencing. Human proteasomes were affinity purified on a large scale from a stable HEK293 cell line harbouring HTBH tagged hRPN11 (a gift from L. Huang). Ten microlitres of USP14 sample were dispensed into 384 well low volume plates in duplicate using a Wellmate dispenser. 33.3 nl of compound from the library were transferred into the wells using a Seiko pin transfer robotic system, followed by pre incubation for ~30 min. To initiate the reaction, 10 μl of VS proteasome plus Ub AMC mixture were added to each well. The sources of compound libraries for screening were as follows: Maybridge, Asinex, ActiMol TimTec, ChemBridge, ChemDiv, Enamine and MMV1. Primary hits were defined by 'robust' *Z* score analysis (Supplementary Fig. 7). To obtain dose response curves, curve fitting was performed by the four parameter logistic model or the three parameter fixed bottom model using SigmaPlot 9.0 according to guidelines from NIH Chemical Genomics Center. The gene trap allele, *Usp14*^{tm1a} (ref. 19), is referred to here as *Usp14*$^{-/-}$.

Full Methods and any associated references are available in the online version of the paper at www.nature.com/nature.

Received 22 April; accepted 14 June 2010.

1. Finley, D. Recognition and processing of ubiquitin-protein conjugates by the proteasome. *Annu. Rev. Biochem.* 78, 477–513 (2009).
2. Schrader, E. K., Harstad, K. G. & Matouschek, A. Targeting proteins for degradation. *Nature Chem. Biol.* 5, 815–822 (2009).

3. Thrower, J. S., Hoffman, L., Rechsteiner, M. & Pickart, C. M. Recognition of the polyubiquitin proteolytic signal. *EMBO J.* **19**, 94–102 (2000).
4. Verma, R. *et al.* Role of Rpn11 metalloprotease in deubiquitination and degradation by the 26S proteasome. *Science* **298**, 611–615 (2002).
5. Yao, T. & Cohen, R. E. A cryptic protease couples deubiquitination and degradation by the proteasome. *Nature* **419**, 403–407 (2002).
6. Lam, Y. A., Xu, W., DeMartino, G. N. & Cohen, R. E. Editing of ubiquitin conjugates by an isopeptidase in the 26S proteasome. *Nature* **385**, 737–740 (1997).
7. Koulich, E., Li, X. & DeMartino, G. N. Relative structural and functional roles of multiple deubiquitylating proteins associated with mammalian 26S proteasome. *Mol. Biol. Cell* **19**, 1072–1082 (2008).
8. Jacobson, A. D. *et al.* The lysine 48 and lysine 63 ubiquitin conjugates are processed differently by the 26S proteasome. *J. Biol. Chem.* **284**, 35485–35494 (2009).
9. Verma, R. *et al.* Proteasomal proteomics: identification of nucleotide-sensitive proteasome-interacting proteins by mass spectrometric analysis of affinity-purified proteasomes. *Mol. Biol. Cell* **11**, 3425–3439 (2000).
10. Borodovsky, A. *et al.* A novel active site-directed probe specific for deubiquitylating enzymes reveals proteasome association of USP14. *EMBO J.* **20**, 5187–5196 (2001).
11. Leggett, D. S. *et al.* Multiple associated proteins regulate proteasome structure and function. *Mol. Cell* **10**, 495–507 (2002).
12. Wilson, S. M. *et al.* Synaptic defects in ataxia mice result from a mutation in Usp14, encoding a ubiquitin-specific protease. *Nature Genet.* **32**, 420–425 (2002).
13. Chernova, T. A. *et al.* Pleiotropic effects of Ubp6 loss on drug sensitivities and yeast prion are due to depletion of the free ubiquitin pool. *J. Biol. Chem.* **278**, 52102–52115 (2003).
14. Anderson, C. *et al.* Loss of Usp14 results in reduced levels of ubiquitin in ataxia mice. *J. Neurochem.* **95**, 724–731 (2005).
15. Hu, M. *et al.* Structure and mechanisms of the proteasome-associated deubiquitinating enzyme Usp14. *EMBO J.* **24**, 3747–3756 (2005).
16. Hanna, J. *et al.* Deubiquitinating enzyme Ubp6 functions noncatalytically to delay proteasomal degradation. *Cell* **127**, 99–111 (2006).
17. Hanna, J., Meides, A., Zhang, D. P. & Finley, D. A ubiquitin stress response induces altered proteasome composition. *Cell* **129**, 747–759 (2007).
18. Crimmins, S. *et al.* Transgenic rescue of ataxia mice with neuronal-specific expression of ubiquitin-specific protease 14. *J. Neurosci.* **26**, 11423–11431 (2006).
19. Crimmins, S. *et al.* Transgenic rescue of ataxia mice reveals a male-specific sterility defect. *Dev. Biol.* **325**, 33–42 (2009).
20. Chen, P.-C. *et al.* The proteasome-associated deubiquitinating enzyme Usp14 is essential for the maintenance of synaptic ubiquitin levels and the development of neuromuscular junctions. *J. Neurosci.* **29**, 10909–10919 (2009).
21. Peth, A., Besche, H. C. & Goldberg, A. L. Ubiquitinated proteins activate the proteasome by binding to Usp14/Ubp6, which cause 20S gate opening. *Mol. Cell* **36**, 794–804 (2009).
22. Catic, A. *et al.* Screen for ISG15-crossreactive deubiquitinases. *PLoS ONE* **2**, e679 (2007).
23. Wang, X. *et al.* Mass spectrometric characterization of the affinity-purified human 26S proteasome complex. *Biochemistry* **46**, 3553–3565 (2007).
24. Yao, T. *et al.* Proteasome recruitment and activation of the Uch37 deubiquitinating enzyme by Adrm1. *Nature Cell Biol.* **8**, 994–1002 (2006).
25. Spires-Jones, T. L., Stoothoff, W. H., de Calignon, A., Jones, P. B. & Hyman, B. T. Tau pathophysiology in neurodegeneration: a tangled issue. *Trends Neurosci.* **32**, 150–159 (2009).
26. Kwong, L. K., Uryu, K., Trojanowski, J. Q. & Lee, V. M. TDP-43 proteinopathies: neurodegenerative protein misfolding diseases without amyloidosis. *Neurosignals* **16**, 41–51 (2008).
27. David, D. C. *et al.* Proteasomal degradation of tau protein. *J. Neurochem.* **83**, 176–185 (2002).
28. Petrucelli, L. *et al.* CHIP and Hsp70 regulate tau ubiquitination, degradation and aggregation. *Hum. Mol. Genet.* **13**, 703–714 (2004).
29. Todi, S. V. *et al.* Cellular turnover of the polyglutamine disease protein ataxin-3 is regulated by its catalytic activity. *J. Biol. Chem.* **282**, 29348–29358 (2007).
30. Varshavsky, A., Turner, G., Du, F. & Xie, Y. The ubiquitin system and the N-end rule pathway. *Biol. Chem.* **381**, 779–789 (2000).
31. Dantuma, N. P., Lindsten, K., Glas, R., Jellne, M. & Masucci, M. G. Short-lived green fluorescent proteins for quantifying ubiquitin/proteasome-dependent proteolysis in living cells. *Nature Biotechnol.* **18**, 538–543 (2000).
32. Saeki, Y., Isono, E. & Toh-E, A. Preparation of ubiquitinated substrates by the PY motif-insertion method for monitoring proteasome activity. *Methods Enzymol.* **399**, 215–227 (2005).
33. Kirkpatrick, D. S. *et al.* Quantitative analysis of *in vitro* ubiquitinated cyclin B1 reveals complex chain topology. *Nature Cell Biol.* **8**, 700–710 (2006).
34. Amerik, A. Y., Li, S. J. & Hochstrasser, M. Analysis of the deubiquitinating enzymes of the yeast *Saccharomyces cerevisiae*. *Biol. Chem.* **381**, 981–992 (2000).
35. Hanna, J., Leggett, D. S. & Finley, D. Ubiquitin depletion as a key mediator of toxicity by translational inhibitors. *Mol. Cell. Biol.* **23**, 9251–9261 (2003).
36. Shabek, N., Herman-Bachinsky, Y. & Ciechanover, A. Ubiquitin degradation with its substrate, or as a monomer in a ubiquitination-independent mode, provides clues to proteasome regulation. *Proc. Natl Acad. Sci. USA* **106**, 11907–11912 (2009).
37. Hoyt, M. A., Zhang, M. & Coffino, P. Probing the ubiquitin/proteasome system with ornithine decarboxylase, a ubiquitin-independent substrate. *Methods Enzymol.* **398**, 399–413 (2005).
38. Stadtman, E. R. Protein oxidation and aging. *Free Radic. Res.* **40**, 1250–1258 (2006).
39. Ahmed, E. K., Picot, C. R., Bulteau, A. L. & Friguet, B. Protein oxidative modifications and replicative senescence of WI-38 human embryonic fibroblasts. *Ann. NY Acad. Sci.* **1119**, 88–96 (2007).
40. Hamazaki, J. *et al.* A novel proteasome interacting protein recruits the deubiquitinating enzyme UCH37 to 26S proteasomes. *EMBO J.* **25**, 4524–4536 (2006).
41. Qiu, X. B. *et al.* hRpn13/ADRM1/GP110 is a novel proteasome subunit that binds the deubiquitinating enzyme, UCH37. *EMBO J.* **25**, 5742–5753 (2006).
42. Husnjak, K. *et al.* Proteasome subunit Rpn13 is a novel ubiquitin receptor. *Nature* **453**, 481–488 (2008).
43. Chauhan, D., Bianchi, G. & Anderson, K. C. Targeting the UPS as therapy in multiple myeloma. *BMC Biochem.* **9** (Suppl. 1), S1 (2008).
44. Muchamuel, T. *et al.* A selective inhibitor of the immunoproteasome subunit LMP7 blocks cytokine production and attenuates progression of experimental arthritis. *Nature Med.* **15**, 781–787 (2009).
45. Chondrogianni, N. *et al.* Overexpression of proteasome β5 subunit increases the amount of assembled proteasome and confers ameliorated response to oxidative stress and higher survival rates. *J. Biol. Chem.* **280**, 11840–11850 (2005).
46. Tonoki, A. *et al.* Genetic evidence linking age-dependent attenuation of the 26S proteasome with the aging process. *Mol. Cell. Biol.* **29**, 1095–1106 (2009).
47. Lehman, N. L. The ubiquitin proteasome system in neuropathology. *Acta Neuropathol.* **118**, 329–347 (2009).
48. Hinault, M. P., Ben-Zvi, A. & Goloubinoff, P. Chaperones and proteases: cellular fold-controlling factors of proteins in neurodegenerative diseases and aging. *J. Mol. Neurosci.* **30**, 249–265 (2006).
49. Balch, W. E., Morimoto, R. I., Dillin, A. & Kelly, J. W. Adapting proteostasis for disease intervention. *Science* **319**, 916–919 (2008).
50. Goldberg, A. L. Protein degradation and protection against misfolded and damaged proteins. *Nature* **426**, 895–899 (2003).

Supplementary Information is linked to the online version of the paper at www.nature.com/nature.

Acknowledgements We thank K. Gordon, J. Y. Suk and N. Bays for advice and assistance, and members of the Finley laboratory for comments on the manuscript. We thank C. Shamu and the staff of the ICCB facility at Harvard Medical School, where the HT screen was carried out. We also thank N. Hathaway for ubiquitinated cyclin B, L. Huang for the tagged proteasome cell line, R. Baker for anti-USP14 antibody, G. DeMartino for anti-UCH37 antibody, K. Wilkinson and K. Walters for DUB enzymes, as well as C. Seong, M. Kim, S. M. Lim and D. Waterman for assistance in some experiments. For plasmids, we thank K. Walters, M. Sowa, W. Harper, V. Lee, F. Baralle, H. Paulson, Y. T. Kwon, M. Masucci, M.-K. Kwak, P. Coffino and C. Kahana. This work was supported by grants from the National Institutes of Health (DK082906 to D.F., GM65592 to D.F., GM66492 to R.W.K. and NS047533 to S.M.W.); the Harvard Technology Development Accelerator Fund (D.F.); Merck & Co. (D.F. and R.W.K.); and Johnson & Johnson (D.F. and R.W.K.).

Author Contributions B.-H.L. carried out screening and most *in vitro* studies, and M.J.L. chemical analysis and most cell-based assays. R.W.K. and D.F. were responsible for overall design and oversight of the project. S.P., S.E. and N.D. provided skilled assistance in proteasome biochemistry and assays. D.-C.O., C.G. and S.P.G. designed and carried out chemistry studies. P.-C.C., S.M.W. and J.H. provided key reagents and intellectual input. Many authors contributed to preparation of the manuscript.

Author Information Reprints and permissions information is available at www.nature.com/reprints. The authors declare competing financial interests: details accompany the full-text HTML version of the paper at www.nature.com/nature. Readers are welcome to comment on the online version of this article at www.nature.com/nature. Correspondence and requests for materials should be addressed to R.W.K. (randy_king@hms.harvard.edu) or D.F. (daniel_finley@hms.harvard.edu).

METHODS

Constructs, antibodies and biochemical reagents. For expression in mammalian cells we used full-length USP14 (WT USP14) and its splice variant lacking exon 4 (USP14(SF)) subcloned into pcDNA3.1 (Invitrogen) as previously described[18]. The USP14(C114A) and USP14(ΔUBL) constructs were generated in the same vector by PCR-mediated mutagenesis. For bacterial expression, glutathione *S*-transferase (GST) USP14 fusion protein constructs were generated using pGEX-2T (GE Healthcare). For the Flag-tagged version, the cDNAs were subcloned into pDONR223 and subsequently recombined into pCMV4-based destination vectors (ref. 51). Vectors expressing tau (from V. M. Lee), TDP-43 (from F. E. Baralle), ATXN3 (from H. Paulson), Ub-X GFPs (from M. G. Masucci), cODC EGFP (from P. Coffino) and luciferase (from M. Kwak) were provided. The pDONR223 vector was provided by M. Sowa and W. Harper. Anti-USP14 and anti-UCH37 antibodies were provided by R. Baker and G. DeMartino, respectively. Sources of other commercial antibodies are as follows: anti-tau (clone TAU-5; Invitrogen); anti-V5 (Invitrogen); anti-cyclin B (Ab-2, Neomarkers); anti-Flag M2 and anti-actin (A5060, Sigma); anti-Ub (UG9510; Enzo Life Sciences), anti-α6 (PW8100; Enzo), anti-α7 (PW8110; Enzo), and anti-RPN13 (PW9910; Enzo); anti-GFP (Ab290, Abcam); anti-T7-HRP (Novagen); anti-HA (12CA5, Roche); IRDye infrared secondary antibodies (Li-Cor). Sources of major biochemical reagents were as follows: IU1 and IU1C (T0502-8593 and T5369385, Enamine); PS-341 (LC Laboratories); epoxomicin and Ub VS (Boston Biochem); ADP (Calbiochem); MG132, ubiquitin and bafilomycin A_1 (Sigma); Suc-LLVY-AMC (Bachem).

Purification of recombinant USP14. GST USP14 (WT and C114A variants) was expressed in *Escherichia coli* strain Rosetta 2 (DE3) cells (Novagen). Cultures were grown at 37 °C until $OD_{600\,nm}$ reached 0.6 to 0.8, and expression was then induced overnight with 1 mM IPTG at room temperature. Cells were harvested in PBS containing protease inhibitors and lysed by French press. The cleared lysates were incubated with GST Sepharose 4B resin (GE Healthcare) at 4 °C for 1 h, and subsequently washed with excess PBS, followed by PBS containing 100 mM NaCl. The GST moiety was removed by thrombin in cleavage buffer (50 mM Tris-HCl (pH 8.0), 150 mM NaCl, 2.5 mM $CaCl_2$ and 0.1% 2-mercaptoethanol) for 3 h at room temperature. GST-tagged USP14 proteins for proteasome binding assays were eluted before thrombin cleavage using elution buffer (10 mM reduced glutathione and 50 mM Tris-HCl (pH 8.0)).

Native gel electrophoretic mobility assays. Native gel analysis using purified proteasomes was performed as in ref. 52, with slight modifications. Briefly, 5 pmol of GST, GST USP14 WT, GST USP14(C114A), untagged wild-type USP14, or untagged USP14(C114A) was mixed with 1 pmol of human proteasomes for 20 min at 30 °C. Complexes were resolved by 3.5% non-denaturing PAGE for 850 Volt-hours. Proteasomes were visualized using the fluorogenic substrate Suc-LLVY-AMC (Bachem) as described[52]. Both wild-type USP14 and catalytically inactive USP14(C114A) bind to 26S human proteasomes (Supplementary Fig. 2b).

For whole-cell lysate analysis, buffer B (50 mM NaH_2PO_4 (pH 7.5), 10% glycerol, 5 mM $MgCl_2$, 0.25% NP-40, 1 mM DTT, 5 mM ATP and 1× protease inhibitor cocktail) was used for lysis, which was carried out on ice for 15 min with intermittent vortexing. Lysates were cleared by centrifugation at 16,000 *g* for 10 min at 4 °C. 75 μg of total protein was loaded on a 3.5% polyacrylamide non-denaturing gel, with electrophoresis for 400 Volt-hours at 4 °C. After the in-gel Suc-LLVY-AMC hydrolysis assay (LAS 3000 imaging system, Fujifilm), gels were pre-soaked in transfer buffer containing 0.1% SDS and no methanol for 15 min (refs 53, 54), followed by protein transfer to PVDF and subsequent immunoblotting against CP subunit α6, which were performed as previously described[55].

Affinity purification of the 26S human proteasome. Human proteasomes were affinity-purified on a large scale from a stable HEK293T cell line harbouring HTBH-tagged hRPN11 (a gift from L. Huang). The cells were Dounce-homogenized in lysis buffer (50 mM NaH_2PO_4 (pH 7.5), 100 mM NaCl, 10% glycerol, 5 mM $MgCl_2$, 0.5% NP-40, 5 mM ATP and 1 mM DTT) containing protease inhibitors. Lysates were cleared, then incubated with NeutrAvidin agarose resin (Thermo Scientific) overnight at 4 °C. The beads were then washed with excess lysis buffer followed by the wash buffer (50 mM Tris-HCl (pH 7.5), 1 mM $MgCl_2$ and 1 mM ATP). For VS-proteasomes, Ub VS was added to the resin at 1 to 1.5 μM, followed by incubation at 30 °C for 2 h. Residual Ub VS was removed by washing the beads with at least 20 bed volumes of wash buffer. 26S proteasomes were eluted from the beads by cleavage, using TEV protease (Invitrogen). VS-proteasomes were tested to confirm the elimination of DUB activity using the Ub AMC hydrolysis assay. Endogenous wild-type USP14 was not found on the proteasome under these purification conditions (see Supplementary Fig. 1).

To purify human proteasomes (together with RP) in the presence of ADP, 'ATP-free' ADP was prepared and used for all the procedures as previously described[55].

High-throughput screening for USP14 inhibitors. Screening was conducted at the ICCB-Longwood screening facility (Harvard Medical School). Ten microlitres of recombinant USP14 protein were dispensed into each well of a 384-well low volume plate (Corning) in duplicate, using a Wellmate plate dispenser. 33.3 nl of compound from the library were pin-transferred into the wells using a Seiko pin transfer robotic system, followed by pre-incubation for about 30 min. The last two columns of each plate were used for positive and negative controls for the assay. To initiate the enzyme reaction, 10 μl of VS-proteasome plus Ub AMC mixture were added to each well, using a Wellmate dispenser. Samples were then incubated for another 45 min. Ub AMC hydrolysis was measured at Ex355/Em460 using an Envision plate reader (PerkinElmer). The final concentrations of USP14, VS-proteasome and Ub AMC were 15 nM, 1 nM and 0.8 μM, respectively. The final concentration of test compound was approximately 17 μM. Enzymes and substrates were prepared in Ub AMC assay buffer (50 mM Tris-HCl (pH 7.5), 1 mM EDTA, 1 mM ATP, 5 mM $MgCl_2$, 1 mM DTT, and 1 mg ml^{-1} ovalbumin). The sources of compound libraries used for screening were as follows: Maybridge, Asinex, ActiMol TimTec, ChemBridge, ChemDiv, Enamine and MMV1 (natural product extracts).

Primary hits were defined by 'robust' *Z*-score analysis as previously described (Supplementary Fig. 7 and ref. 56). In summary, the raw measurements of each sample from two replicates were averaged, and then *Z*-score was calculated by $(X_i - X)/\mathrm{MADe}$, where X_i is the averaged raw measurement of each sample, X is the median, and MADe is an adjusted median absolute deviation for each replicate plate. This normalization was performed for each plate to adjust for possible plate-to-plate variation. Strong hits were defined as *Z*-score < -10, medium hits as $-10 < Z < -7$, and weak hits as $-7 < Z < -3.5$.

Secondary screening. A total of 312 primary hits were first tested, in a 384-well plate format, for quenching the fluorescence of AMC amine to eliminate false positives. To exclude quenching compounds that only affect AMC fluorescence, each compound (17 μM) was first tested for quenching of AMC amine (50 nM). Quenchers were retested for inhibition of proteasome-associated USP14 activity and the strength of this effect was compared to their quenching effect in a dose- and time-dependent manner. Pure quenchers were thus scored as false positives and excluded from further analysis.

To test the specificity of potential USP14 inhibitors, each candidate was first counter-screened against human IsoT, a DUB that is closely related to USP14. Only compounds having significant activity for USP14 over IsoT were considered for further analysis with a panel of other human DUBs. IsoT and BAP1 were provided by K. Wilkinson, and UCH37 by K. Walters. UCH-L1, UCH-L3, USP2 catalytic domain (CD), USP7(CD) and USP15 were purchased from Boston Biochem. The final concentrations of DUBs in these reactions were as follows: USP14 (30 nM in the presence of 2.5 nM VS-proteasome), IsoT (1.5 nM), UCH37 (0.7 nM), BAP1 (2.5 nM), UCH-L1 (8 nM), UCH-L3 (0.3 nM), USP2 (50 nM), USP7 (50 nM) and USP15 (50 nM). To activate IsoT, 0.02 μM ubiquitin was added to the reaction. UCH37 was assayed in purified recombinant form in Fig. 2b, c. The proteasome-associated form of UCH37 was also assayed against IU1, with equivalent results (Supplementary Fig. 8b). In these experiments, we used proteasomes affinity-purified from tagged HEK293 cells without Ub VS treatment, at both 0.5 and 1.0 nM. Ub AMC (0.1 to 1 μM) was used as substrate for all quantitative DUB assays.

IC_{50} value determination. To measure IC_{50} values, various concentrations of IU1 (100 μM to 50 nM for proteasome-bound USP14, and 2 mM to 50 nM for IsoT and UCH37) were pre-incubated with corresponding DUBs for 30 min. The reaction was initiated by adding 1 μM of Ub AMC. These experiments were done in triplicate and represented as mean ± s.d. Fluorescence was measured by monitoring the reactions at room temperature for 45 min in real time using an Envision plate reader. IC_{50} determination for IU1C was performed with 2 mM to 50 nM of compound. To obtain a dose response curve, the per cent inhibition for each reaction was first determined, and then curve fitting was performed by the four parameter logistic model or the three parameter fixed bottom model using SigmaPlot 9.0 according to guidelines from NIH Chemical Genomics Center (http://ncgc.nih.gov/guidance/manual_toc.html).

Ubiquitination and purification of $Sic1^{PY}$. Ubiquitination of $Sic1^{PY}$ was carried out essentially as described[35], but with some modifications. The conjugation mixture contained 1.2 μM $Sic1^{PY}$, 0.17 μM Ubа1, 0.62 μM Ubc4, 0.71 μM Rsp5 and 20 μM ubiquitin, in a buffer of 50 mM Tris-HCl (pH 7.4), 100 mM NaCl, 1 mM DTT, 5 mM ATP and 10 mM $MgCl_2$. Conjugation proceeded for 100 min at 25 °C. To purify the conjugates, they were absorbed to Qiagen Ni-NTA resin, washed with buffer (50 mM Tris-HCl (pH 8.0), 50 mM NaCl and 40% glycerol), eluted with 200 mM imidazole in wash buffer, and dialysed into wash buffer containing 10% glycerol.

***In vitro* protein degradation and chain-trimming assays.** Purified human proteasomes (4 to 5 nM) were incubated with polyubiquitinated cyclin B (Ub_n CCNB; ~40 nM final) or polyubiquitinated $Sic1^{PY}$ (Ub_n $Sic1^{PY}$; ~240 nM final)

in proteasome assay buffer (50 mM Tris-HCl (pH 7.5), 5 mM $MgCl_2$ and 5 mM ATP). Where indicated, purified recombinant USP14 was incubated with proteasome for 5 min before initiating the reaction. To test the effect of IU1, 34 or 75 μM IU1 was pre-incubated with USP14 for 5 min before adding proteasome. Proteasome inhibitor cocktail (5 μM each of PS-341 and epoxomicin) was added 10 min in advance of the assay to inhibit the catalytic activity of proteasomes. For chain-trimming assays with ADP, the reaction was performed in the presence of ADP, with the proteasome-containing sample purified in the presence of ADP. This sample was pre-incubated with IU1 for 30 min (rather than 5 min) for Supplementary Fig. 14e. Reactions were terminated by adding 5× SDS PAGE sample buffer and subsequently subjected to SDS PAGE/immunoblot analysis using anti-cyclin B1 polyclonal antibody or anti-T7 HRP antibody. Ub_n CCNB was prepared as previously described[59].

IU1 reversibility test. The reversibility of IU1 inhibition of USP14 was examined by gel filtration using Centrispin-10 spin columns (Princeton Separations). 60 nM of USP14 and 5 nM of VS-proteasome were treated with vehicle or 100 μM IU1 for each indicated time point, at room temperature. The protein complex was then centrifuged through a gel-filtration column and assayed for DUB activity by adding Ub AMC (1 μM). Each error bar for Fig. 2b–d indicates standard deviation of three comparable experiments. To test IU1 inhibition of proteasome-bound USP14 for a prolonged incubation, the decay of activity or the stability of the enzyme complex was also investigated up to 8 h (Supplementary Fig. 13c). The DUB activity of each vehicle-treated control was normalized to 100%, and IU1-treated enzyme activity was expressed as a percentage of inhibition for each control. For Supplementary Fig. 13d, DUB activity was further normalized to Suc-LLVY-AMC hydrolytic peptidase activity. To confirm the reversibility of IU1, USP14 (60 nM) and VS-proteasome (5 nM) were incubated with vehicle or 100 μM of IU1 for 2 h at 4 °C. Each sample was then subjected to three rounds of ultrafiltration, using a Microcon-YM3 filter (3-kDa cutoff, Millipore). After each spin, the protein complex was re-suspended to the original volume and assayed for DUB activity. In some cases, the filtrate before and after centrifugation was saved for SDS PAGE and immunoblot analyses using anti-USP14 and anti-α7 antibodies (see Supplementary Fig. 13e).

Mammalian cell cultures and transient expression. Homozygous *Usp14* null mice have been previously generated by a gene-trap strategy, which exhibited embryonic lethality at approximately E13.5 (ref. 19). The gene trap allele, $Usp14^{mk114}$, is referred to here as $Usp14^{-/-}$. Cultures of primary mouse embryonic fibroblasts (MEFs) were established from E12.5 $Usp14^{-/-}$ and littermate wild-type embryos produced through intercrosses of 129/BL6 $Usp14^{+/-}$ mice. Primary MEFs were immortalized using the pEF321-T plasmid, which expresses Simian Virus 40 (SV40) large T-antigen[57,58]. MEFs, human kidney cells (HEK293) and HeLa cells were grown in DMEM supplemented with 10% FBS, 2 mM glutamine and 100 units ml^{-1} penicillin/streptomycin. Cells were transfected with 2–4 μg of total plasmid DNA in a 6-well culture plate for 4 h using LipofectAMINE 2000 (Invitrogen) when cells were >95% confluent or at a density of 10^6 cells per well. Cell lysates were prepared 36–48 h after transfection in RIPA buffer and used for immunoblotting. In a given panel, each lane is loaded with extract from an equal cell number, generally corresponding to 10–20 μg per lane, or 1/10 of the sample recovered from one well of a 6-well plate. For chase analysis, MEFs were treated with 75 μg ml^{-1} cycloheximide and samples were isolated at chase times 0, 0.5, 1, 2 and 4 h. Autophagic vacuole formation was inhibited by the treatment of 200 μM of bafilomycin A_1 for 6 h, which was verified by marked increase of transiently expressed mCherry-NBR1 (ref. 59). For quantitative immunoblot, proteins were visualized by infrared fluorescence antibodies using an Odyssey Imaging System (Li-Cor) and quantified using Odyssey software version 3.0 from three independent experiments. Tau signal was normalized to that of endogenous actin and values are represented as mean ± s.d.

Quantitative RT–PCR analysis. Total RNA from cultured cells was prepared using the TRIzol reagent (Invitrogen), followed by further purification through RNeasy mini-column (Qiagen) with on-column DNase I treatment. 250 ng of extracted RNA was used for quantitative RT–PCR in a LightCycler Carousel-Based System (Roche), using RNA Master SYBR Green I (Roche) as reporter dye. Reverse transcription was performed at 61 °C for 20 min and amplifications were performed for 40 cycles of 95 °C for 5 s, 60 °C for 20 s, and 72 °C for 30 s. Each mRNA level was normalized to that of GAPDH and the values were plotted as means ± s.d. of three independent experiments. Primer sequences used were as follows: for tau, forward 5′-AAGGTGACCTCCAAGTGTGG-3′ and reverse 5′-GGGACGTGGGTGATATTGTC-3′; for TDP-43, forward 5′-ATGGAAAA CAACCGAACAGG-3′ and reverse 5′-CAGTCACACCATCGTCCATC-3′; for GFAP, forward 5′-AGGAAGATTGAGTCGCTGGA-3′ and reverse 5′-ATACT GCGTGCGGATCTCTT-3′; for USP14, forward 5′-AAATGGCTTCAGCGC AGTAT-3′ and reverse 5′-TTCACCTTTCTCGGCAAACT-3′; for UbB, forward 5′-AGACCATCACCCTGGAAGTG-3′ and reverse 5′-AGGGTCGACTCCTT CTGGAT-3′; for α5, forward 5′-CGTGTGGCCTTTGGGAAC-3′ and reverse 5′-CACAACCTATATGAGCATCG-3′; for α7, forward 5′-ACAGTGGAGGA CCCAGTGAC-3′ and reverse 5′-CAATTAGGGCCGAGATACCA-3′; for GAPDH, forward 5′-GAGTCAACGGATTTGGTCGT-3′ and reverse 5′-GAC AAGCTTCCCGTTCTCAG-3′.

Determination of cell viability. Cell viability was assessed by the MTT assay[60]. Briefly, cells were grown in 96-well plates at a density of 2×10^4 cells per well. After IU1 or DMSO treatment, thiazolyl blue tetrazolium bromide (MTT, Sigma Aldrich) was added to each well of cells (final 0.5 mg ml^{-1}) and incubated for 1.5 h at 37 °C in a humidified atmosphere of 95% air/5% CO_2. DMSO was added to solubilize the blue MTT-formazan product and the sample was incubated for a further 30 min at room temperature. Absorbance of the solution was read at a test wavelength of 570 nm against a reference wavelength of 630 nm. IC_{50} values were determined using GraphPad Prism version 4.0 (GraphPad Software, Inc.). For cell survival upon oxidative stress, cells were pre-treated with 50 μM of IU1 for 2 h and a series of concentrations of menadione was then added, followed by incubation for 4 h before the MTT assay. Data in MTT assays represent mean values ± s.d. from three independent experiments. Apoptotic cells induced by IU1 were detected by TUNEL assay[61] using a fluorescence-based *in situ* cell death detection kit (Roche) and DAPI (Invitrogen) counterstaining according to the manufacturers' protocols. The extent of fluorescein-labelled DNA-strand breakage was evaluated from at least 1,000 cells out of ten different ×200 fields. For live-cell proliferation measurement, HeLa cells and MEFs were plated on 24-well plates (BD Biosciences) at around 35,000 cells per well or no more than 30% confluency. The next day, various concentrations of IU1 or the equivalent amounts of vehicle were added to each well in duplicate. Plates were then placed into an IncuCyte instrument (Essen Instruments) to automatically image cells every 2 h and measure confluence. Cells were imaged for 72 h or until they reached full confluence.

Oxidized protein analysis. Oxidized proteins were detected using the OxyBlot protein oxidation detection kit (Millipore). Total proteins from cells were isolated after treatment with 300 μM of menadione for 1 h, 75 μM of IU1 for 4 h, and/or proteasome inhibitors (20 μM of MG132; 10 μM of PS-341) for 4 h, and 15 μg of protein was used for derivatization with 2-4-dinitrophenyl hydrazine (DNPH) for 25 min. Samples were resolved by SDS PAGE and anti-DNP antibody was used for subsequent immunoblotting. IU1 does not inactivate menadione, as determined by LC-MS (data not shown).

Compound analysis. ^{1}H spectra were acquired on a Varian Inova 600 MHz spectrometer. Chemical shifts are reported as parts per million (p.p.m.) downfield from tetramethylsilane. Data are reported as follows: chemical shift, multiplicity (s = singlet, d = doublet, t = triplet, m = multiplet, br = broad), coupling constant and integration. Analytical LC-MS chromatography was performed using the Agilent 1200 Series HPLC/6130 Series mass spectrometer with a gradient solvent system from 10% to 50% CH_3CN (0.1% formic acid) over 15 min (IU1) or 10% to 100% CH_3CN (0.1% formic acid) over 23 min (IU1C). The collected LC-MS profiles were further analysed by extracting specific ions such as 301.0 (IU1) and 315.0 (IU1C) in the positive ion MS mode. IU1 and IU1C were determined to be >99% pure by LC-MS. High-resolution mass spectrometry (HRMS) was performed by the University of Illinois Mass Spectrometry Laboratory.

^{1}H-NMR (600 MHz, DMSO-d_6) of IU1: δ = 7.38 (m, 4H), 6.44 (s, 1H), 3.65 (s, 2H), 2.57 (m, 4H), 2.21 (s, 3H), 1.93 (s, 3H), 1.70 (m, 4H) p.p.m. HRMS (ESI) = *m/z* calculated for $C_{18}H_{21}FN_2O$ $[M+H]^+$ 301.1716, found 301.1729.

^{1}H-NMR (600 MHz, DMSO-d_6) of IU1C: δ = 7.38 (m, 4H), 5.93 (s, 1H), 4.21 (br, 2H), 2.82 (br, 2H), 1.97 (s, 3H), 1.96 (s, 3H), 1.62 (m, 4H), 1.02 (m, 1H), 0.92 (d, J = 6.0 Hz, 3H) p.p.m. HRMS (ESI) = *m/z* calculated for $C_{19}H_{23}FN_2O$ $[M+H]^+$ 315.1873, found 315.1872.

For the extraction of internalized small molecules, cells were washed 3× with PBS and lysed in LC-MS lysis buffer A (10 mM K_2HPO_4 (pH 7.5), 0.1 mM EDTA, 0.5 mM EGTA, 0.5% Triton X-100, and 1 mM DTT) containing 1× Complete protease inhibitors and 1× PhosSTOP phosphatase inhibitors (Roche), followed with the addition of 2.5 vol. ethyl acetate. The organic phase was separated from the aqueous phase and dried with anhydrous sodium sulphate. The extracts were dried *in vacuo*, then re-suspended in 200 μl of methanol for LC-MS analysis. LC-MS data were obtained using an Agilent series 1200 LC/6130 MS system with a reversed-phase C_{18} column (Phenomenex Luna C_{18}(2), 4.6 mm × 100 mm, 5 μm) and a CH_3CN/H_2O gradient solvent system, beginning with 10% aqueous CH_3CN and ending at 50% CH_3CN at 15 min. 10 μl of each sample was injected for each analysis. The collected LC-MS profiles were further analysed by extracting specific ions such as 301.0 (IU1) and 172.2 (menadione) in the positive ion MS mode. IU1 and menadione were eluted at 8.8 min and 14.9 min, respectively. To determine the excluded cell volume, [^{3}H]methoxyinuline (25 μCi) was added to cell pellets before collection to measure extracellular volume[62]. The intracellular concentrations of IU1 were normalized by cell number.

Reporter gene assays. To examine the promoter activities of *Psmb5* in the presence or absence of IU1, wild-type and $Usp14^{-/-}$ MEFs seeded on 6-well

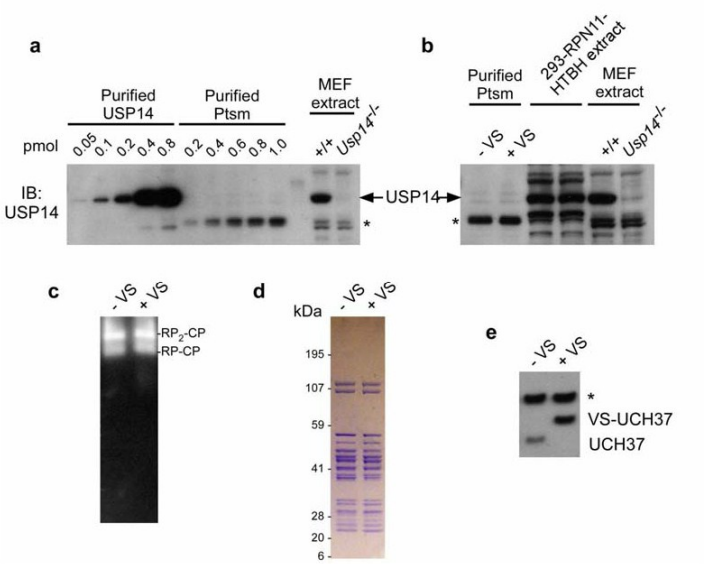

Figure S1. A preparation of purified human proteasomes that lack endogenous USP14, but contain UCH37. a, b, Human proteasomes were affinity-purified from an hRPN11-tagged line of HEK293T cells[1] as described in **Methods.** Indicated amounts of proteasomes were analyzed by SDS-PAGE and immunoblotted with anti-USP14 antibody. Samples were compared to recombinant USP14 protein and lysates from wild-type and *Usp14*$^{-/-}$ MEFs. Lanes 1 and 2 of panel b were loaded with 0.6 pmol of proteasome. **c,** Nondenaturing gel analysis of purified human proteasomes (7 μg) pre-treated with Ub-VS (+VS) or untreated (-VS) with Suc-LLVY-AMC staining. **d,** One dimensional SDS-PAGE and Coomassie Brilliant Blue (CBB) staining of human proteasomes (6 μg). This, together with **c,** suggests that there is essentially no change in proteasome integrity upon Ub-VS treatment of human proteasomes. **e,** Immunoblot analysis with anti-UCH37 antibody demonstrates the presence of endogenous UCH37 in the purified proteasomes (1.5 μg). Reactivity with Ub-VS indicates that the band represents active UCH37. Asterisks (*) indicate nonspecific signals. Note that, in a separate experiment, the stoichiometry of UCH37 on proteasomes purified from tagged HEK293T cells was estimated using purified, recombinant UCH37 as a standard. This visual assay allowed for a rough estimate of one UCH37 molecule to one proteasome (data not shown).

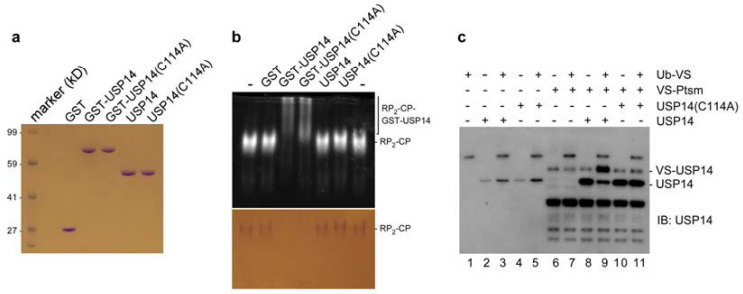

Figure S2. Reconstitution of USP14-proteasome complexes. **a**, CBB staining of purified recombinant proteins (0.5 μg protein/lane). **b**, Gel-shift assay of USP14-proteasome binding. Purified human proteasomes (1 pmol per reaction) were incubated for 20 min at 30°C with 5 pmol of GST, GST-USP14 (i.e., wild-type), GST-USP14{C114A}, untagged USP14, or untagged USP14{C114A}. Samples were resolved by nondenaturing PAGE and proteasomes visualized by Suc-LLVY-AMC in-gel hydrolysis. Binding of GST-USP14 to proteasomes significantly reduced their electrophoretic mobility. Bottom, CBB staining of the gel after gel-shift assay. **c**, Ub-VS labeling of recombinant USP14. 11 nM of recombinant USP14 was incubated with 110 nM of VS-Ptsm in the absence or presence of Ub-VS (1 μM) at 30°C for 1 hr. Samples were analyzed by SDS-PAGE/immunoblot. The result is a representative of two comparable experiments. This experiment shows that the bulk of recombinant USP14 is Ub-VS modifiable and thus functionally intact.

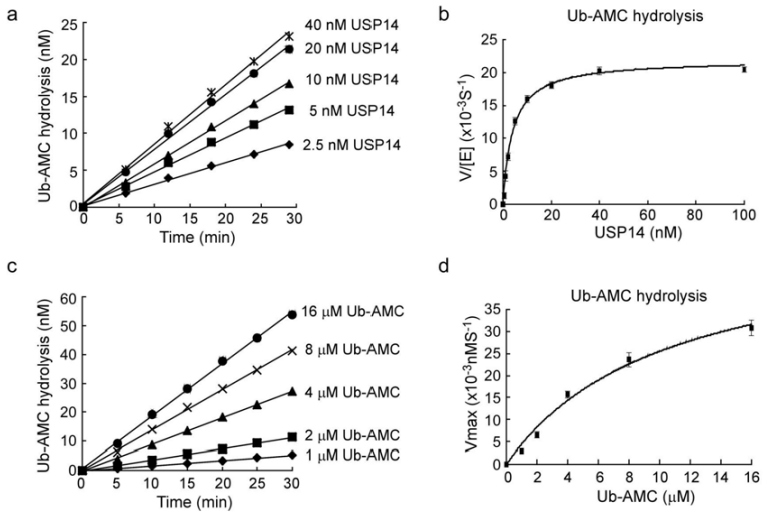

Figure S3. Kinetic analysis of reconstituted USP14-proteasome complexes. a, Linear kinetics ($R^2 > 0.99$) of the initial rates of Ub-AMC (1 μM) hydrolysis by USP14 and proteasome (1 nM). **b,** Michaelis-Menten plot of USP14-dependent Ub-AMC (1 μM) hydrolysis in the presence of human proteasome (1 nM) for 25 min. The data were fit to a hyperbolic curve by nonlinear regression ($R^2 > 0.99$). Approximate K_M and k_{cat} were determined as 4.0 ± 0.5 nM and (22 ± 0.4) x10^{-2} sec^{-1}, respectively. **c,** Linear kinetics ($R^2 > 0.99$) of Ub-AMC hydrolysis at 4 nM USP14 and 1 nM proteasome. **d,** Michaelis-Menten plot of concentration-dependent Ub-AMC cleavage in the presence of USP14 (4 nM) and proteasome (1 nM) for 30 min. The data are fit to a hyperbolic curve by nonlinear regression ($R^2 > 0.99$). Approximate K_M and k_{cat} were determined as 11 ± 2.7 μM and (53 ± 7.1) x10^{-2} sec^{-1}, respectively. The graphs shown are representative of at least three independent determinations and each data point is the mean ± s.d. of triplicate determinations.

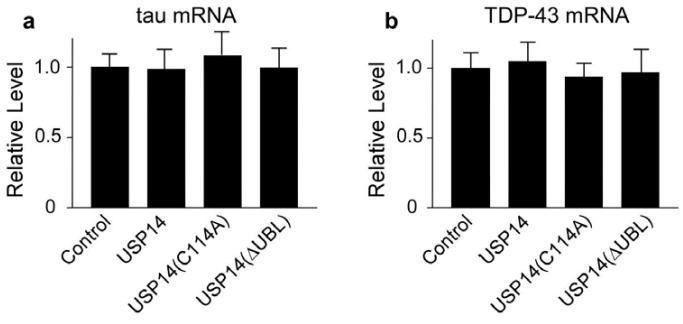

Figure S4. USP14 does not regulate mRNA encoding tau or TDP-43. *Usp14*$^{-/-}$ MEFs were cotransfected with plasmids expressing tau (a) or TDP-43 (b) and USP14 wild-type or a mutant. Control indicates pcDNA3 empty vector cotransfection. After 2 days, total RNA was isolated through Trizol extraction and further purified using an RNeasy column. Quantitative RT-PCR was performed using primers for tau (Forward: AAGGTGACCTCCAAGTGTGG, Reverse: GGGACGTGGGTGATATTGTC) and TDP-43 (Forward: ATGGAAAACAACCGAACAGG, Reverse: CAGTCACACCATCGTCCATC). mRNA levels were normalized to that of to the GAPDH gene (Forward: GAGTCAACGGATTTGGTCGT, Reverse: GACAAGCTTCCCGTTCTCAG). The values plotted are means ± s.d. of three independent experiments.

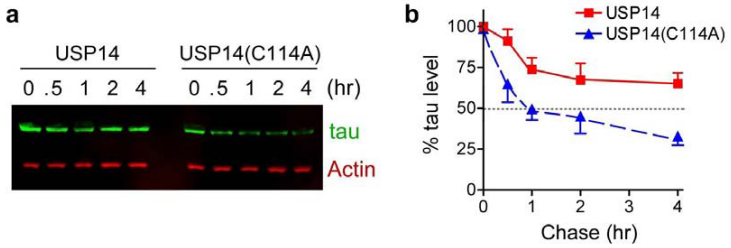

Figure S5. Stabilization of tau by wild-type USP14. *Usp14*$^{-/-}$ MEFs were cotransfected with a plasmid expressing tau and a plasmid expressing either wild-type USP14 or its catalytically inactive mutant USP14(C114A). Chase experiments (**a**) and quantification (**b**) were carried out at indicated time points after the addition of 75 μg/mL cycloheximide at time zero. The chase was initiated 36 hrs after transfection. Anti-tau and anti-actin antibodies were simultaneously incubated for immunoblot. For each time point, the tau signal was normalized to that of endogenous actin. Band intensities were quantified using Odyssey software ver. 3.0 from three independent experiments (n=3). Note that tau levels were reduced in the mutant already at time zero (to 67% of wild-type), presumably as a result of elevated tau degradation prior to cycloheximide addition. This effect is normalized out in panel b.

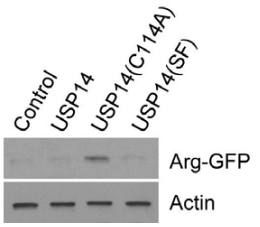

Figure S6. USP14(SF) does not significantly stabilize Arg-GFP in *Usp14*$^{-/-}$ MEF cells. An N-end rule substrate, Arg-GFP, is responsive to the USP14 noncatalytic effect as shown in **Fig. 1f.** Arg-GFP (3 μg plasmid DNA transfected per sample) was coexpressed with either wild-type USP14, catalytically inactive USP14(C114A), or a naturally occurring splice variant, the short form of USP14 (USP14[SF]) (2 μg DNA /sample) in *Usp14*$^{-/-}$ MEFs. Protein extracts were prepared two days after transfection, and analyzed by SDS-PAGE and anti-GFP immunoblot as in **Fig. 1f.**

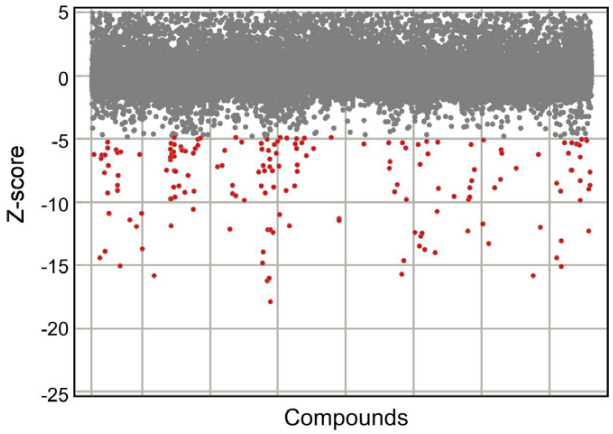

Figure S7. Primary screening of small-molecule libraries for USP14 inhibition. Statistical plot of high-throughput compound screening. 83,052 compounds were screened in duplicate for inhibition of USP14 (15 nM) in the presence of proteasome (1 nM). A 384-well, low volume (20 µl) plate format was used. Data processing was done by a 'robust' Z-score method as previously described[2] and each compound was plotted using Spotfire software. The Z-score is a normalized value that takes into account plate-to-plate variation that would otherwise make it difficult to compare data from different plates across the screen. Here, weak hits are designated as -3.5 > Z > -7, medium hits as -7 > Z > -10, and strong hits as Z < -10. Compounds with a Z score less than –3.5 were selected for secondary screening. Compounds over the cut-off of Z > 5 are mostly autofluorescent molecules and were not plotted.

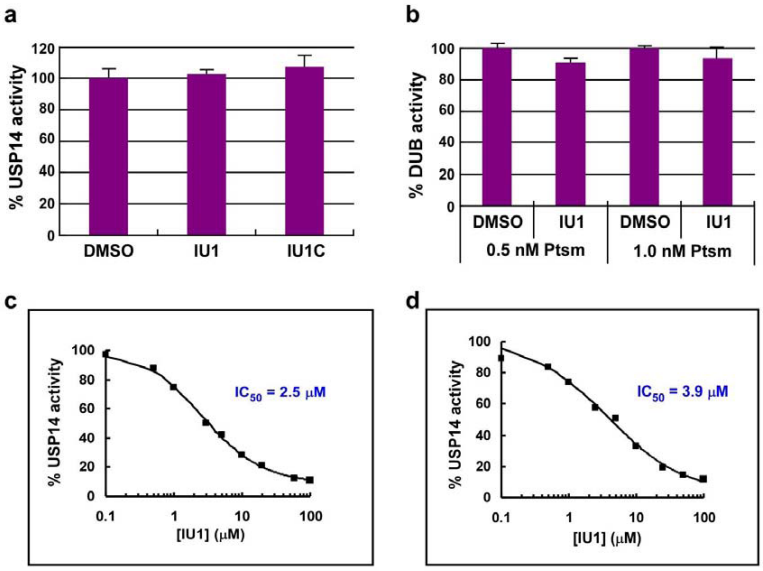

Figure S8. IU1, a USP14 inhibitor, inhibits the catalytic activity of proteasome-associated USP14 *in vitro*. a, IU1 is only weakly inhibitory towards proteasome-free USP14. 2 μM of recombinant USP14 protein in the absence of proteasome was treated with either IU1 or IU1C (17 μM). **b,** IU1 (17 μM) shows little inhibitory activity in Ub-AMC hydrolysis assays of human proteasomes not treated with Ub-VS. These data complement **Fig. 2c** and demonstrate that IU1 does not affect the DUB activity of proteasome-bound UCH37. **c, d,** Two independent IC_{50} curves of proteasome-associated USP14 treated with IU1. USP14 was preincubated with IU1 for either 45 min (Exp1) or 30 min (Exp2). The data were fit to a four parameter logistic model (the Hill-slope model) based on guidelines from NIH Chemical Genomics Center (http://ncgc.nih.gov/guidance/manual_toc.html). Error bars indicate s.d. (n=3). Note that, in related experiments, IU1 was shown not to be a fluorescent quencher for AMC (data not shown). See ***Methods*** for the detailed assay conditions.

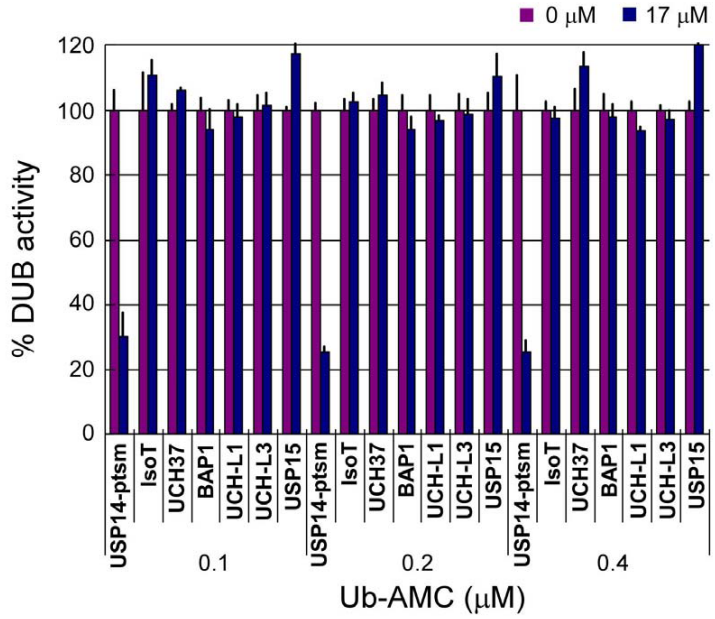

Figure S9. The specificity of IU1 for USP14 is observed independently of Ub-AMC concentration. Assays of Ub-AMC hydrolysis were done as in **Fig. 2c,** except lower concentrations of Ub-AMC were used. Similar results were obtained for USP2 (data not shown).

Enzyme	K_M (μM)	Substrates	References for K_M
USP14-26S	11	Ub-AMC	This study
BAP1	7.0	Ub-AMC	Personal communication, K. Wilkinson
IsoT	1.4	Ub-AMC	Dang et al (1998) Biochemistry, 37: 1868
UCH37	13	Ub-AMC	Yao et al (2006) Nat Cell Biol, 8: 994
UCH-L1	0.041	Ub-AMC	Liu et al (2003) Chem Biol, 10: 837
UCH-L3	0.039	Ub-AMC	Dang et al (1998) Biochemistry, 37: 1868
USP2 CD	0.55	Ub-AMC	Hassiepen et al (2007) Anal Biochem, 371: 201
USP7 CD	44	Ub-AMC	Fernandez-Montalvan et al (2007) FEBS J, 274: 4256
USP15	3.0	Ub-AMC	This study

Figure S10. Summary of K_M values for Ub-AMC of deubiquitinating enzymes in this study. K_M values of DUBs used in the selectivity assays were obtained from the literature. Unknown K_M values were determined in this study, as indicated. These values are significant because the DUB assays (of **Supplementary Fig. 9**) should be most sensitive to inhibition when substrate is at a low concentration as compared to the K_M of the enzyme in question. CD, catalytic domain.

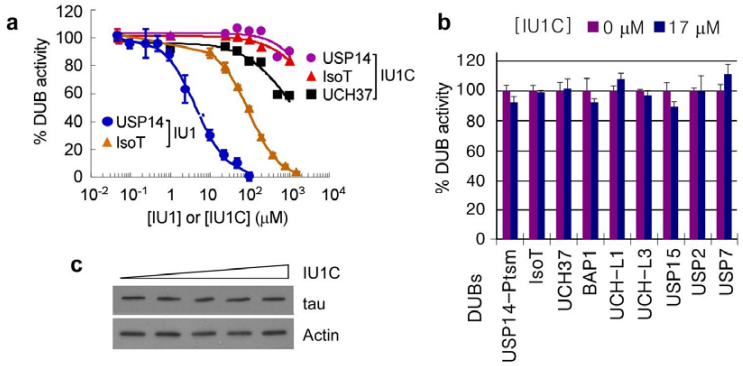

Figure S11. Characterization of IU1C, an inactive variant of IU1. a, Dose-response curves for inhibition of various deubiquitinating enzymes by IU1C *versus* IU1. IU1 data are taken from **Fig. 2b. b,** Assays of deubiquitinating enzyme inhibition by IU1C. Compare to **Fig. 2c.** Conditions as in **Fig. 2c.** All values are presented as mean ± s.d. (n=3). **c,** IU1C does not significantly affect tau levels in wild-type MEF cells. Compare to **Fig. 4a.** Conditions as in **Fig. 4a** except no LacZ coexpression (i.e., IU1C was used at 0, 25, 50, 75, or 100 μM in a 6-hr treatment).

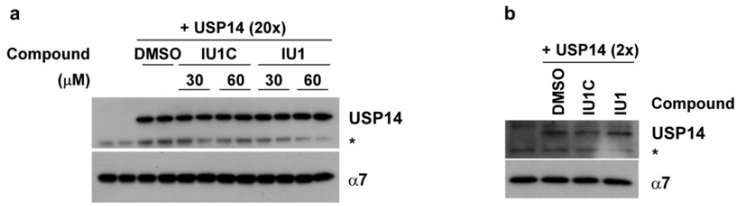

Figure S12. IU1 does not interfere with USP14 binding to human proteasomes. a, Human proteasomes (~ 4 nM) were first collected, using NeutrAvidin agarose (Thermo Scientific), from ~2 mg of lysate from HEK293T cells harboring hRPN11-HTBH. After incubating with recombinant USP14 (80 nM) in the presence or absence of the indicated compound, followed by washing with low salt lysis buffer, the association between USP14 and the proteasome was determined by immunoblotting. The experiment was performed in duplicate and additionally repeated. b, as in a, except ~2-fold molar excess of USP14 was incubated with the proteasome in the absence or presence of the indicated compound (30 μM). The asterisk (*) denotes a nonspecific signal generated by the anti-USP14 antibody.

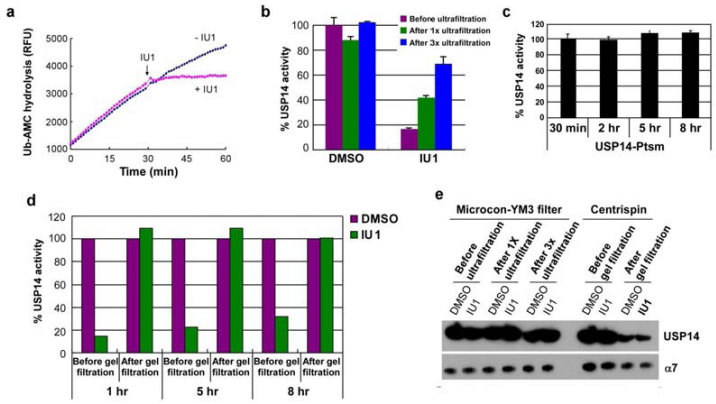

Figure S13. Reversibility of USP14 inhibition by IU1 after prolonged incubation. **a**, IU1 inhibits proteasome-associated USP14 activity without a detectable lag period. 2.5 nM of human proteasome was mixed with 30 nM of recombinant USP14 protein. The reaction was then initiated by adding 1 μM Ub-AMC. After 30 min, IU1 (100 μM) or vehicle (DMSO) was added to the sample. **b**, These data complement **Fig. 2d**. 60 nM of USP14 and 5 nM human proteasome were treated with vehicle or 100 μM of IU1 for 2 hr. The sample was then subjected to three rounds of ultrafiltration, using a Microcon-YM3 filter (3 kDa cutoff, Millipore). After each spin, the protein complex was resuspended to the original volume and assayed for DUB activity. **c**, The DUB activity of USP14 is stable in the presence of human proteasome for at least 8 hrs. **d**, As in **Fig. 2d** except prolonged incubation (5 and 8 hr) was tested and the percent DUB activity was normalized to 26S peptidase activity (i.e. LLVY-AMC hydrolysis). IU1 was added to 100 μM. **e**, Immunoblot analysis showing that there are essentially no changes of protein level after multiple rounds of sample concentration using Microcon-YM3 filters. There is some protein loss after gel filtration by Centrispin-10, but the amount of protein is comparable between IU1 treated and nontreated samples. SDS-PAGE/immunoblot was done with the same samples as used in **Fig. 2d** and **Supplementary Fig. 13b**.

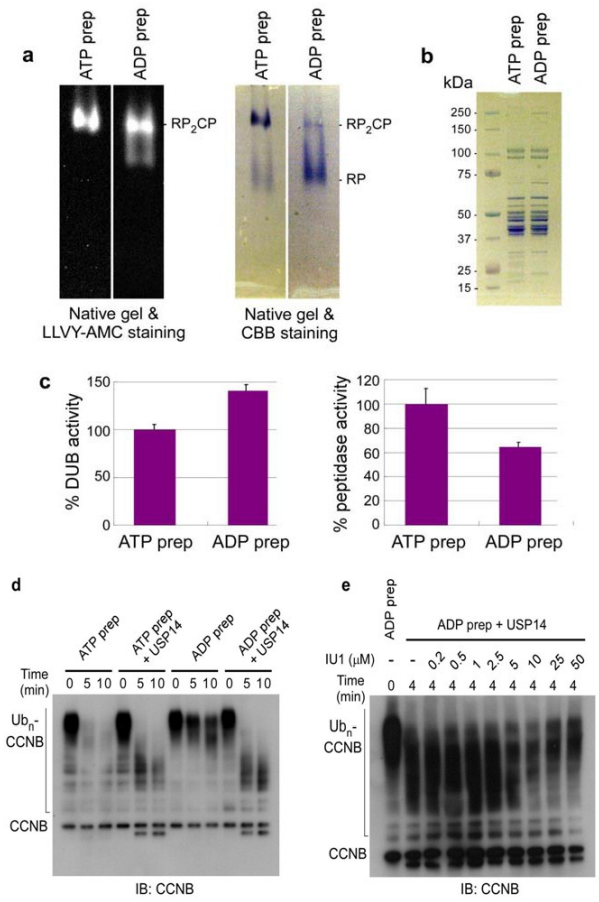

Figure S14. Chain trimming assays with human proteasome and RP purified in the presence of ADP. a, b, Nondenaturing gels (**a**) and SDS-PAGE gel analysis (**b**) of purified human proteasomes with ATP (ATP prep) or ADP (ADP prep). 7 μg was used for nondenaturing gel analysis and 6 μg for SDS-PAGE. Note that the ADP sample contains a mixture of proteasome 26S holoenzyme and 19S RP, due to CP-RP dissociation during purification (see also ref 3). **c,** Ub-AMC and LLVY-AMC hydrolysis assays. **d,** *In vitro* Ub_n-CCNB degradation assays with samples prepared and assayed in the presence of ATP or ADP. Samples were analyzed by SDS-PAGE/immunoblotting. These data complement **Fig. 3a**. **e,** *In vitro* Ub_n-CCNB chain trimming assays with samples prepared and assayed in the presence of ADP. IU1 is effective at inhibition of chain trimming at approximately 5 μM, as expected from Ub-AMC hydrolysis data.

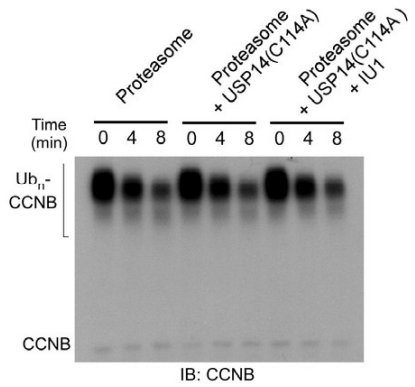

Figure S15. IU1 does not affect CCNB degradation in the presence of USP14(CA).
Assays were done as in **Figs. 1b** and **3b.**

Supplementary Fig. 16

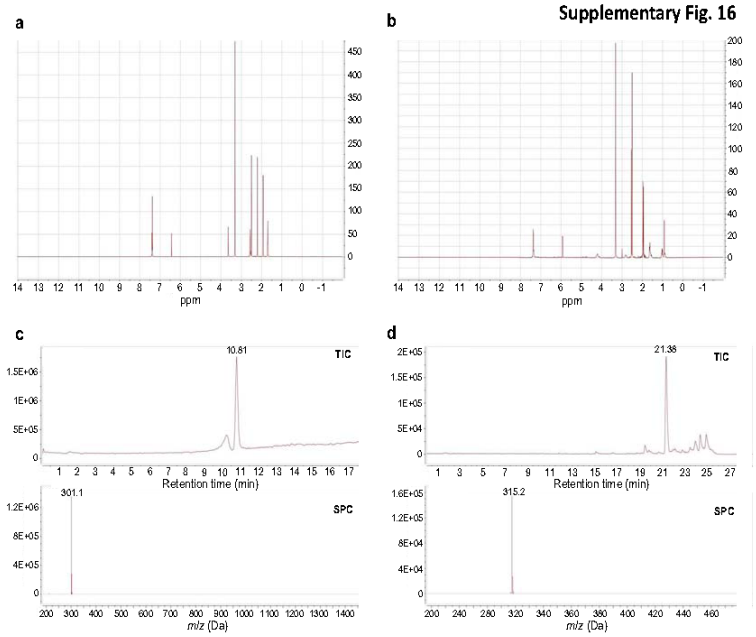

Figure S16. Chemical analysis of IU1 and IU1C. a, b, ^{1}H-NMR spectroscopic data of IU1 (**a**) and IU1C (**b**). LC/MS analysis using IU1 (**c**) and IU1C (**d**). TIC, total ion count. SPC, shared peak count extracted from the peak with retention time 15 min (IU1) or 23 min (IU1C). Additional information is available in ***Methods***.

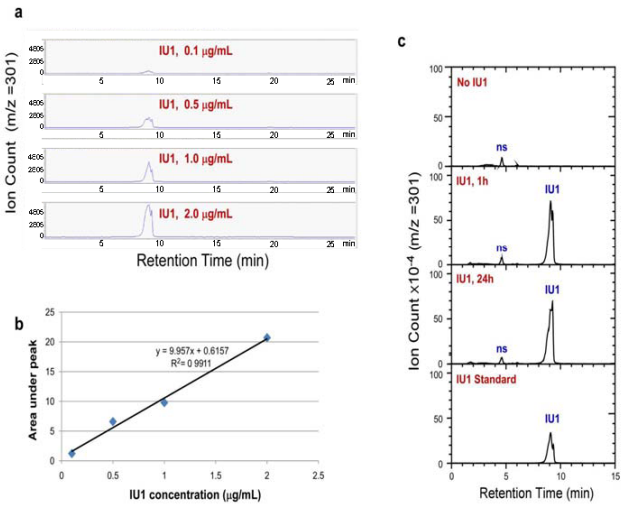

Figure S17. IU1 uptake into cells measured by LC/MS. **a**, Standardization of LC/MS for IU1 detection. Ion count LC/MS traces (*m/z* at 301) of various concentrations of IU1. Cell-associated IU1 was monitored using an Agilent series 1200 LC/6130 system with a reversed-phase C_{18} column. The retention time for IU1 is ~8.8 min. **b**, Ion count peak areas *versus* concentration of IU1. The LC/MS shows linear responses in the given range of concentration (R^2=0.99). **c**, Wild-type MEFs were treated with 50 μM of IU1 for various times as indicated. Cell lysates were collected, extracted with ethyl acetate, and subjected to mass spectrometry (see details in ***Methods***). Ion counts of LC/MS traces (m/z at 301) at 0 hr, 1 hr, 24 hr, and an IU1 standard solution at 1 μg/mL, are shown. ns, nonspecific.

Supplementary Fig. 18

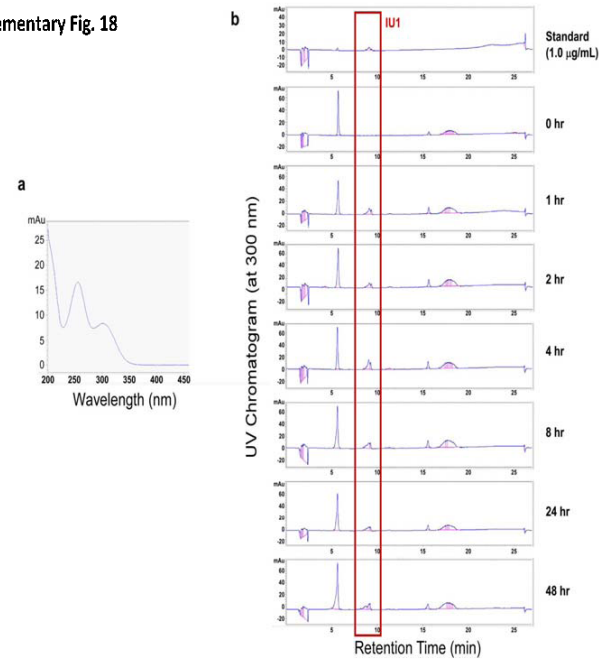

Figure S18. Entry of IU1 into wild-type MEF cells monitored by HPLC with UV detection. **a**, The UV spectrum of IU1. IU1 shows absorption maxima at 255 nm and 305 nm. **b**, HPLC chromatograms showing the time-dependence of IU1 internalization at 300 nm. Cell lysates were processed as described in the legend to **Supplementary Fig. 17**. The standard shows results obtained using purified IU1 at 1 μg/mL. It is assumed that the retention of IU1 with the cell fraction reflects IU1 internalization.

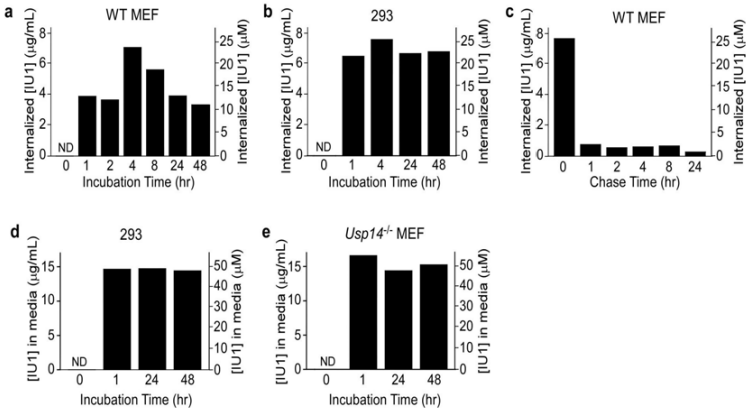

Figure S19. Time-course of IU1 levels in cells and media. **a**, **b**, The IU1 concentration in wild-type MEF cells and HEK293 cells, determined by LC/MS. IU1 was added to cultures at 50 μM at time zero. ND, not detected. Similar results were obtained in *Usp14*$^{-/-}$ MEF cells. **c**, Internalized IU1 was rapidly released from cells. After wild-type MEFs were incubated with 50 μM of IU1 for one hour, the culture media were replaced with fresh media without IU1. Internalized IU1 was monitored at the indicated times. **d**, **e**, IU1 concentration in the media of HEK293 cells and *Usp14*$^{-/-}$ MEF cells. The comparable concentrations of IU1 from 1 hr to 48 hr indicate its stability in serum-containing media.

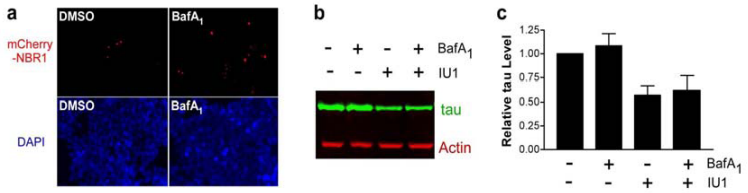

Figure S25. The stimulation of tau degradation by IU1 is not mediated by autophagy. a, Transiently expressed mCherry-NBR1 levels in wild-type MEFs were significantly increased after treatment with 200 μM of bafilomycin A_1 ($BafA_1$), an autolysosome formation inhibitor[4], for 6 hr. **b,** Cells transfected with a plasmid expressing tau were treated with 200 μM of $BafA_1$ and/or 75 μM of IU1 for 6 hrs, and analyzed by SDS-PAGE/immunoblot using the Odyssey infrared imaging system. **c,** Band intensities were quantified from three independent experiments (mean ± s.d.) using Odyssey software.

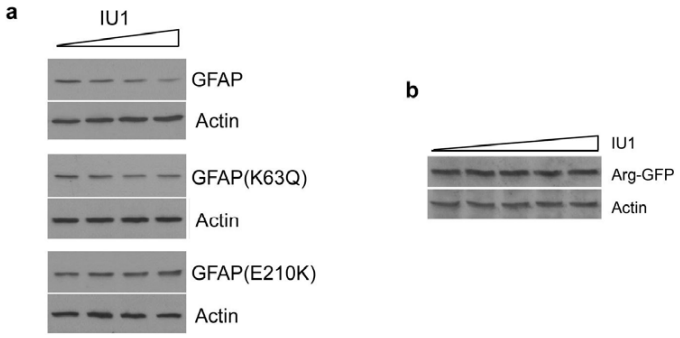

Figure S26. IU1 treatment reduces the level of GFAP expressed in wild-type MEF cells but does not affect Arg-GFP. **a**, Wild-type MEF cells transfected with plasmids expressing wild-type GFAP or its more aggregation-prone mutations, GFAP(K63Q) or GFAP(E210K) were treated with 0, 25, 50, or 100 μM of **IU1** for 6 hr, and analyzed by SDS-PAGE/immunoblot. **b**, Lack of effect of **IU1** on the degradation of Arg-GFP, which was stabilized by catalytically inactive USP14(C114A) as in **Fig. 1f**. Otherwise short-lived Arg-GFP was coexpressed with USP14(C114A) in *Usp14*$^{-/-}$ MEF cells and treated with 0 - 100 μM of **IU1** for 6 hrs. Anti-GFP and anti-actin antibodies were used for immunoblotting. The noncatalytic effect of USP14, which is best visualized in this assay, is not reversed by **IU1**.

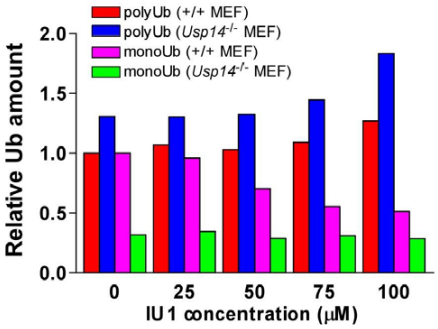

Figure S27. Quantification of ubiquitin levels in Fig. 4g. Polyubiquitin and monoubiquitin levels from wild-type and *Usp14*$^{-/-}$ MEF were quantified after treatment of various concentration of IU1. Ub signals were normalized to that of endogenous actin. Quantification was achieved by densitometry of a film image.

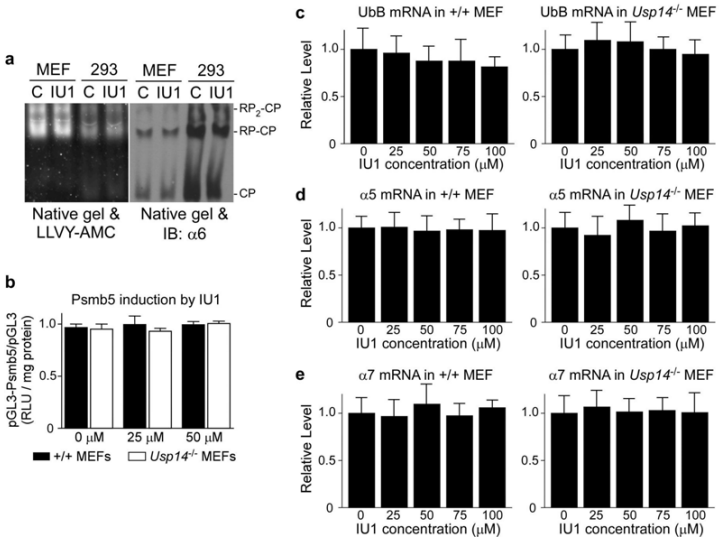

Figure S28. IU1 treatment does not induce transcription of proteasome subunit genes. a, The level and peptidase activity of the proteasome were determined before and after a 6-hr IU1 treatment (100 μM). Total cell extracts (50 μg/lane) were resolved by native PAGE, and the proteasome was visualized using either an in-gel activity stain with a fluorogenic peptide substrate (LLVY-AMC), or immunoblotting with antibodies to subunit α6. RP_2-CP and RP-CP are distinct forms of the 26S proteasome. **b,** A luciferase reporter gene containing the murine *Psmb5* promoter (-1 kb to 0 kb) was transiently expressed in wild-type and *Usp14*$^{-/-}$ MEFs and promoter activity was assessed following incubation of 25 or 50 μM of IU1 for 8 hr. For normalization of luciferase activity, a control experiment using the promoter-less pGL3 plasmid was performed. This reporter construct has previously been used as a representative measure of proteasome subunit gene induction[5,6]. Values are mean ± s.d. from three independent experiments. RLU, relative light units. **c-e,** Quantitative RT-PCR for a ubiquitin gene (UbB) and two proteasome subunit genes (α5 and α7) was performed using total mRNA from +/+ (left panels) and *Usp14*$^{-/-}$ MEFs (right) after incubation with a graded doses of IU1 for 8 hr. These data supplement **Fig. 4h**.

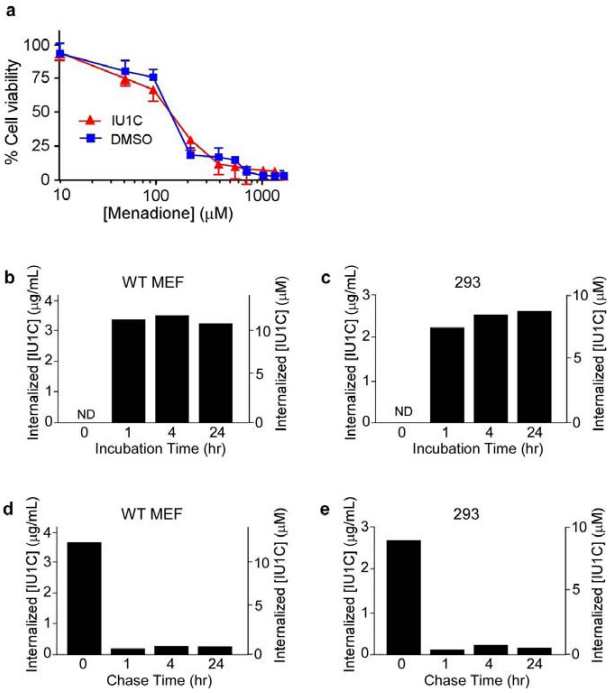

Figure S29. IU1C does not significantly affect oxidative stress-induced cytotoxicity. a, HEK293 cells were treated with 50 μM of IU1C for 6 hr and graded concentrations of menadione for 4 hr, followed by MTT assay. Values represent the mean ± s.d. of triplicate cultures. These data supplement **Fig. 5b.** Time-course of IU1C levels in wild-type MEFs (**b**) and HEK293 cells (**c**) were measure by using LC/MS. As in **Supplementary Figs. 19a** and **19b**, respectively, except IU1C, a functionally inactive control for IU1, was used. ND, not detected. **d and e,** See legend to **Supplementary Fig. 19c.** IU1C concentrations in the media (data not shown) of wild-type MEFs or HEK293 cells are comparable to those of IU1 (**Supplementary Fig. 19**).

References accompanying supplementary figures

1. Wang, X. *et al*. Mass spectrometric characterization of the affinity-purified human 26S proteasome complex. *Biochemistry* **46**, 3553-65 (2007).
2. Malo, N., Hanley, J., Cerquozzi, S., Pelletier, J. & Nadon, R. Statistical practice in high-throughput screening data analysis. *Nat. Biotechnol.* **24**, 167-75 (2006).
3. Liu, C.W. *et al*. ATP binding and ATP hydrolysis play distinct roles in the function of the 26S proteasome. *Mol. Cell* **24**, 39-50 (2006).
4. Mizushima, N., Yoshimori, T., & Levine, B. Methods in mammalian autophagy research. *Cell* **140**, 313-26 (2010).
5. Kwak, M.K. *et al*. Antioxidants enhance mammalian proteasome expression through the Keap1-Nrf2 signaling pathway. *Mol. Cell. Biol.* **23**, 8786-94 (2003).
6. Chondrogianni, N. *et al*. Central role of the proteasome in senescence and survival of human fibroblasts. *J. Biol. Chem.* **278**, 28026-37 (2003).

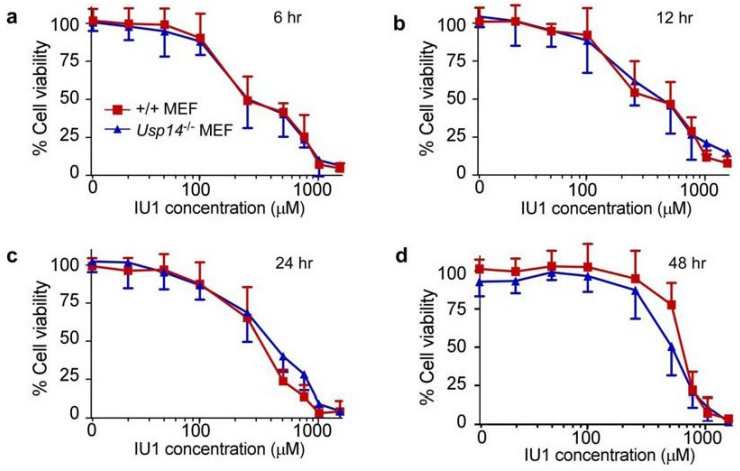

Figure S20. Assessment of IU1 cytotoxicity in MEF cells, using the MTT assay. IU1 was added at various concentrations (12.5 μM to 1.5 mM) to +/+ (red squares) or *Usp14*$^{-/-}$ MEFs (blue triangles). After the indicated incubation times, 25 μL of a 5 mg/mL MTT solution was added to sample and the plates were incubated for 2 hr at 37°C. The MTT-formazan crystals that had formed were dissolved by adding 200 μl DMSO and the absorbance was measured at 550 nm. Each data point is a mean ± s.d. of three independent experiments.

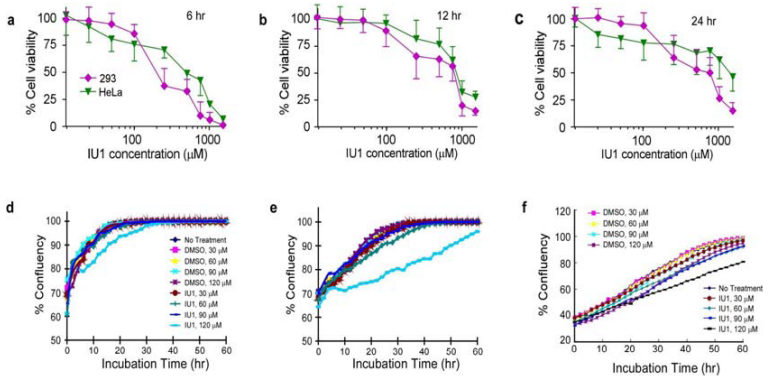

Figure S21. IU1 cytotoxicity assayed in MEF, HEK293, and HeLa cells. a-c, See legend to **Supplementary Fig. 20. d, e,** Live-cell imaging of **IU1** effects on proliferation of MEFs. Wild-type (**d**) or *Usp14*$^{-/-}$ (**e**) MEFs were plated into each well of a 24-well plate at 35,000 cells/well. On the following day, **IU1** or vehicle was added, as indicated. Live cell proliferation was monitored over 72 hrs using an automated imaging system. Data points are means of duplicate measurements. **f,** Live-cell imaging of **IU1** effects on HeLa cell proliferation.

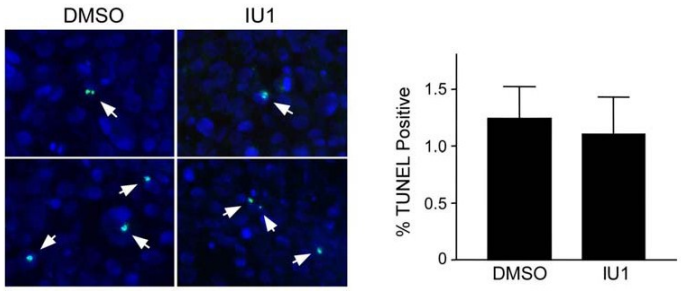

Figure S22. IU1 does not induce apoptosis in wild-type MEF cells. Cells were treated with 100 μg/mL of IU1 or DMSO control for 6 hr and a fluorescent TUNEL assay was performed with DAPI counterstaining. TUNEL-positive cells (arrow) were quantified and compared (right). Bars are the mean ± s.e.m. of percentage of TUNEL positive cells from four independent experiments.

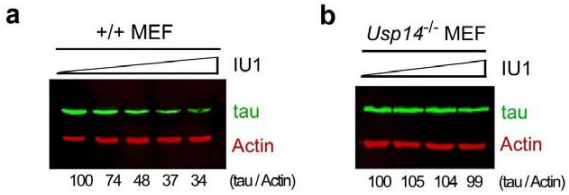

Figure S23. Quantitative analysis of tau levels after IU1 treatment in wild-type and *Usp14*$^{-/-}$ MEFs. **a** and **b**, As in **Figs. 4a** and **4b** except infrared dye-conjugated secondary antibodies were used for quantification using Odyssey imaging system. Tau signal intensities were normalized to that of endogenous actin and relative amounts are shown. Primary antibodies were simultaneously incubated for immunoblot and band intensities were quantified using the Odyssey software.

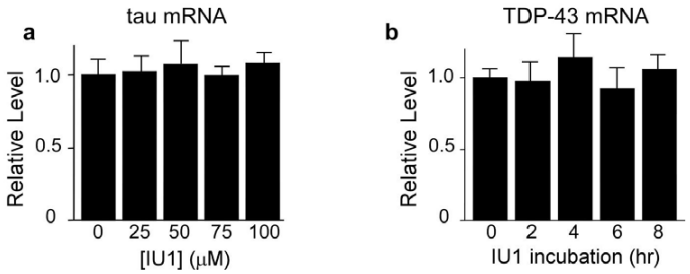

Figure S24. IU1 reduces tau and TDP-43 levels through a post-transcriptional effect. Tau (**a**) or TDP-43 (**b**) was transiently overexpressed in wild-type MEFs, which were then treated with **IU1** as in **Figs. 4a** and **4e**, respectively. Total RNA was isolated and quantitative RT-PCR was performed as in **Supplementary Fig. 4.**

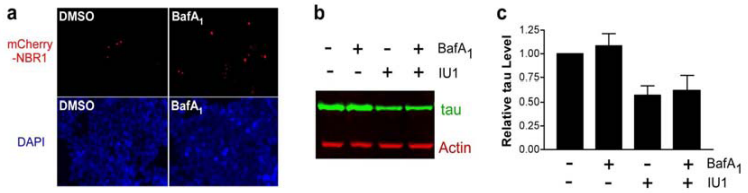

Figure S25. The stimulation of tau degradation by IU1 is not mediated by autophagy. a, Transiently expressed mCherry-NBR1 levels in wild-type MEFs were significantly increased after treatment with 200 μM of bafilomycin A_1 ($BafA_1$), an autolysosome formation inhibitor[4], for 6 hr. **b,** Cells transfected with a plasmid expressing tau were treated with 200 μM of $BafA_1$ and/or 75 μM of IU1 for 6 hrs, and analyzed by SDS-PAGE/immunoblot using the Odyssey infrared imaging system. **c,** Band intensities were quantified from three independent experiments (mean ± s.d.) using Odyssey software.

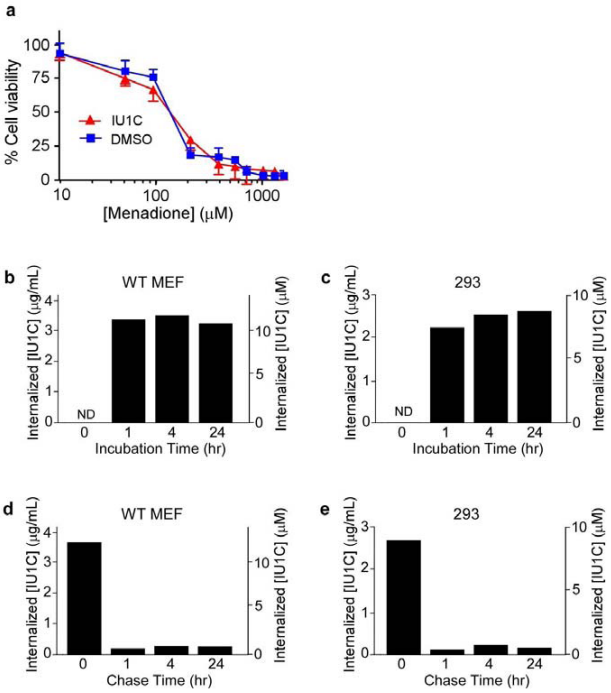

Figure S29. IU1C does not significantly affect oxidative stress-induced cytotoxicity. a, HEK293 cells were treated with 50 μM of IU1C for 6 hr and graded concentrations of menadione for 4 hr, followed by MTT assay. Values represent the mean ± s.d. of triplicate cultures. These data supplement **Fig. 5b.** Time-course of IU1C levels in wild-type MEFs (**b**) and HEK293 cells (**c**) were measure by using LC/MS. As in **Supplementary Figs. 19a** and **19b**, respectively, except IU1C, a functionally inactive control for IU1, was used. ND, not detected. **d and e,** See legend to **Supplementary Fig. 19c.** IU1C concentrations in the media (data not shown) of wild-type MEFs or HEK293 cells are comparable to those of IU1 (**Supplementary Fig. 19**).

References accompanying supplementary figures

1. Wang, X. *et al*. Mass spectrometric characterization of the affinity-purified human 26S proteasome complex. *Biochemistry* **46**, 3553-65 (2007).
2. Malo, N., Hanley, J., Cerquozzi, S., Pelletier, J. & Nadon, R. Statistical practice in high-throughput screening data analysis. *Nat. Biotechnol.* **24**, 167-75 (2006).
3. Liu, C.W. *et al*. ATP binding and ATP hydrolysis play distinct roles in the function of the 26S proteasome. *Mol. Cell* **24**, 39-50 (2006).
4. Mizushima, N., Yoshimori, T., & Levine, B. Methods in mammalian autophagy research. *Cell* **140**, 313-26 (2010).
5. Kwak, M.K. *et al*. Antioxidants enhance mammalian proteasome expression through the Keap1-Nrf2 signaling pathway. *Mol. Cell. Biol.* **23**, 8786-94 (2003).
6. Chondrogianni, N. *et al*. Central role of the proteasome in senescence and survival of human fibroblasts. *J. Biol. Chem.* **278**, 28026-37 (2003).

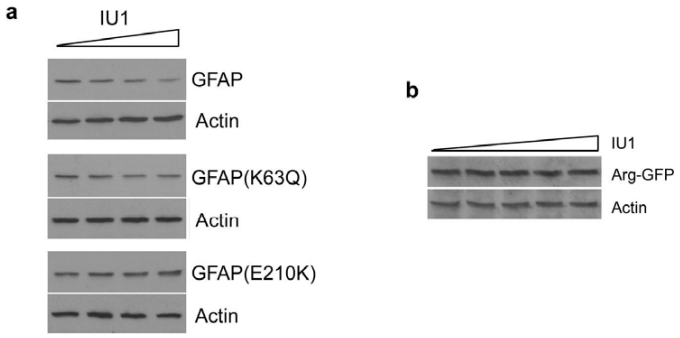

Figure S26. IU1 treatment reduces the level of GFAP expressed in wild-type MEF cells but does not affect Arg-GFP. **a**, Wild-type MEF cells transfected with plasmids expressing wild-type GFAP or its more aggregation-prone mutations, GFAP(K63Q) or GFAP(E210K) were treated with 0, 25, 50, or 100 μM of **IU1** for 6 hr, and analyzed by SDS-PAGE/immunoblot. **b**, Lack of effect of **IU1** on the degradation of Arg-GFP, which was stabilized by catalytically inactive USP14(C114A) as in **Fig. 1f**. Otherwise short-lived Arg-GFP was coexpressed with USP14(C114A) in *Usp14*$^{-/-}$ MEF cells and treated with 0 - 100 μM of **IU1** for 6 hrs. Anti-GFP and anti-actin antibodies were used for immunoblotting. The noncatalytic effect of USP14, which is best visualized in this assay, is not reversed by **IU1**.

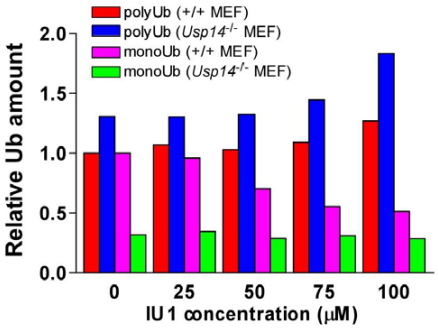

Figure S27. Quantification of ubiquitin levels in Fig. 4g. Polyubiquitin and monoubiquitin levels from wild-type and *Usp14*$^{-/-}$ MEF were quantified after treatment of various concentration of IU1. Ub signals were normalized to that of endogenous actin. Quantification was achieved by densitometry of a film image.

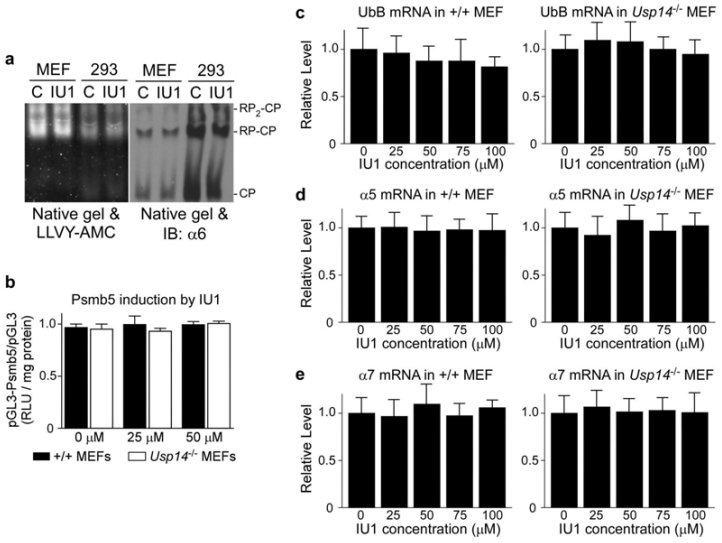

Figure S28. IU1 treatment does not induce transcription of proteasome subunit genes. a, The level and peptidase activity of the proteasome were determined before and after a 6-hr IU1 treatment (100 μM). Total cell extracts (50 μg/lane) were resolved by native PAGE, and the proteasome was visualized using either an in-gel activity stain with a fluorogenic peptide substrate (LLVY-AMC), or immunoblotting with antibodies to subunit α6. RP_2-CP and RP-CP are distinct forms of the 26S proteasome. **b,** A luciferase reporter gene containing the murine *Psmb5* promoter (-1 kb to 0 kb) was transiently expressed in wild-type and *Usp14*$^{-/-}$ MEFs and promoter activity was assessed following incubation of 25 or 50 μM of IU1 for 8 hr. For normalization of luciferase activity, a control experiment using the promoter-less pGL3 plasmid was performed. This reporter construct has previously been used as a representative measure of proteasome subunit gene induction[5,6]. Values are mean ± s.d. from three independent experiments. RLU, relative light units. **c-e,** Quantitative RT-PCR for a ubiquitin gene (UbB) and two proteasome subunit genes (α5 and α7) was performed using total mRNA from +/+ (left panels) and *Usp14*$^{-/-}$ MEFs (right) after incubation with a graded doses of IU1 for 8 hr. These data supplement **Fig. 4h**.

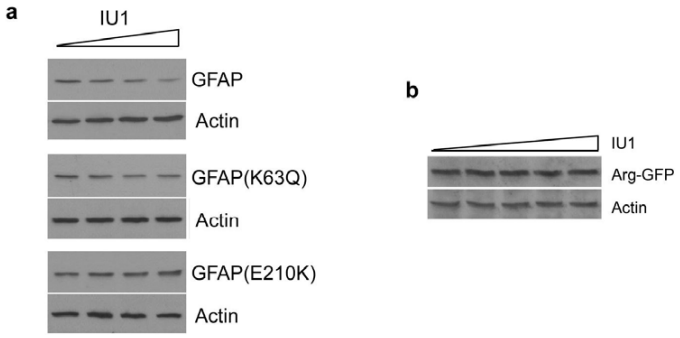

Figure S26. IU1 treatment reduces the level of GFAP expressed in wild-type MEF cells but does not affect Arg-GFP. **a**, Wild-type MEF cells transfected with plasmids expressing wild-type GFAP or its more aggregation-prone mutations, GFAP(K63Q) or GFAP(E210K) were treated with 0, 25, 50, or 100 μM of **IU1** for 6 hr, and analyzed by SDS-PAGE/immunoblot. **b**, Lack of effect of **IU1** on the degradation of Arg-GFP, which was stabilized by catalytically inactive USP14(C114A) as in **Fig. 1f**. Otherwise short-lived Arg-GFP was coexpressed with USP14(C114A) in *Usp14*$^{-/-}$ MEF cells and treated with 0 - 100 μM of **IU1** for 6 hrs. Anti-GFP and anti-actin antibodies were used for immunoblotting. The noncatalytic effect of USP14, which is best visualized in this assay, is not reversed by **IU1**.

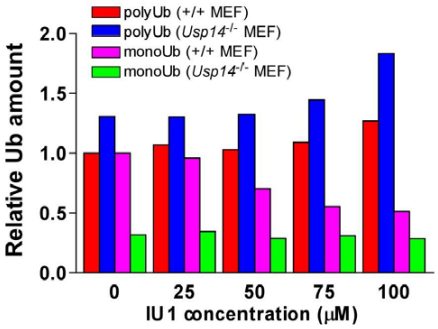

Figure S27. Quantification of ubiquitin levels in Fig. 4g. Polyubiquitin and monoubiquitin levels from wild-type and *Usp14*$^{-/-}$ MEF were quantified after treatment of various concentration of IU1. Ub signals were normalized to that of endogenous actin. Quantification was achieved by densitometry of a film image.

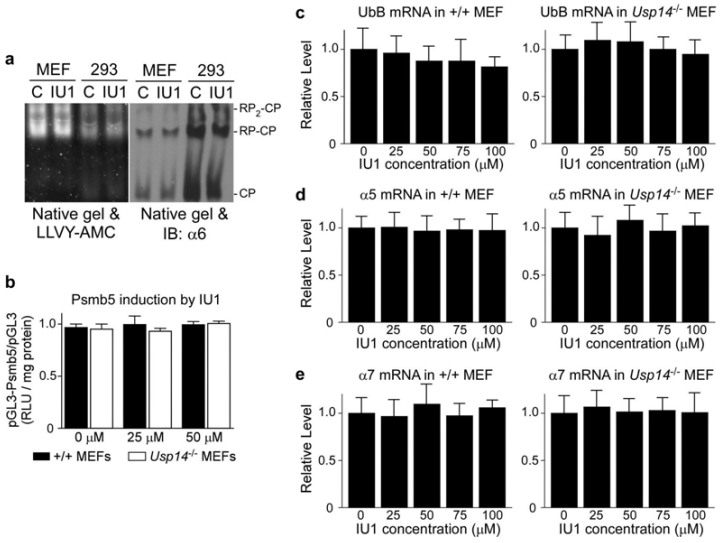

Figure S28. IU1 treatment does not induce transcription of proteasome subunit genes. a, The level and peptidase activity of the proteasome were determined before and after a 6-hr IU1 treatment (100 μM). Total cell extracts (50 μg/lane) were resolved by native PAGE, and the proteasome was visualized using either an in-gel activity stain with a fluorogenic peptide substrate (LLVY-AMC), or immunoblotting with antibodies to subunit α6. RP_2-CP and RP-CP are distinct forms of the 26S proteasome. **b,** A luciferase reporter gene containing the murine *Psmb5* promoter (-1 kb to 0 kb) was transiently expressed in wild-type and *Usp14*$^{-/-}$ MEFs and promoter activity was assessed following incubation of 25 or 50 μM of IU1 for 8 hr. For normalization of luciferase activity, a control experiment using the promoter-less pGL3 plasmid was performed. This reporter construct has previously been used as a representative measure of proteasome subunit gene induction[5,6]. Values are mean ± s.d. from three independent experiments. RLU, relative light units. **c-e,** Quantitative RT-PCR for a ubiquitin gene (UbB) and two proteasome subunit genes (α5 and α7) was performed using total mRNA from +/+ (left panels) and *Usp14*$^{-/-}$ MEFs (right) after incubation with a graded doses of IU1 for 8 hr. These data supplement **Fig. 4h**.

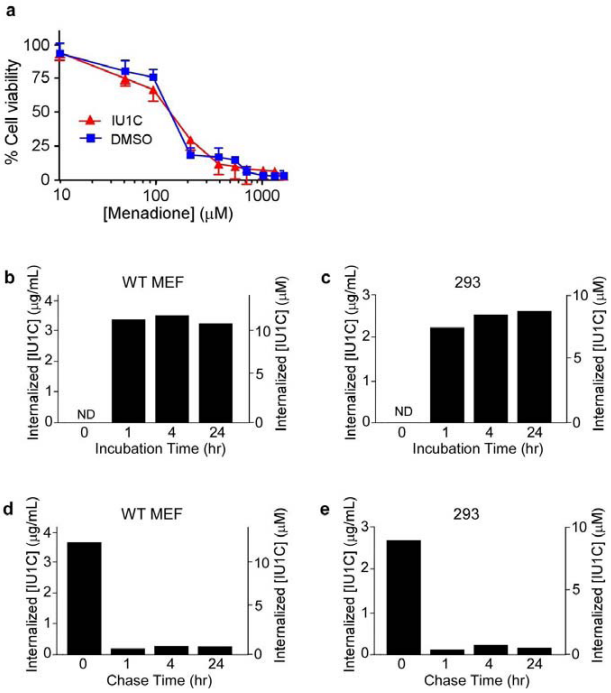

Figure S29. IU1C does not significantly affect oxidative stress-induced cytotoxicity. a, HEK293 cells were treated with 50 μM of IU1C for 6 hr and graded concentrations of menadione for 4 hr, followed by MTT assay. Values represent the mean ± s.d. of triplicate cultures. These data supplement **Fig. 5b.** Time-course of IU1C levels in wild-type MEFs (**b**) and HEK293 cells (**c**) were measure by using LC/MS. As in **Supplementary Figs. 19a** and **19b**, respectively, except IU1C, a functionally inactive control for IU1, was used. ND, not detected. **d and e,** See legend to **Supplementary Fig. 19c.** IU1C concentrations in the media (data not shown) of wild-type MEFs or HEK293 cells are comparable to those of IU1 (**Supplementary Fig. 19**).

References accompanying supplementary figures

1. Wang, X. *et al*. Mass spectrometric characterization of the affinity-purified human 26S proteasome complex. *Biochemistry* **46**, 3553-65 (2007).
2. Malo, N., Hanley, J., Cerquozzi, S., Pelletier, J. & Nadon, R. Statistical practice in high-throughput screening data analysis. *Nat. Biotechnol.* **24**, 167-75 (2006).
3. Liu, C.W. *et al*. ATP binding and ATP hydrolysis play distinct roles in the function of the 26S proteasome. *Mol. Cell* **24**, 39-50 (2006).
4. Mizushima, N., Yoshimori, T., & Levine, B. Methods in mammalian autophagy research. *Cell* **140**, 313-26 (2010).
5. Kwak, M.K. *et al*. Antioxidants enhance mammalian proteasome expression through the Keap1-Nrf2 signaling pathway. *Mol. Cell. Biol.* **23**, 8786-94 (2003).
6. Chondrogianni, N. *et al*. Central role of the proteasome in senescence and survival of human fibroblasts. *J. Biol. Chem.* **278**, 28026-37 (2003).

Cancer Cell
Article

Pharmacologic Inhibition of the Anaphase-Promoting Complex Induces A Spindle Checkpoint-Dependent Mitotic Arrest in the Absence of Spindle Damage

Xing Zeng,[1] Frederic Sigoillot,[1] Shantanu Gaur,[1] Sungwoon Choi,[2] Kathleen L. Pfaff,[1] Dong-Chan Oh,[3,4] Nathaniel Hathaway,[1] Nevena Dimova,[1] Gregory D. Cuny,[2] and Randall W. King[1,*]
[1]Department of Cell Biology, 240 Longwood Avenue, Harvard Medical School, Boston, MA 02115, USA
[2]Laboratory for Drug Discovery in Neurodegeneration, Brigham & Women's Hospital and Harvard Medical School, 65 Landsdowne Street, Cambridge, MA 02139, USA
[3]Department of Biological Chemistry and Molecular Pharmacology, 240 Longwood Avenue, Harvard Medical School, Boston, MA 02115, USA
[4]Natural Products Research Institute, College of Pharmacy, 599 Gwanak-ro, Gwanak-gu, Seoul 151-742, Republic of Korea
*Correspondence: randy_king@hms.harvard.edu
DOI 10.1016/j.ccr.2010.08.010

SUMMARY

Microtubule inhibitors are important cancer drugs that induce mitotic arrest by activating the spindle assembly checkpoint (SAC), which, in turn, inhibits the ubiquitin ligase activity of the anaphase-promoting complex (APC). Here, we report a small molecule, tosyl-L-arginine methyl ester (TAME), which binds to the APC and prevents its activation by Cdc20 and Cdh1. A prodrug of TAME arrests cells in metaphase without perturbing the spindle, but nonetheless the arrest is dependent on the SAC. Metaphase arrest induced by a proteasome inhibitor is also SAC dependent, suggesting that APC-dependent proteolysis is required to inactivate the SAC. We propose that mutual antagonism between the APC and the SAC yields a positive feedback loop that amplifies the ability of TAME to induce mitotic arrest.

INTRODUCTION

Microtubule inhibitors such as taxanes and the vinca alkaloids represent one of the most important classes of cancer drugs, used in the treatment of breast, ovarian, and lung cancer (Montero et al., 2005). However, the response of cells to microtubule inhibitors is highly variable (Brito et al., 2008; Gascoigne and Taylor, 2008; Orth et al., 2008; Shi et al., 2008), potentially compromising clinical efficacy. How these drugs cause cell death remains unclear, but induction of mitotic arrest appears to be a key aspect of the mechanism (Bekier et al., 2009; Huang et al., 2009). By perturbing the mitotic spindle, these drugs activate the spindle assembly checkpoint (SAC), which delays mitotic exit by inhibiting the ubiquitin ligase activity of the anaphase-promoting complex/cyclosome (APC). In principle, a compound that directly inhibits APC-dependent proteolysis should arrest cells in mitosis without causing side effects that result from microtubule inhibition such as peripheral neuropathy.

The APC is the most complex ubiquitin ligase known, consisting of more than 11 subunits. The activator proteins Cdh1 and Cdc20 bind to the APC at different cell cycle stages to stimulate APC-dependent ubiquitination of substrates and their subsequent destruction by the 26S proteasome (Peters, 2006). The activators assist in recruitment of APC substrates and may also stimulate ligase activity (Yu, 2007). Cdh1 binds to the APC during G1 to promote degradation of APC substrates during interphase. In contrast, the initiation of anaphase and exit from mitosis require Cdc20-dependent ubiquitination of APC substrates such as securin and mitotic cyclins. Prior to anaphase, the ability of APC-Cdc20 to ubiquitinate certain substrates is inhibited by the SAC (Musacchio and Salmon, 2007). Unattached

Significance

The anaphase-promoting complex (APC) is required for mitotic exit, making the APC a potential target for antimitotic chemotherapy. Here, we identify TAME as a small molecule inhibitor of the APC and develop a cell-permeable derivative, proTAME. Treatment of cells with proTAME causes a surprisingly robust mitotic arrest because APC-dependent proteolysis is required for inactivation of the spindle assembly checkpoint (SAC). In contrast, SAC-activating compounds such as microtubule inhibitors do not suppress APC activity as completely. As a result, cells rely on continued protein synthesis to maintain mitotic arrest, providing an explanation for the known variability in cellular response to microtubule inhibitors. Direct APC inhibitors may therefore provide a more uniform and specific method for inducing mitotic arrest.

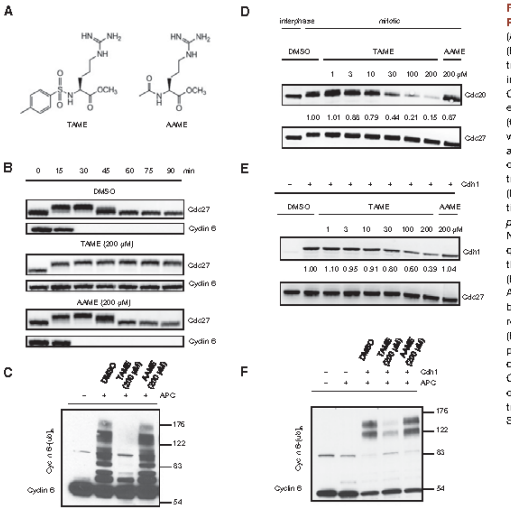

Figure 1. TAME Inhibits APC Activation by Perturbing Binding of Cdc20 or Cdh1

(A) Structures of TAME and AAME.

(B) TAME induces mitotic arrest in *Xenopus* extract. Recombinant cyclin B1/Cdk1 was added to interphase extract in the presence of compounds. Cdc27 phosphorylation and cyclin B1 levels were examined by immunoblot.

(C) TAME inhibits APC activation. Compounds were added to mitotic *Xenopus* extract immediately before APC immunoprecipitation. The activity of the isolated APC was measured in a reconstituted assay.

(D) TAME inhibits Cdc20 association with mitotic APC. Compounds were added to mitotic *Xenopus* extract prior to APC immunoprecipitation. Numbers represent CCD-imaging based-intensity quantitation of the immunoblot and show the relative amount of Cdc20 normalized to Cdc27.

(E) TAME inhibits Cdh1 association with interphase APC. Interphase *Xenopus* extract was preincubated with compounds for 30 min prior to adding recombinant Cdh1 and APC immunoprecipitation. The activity of the isolated APC was measured in a reconstituted assay.

(F) TAME inhibits APC activation by Cdh1. Interphase *Xenopus* extract was preincubated with compound for 30 min prior to adding recombinant Cdh1 and APC immunoprecipitation. The activity of the isolated APC was measured in a reconstituted assay.

See also Figure S1.

kinetochores catalyze the formation of an inhibitory protein complex, containing the proteins Mad2, BubR1, and Bub3, that sequesters Cdc20 or interferes with its ability to activate the APC. Attachment of kinetochores to the mitotic spindle diminishes their ability to generate an inhibitory signal. Subsequently, the SAC-inhibited APC-Cdc20 complex is activated, by a mechanism that remains incompletely understood.

Because the APC regulates multiple cell-cycle events, it is not clear whether pharmacological inhibition of its activity will lead to selective or prolonged arrest in mitosis as is the case with microtubule inhibitors. Proteasome inhibitors can block APC-dependent proteolysis without perturbing the mitotic spindle (Famulski and Chan, 2007), but they also inhibit the degradation of many other substrates of the ubiquitin-proteasome system, and therefore also cause cell-cycle arrest during interphase (Wojcik et al., 1996). It may be difficult to achieve mitotic arrest by pharmacologic APC inhibition, as RNAi approaches indicate that Cdc20 expression must be severely reduced to induce mitotic arrest (Huang et al., 2009; Wolthuis et al., 2008). Even when the SAC is maximally activated by complete microtubule depolymerization, some cells escape mitotic arrest due to residual APC activity (Brito and Rieder, 2006), suggesting that the SAC cannot fully inhibit the APC during mitosis. For this reason, microtubule inhibitors may suffer from limited effectiveness because some cells escape mitotic arrest before dying (Bekier et al., 2009; Huang et al., 2009). Whether an APC inhibitor can better extinguish APC activity and induce a more persistent mitotic arrest is therefore an important question in contemplating development of APC inhibitors as a therapeutic strategy for cancer.

RESULTS

TAME Inhibits APC Activation by Perturbing Activator Protein Binding

We identified TAME (Figure 1A) in an earlier study (Verma et al., 2004) as an inhibitor of cyclin proteolysis in mitotic *Xenopus* egg extract (IC_{50} of 12 μM; Figure S1A), but its mechanism of action has remained unknown. TAME also inhibited cyclin degradation in interphase extract activated by exogenous Cdh1, but had no effect on SCF-dependent proteolysis of β-catenin-luciferase (Verma et al., 2004), indicating that it is not a general inhibitor of the ubiquitin-proteasome system. Testing of TAME derivatives indicated that the tosyl group, arginine, and the methyl ester are each important for activity (Figures S1B and S1C). Acetyl-L-arginine methyl ester (AAME; Figure 1A) showed only low activity and was therefore used as a negative control in subsequent experiments. When added to interphase extract treated with recombinant cyclin B1/Cdc2 complex, TAME, but not AAME, arrested the extract in mitosis, with stable cyclin B1 and phosphorylated Cdc27 (Figure 1B). Another APC substrate, cyclin A2, was also stabilized by TAME in *Xenopus* extract (data not shown). TAME

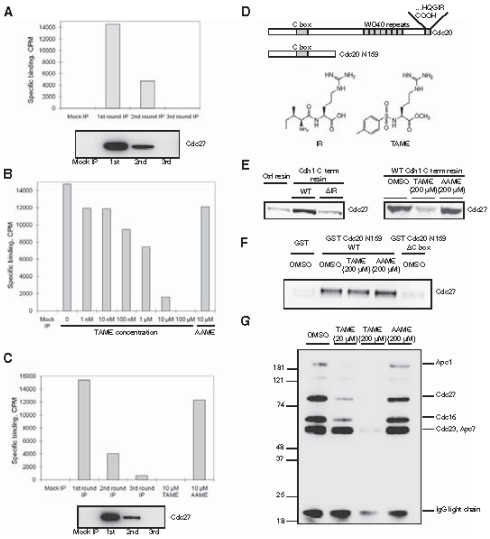

Figure 2. TAME Binds to the APC and Inhibits Binding of the IR Tail of Activator Proteins

(A) TAME binds *Xenopus* APC. ^{3}H-TAME was added to interphase extract or to extract that had been partially or completely immunodepleted of APC. Remaining APC was then immunoprecipitated, and the associated radioactivity was measured by scintillation counting. Residual APC levels were measured by immunoblot with Cdc27 antibody. Specific binding was calculated as described in the methods.

(B) Unlabeled TAME competes with ^{3}H-TAME for binding to *Xenopus* APC. ^{3}H-TAME was added to interphase extract with unlabeled TAME or AAME prior to APC immunoprecipitation.

(C) ^{3}H-TAME binds to human APC. The experiment in 2A was repeated with lysate from asynchronous HeLa cells.

(D) Schematic of Cdc20, the C-box containing fragment, and structures of the IR tail and TAME.

(E) TAME inhibits the interaction between the Cdh1 C-terminal IR peptide and the APC. Left: Resin coupled with cysteine (Ctrl resin), Cdh1 C-terminal peptide (WT), or the peptide lacking the C-terminal isoleucine and arginine (ΔIR) was incubated with interphase *Xenopus* extract, washed, and the amount of bound Cdc27 was analyzed by immunoblot. Right: Cdh1 C-terminal resin was incubated with interphase extract in the presence of compounds and the amount of Cdc27 was analyzed as above.

(F) TAME does not inhibit the interaction between the C-box and the APC. A 159 amino acid N-terminal fragment of Cdc20 containing the C-box fused to GST (GST-CDC20 N159 WT) or the same fragment lacking the C-box (GST-CDC20 N159 ΔC-box) were bound to glutathione resin and incubated with mitotic *Xenopus* extract in the presence of compounds. Bound Cdc27 was analyzed by immunoblot.

(G) TAME inhibits IR-peptide crosslinking to APC subunits. Purified interphase *Xenopus* APC was incubated with an IR peptide coupled to a biotin-containing label-transfer reagent, in the presence or absence of compounds, prior to photocrosslinking. Reaction products were detected by streptavidin-HRP.

See also Figure S2.

had no effect on the ability of *Xenopus* extract to degrade cyclin B1 that had been preubiquitinated in vitro (Figure S1D), indicating that TAME does not inhibit the proteasome or its ability to recognize ubiquitinated substrates.

Because the SAC is not active in *Xenopus* extracts (Minshull et al., 1994), we reasoned that TAME might inhibit cyclin proteolysis by perturbing the APC. Indeed, when TAME was added to mitotic *Xenopus* extract during APC isolation, the APC showed a dramatic loss of activity in a reconstituted ubiquitination reaction (Figure 1C). Consistent with this finding, TAME addition to extract reduced Cdc20 association with the APC in a dose-dependent manner (Figure 1D), but did not otherwise affect APC composition (Figure S1E). TAME also inhibited the binding of Cdh1 to APC when Cdh1 and TAME were added together to interphase extract (Figure 1E). The reduction in Cdh1 binding was accompanied by a reduction in APC activation (Figure 1F). These findings suggested that TAME might block APC activation by perturbing the interaction between APC and its activator proteins Cdc20 or Cdh1.

To understand how TAME disrupts the interaction between the activator proteins and the APC, we first tested whether TAME binds to the APC. We added ^{3}H-TAME to interphase *Xenopus* extract, or to extract immunodepleted of APC, and then isolated residual APC with Cdc27 antibodies and measured the amount of radioactivity associated with the beads. We found that binding of ^{3}H-TAME correlated with the amount of immunoprecipitated Cdc27 (Figure 2A). Unlabeled TAME competitively inhibited the binding of ^{3}H-TAME, whereas AAME did not (Figure 2B). Other TAME derivatives competed with ^{3}H-TAME for APC binding in a manner that correlated with their ability to inhibit cyclin-luciferase proteolysis in *Xenopus* extract (Figure S2A). A similar approach demonstrated that TAME binds to human APC isolated from HeLa cells (Figure 2C). Together these findings indicate that TAME binds to the APC, potentially explaining its ability to perturb activator protein association.

To understand how TAME disrupts activator binding to the APC, we determined whether TAME could inhibit the interaction between APC and motifs of the activator proteins that have been

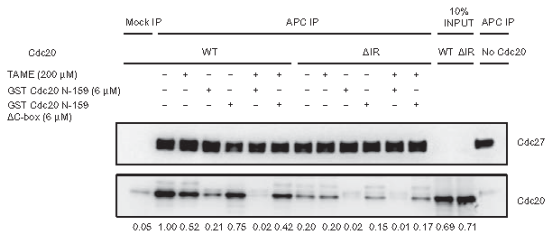

Figure 3. TAME Inhibits Binding of Wild-Type Cdc20 to the APC, but Not Binding of a ΔIR Mutant

Mitotic APC immunoprecipitated from *Xenopus* extract was washed with XB high salt (500 mM KCl) and XB to remove endogenous Cdc20 prior to incubation with in vitro translated wild-type *Xenopus* Cdc20 or the ΔIR mutant. Various competitors were added during incubation as indicated. Unbound proteins were washed away and bound Cdc20 was analyzed by immunoblot. Numbers represent the amount of Cdc20 normalized to Cdc27.

implicated in APC binding, including the C-box (Schwab et al., 2001) and the C-terminal isoleucine-arginine (IR) tail (Figure 2D; Burton et al., 2005; Vodermaier et al., 2003). Because TAME structurally resembles the IR tail of Cdc20 and Cdh1 (Figure 2D), we hypothesized that TAME might bind to the APC in the same site normally occupied by the IR tail. Previous work has demonstrated that a C-terminal 20 amino acid peptide derived from Cdh1 ("IR peptide") is sufficient to isolate *Xenopus* APC from interphase extract (Vodermaier et al., 2003). We confirmed this finding and found that TAME, but not AAME, was sufficient to block APC recruitment by the IR peptide (Figure 2E). In contrast, TAME had no effect on recruitment of APC from mitotic extract by an N-terminal fragment of Cdc20 containing only the C-box interaction motif (Figure 2F), indicating that TAME specifically inhibits the IR-tail-dependent interaction.

The APC subunits Cdc27 and APC7 have been implicated in binding of the IR tail of Cdh1 to the APC (Matyskiela and Morgan, 2009; Vodermaier et al., 2003). To determine whether TAME could competitively inhibit the binding of the IR-tail to these proteins, we conjugated the IR peptide to a photo-affinity reagent and performed crosslinking studies with APC immunopurified from interphase *Xenopus* extract. Four proteins known to exist in an APC subcomplex, namely, Cdc27, Cdc16, Cdc23, and Apc7, were crosslinked in an IR-dependent manner that could be competed by excess unlabeled IR peptide (Figures S2B and S2C). At low concentration (20 μM), TAME efficiently inhibited crosslinking of the IR peptide to Cdc27 and Cdc16 but only slightly reduced crosslinking to Cdc23 and Apc7 (Figure 2G). At high concentration (200 μM), TAME strongly inhibited crosslinking to all APC subunits (Figure 2G). Together these findings support the hypothesis that TAME binds to APC subunits that recruit the IR tail, thereby preventing activator proteins from associating with the APC.

To confirm that TAME specifically antagonizes IR-tail-dependent interactions between Cdc20 and the APC, we tested the ability of TAME to inhibit the binding of Cdc20 to the APC in a reconstituted system. APC was purified from mitotic *Xenopus* extracts and washed with high salt to remove most Cdc20. Purified mitotic APC was then incubated in reticulocyte lysate expressing wild-type or mutant Cdc20, and Cdc20 binding to APC was measured by coimmunoprecipitation. We found that efficient binding of Cdc20 to the APC under these conditions indeed requires the IR-tail, as a mutant lacking these two residues (Cdc20ΔIR) did not bind as efficiently to the APC (Figure 3). TAME also strongly reduced Cdc20 binding to the APC under these conditions (Figure 3). Importantly, addition of TAME had no further effect on binding of the Cdc20ΔIR mutant, confirming that TAME does not perturb other interactions between Cdc20 and the APC.

We found that TAME addition or IR-tail deletion was not sufficient to fully inhibit Cdc20 association under these conditions. We suspected that other interactions, such as C-box-dependent binding, might promote Cdc20 association with the APC, thereby masking the effect of TAME addition or IR-tail deletion. Consistent with this hypothesis, we found that addition of a C-box-containing N-terminal fragment of Cdc20 could competitively inhibit binding of full-length Cdc20 to the APC (Figure 3). In the presence of the C-box fragment, addition of TAME or deletion of the IR-tail was sufficient to completely suppress Cdc20 association with the APC. These results indicate that both C-box-dependent and IR-tail-dependent interactions are important for Cdc20 binding in these conditions, and that TAME specifically disrupts the IR-dependent interaction. We conclude that the target of TAME is the APC, and that it inhibits APC activation by interfering specifically with IR-tail-dependent interactions between Cdc20 or Cdh1 and the APC.

A TAME Prodrug Inhibits APC-Cdh1 Activation in Cells

Having established the mechanism by which TAME inhibits APC activation in *Xenopus* extract, we next wanted to determine whether TAME inhibits APC activation in human cells. Because TAME is not cell permeable, we synthesized a TAME prodrug (proTAME), and its control compound proAAME, by modifying the guanidino group to produce an N,N'-bis(acyloxymethyl carbamate) derivative (Figure 4A). Such prodrugs can be processed by intracellular esterases to yield the parent compound. In *Xenopus* extract, proTAME was indeed rapidly converted to TAME (Figure S3A), which efficiently inhibited cyclin B-luciferase

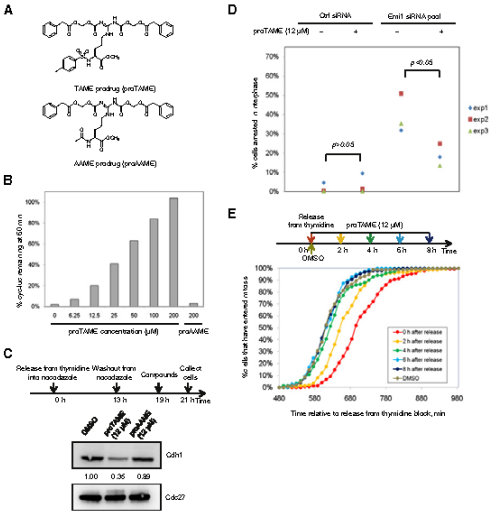

Figure 4. ProTAME Inhibits APC Activity in *Xenopus* Extract and Inhibits Cdh1-Dependent APC Activity during Interphase in HeLa Cells

(A) Structures of proTAME and proAAME.

(B) ProTAME inhibits cyclin B-luciferase degradation in mitotic *Xenopus* extract. Different concentrations of proTAME or proAAME were added to mitotic *Xenopus* extract containing cyclin B-luciferase reporter. Samples were collected at 60 min and the remaining reporter level was measured by luminescence.

(C) ProTAME blocks Cdh1 association with the APC. HeLa cells were released from nocodazole and treated with proTAME in G1. APC was immunoprecipitated from cell lysates and the amount of Cdc27 and Cdh1 was analyzed by immunoblot.

(D) ProTAME restores mitotic entry in Emi1-depleted cells. HeLa cells were transfected with control siRNA or Emi1 siRNA and treated with DMSO or proTAME 24 hr after transfection and then imaged for 48 hr. About 400 cells were analyzed in each experiment, and the proportion that failed to enter mitosis during the 48 hr of imaging was calculated. Results of three independent experiments are shown. Statistical significance was calculated using an unpaired t test.

(E) ProTAME causes a mitotic entry delay if added during S phase. HeLa H2B-GFP cells were released from a double thymidine block and proTAME (12 μM) was added at different time points as indicated. Mitotic entry was monitored by time-lapse imaging. Cumulative frequency curves of the time of mitotic entry are shown. Statistical analysis, including mean, median, statistical significance, and number of cells analyzed per condition for all experiments is included in Table S1.

See also Figure S3.

proteolysis (Figure 4B). ProTAME was also activated efficiently in HeLa cells, but not in MCF10A cells (Figure S3B).

We first examined whether proTAME could inhibit association of Cdh1 with the APC in cells. We released HeLa cells expressing H2B-GFP from a nocodazole block and added 12 μM proTAME after cells had entered G1, when the APC is activated by Cdh1. We found that addition of proTAME inhibited Cdh1 association with the APC (Figure 4C) but proAAME did not. However, proTAME was not sufficient to cause premature accumulation of endogenous APC substrates in G1 or S phase (Figure S3C). During S phase, when APC substrates are known to be expressed, the effect of proTAME may be masked by Emi1-dependent inhibition of APC-Cdh1 (Hsu et al., 2002). To test this idea, we depleted cells of Emi1, which leads to degradation of APC substrates and prevents mitotic entry (Hsu et al., 2002). We confirmed that Emi1 depletion prevents mitotic entry, and found that addition of 12 μM proTAME substantially rescued the mitotic entry defect caused by depletion of Emi1 (Figure 4D). Therefore, we conclude that proTAME is capable of inhibiting APC-Cdh1 function in cells.

Previous studies have shown that knockdown of Cdh1 induces prolonged S phase and mitotic entry delay in human cells (Engelbert et al., 2008; Sigl et al., 2009). Consistent with these findings, proTAME caused a 2 hr delay in mitotic entry when added during release from a double thymidine block (Figure 4E). However, adding proTAME 6 hr or later after release did not delay mitotic entry (Figure 4E), suggesting the delay may be a consequence of inhibiting APC-Cdh1 in S phase. These findings indicate that, although proTAME can inhibit APC-Cdh1 activation, it has only modest effects on cell cycle progression during interphase.

ProTAME Induces Mitotic Arrest in the Absence of Spindle Damage

To examine effects of proTAME treatment on mitosis, we released HeLa H2B-GFP cells from a double thymidine block and added proTAME 8 hr after release, a time when proTAME addition does not delay mitotic entry (Figure 4E). Mitotic duration was then measured by time-lapse imaging. Cells treated with low doses of proTAME (780 nM or 3 μM) remained in metaphase for as long as 5 hr, but then proceeded through a normal anaphase, whereas cells treated with 12 μM proTAME arrested in metaphase and subsequently died (Figure 5A). In contrast, treatment of cells with 12 μM proAAME had no effect. ProTAME greatly increased mitotic duration in asynchronous hTERT-RPE1 cells as well, as 6 μM proTAME increased median mitotic duration to over 8 hr, compared with 24 min in proAAME-treated cells (Figure S4A). ProTAME had no effect at similar doses in

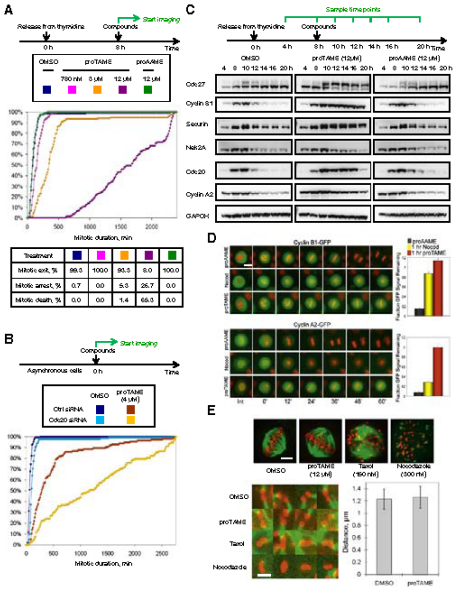

Figure 5. ProTAME Induces Mitotic Arrest without Disrupting the Mitotic Spindle

(A) ProTAME induces mitotic arrest in HeLa cells. Double thymidine synchronized HeLa H2B-GFP cells were treated with compounds and analyzed by time-lapse imaging. Cumulative frequency curves of mitotic duration and cell fate distributions are shown.

(B) Partial Cdc20 knockdown sensitizes cells to proTAME treatment. Asynchronous HeLa H2B-GFP cells were transfected with control or Cdc20 siRNA 24 hr prior to treatment with compounds.

(C) ProTAME stabilizes endogenous APC substrates. Double thymidine synchronized HeLa cells were treated with compounds.

(D) ProTAME stabilizes exogenous cyclin B1-GFP and cyclin A2-GFP in HeLa cells. HeLa H2B-RFP cells transduced with cyclin-GFP adenoviruses were treated with 20 μM proTAME or proAAME, or 150 nM nocodazole. Bar: 12 μm. Representative cells are shown. For quantitation, the fraction of GFP intensity remaining at 60 min as compared with the onset of mitosis was determined ($n \geq 30$ individual cells per treatment). Error bars represent standard error of the mean.

(E) ProTAME does not disrupt mitotic spindles or alter interkinetochore distance. Asynchronous HeLa cells were treated with compounds for 2 hr and then stained with anti-tubulin (green) and CREST (red) antibody. Representative images are shown. Bar: 3 μm. Representative images of kinetochore pairs are shown. Bar: 1.2 μm. Interkinetochore distance was measured in DMSO or proTAME treated cells ($n = 55$, $p = 0.23$). Error bars represent standard deviation.

See also Figure S4 and Movies S1–S4.

MCF10A cells (data not shown), because the prodrug was not efficiently activated (Figure S3B).

If proTAME blocks mitotic progression by disrupting the APC-Cdc20 interaction, then reducing Cdc20 expression should enhance the mitotic exit delay induced by proTAME treatment. In control-transfected cells, 4 μM proTAME increased mitotic duration from 1.0 to 4.8 hr (Figure 5B). However, when Cdc20 levels were reduced by 50% using siRNA-mediated knockdown (Figure S4B), proTAME prolonged mitotic duration to 19.4 hr (Figure 5B). This effect was synergistic, because Cdc20 knockdown by itself only increased mitotic duration to 1.6 hr. These results show that reducing the expression of Cdc20 strongly sensitizes cells to the effect of proTAME, consistent with the APC-Cdc20 interaction as the relevant target of the compound.

We next investigated the effect of proTAME treatment on degradation of APC substrates. Because the SAC does not stabilize all APC substrates during mitosis, some substrates such as cyclin A2, Cdc20, and Nek2A are degraded in cells treated with microtubule inhibitors (den Elzen and Pines, 2001; Hayes et al., 2006; Nilsson et al., 2008). In contrast, substrates such as cyclin B1 and securin are stabilized by SAC activation. If proTAME directly inhibits APC activation, we predicted it would stabilize all APC substrates during mitosis, not just those whose stability depends on the SAC. Consistent with this hypothesis, cells treated with proTAME accumulated cyclin A2, Cdc20, and Nek2A in addition to cyclin B1 and securin (Figure 5C). These results were confirmed in live cell imaging experiments, where proTAME stabilized cyclinA2-GFP but the microtubule depolymerizer nocodazole did not (Figure 5D). Interestingly, proTAME treatment caused greater accumulation of cyclin B1-GFP than nocodazole treatment, consistent with proTAME's ability to directly inhibit APC activation.

We next assessed the effects of proTAME treatment on mitotic spindle morphology and chromosome congression and compared this with the effects of treatment of cells with microtubule inhibitors. Compared with DMSO-treated cells, treatment of asynchronous HeLa cells with 12 μM proTAME for 2 hr yielded no measurable differences in mitotic spindle morphology or interkinetochore distance, indicating that proTAME did not perturb establishment of proper kinetochore tension (Figure 5E). In contrast, treatment of cells with nocodazole or taxol for 2 hr strongly perturbed spindle organization (Figure 5E). In live cell imaging experiments, treatment of cells with 3 μM proTAME or 10 μM MG132 caused no delay in chromosome congression (Figure S4C). Treatment of cells with 10 nM nocodazole or 12 μM proTAME caused a similar mild congression delay of

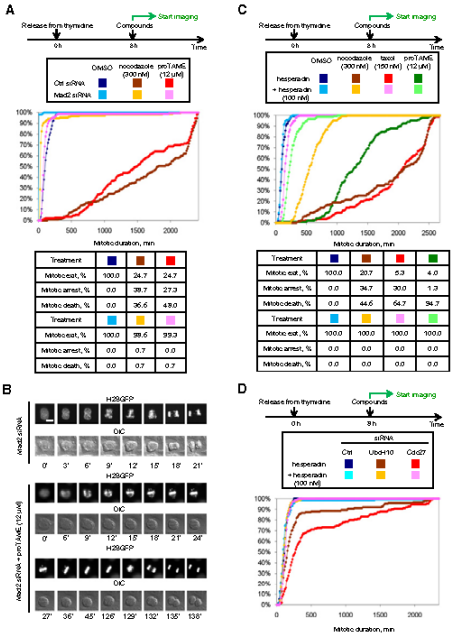

Figure 6. ProTAME-Induced Mitotic Arrest Is SAC Dependent

(A) ProTAME-induced mitotic arrest is Mad2 dependent. HeLa H2B-GFP cells were transfected with indicated siRNAs between rounds of thymidine treatment. Following release, cells were treated with compounds and analyzed by time-lapse imaging. A graph of the same data with an expanded x axis is shown in Figure S5A.

(B) ProTAME rescues the mitotic defect induced by Mad2 knockdown. Asynchronous HeLa H2B-GFP cells were treated with Mad2 siRNA 24 hr prior to addition of compound. Bar: 10 μm.

(C) ProTAME-induced mitotic arrest is hesperadin sensitive. Double thymidine synchronized HeLa H2B-GFP cells were treated with compounds 8 hr following release.

(D) UbcH10 or Cdc27 knockdown induces a hesperadin-sensitive mitotic delay. HeLa H2B-GFP cells were transfected with indicated siRNA between rounds of thymidine synchronization and treated with hesperadin 8 hr following release.

See also Figure S5 and Movies S5 and S6.

6 min (Figure S4C), but these treatments produced contrasting effects on the metaphase plate. In cells treated with 10 nM nocodazole, the metaphase plate appeared loose and was prone to bending (Movies S1–S3), whereas in cells treated with 12 μM proTAME the metaphase plate appeared tight and did not bend (Movie S4). Importantly, 10 nM nocodazole prolonged mitosis by only 20 min (data not shown), whereas 12 μM proTAME induced a mitotic arrest of over 28 hr (Figure 5A). Thus, the mild delay in congression is not sufficient to explain the ability of proTAME to arrest cells in mitosis. We conclude that proTAME induces arrest in metaphase without perturbing the morphology or function of the mitotic spindle.

ProTAME-Induced Mitotic Arrest Is SAC Dependent

Because TAME directly inhibits the APC, and causes arrest in metaphase with kinetochores that develop tension, we predicted that the proTAME-induced mitotic arrest in human cells would be independent of the SAC. We were therefore surprised to find that the SAC is in fact essential for the prolonged mitotic arrest of cells treated with proTAME. In double-thymidine synchronized cells, Mad2 knockdown greatly shortened the duration of proTAME-induced arrest, from 24.6 to 1.4 hr (Figure 6A; Figure S5A). As expected, Mad2 knockdown abrogated nocodazole-induced arrest, shortening the average mitotic duration from 30 to 0.6 hr. The Mad2 dependence of the proTAME-induced arrest was confirmed by measurement of APC substrate levels in synchronized cells (Figure S5B).

These experiments also revealed the ability of proTAME to delay mitotic exit independent of Mad2, as expected based on TAME's ability to directly inhibit APC activation. In Mad2 knockdown cells, proTAME treatment increased median mitotic duration from 12 to 84 min (Figure 6A; Figure S5A). Strikingly, this mitotic exit delay was sufficient to give Mad2 knockdown cells enough time to build a normal metaphase plate before initiating anaphase, rescuing the chromosome segregation defect caused by Mad2 knockdown (Figure 6B; Figure S5C; Movies S5 and S6). The ability of proTAME to restore normal mitotic division in cells depleted of Mad2 demonstrates that proTAME is unlikely to perturb microtubules or interfere with kinetochore function. The fact that 12 μM proTAME delays mitotic exit by only 72 min in the absence of the SAC indicates that this dose of proTAME does not fully inhibit APC activation. The ability of this dose of proTAME to cause mitotic arrest in SAC-proficient cells must therefore arise from significant amplification of APC inhibition by the SAC.

Whereas TAME reduced Cdc20 binding to the APC when added to *Xenopus* extracts, proTAME treatment did not decrease Cdc20 binding to the APC during mitotic arrest in HeLa cells (data not shown). We suspected that persistent Cdc20 association might result from the ability of the SAC to promote IR-tail-independent binding of Cdc20 to the APC. We

therefore examined the effect of depleting SAC proteins on the ability of proTAME to disrupt the APC-Cdc20 interaction. Indeed, when we arrested HeLa cells in mitosis by expression of nondegradable cyclin B, proTAME induced significant dissociation of Cdc20 from the APC, but only if SAC proteins were depleted by RNAi (Figure S5D). These results show that a proTAME-induced mitotic arrest occurs without substantial dissociation of Cdc20 from the APC, as a consequence of persistent activity of the SAC.

To further understand the SAC dependence of the proTAME arrest, we pharmacologically inactivated SAC signaling by treating cells with hesperadin (Hauf et al., 2003), an inhibitor of Aurora B kinase. This kinase phosphorylates proteins at kinetochores that are not under tension, leading to destabilization of microtubule-kinetochore interactions and activation of the SAC (Biggins and Murray, 2001; Cheeseman et al., 2006; DeLuca et al., 2006). Recent work using phosphospecific antibodies that recognize Aurora B substrates indicates that kinetochore proteins remain phosphorylated at a basal rate during metaphase (Welburn et al., 2010). We hypothesized that this basal rate of Aurora B-dependent phosphorylation may produce a persistent SAC signal during metaphase that contributes to the proTAME-induced arrest. Three observations are consistent with this hypothesis. First, hesperadin treatment dramatically shortened proTAME-induced mitotic arrest (Figure 6C) and led to dissociation of Mad2 and BubR1 from the APC in proTAME-arrested cells (Figure S5E). As expected, hesperadin also substantially shortened taxol-induced mitotic arrest, with a less pronounced effect on nocodazole-induced arrest (Figure 6C). Second, hesperadin treatment caused deformation of the metaphase plate in proTAME-arrested cells (Figure S5F), suggesting that Aurora B-dependent phosphorylation is required to maintain proper kinetochore-microtubule attachments in metaphase. Third, knockdown of the APC component Cdc27 or the APC-specific E2 UbcH10 caused a mitotic exit delay that could be completely suppressed by hesperadin treatment (Figure 6D). Together, these experiments are consistent with the idea that the SAC remains active at a basal rate during metaphase, despite the presence of properly attached chromosomes, and that kinetochore-dependent SAC signaling is important for the prolonged mitotic arrest induced by APC inhibition.

One possible explanation for the SAC dependence of the proTAME arrest is that proTAME stabilizes APC substrates such as Nek2A or cyclin A that are normally degraded in early mitosis. For example, overexpression of cyclin A has been reported to delay chromosome congression (den Elzen and Pines, 2001). To test whether stabilization of these substrates is important for the proTAME-induced arrest, we released HeLa cells from double thymidine block into nocodazole for 15 hr to allow degradation of cyclin A and other APC substrates that are not efficiently stabilized by the SAC. We then washed cells out of nocodazole into proTAME. Under this condition, proTAME remained capable of inducing a prolonged mitotic arrest that was highly hesperadin sensitive (Figure S5G). This result indicates that the SAC dependence of proTAME-induced mitotic arrest is unlikely to be caused by stabilization of APC substrates that are normally degraded in a SAC-independent fashion.

Metaphase Arrest Induced by a Proteasome Inhibitor Is SAC Dependent

Previous work has shown that APC-dependent ubiquitination promotes SAC inactivation in cell lysates (Reddy et al., 2007). In this system, APC-dependent ubiquitination of Cdc20, but not APC-dependent proteolysis, was suggested to be important for release of Cdc20 from SAC proteins (Reddy et al., 2007). However, a recent study found that proteasome activity is required for dissociation of the Mad2-Cdc20 complex in cells (Visconti et al., 2010). Together with our findings, these studies suggested that APC-dependent proteolysis could be important for SAC inactivation. A prediction of this model is that mitotic arrest induced by treatment with a low dose of proteasome inhibitor should be SAC dependent. To test this idea, we treated cells with a dose of MG132 (3 μM) that was just sufficient to arrest cells in mitosis (median duration of 15 hr). At this concentration, the duration of arrest was limited by cell death rather than mitotic exit, as only 10% of cells exited mitosis over 30h (Figure 7A). In MG132-treated cells depleted of Mad2 by RNAi, we observed that 50% of the cells exited mitosis (Figure 7A), indicating that the SAC is indeed required for efficient induction of mitotic arrest by proteasome inhibition.

Like proTAME-treated cells, MG132-treated cells arrest in metaphase with kinetochores that develop normal tension (Famulski and Chan, 2007). If metaphase chromosomes are indeed competent to generate a checkpoint signal, we predicted that the MG132-induced arrest should be hesperadin sensitive. To test this idea, 10 hr following thymidine release, HeLa H2B-GFP cells were treated with 3 μM MG132 in the presence or absence of hesperadin. Strikingly, hesperadin induced rapid mitotic exit in half of the cells, with the remainder exiting mitosis more slowly (Figure 7B). These distinct behaviors correlated with the timing of drug administration: cells that encountered drug while in mitosis exited mitosis quickly, whereas cells that encountered drug before mitosis exited slowly (Figure S6A). Hesperadin treatment induced dephosphorylation of Cdc27 and reduced levels of Mad2 and BubR1 bound to the APC compared with cells treated with MG132 alone (Figure S6B). Coaddition of proTAME to MG132 abrogated the ability of hesperadin to drive mitotic exit (Figure 7B), indicating that mitotic exit remains dependent on APC-dependent ubiquitination. In contrast, coaddition of taxol to MG132 did not efficiently suppress hesperadin-induced mitotic exit (Figure 7C), underscoring the distinct mechanisms underlying taxol and proTAME-induced mitotic arrests. Similar results were obtained when the proteasome was more fully inhibited by increasing the MG132 concentration to 10 μM (Figure 7D), indicating that the SAC continues to be important for complete inhibition of APC-dependent proteolysis even when the proteasome is more completely inhibited by drug.

The hesperadin sensitivity of the MG132-induced arrest suggested that Aurora B activity could be important for maintaining the metaphase plate, as we observed in proTAME treated cells. We found that treatment of MG132-arrested cells with hesperadin induced deformation of the metaphase plate within 30 min, whereas cells arrested with MG132 alone maintained a normal-appearing metaphase plate for over 5 hr (Figure S6C). These findings provide further support for the idea that Aurora B-dependent pathways remain active in metaphase. Together our findings indicate that mitotic arrest induced by a low

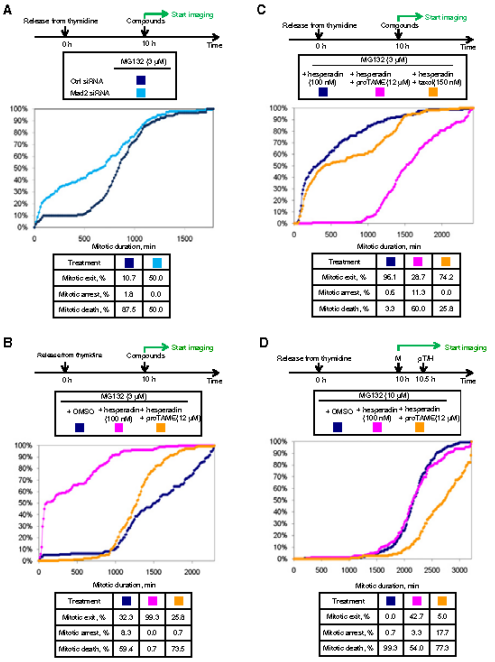

Figure 7. MG132-Induced Mitotic Arrest Is SAC Dependent

(A) MG132-induced arrest is Mad2 dependent. HeLa H2B-GFP cells were transfected with indicated siRNAs between rounds of thymidine synchronization, treated with compounds, and followed by time-lapse imaging.

(B) MG132-induced arrest is hesperadin sensitive, but mitotic exit can be suppressed by proTAME. Double thymidine synchronized HeLa cells were treated with compounds.

(C) Taxol cannot restore mitotic arrest in the presence of MG132 and hesperadin. Double thymidine synchronized HeLa cells were treated with compounds.

(D) Mitotic arrest induced by a higher concentration of MG132 remains hesperadin sensitive. Double thymidine synchronized HeLa cells were treated with compounds. M: MG132; pT: proTAME; H: hesperadin.

See also Figure S6.

concentration of proteasome inhibitor is not a simple consequence of direct inhibition of the proteasome by the drug, but also depends on continued inhibition of APC-dependent ubiquitination by the SAC.

Protein Synthesis Is Required for Mitotic Arrest Induced by Microtubule Inhibitors but Not by APC or Proteasome Inhibitors

Our data support a model in which APC-dependent proteolysis is required to inactivate the SAC. However, this model yields a paradox: How could the APC initiate SAC inactivation if it is fully inhibited by the SAC? One possibility is that SAC inhibition of APC is never complete, with residual APC remaining active to initiate SAC inactivation. Indeed, it has been shown that cyclin B1 and securin are slowly degraded even in the presence of a fully active SAC (Brito and Rieder, 2006; Nilsson et al., 2008). Prolonged arrest in mitosis might therefore require the continued synthesis of APC substrates during mitosis. Consistent with this hypothesis, we found that cycloheximide promoted mitotic exit of nocodazole- or taxol-arrested cells (Figure 8A). In striking contrast, cycloheximide did not accelerate mitotic exit in proTAME-treated cells, but rather extended mitotic arrest by delaying cell death (Figure 8A). Cycloheximide addition produced similar effects in MG132-treated cells, suppressing cell death without promoting mitotic exit (Figure 8B). Consistent with these findings, labeling experiments demonstrated that known APC substrates such as cyclin B1 and BubR1 are translated during mitotic arrest (Figure S7). Together these findings indicate that ongoing mitotic protein synthesis is essential to maintain a SAC-dependent mitotic arrest, perhaps by replenishing components that are degraded by residual APC-dependent proteolysis.

We next wanted to understand why the MG132-induced arrest is resistant to cycloheximide. We hypothesized that persistent SAC activity cooperates with direct pharmacologic inhibition of the proteasome to slow the rate of APC-dependent proteolysis to such a great extent that mitotic arrest no longer depends upon protein synthesis. If this hypothesis is correct, then inactivating the SAC should make the MG132-induced arrest sensitive to cycloheximide, as protein synthesis would now be required to balance the increased rate of APC-dependent degradation. This was indeed the case, as depletion of Mad2 (Figure 8B) or inactivation of the SAC with hesperadin (Figure 8C) led to mitotic exit in cells treated with cycloheximide and 10 μM MG132. Addition of proTAME suppressed the effect of hesperadin (Figure 8C), indicating that mitotic exit remains dependent on APC-mediated

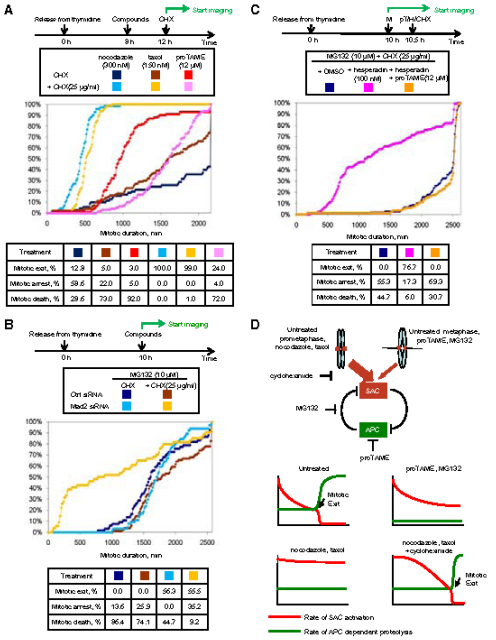

Figure 8. Microtubule Inhibitors Require Protein Synthesis for Mitotic Arrest whereas proTAME and MG132 Do Not

(A) Mitotic arrest induced by microtubule inhibitors requires protein synthesis but proTAME-induced arrest does not. Double thymidine synchronized HeLa-H2B-GFP cells were treated with compounds and followed by time-lapse imaging. CHX: cycloheximide.

(B) MG132 (10 μM)-induced arrest is cycloheximide resistant but Mad2 dependent. HeLa cells were transfected with indicated siRNAs between rounds of thymidine synchronization.

(C) MG132 (10 μM)-induced arrest is cycloheximide resistant but hesperadin sensitive. Double thymidine synchronized HeLa cells were treated with compounds.

(D) Model. In the bottom panels, the x axis indicates time from mitotic entry.

See also Figure S7.

ubiquitination. Together these results indicate that the ability of proTAME or MG132 to induce mitotic arrest independent of protein synthesis requires persistent inhibition of the APC by the SAC.

DISCUSSION

Here, we identify the mechanism of action of a small molecule inhibitor of cyclin proteolysis discovered in a phenotypic screen in *Xenopus* extract (Verma et al., 2004). TAME binds to the APC and displaces the IR tail of Cdc20 or Cdh1, preventing efficient APC activation. In human cells, proTAME treatment causes arrest in metaphase without perturbing the mitotic spindle. Despite development of normal kinetochore tension that should silence the SAC, the SAC is required for proTAME to induce mitotic arrest. Similar results were obtained using a proteasome inhibitor. We propose that kinetochore-dependent SAC signaling persists at a low rate in metaphase, and is inactivated by residual APC-dependent proteolysis, creating a positive feedback loop between the APC and the SAC (Figure 8D). The ability of low doses of proTAME or MG132 to induce metaphase arrest is strongly enhanced by this feedback loop, enabling mitotic arrest to be achieved at drug concentrations below those necessary to fully inhibit the APC or the proteasome.

TAME Interferes with IR-Tail-Dependent APC Activation

Our findings indicate that TAME prevents APC activation by perturbing the binding of the IR-tail of Cdc20 and Cdh1 to the APC. The importance of the IR motif in promoting Cdh1 association with yeast and human APC is well established (Burton et al., 2005; Kraft et al., 2005; Matyskiela and Morgan, 2009; Vodermaier et al., 2003). However, the role of the Cdc20 IR motif is less clear, because the Cdc20 IR tail is not essential in budding yeast (Thornton et al., 2008), and a Cdc20ΔIR mutant can support APC-dependent degradation of Nek2A in *Xenopus* extract (Kimata et al., 2008). Our data show that the IR motif of Cdc20 indeed contributes significantly to APC-association in vitro, as Cdc20ΔIR binds the APC with lower affinity than the wild-type protein, and TAME competes with wild-type Cdc20 for APC association. Moreover, TAME induces significant dissociation of Cdc20 from the APC in *Xenopus* extract, and proTAME can antagonize Cdc20 binding in human cells if the SAC is inactivated. Functionally, TAME stabilizes APC substrates in *Xenopus* extract and proTAME inhibits both Cdc20 and Cdh1-dependent degradation in HeLa cells. Taken together, these data show that proper engagement of the IR motif of Cdc20 or Cdh1 is critical for APC activation.

TAME Exploits a Positive Feedback Loop between the SAC and the APC

We found that proTAME-induced mitotic arrest requires sustained SAC activity. This finding was unexpected, because proTAME-treated cells arrest in metaphase with kinetochores that develop normal tension, a condition that should inactivate the SAC. In principle, the requirement for the SAC in the proTAME arrest could be explained in one of two ways. First, proTAME treatment could produce defects in microtubule-kinetochore interactions that generate an abnormally high degree of checkpoint signal compared with normal metaphase kinetochores. Alternatively, proTAME may hamper SAC inactivation, despite normal microtubule-kinetochore interactions. We favor the latter model because the degree of checkpoint dependence far exceeds the degree of kinetochore-microtubule perturbation that we observe.

Defects in microtubule-kinetochore attachment could arise from an off-target effect of TAME on microtubules, or be a consequence of specific APC inhibition. We found that knockdown of Cdc27 or UbcH10 each produced a mitotic exit delay that was SAC dependent. Furthermore, treatment of cells with a proteasome inhibitor yielded a SAC-dependent mitotic arrest, consistent with a recent study showing that MG132-treated mitotic cells show persistent Mad2-Cdc20 interaction (Visconti et al., 2010), and work in *Schizosaccharomyces pombe* showing that Mad2 and Mad3 remain APC-bound in proteasome mutants (Ohi et al., 2007). Together these findings suggest that if defective microtubule-kinetochore interactions are indeed present in proTAME-treated cells, they are likely to result from specific inhibition of APC-dependent proteolysis rather than from nonspecific effects of proTAME on microtubules.

If defective microtubule-kinetochore interactions exist in proTAME-treated cells, they must be subtle. Cells treated with 12 μM proTAME arrest in mitosis until they die, yet form a normal-appearing metaphase plate and develop normal kinetochore tension. Furthermore, cells treated with 12 μM proTAME undergo a normal-appearing anaphase when the SAC is inactivated, indicating that the mitotic spindle functions properly in the presence of proTAME. The only change in chromosome behavior caused by this dose of proTAME is a slight delay in chromosome congression. A lower dose of proTAME (3 μM) causes no delay in chromosome congression, yet still extends mitotic duration to 5 hr. Although we cannot completely rule out subtle defects in microtubule-kinetochore interactions in proTAME-treated cells, we believe such defects are not of sufficient magnitude to explain the strong dependence of the proTAME arrest on the SAC.

The alternative explanation for the SAC dependence of the proTAME arrest is that APC-dependent ubiquitination or proteolysis is required to inactivate the SAC. Such mutual antagonism between the APC and the SAC is predicted to create a positive feedback loop that would amplify the inhibitory effects of proTAME or a proteasome inhibitor in a SAC-dependent manner. This is what we observed. If the SAC is inactivated by Mad2 depletion, 12 μM proTAME extends mitotic duration by only 72 min, indicating that this dose only partially inhibits APC activation (consistent with the measured IC_{50} of 12 μM in *Xenopus* extract). However, when the same dose of proTAME is used in cells with an intact SAC, proTAME extends mitotic duration by 23 hr, indicating that the effect of proTAME is greatly amplified by the SAC. This degree of amplification cannot be explained by the mild effect of proTAME on chromosome congression, because a dose of nocodazole (10 nM) that causes a similar delay in chromosome congression extends mitotic duration by only 20 min in SAC-proficient cells. Because we obtained similar results with a proteasome inhibitor, we believe this amplification is best explained by a requirement for APC-dependent proteolysis to inactivate the SAC.

It is unclear which APC substrates play the most important role in mediating the mutual antagonism between the APC and the SAC. APC-dependent ubiquitination of Cdc20 has been proposed to release the APC from the inhibitory effects of the SAC (Reddy et al., 2007; Stegmeier et al., 2007). However, this process does not require proteasome activity in cell lysates (Reddy et al., 2007), and others argue that Cdc20 ubiquitination targets Cdc20 for proteasomal degradation in a manner that sustains the SAC (Ge et al., 2009; Nilsson et al., 2008). Alternatively, many SAC proteins are APC substrates and may need to be degraded to inactivate the SAC. Consistent with this possibility, expression of a stable BubR1 mutant induces a mitotic arrest (Choi et al., 2009). Another candidate is cyclin B1, because it is degraded prior to anaphase (Clute and Pines, 1999) and cyclin-dependent kinase activity is required to maintain the SAC (Chung and Chen, 2003; D'Angiolella et al., 2003). Other SAC proteins, including Mps1, Bub1, and Aurora B are also APC substrates, but their bulk population is not degraded until after anaphase (Palframan et al., 2006; Qi and Yu, 2007; Stewart and Fang, 2005). It is possible that degradation of these proteins prior to anaphase is masked by their resynthesis. The mutual antagonism between the APC and the SAC may reflect a system-level behavior that is regulated by small changes in the abundance of multiple SAC proteins prior to anaphase. If so, confirmation of our model will require quantitative measurements of the relative rates of synthesis and degradation of APC substrates that regulate SAC activity.

Our results indicate that it is possible to induce mitotic arrest without fully inhibiting the APC or the proteasome pharmacologically. This result was unexpected, because RNAi-based experiments indicated that Cdc20 must be reduced to very low levels to induce mitotic arrest (Wolthuis et al., 2008). Unlike the proTAME-induced arrest, the mitotic arrest induced by Cdc20 knockdown does not depend on the SAC (Huang et al., 2009). One possible explanation for the lack of SAC dependence in the context of Cdc20 depletion is that Cdc20 is the target of the SAC (Yu, 2007). Therefore, when Cdc20 levels are reduced, the SAC is no longer required to inhibit Cdc20 function. In contrast, other methods of perturbing APC function, including knockdown of core APC subunits or the E2 enzyme UbcH10, or proTAME treatment, all produce an arrest that is SAC dependent. This is likely a consequence of the fact that Cdc20 remains present under each of these conditions.

A Model for Regulation of Mitotic Exit

Based on our findings, we propose the following model (Figure 8D). A positive feedback loop between the SAC and the APC has the potential to adopt one of two stable states: high SAC activity (mitotic arrest) or high APC activity (mitotic exit). During normal division, it is important that cells do not become

permanently arrested in mitosis. We propose that the SAC does not fully inhibit the APC during mitosis because residual APC activity must be preserved to prevent cells from becoming locked in mitosis. This residual APC activity may explain why cyclin B1 is degraded prior to the initiation of anaphase (Clute and Pines, 1999) and during prolonged SAC-dependent mitotic arrest (Brito and Rieder, 2006; Gascoigne and Taylor, 2008; Huang et al., 2009; Nilsson et al., 2008). To remain in mitosis for a prolonged period, a cell may need to continue to resynthesize APC substrates that are degraded by residual APC-dependent proteolysis.

During normal mitosis, the development of kinetochore tension reduces the rate of SAC activation, but SAC activation is unlikely to be completely suppressed during metaphase. Anaphase is triggered when the rate of SAC activation falls below the rate at which APC-dependent proteolysis inactivates the SAC, tipping the feedback loop toward rapid APC activation and mitotic exit. The timing of anaphase initiation therefore depends not only on how kinetochore attachment controls SAC activation, but also on the level of residual APC activity.

During nocodazole or taxol treatment, the rate of SAC activation remains above the rate at which the APC inactivates the SAC, tipping the loop in the direction of APC inhibition, thereby preventing mitotic exit. Because APC-dependent proteolysis is not fully inhibited by the SAC, mitotic arrest is dependent on protein synthesis to resupply APC substrates. If the rate of protein synthesis is not sufficient, the rate of SAC signal production will fall below the rate at which it is inactivated by the APC, leading to rapid APC activation and mitotic slippage. Therefore, the rate of protein synthesis in mitosis may be an important determinant of the duration of mitotic arrest in cells treated with microtubule inhibitors.

In contrast to microtubule inhibitors, proTAME and MG132 induce mitotic arrest by inhibiting residual APC-dependent proteolysis rather than by stimulating SAC activation. The rate of SAC signal production by kinetochores may decline normally in proTAME- or MG132-treated cells because kinetochores develop proper tension. However, because the rate of residual APC-dependent proteolysis is lowered by proTAME or MG132, the rate of SAC signal production cannot fall below the rate at which it is inactivated by APC-dependent proteolysis, leading to mitotic arrest. The strong hesperadin sensitivity of both proTAME and MG132-induced arrests indicates the importance of metaphase kinetochores in generating a SAC signal to sustain mitotic arrest. Compared with microtubule inhibitors, this mechanism of mitotic arrest shows reduced dependence on protein synthesis because the rate of residual APC activity is lower in proTAME and MG132-treated cells, yielding a lower requirement for protein synthesis to replenish APC substrates.

An Opportunity for Antimitotic Cancer Therapy

Our study has identified a potential explanation for the variability in cellular responses to microtubule inhibitors that could limit their therapeutic effectiveness. Because the SAC does not completely inhibit the APC, mitotic arrest induced by microtubule inhibition depends on protein synthesis. As a result, variation in the rates of protein synthesis among cells may be one factor that explains the highly variable response of cells to microtubule inhibitors. In contrast, cells treated with an APC inhibitor may be less prone to mitotic slippage because residual APC activity is inhibited. APC inhibitors may therefore be more effective in promoting mitotic arrest, inducing a greater proapoptotic effect. Furthermore, low doses of an APC inhibitor may be useful in combination with microtubule inhibitors to sustain mitotic arrest and enhance cell death.

EXPERIMENTAL PROCEDURES

A list of reagents, methods of synthesis of proTAME and additional experimental procedures are provided in the Supplemental Information.

^{3}H-TAME Binding Assay

^{3}H-TAME (200 nM; 15 Ci/mmol) was added to 100 µl interphase *Xenopus* extract or HeLa cell lysate. APC was immunoprecipitated with Cdc27 antibody (Santa Cruz, AF3.1) coupled to affiprep beads (Bio-Rad) as previously described (Kirkpatrick et al., 2006). The beads were washed with XB and radioactivity measured by scintillation counting. Alternatively, ^{3}H-TAME was added and Cdc27 immunoprecipitation was performed after one or two rounds of APC immunodepletion. Specific binding was calculated as the difference between counts associated with Cdc27 antibody beads compared with beads lacking antibody (mock IP).

APC Isolation by IR Peptide or C-Box Fragment and Crosslinking

A cysteine-containing 20 amino acid peptide derived from the C terminus of Cdh1, or a control peptide lacking the C-terminal isoleucine and arginine residues, was reduced with TCEP at RT for 15 min and coupled to Ultralink iodoacetyl resin (Pierce). Ten microliters of resin was mixed with 100 µl interphase *Xenopus* egg extract and incubated on a rotator for 30 min at 4°C. The resin was then washed with XB (100 mM KCl, 0.1 mM $CaCl_2$, 1 mM $MgCl_2$, and 10 mM HEPES [pH 7.7]) and bound Cdc27 was analyzed by immunoblot. To investigate the effect of TAME on C-box interactions, a GST fusion protein containing the N-terminal 159 residues of *Xenopus* Cdc20, or the same protein lacking the C-box, were expressed and purified as described previously (Kimata et al., 2008). The proteins (10 µg) were preloaded on 5 µl Glutathione-Sepharose 4B resin (GE Healthcare) and incubated with cyclin B1Δ90-arrested mitotic *Xenopus* extract at RT for 30 min in the presence of 1% DMSO, 200 µM TAME, or 200 µM AAME. The resin was then washed with XB and bound Cdc27 was analyzed by immunoblot. For crosslinking studies, the Cdh1-derived C-terminal peptide was conjugated to Profound Mts-Atf-Biotin label transfer reagent (Pierce) and crosslinked as described in the supplemental experimental procedures.

APC-Cdc20/Cdh1 Association Assay

APC was immunoprecipitated from cyclin B1Δ90-arrested mitotic *Xenopus* extract or interphase extract supplemented with 0.5 µg/ml recombinant Cdh1 as previously described (Kirkpatrick et al., 2006). Compounds were added to mitotic extract immediately before immunoprecipitating the APC. Interphase extracts were preincubated with compounds for 30 min before adding recombinant Cdh1 and immunoprecipitating the APC. The beads were washed with XB high salt (XB with 500 mM KCl) and then XB, and bound Cdc27 and Cdc20/Cdh1 were analyzed by immunoblot. Alternatively, Cdc20 was expressed using an in vitro coupled transcription/translation reticulocyte lysate system following the manufacturer's instruction (Promega L1170). The lysate was diluted with XB so that the concentration of Cdc20 was approximately equal to that of the endogenous Cdc20 in *Xenopus* extract. APC was immunoprecipitated from mitotic extract as described above and the beads were washed with XB high salt and XB. For each binding assay, 5 µl beads were mixed with 50 µl diluted lysate plus 1 µM okadaic acid, 0.05% IGEPAL CA-630 and various competitors as indicated for 30 min with constant shaking. The beads were then washed with XB + 0.05% IGEPAL CA-630 and bound Cdc27 and Cdc20 were analyzed by immunoblot.

SUPPLEMENTAL INFORMATION

Supplemental Information includes Experimental Procedures, references, seven figures, one table, and six movies and can be found online at doi:10.1016/j.ccr.2010.08.010.

ACKNOWLEDGMENTS

We thank Mike Aguilar and Steve Gygi for assistance with mass spectrometry and Jonathan Iaconelli for technical assistance. We thank Daniel Finley, David Pellman, and Tom Rapoport for comments on the manuscript. This work was supported by NIH Grant GM66492 to R.W.K. and a grant from the Stewart Trust. R.W.K. is a member of the Dana Farber-Harvard Cancer Center Breast Cancer SPORE, supported by NIH grant CA089393. K.L.P. was supported by fellowship GM085923. Immunofluorescence microscopy data for this study were acquired in the Nikon Imaging Center at Harvard Medical School. The authors declare no financial conflict of interest.

Received: April 9, 2010
Revised: July 1, 2010
Accepted: August 10, 2010
Published: October 18, 2010

REFERENCES

Bekier, M.E., Fischbach, R., Lee, J., and Taylor, W.R. (2009). Length of mitotic arrest induced by microtubule-stabilizing drugs determines cell death after mitotic exit. Mol. Cancer Ther. *8*, 1646–1654.

Biggins, S., and Murray, A.W. (2001). The budding yeast protein kinase Ipl1/Aurora allows the absence of tension to activate the spindle checkpoint. Genes Dev. *15*, 3118–3129.

Brito, D.A., and Rieder, C.L. (2006). Mitotic checkpoint slippage in humans occurs via cyclin B destruction in the presence of an active checkpoint. Curr. Biol. *16*, 1194–1200.

Brito, D.A., Yang, Z., and Rieder, C.L. (2008). Microtubules do not promote mitotic slippage when the spindle assembly checkpoint cannot be satisfied. J. Cell Biol. *182*, 623–629.

Burton, J.L., Tsakraklides, V., and Solomon, M.J. (2005). Assembly of an APC-Cdh1-substrate complex is stimulated by engagement of a destruction box. Mol. Cell *18*, 533–542.

Cheeseman, I.M., Chappie, J.S., Wilson-Kubalek, E.M., and Desai, A. (2006). The conserved KMN network constitutes the core microtubule-binding site of the kinetochore. Cell *127*, 983–997.

Choi, E., Choe, H., Min, J., Choi, J.Y., Kim, J., and Lee, H. (2009). BubR1 acetylation at prometaphase is required for modulating APC/C activity and timing of mitosis. EMBO J. *28*, 2077–2089.

Chung, E., and Chen, R.H. (2003). Phosphorylation of Cdc20 is required for its inhibition by the spindle checkpoint. Nat. Cell Biol. *5*, 748–753.

Clute, P., and Pines, J. (1999). Temporal and spatial control of cyclin B1 destruction in metaphase. Nat. Cell Biol. *1*, 82–87.

D'Angiolella, V., Mari, C., Nocera, D., Rametti, L., and Grieco, D. (2003). The spindle checkpoint requires cyclin-dependent kinase activity. Genes Dev. *17*, 2520–2525.

DeLuca, J.G., Gall, W.E., Ciferri, C., Cimini, D., Musacchio, A., and Salmon, E.D. (2006). Kinetochore microtubule dynamics and attachment stability are regulated by Hec1. Cell *127*, 969–982.

den Elzen, N., and Pines, J. (2001). Cyclin A is destroyed in prometaphase and can delay chromosome alignment and anaphase. J. Cell Biol. *153*, 121–136.

Engelbert, D., Schnerch, D., Baumgarten, A., and Wasch, R. (2008). The ubiquitin ligase APC(Cdh1) is required to maintain genome integrity in primary human cells. Oncogene *27*, 907–917.

Famulski, J.K., and Chan, G.K. (2007). Aurora B kinase-dependent recruitment of hZW10 and hROD to tensionless kinetochores. Curr. Biol. *17*, 2143–2149.

Gascoigne, K.E., and Taylor, S.S. (2008). Cancer cells display profound intra- and interline variation following prolonged exposure to antimitotic drugs. Cancer Cell *14*, 111–122.

Ge, S., Skaar, J.R., and Pagano, M. (2009). APC/C- and Mad2-mediated degradation of Cdc20 during spindle checkpoint activation. Cell Cycle *8*, 167–171.

Hauf, S., Cole, R.W., LaTerra, S., Zimmer, C., Schnapp, G., Walter, R., Heckel, A., van Meel, J., Rieder, C.L., and Peters, J.M. (2003). The small molecule Hesperadin reveals a role for Aurora B in correcting kinetochore-microtubule attachment and in maintaining the spindle assembly checkpoint. J. Cell Biol. *161*, 281–294.

Hayes, M.J., Kimata, Y., Wattam, S.L., Lindon, C., Mao, G., Yamano, H., and Fry, A.M. (2006). Early mitotic degradation of Nek2A depends on Cdc20-independent interaction with the APC/C. Nat. Cell Biol. *8*, 607–614.

Hsu, J.Y., Reimann, J.D., Sorensen, C.S., Lukas, J., and Jackson, P.K. (2002). E2F-dependent accumulation of hEmi1 regulates S phase entry by inhibiting APC(Cdh1). Nat. Cell Biol. *4*, 358–366.

Huang, H.C., Shi, J., Orth, J.D., and Mitchison, T.J. (2009). Evidence that mitotic exit is a better cancer therapeutic target than spindle assembly. Cancer Cell *16*, 347–358.

Kimata, Y., Baxter, J.E., Fry, A.M., and Yamano, H. (2008). A role for the Fizzy/Cdc20 family of proteins in activation of the APC/C distinct from substrate recruitment. Mol. Cell *32*, 576–583.

Kirkpatrick, D.S., Hathaway, N.A., Hanna, J., Elsasser, S., Rush, J., Finley, D., King, R.W., and Gygi, S.P. (2006). Quantitative analysis of in vitro ubiquitinated cyclin B1 reveals complex chain topology. Nat. Cell Biol. *8*, 700–710.

Kraft, C., Vodermaier, H.C., Maurer-Stroh, S., Eisenhaber, F., and Peters, J.M. (2005). The WD40 propeller domain of Cdh1 functions as a destruction box receptor for APC/C substrates. Mol. Cell *18*, 543–553.

Matyskiela, M.E., and Morgan, D.O. (2009). Analysis of activator-binding sites on the APC/C supports a cooperative substrate-binding mechanism. Mol. Cell *34*, 68–80.

Minshull, J., Sun, H., Tonks, N.K., and Murray, A.W. (1994). A MAP kinase-dependent spindle assembly checkpoint in Xenopus egg extracts. Cell *79*, 475–486.

Montero, A., Fossella, F., Hortobagyi, G., and Valero, V. (2005). Docetaxel for treatment of solid tumours: a systematic review of clinical data. Lancet Oncol. *6*, 229–239.

Musacchio, A., and Salmon, E.D. (2007). The spindle-assembly checkpoint in space and time. Nat. Rev. Mol. Cell Biol. *8*, 379–393.

Nilsson, J., Yekezare, M., Minshull, J., and Pines, J. (2008). The APC/C maintains the spindle assembly checkpoint by targeting Cdc20 for destruction. Nat. Cell Biol. *10*, 1411–1420.

Ohi, M.D., Feoktistova, A., Ren, L., Yip, C., Cheng, Y., Chen, J.S., Yoon, H.J., Wall, J.S., Huang, Z., Penczek, P.A., et al. (2007). Structural organization of the anaphase-promoting complex bound to the mitotic activator Slp1. Mol. Cell *28*, 871–885.

Orth, J.D., Tang, Y., Shi, J., Loy, C.T., Amendt, C., Wilm, C., Zenke, F.T., and Mitchison, T.J. (2008). Quantitative live imaging of cancer and normal cells treated with Kinesin-5 inhibitors indicates significant differences in phenotypic responses and cell fate. Mol. Cancer Ther. *7*, 3480–3489.

Palframan, W.J., Meehl, J.B., Jaspersen, S.L., Winey, M., and Murray, A.W. (2006). Anaphase inactivation of the spindle checkpoint. Science *313*, 680–684.

Peters, J.M. (2006). The anaphase promoting complex/cyclosome: a machine designed to destroy. Nat. Rev. Mol. Cell Biol. *7*, 644–656.

Qi, W., and Yu, H. (2007). KEN-box-dependent degradation of the Bub1 spindle checkpoint kinase by the anaphase-promoting complex/cyclosome. J. Biol. Chem. *282*, 3672–3679.

Reddy, S.K., Rape, M., Margansky, W.A., and Kirschner, M.W. (2007). Ubiquitination by the anaphase-promoting complex drives spindle checkpoint inactivation. Nature *446*, 921–925.

Schwab, M., Neutzner, M., Mocker, D., and Seufert, W. (2001). Yeast Hct1 recognizes the mitotic cyclin Clb2 and other substrates of the ubiquitin ligase APC. EMBO J. *20*, 5165–5175.

Shi, J., Orth, J.D., and Mitchison, T. (2008). Cell type variation in responses to antimitotic drugs that target microtubules and kinesin-5. Cancer Res. *68*, 3269–3276.

Sigl, R., Wandke, C., Rauch, V., Kirk, J., Hunt, T., and Geley, S. (2009). Loss of the mammalian APC/C activator FZR1 shortens G1 and lengthens S phase but has little effect on exit from mitosis. J. Cell Sci. *122*, 4208–4217.

Stegmeier, F., Rape, M., Draviam, V.M., Nalepa, G., Sowa, M.E., Ang, X.L., McDonald, E.R., 3rd, Li, M.Z., Hannon, G.J., Sorger, P.K., et al. (2007). Anaphase initiation is regulated by antagonistic ubiquitination and deubiquitination activities. Nature *446*, 876–881.

Stewart, S., and Fang, G. (2005). Destruction box-dependent degradation of aurora B is mediated by the anaphase-promoting complex/cyclosome and Cdh1. Cancer Res. *65*, 8730–8735.

Thornton, B.R., Ng, T.M., Matyskiela, M.E., Carroll, C.W., Morgan, D.O., and Toczyski, D.P. (2006). An architectural map of the anaphase-promoting complex. Genes Dev. *20*, 449–460.

Verma, R., Peters, N.R., D'Onofrio, M., Tochtrop, G.P., Sakamoto, K.M., Varadan, R., Zhang, M., Coffino, P., Fushman, D., Deshaies, R.J., and King, R.W. (2004). Ubistatins inhibit proteasome-dependent degradation by binding the ubiquitin chain. Science *306*, 117–120.

Visconti, R., Palazzo, L., and Grieco, D. (2010). Requirement for proteolysis in spindle assembly checkpoint silencing. Cell Cycle *9*, 564–569.

Vodermaier, H.C., Gieffers, C., Maurer-Stroh, S., Eisenhaber, F., and Peters, J.M. (2003). TPR subunits of the anaphase-promoting complex mediate binding to the activator protein CDH1. Curr. Biol. *13*, 1459–1468.

Welburn, J.P., Vleugel, M., Liu, D., Yates, J.R., 3rd, Lampson, M.A., Fukagawa, T., and Cheeseman, I.M. (2010). Aurora B phosphorylates spatially distinct targets to differentially regulate the kinetochore-microtubule interface. Mol. Cell *38*, 383–392.

Wojcik, C., Schroeter, D., Stoehr, M., Wilk, S., and Paweletz, N. (1996). An inhibitor of the chymotrypsin-like activity of the multicatalytic proteinase complex (20S proteasome) induces arrest in G2-phase and metaphase in HeLa cells. Eur. J. Cell Biol. *70*, 172–178.

Wolthuis, R., Clay-Farrace, L., van Zon, W., Yekezare, M., Koop, L., Ogink, J., Medema, R., and Pines, J. (2008). Cdc20 and Cks direct the spindle checkpoint-independent destruction of cyclin A. Mol. Cell *30*, 290–302.

Yu, H. (2007). Cdc20: a WD40 activator for a cell cycle degradation machine. Mol. Cell *27*, 3–16.

Cancer Cell, Volume *18*

Supplemental Information

Pharmacologic Inhibition of the Anaphase-Promoting Complex Induces A Spindle Checkpoint-Dependent Mitotic Arrest in the Absence of Spindle Damage

Xing Zeng, Frederic Sigoillot, Shantanu Gaur, Sungwoon Choi, Kathleen L. Pfaff, Dong-Chan Oh, Nathaniel Hathaway, Nevena Dimova, Gregory D. Cuny, and Randall W. King

Supplemental Movie Legends

Movie S1: Chromosome congression of untreated HeLa H2B-GFP cell. Double thymidine synchronized HeLa H2B-GFP cells were imaged at 3 min interval with a 40x objective. The H2B-GFP channel of a representative mitotic cell is shown here.

Movie S2: Nocodazole (10 nM) treatment induces a delay in chromosome congression. Double thymidine synchronized HeLa H2B-GFP cells were treated with 10 nM nocodazole at 8 h after thymidine release and imaged at 3 min interval with a 40x objective. The H2B-GFP channel of a representative mitotic cell is shown here.

Movie S3: Nocodazole (10 nM) treatment induces bending of the metaphase plate. Double thymidine synchronized HeLa H2B-GFP cells were treated with 10 nM nocodazole at 8 h after thymidine release and imaged at 3 min interval with a 40x objective. The H2B-GFP channel of a representative mitotic cell is shown here.

Movie S4: ProTAME (12 μM) treatment induces a delay in chromosome congression but does not perturb the metaphase plate. Double thymidine synchronized HeLa H2B-GFP cells were treated with 12 μM proTAME at 8 h after thymidine release and imaged at 3 min interval with a 40x objective. The H2B-GFP channel of a representative mitotic cell is shown here.

Movie S5: Mad2-knockdown cell initiates anaphase before full chromosome congression. Asynchronous HeLa H2B-GFP cells were transfected with Mad2 siRNA 24 h prior to imaging. Cells were imaged at 3 min interval with a 40x objective. A representative mitotic cell is shown here. Red: DIC. Green: H2B-GFP.

Movie S6: ProTAME rescues the mitotic defect in cells lacking Mad2 by delaying anaphase onset to allow time for chromosome congression. Asynchronous HeLa H2B-GFP cells were transfected with Mad2 siRNA 24 h prior to imaging. Cells were treated with 12 μM proTAME and imaged at 3 min interval with a 40x objective. A representative mitotic cell is shown here. Red: DIC. Green: H2B-GFP.

Supplemental Experimental Procedures

Preparation of *Xenopus* egg extract

Interphase *Xenopus* egg extract was prepared from eggs laid overnight according to the protocol of Murray (Murray, 1991) with the exception that eggs were activated with 2 μg/ml calcium ionophore (A23187, free acid form, Calbiochem) for 30 minutes prior to the crushing spin. Extract was frozen in liquid nitrogen and stored at -80 ºC. To make mitotic extract, MBP-cyclin B1Δ90 was added to interphase extract at 20 μg/ml and incubated at 22 ºC for 30 min.

Chemicals

Tosyl-L-arginine methyl ester (T4626), tosyl-L-arginine (S365157), tosyl-L-argininamide (T4501), benzoyl-L-arginine methyl ester (B1007), benzoyl-L-argininamide (B4375) and tosyl-L-lysine methyl ester (T5012) were from Sigma. Acetyl-L-arginine methyl ester was from BACHEM (E-1030). Cdh1 C-terminal peptide and the ΔIR control peptide (sequence: CFSKTRSTKESVSVLNLFTRIR and CFSKTRSTKESVSVLNLFTR) were synthesized by the core facility of Tufts medical school. ^{3}H-TAME (15 Ci/mmol, >97% radiochemical purity) was synthesized by AmBios Labs (Newington, CT). Hesperadin was a gift from Boehringer Ingelheim. MG132 was from Sigma (C2211). Okadaic acid was from MP Biomedicals (IC15897425). Cycloheximide was from Calbiochem (239764).

Antibodies

Cdc27 antibody for APC immunoprecipitation was from Santa Cruz (sc-9972, AF3.1). Cdc27 antibody for Western blot was from BD Transduction Laboratories (610454). Cyclin B1 antibody was from NeoMarker (RB-008-P). *Xenopus* Cdc20 antibody was from Abcam (ab18217). Human Cdc20 antibody was from Santa Cruz (sc-8358 H-175). Cdh1 antibody was from Santa Cruz (sc-19398). Streptavidin-HRP was from Invitrogen (SNN1004). Securin antibody was from Abcam (ab3305). Cyclin A antibody was from Santa Cruz (sc H-432). Nek2 antibody was from BD Transduction Laboratories (610593). UbcH10 antibody was from Boston Biochem (A-650). Mad2 antibody was from Bethyl Laboratories (BL1461). GAPDH antibody was from Abcam (ab8245). Anti-α-tubulin-FITC was from Sigma (F2168). CREST antiserum was from Antibodies Incorporated (15-234). Goat anti-human-Alexa 568 was from Invitrogen (A21090). HA antibody was from Santa Cruz (sc-805, Y-11). Apc10 antibody was from Santa Cruz (sc-20989). BubR1 antibody was a kind gift from Frank Mckeon's lab at Harvard medical school.

Luciferase assay

A fusion of the N-terminal domain of cyclin B1 to luciferase (Verma et al., 2004) was added to mitotic extract at 3 μg/ml. The extract was incubated at 23 ºC and 3 μl samples were taken at 0, 30, 60, 90 and 120 min. The samples were mixed quickly with 30 μl of luciferin assay buffer (270 μM coenzyme A, 20 mM tricine, 3.67 mM $MgSO_4$, 0.1 mM

EDTA, 33.3 mM DTT, 530 μM ATP and 470 μM luciferin, pH 7.8) and the level of luminescence was measured on Wallac 1420 multilabel counter.

TAME induction of mitotic arrest in *Xenopus* egg extract

Human cyclin B1/cdc2 complex (MPF) was prepared by baculovirus expression and purification as described (Kirkpatrick et al., 2006), and added to interphase extract at 12.5 μg/ml supplemented with 1% DMSO, 200 μM TAME or 200 μM AAME. Extract samples were collected every 15 min following addition of MPF. Cdc27 and cyclin B1 levels were analyzed by Western blot.

***In vitro* ubiquitination assay**

For a single reaction, 5 μl protein A affiprep beads (Bio-Rad 156-0006) were washed with TBST (10 mM Tris, 150 mM NaCl and 0.01% Tween-20, pH 7.5) twice and incubated with 2 μg Cdc27 antibody for 75 min at 4 ºC. Beads were then washed with TBST twice and XB (100 mM KCl, 0.1 mM $CaCl_2$, 1 mM $MgCl_2$ and 10 mM HEPES, pH 7.7) twice before APC immunoprecipitation. For APC-Cdc20 reaction, MBP-cyclin B1Δ90 was added to interphase extract at 20 μg/ml and incubated at 22 ºC for 30 min before immunoprecipitation. To immunoprecipitate APC, 100 μl extract was incubated with 5 μl antibody beads at 4 ºC for 1 h. The beads were then washed with XB high salt (XB with 500 mM KCl) twice, XB twice and ubiquitin chain buffer (20 mM Tris, 100 mM KCl, 2 mM ATP and 2.5 mM $MgCl_2$, pH 7.7) three times. A reaction mixture containing 200

μg/ml MBP-E1, 66 μg/ml His_6-Ubc4, 25 μg/ml MPF, 1 mg/ml ubiquitin (Sigma) in ubiquitin chain buffer was prepared and 5 μl of this was added to 5 μl antibody beads. Beads were incubated at 22 ºC on a Eppendorf Thermomixer with shaking at 1500 rpm for 60 min and the whole mixture was then boiled with 10 μl sample buffer for 5 min. Ubiquitinated cyclin B1 was visualized by cyclin B1 immunoblot.

Degradation of ^{35}S labeled pre-ubiquitinated cyclin B1

Human ^{35}S-cyclin B1/cdc2 complex was prepared by metabolic labeling of SF9 cultures expressing cyclin B1. The labeled lysate containing cyclin B1 was mixed with an unlabeled lysate from cells expressing cdc2, followed by purification of the cyclin B1/cdc2 complex as described above. The labeled complex was ubiquitinated in a reconstituted APC reaction as described above. Interphase *Xenopus* extract was pre-incubated with 200 μM TAME or control compounds for 22 ºC for 30 min. Pre-incubation was performed in the presence of 100ug/ml cycloheximide to prevent re-incorporation of free labeled amino acid and 1/20th volume of energy mix (150 mM creatine phosphate, 20 mM ATP, 2 mM EGTA and 20 mM $MgCl_2$, pH 7.7). 90 μl of extract was then added to 15 μl of labeled cyclin B1-ubiquitin conjugates and incubated at 22°C for the indicated amount of time. Reactions were stopped by the addition of an equal volume (105ul) of chilled 2% perchloric acid. The mixture was incubated on ice for 30 min and centrifuged at 14,000 rpm for 10 min at 4 ºC. 168 μl of supernatant was mixed with 20 μl 2 M Tris base and 6 ml ultima gold scintillation fluid (Perkin Elmer).

Samples were mixed well and counted with a scintillation counter.

Covalent coupling of Cdc27 antibody to protein A beads

Protein A affiprep beads were coupled with Cdc27 antibody as described above. After coupling, the beads were washed with TBST for 10 min followed by two additional quick washes with TBST. Dimethyl pimelimidate (DMP, PIERCE, 21666) was freshly dissolved in 100 mM sodium tetraborate decahydrate, pH 9.0 at 20 mM. The beads were mixed with ten beads volume of DMP solution and incubated on a rotating wheel for 45 min in the dark at room temperature. The beads were then washed twice quickly with 200 mM Tris, pH 8.0 twice, followed by a final 1 h wash. Beads were then washed twice in TBST and twice in XB prior to APC immunoprecipitation.

IR peptide immobilization on iodoacetyl resin

A 20-aa Cdh1 C-terminal peptide with one cysteine residue added at the N-terminus was synthesized along with a control peptide lacking the C-terminal IR residues. The lyophilized peptide was re-dissolved at 400 μM in 100 mM HEPES, 5 mM EDTA, pH 7.9. To reduce the disulfide bonds, TCEP (Sigma C4706) was dissolved at 10 mM in 100 mM HEPES, 5 mM EDTA, pH 7.9 and added to the peptide solution at a final concentration of 200 μM (stoichiometric amount to reduce disulfide bonds). The peptide was reduced at room temperature for 15 min before mixing with Ultralink iodoacetyl resin (Pierce 53155) that was pre-equilibrated with 100 mM HEPES, 5 mM EDTA, pH

7.9. A ratio of 35 µl resin volume per 110 µl reduced peptide was used. For the negative control, freshly prepared 50 mM cysteine in 100 mM HEPES, 5 mM EDTA, pH 7.9 was used instead of the peptide. The coupling reaction was carried out at room temperature on a rotating wheel for 1 h and unreacted sites on the resin were blocked by further incubation with 50 mM cysteine for 30 min. The resin was then washed with 1 M NaCl followed by two washes with XB and stored at 4 ºC before APC pull down.

APC pull down by IR peptide resin

10 µl of resin coupled with IR peptide, ΔIR peptide or cysteine as described above was mixed with 100 µl interphase *Xenopus* egg extract and incubated on a rotating wheel for 30 min at 4 ºC. The resin was then washed twice with XB high salt and once with PBS. The resin was boiled with 10 µl sample buffer and the amount of Cdc27 was analyzed by immunoblot.

Conjugation of IR peptide with photoactive crosslinker

The IR and ΔIR peptides were reduced as described above. The photoactive crosslinker, Profound Mts-Atf-Biotin label transfer reagent (Pierce 33093), was dissolved at 40 mg/ml in DMSO. The crosslinker was added to the reduced peptide at a 1.1 molar excess and the reaction was left at room temperature in the dark for 1 h. The reaction mixture was centrifuged at 12,000 rpm for 1 min and the supernatant was loaded onto HPLC for purification. The purified conjugated peptide showed >99% purity on HPLC. The identity

of the conjugated peptide was confirmed by mass spectrometry.

Crosslinking assay

Purified conjugated IR or ΔIR peptide was diluted in XB to a final concentration of approximately 2 μM. The following additives were included when necessary: 10 μM of unconjugated IR peptide with the cysteine modified with N-ethyl maleimide to show competition with the conjugated peptide, 20 μM or 200 μM TAME to show inhibition of crosslinking, and 200 μM AAME as a negative control. APC was immunoprecipitated with protein A affiprep beads covalently crosslinked with Cdc27 antibody as described above. After washing, 5 μl aliquot of beads were mixed with 50 μl conjugated peptide and transferred to a 96-well polypropylene clear conical bottom plate. The plate was illuminated at a distance of 10 cm from a 300 watt long wavelength UV lamp for 3 min. The beads were then transferred back to 0.5 ml tubes and mixed with 10 μl sample buffer and boiled for 5 min. APC subunits that were crosslinked were analyzed by streptavidin-HRP blot. To confirm the nature of the crosslinked subunits, APC was immunoprecipitated from interphase extract as described above and run on the same gel of the crosslinked sample and coomassie stained. The bands were subjected to mass spectrometry analysis.

^{3}H-TAME binding assay in interphase extract

^{3}H-TAME (15 Ci/mmol) was added to interphase extract (100 μl) to a final concentration

of 200 nM, and subject to immunoprecipitation (4 ºC for 1.5 h) using 5 µl protein A affiprep beads coupled with Cdc27 antibody as described above. Protein A beads without Cdc27 antibody were used as a negative control to measure background level of binding (mock IP). The beads were washed quickly twice with XB high salt and twice with XB. The beads were then transferred to scintillation vials, mixed with scintillation fluid, and counted in a scintillation counter. Alternatively, the extract was subjected to one or two rounds of immunoprecipitation before the addition of ^{3}H-TAME. For competition assays, different concentrations of unlabeled TAME or other derivatives were added along with 200 nM ^{3}H-TAME into the extract. Specific binding under each condition was obtained by subtracting the value of mock IP.

^{3}H-TAME binding assay in HeLa cell lysate

Protein A affiprep beads coupled with Cdc27 antibody were prepared as described above. HeLa cells were harvested in lysis buffer (10mM potassium phosphate pH 7.5, 0.1mM EDTA, 0.5mM EGTA, 50mM β-glycerophosphate, 1mM sodium vanadate, 1mM DTT, 0.5% Triton X-100 and leupeptin, chymostatin and pepstatin each at 10 µg/ml). For 4,000,000 cells, 100 µl lysis buffer was used. The cell lysate was centrifuged at 10,000 rpm for 10 min to remove cell debris. ^{3}H-TAME (15 Ci/mmol) was added to cell lysate to a final concentration of 200 nM. For each aliquot of 5 µl beads, 100 µl lysate was used for APC immunoprecipitation at 4 ºC for 1 h. Protein A beads without Cdc27 antibody was used as a negative control to measure background level of binding (mock IP). The

beads were washed quickly with lysis buffer high salt (500 mM sodium chloride in addition to above components) twice and lysis buffer twice. The beads were then transferred to scintillation vials, mixed with scintillation fluid, and radioactivity measured by scintillation counting. Alternatively, the lysate was subjected to one or two rounds of immunoprecipitation before the addition of ^{3}H TAME. For competition assays, 10 μM unlabeled TAME or AAME was added along with 200 nM ^{3}H TAME into the lysate. Specific binding under each condition was obtained by subtracting the value of mock IP.

Synthesis of proTAME (14) and proAAME (15)

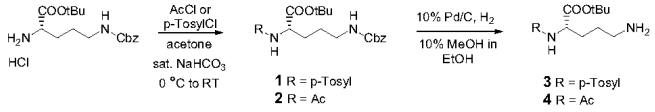

1 R = p-Tosyl
2 R = Ac

3 R = p-Tosyl
4 R = Ac

N^2-[(4-methylphenyl)sulfonyl]-N^5-[(phenylmethoxy)carbonyl]-L-ornithine 1,2,-dimethylethyl ester (1): A mixture of N^5-[(phenylmethoxy)carbonyl]-L-ornithine 1,2,-dimethylethyl ester HCl (718 mg, 2 mmol), acetone (15 mL) and sat. aq. $NaHCO_3$ (15 mL) was treated with *p*-toluenesulfonyl chloride (420mg, 2.2 mmole) in acetone (15 mL) at 0 ºC and then stirred at room temperature for 16 h. The mixture was diluted with EtOAc, washed with brine, dried over anhydrous sodium sulfate, filtered, concentrated *in vacuo* to afford an oil, which was purified by silica gel column chromatography using 40% EtOAc in hexane to give compound **1** (910mg, 95%): ^{1}H NMR (500 MHz, $CDCl_3$): δ1.23 (s, 9H), 1.56 – 1.65 (m, 3H), 1.73 – 1.77 (m, 1H), 2.39 (s, 3H), 3.21 (q, *J* = 6.0, 2H), 3.72 –

3.77 (m, 1H), 4.77 (br, 1H), 5.10 (s, 2H), 5.16 (br, 1H), 7.26 – 7.28 (m, 2H), 7.31 – 7.36 (m, 5H), 7.70 – 7.72 (m, 2H).

N^2-acetyl-N^5-[(phenylmethoxy)carbonyl]-L-ornithine 1,2,-dimethylethyl ester (2) was prepared in a manner similar as **1**, with acetyl chloride used in place of *p*-toluenesulfonyl chloride. ^{1}H NMR (500 MHz, $CDCl_3$): δ1.46 (s, 9H), 1.49 – 1.57 (m, 2H), 1.63 – 1.69 (m, 1H), 1.81 – 1.88 (m, 1H), 2.01 (s, 3H), 3.22 (q, J = 6.5, 2H), 4.47 – 4.51 (m, 1H), 4.94 (br, 1H), 5.09 (s, 2H), 6.11 (br d, J = 7.5, 1H), 7.30 – 7.36 (m, 5H).

N^2-[(4-methylphenyl)sulfonyl]- L-ornithine 1,2,-dimethylethyl ester (3): A mixture of **1** (500 mg, 1.05 mmole), methanol (1.5 mL), ethanol (15 mL) and 10% Pd-C (200 mg) was stirred under a hydrogen atmosphere at room temperature for 3 h. The mixture was filtered through a pad of Celite, concentrated *in vacuo* to give crude compound **3** (399mg, 99%). This material was stored in the freezer and then used without further purification.

N^2-acetyl- L-ornithine 1,2,-dimethylethyl ester (4) was prepared in a manner similar as **3**.

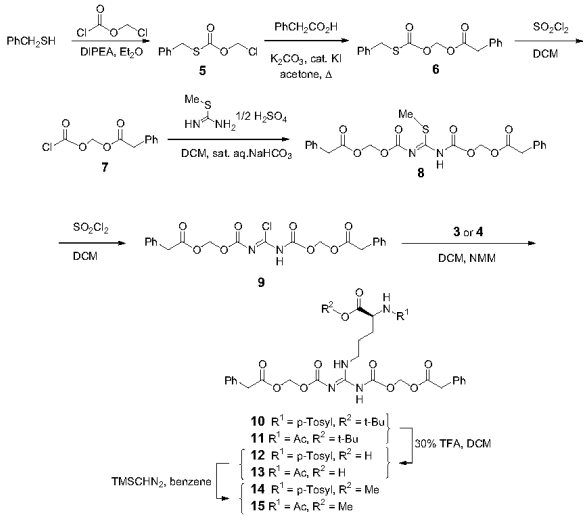

O-Chloromethyl S-(phenylmethyl) carbothioate (5): was prepared following a literature procedure (Folkmann, 1990).

[[(phenylmethylthio)carbonyl]oxy]methyl benzeneacetate (6): A mixture of **5** (6.327g, 29.2 mmol), phenylacetic acid (3.68g, 27 mmole), K_2CO_3 (3.74g, 27 mmole), and cat. KI in acetone (100 mL) was refluxed for 16 h. The mixture was diluted with EtOAc, washed with brine, dried over anhydrous sodium sulfate, filtered, concentrated *in vacuo* to afford an oil, which was purified by silica gel column chromatography with 5% EtOAc in hexane to give

1 (5.80g, 92%): ^{1}H NMR (500 MHz, $CDCl_3$): δ 3.68 (s, 4H), 4.12 (s, 4H), 5.82 (s, 4H), 7.26 – 7.33 (m, 10H).

[(chlorocarbonyl)oxy]methyl benzeneacetate (7): was prepared following a literature procedure (Folkmann, 1990).

3-(methylthio)-5,9-dioxo-10-phenyl-[(phenylacetyl)oxy]methyl 6,8-dioxa-2,4-diazadec-2-enoate (8): was prepared following a literature procedure (Saulnier, 1994). ^{1}H NMR (500 MHz, $CDCl_3$): δ 2.44 (s, 3H), 3.70 (s, 4H), 5.84 (s, 4H), 7.26 – 7.35 (m, 10H).

3-chloro-5,9-dioxo-10-phenyl-[(phenylacetyl)oxy]methyl 6,8-dioxa-2,4-diazadec-2-enoate (9): was prepared following a literature procedure (Saulnier, 1994).

1,2,-dimethylethyl (S)-2-[(4-methylphenyl)sulfonyl]amino-4-[[bis[[[[(phenylacetyl)oxy]methoxy]carbonyl]amino]methylene]amino]pentanoate (10) and 1,2,-dimethylethyl (S)-2-(acetyl)amino-4-[[bis[[[[(phenylacetyl)oxy]methoxy]carbonyl]amino]methylene]amino]pentanoate (11): were prepared following a literature procedure (Saulnier, 1994).

10: ^{1}H NMR (500 MHz, $CDCl_3$): δ 1.23 (s, 9H), 1.57 – 1.62 (m, 1H), 1.71 – 1.77 (m, 3H), 2.39 (s, 3H), 3.45 (q, J = 6.5, 2H), 3.68 (s, 2H), 3.71 (s, 2H), 3.77 – 3.79 (m, 1H), 5.23 (d, J = 8.5 Hz, 1H), 5.80 (s, 2H), 5.82 (s, 2H), 7.24 – 7.36 (m, 12H), 7.71 – 7.73 (m, 2H), 8.29 (br t, J = 5.3 Hz, 1H), 11.61 (br s, 1H).

11: ^{1}H NMR (500 MHz, $CDCl_3$): δ 1.46 (s, 9H), 1.56 – 1.71 (m, 3H), 1.86 – 1.90 (m, 1H), 2.02 (s, 3H), 3.42 – 3.48 (m, 2H), 3.67 (s, 2H), 3.71 (s, 2H), 4.51 – 4.54 (m, 1H), 5.80 (s, 2H), 5.82 (s, 2H), 6.19 (d, J = 7.5 Hz, 1H), 7.26 – 7.36 (m, 10H), 8.31 (br t, J = 5.5 Hz, 1H), 11.61 (br s, 1H).

(S)-2-[(4-methylphenyl)sulfonyl]amino-4-[[bis[[[[(phenylacetyl)oxy]methoxy]carbonyl]amino]methylene]amino]pentanoic acid (12) and (S)-2-(acetyl)amino-4-[[bis[[[[(phenylacetyl)oxy]methoxy]carbonyl]amino]methylene]amino]pentanoic acid (13) : were prepared following a literature procedure (Bryan, 1977). Briefly, each ester (**10** and **11**) was deprotected with 30% TFA in DCM at room temperature for 2 h and then purified by silica gel column chromatography with 2.5% MeOH in dichloromethane to give each acid **12** and **13** in 30-40% yield.

12: ^{1}H NMR (500 MHz, $CDCl_3$): δ1.66 – 1.75 (m, 3H), 1.83 – 1.89 (m, 1H), 2.40 (s, 3H), 3.36 – 3.46 (m, 2H), 3.68 (s, 2H), 3.71 (s, 2H), 4.01 – 4.05 (m, 1H), 5.48 (d, J = 8.5 Hz, 1H), 5.78 (s, 2H), 5.82 (s, 2H), 7.24 – 7.35 (m, 12H), 7.72 – 7.74 (m, 2H), 8.32 (br t, J = 5.3 Hz, 1H), 11.55 (br, 1H).

13: ^{1}H NMR (500 MHz, $CDCl_3$): δ 1.67 – 1.77 (m, 3H), 1.93 – 1.97 (m, 1H), 2.04 (s, 3H), 3.36 – 3.40 (m, 1H), 3.51 – 3.55 (m, 1H), 3.67 (s, 2H), 3.70 (s, 2H), 4.54 – 4.58 (m, 1H), 5.78 (s, 2H), 5.81 (s, 2H), 6.93 (d, J = 7.5 Hz, 1H), 7.26 – 7.35 (m, 10H), 8.41 (br t, J = 5.5 Hz, 1H), 11.63 (br, 1H).

Methyl(S)-2-[(4-methylphenyl)sulfonyl]amino-4-[[bis[[[[(phenylacetyl)oxy]methoxy] carbonyl]amino]methylene]amino]pentanoate (14) and methyl (S)-2-(acetyl)amino-4-[[bis[[[[(phenylacetyl)oxy]methoxy]carbonyl]amino]methylene]amino]pentanoate (15): were prepared following a literature procedure (Tangirala, 2006). Briefly, each acid (**12** and **13**) was methylated with $TMSCHN_2$ (2 M solution in hexane) in dry benzene at room temperature and then purified by silica gel column chromatography with 40% EtOAc in hexane for **14**, 80% EtOAc in hexane for **15** to give each ester **14** and **15** in 40 to 45% yield, respectively.

14: ^{1}H NMR (500 MHz, $CDCl_3$): δ1.65 – 1.72 (m, 2H), 1.76 – 1.81 (m, 1H), 2.41 (s, 3H), 3.34 (q, J = 6.5, 2H), 3.48 (s, 3H), 3.68 (s, 2H), 3.71 (s, 2H), 3.93 – 3.97 (m, 1H), 5.28 (d, J = 9.0 Hz, 1H), 5.80 (s, 2H), 5.83 (s, 2H), 7.24 – 7.36 (m, 12H), 7.71 – 7.72 (m, 2H), 8.28 (br t, J = 5.8 Hz, 1H), 11.61 (s, 1H). ^{13}C NMR (125 MHz,$CDCl_3$): . 21.5, 24.8, 30.2, 40.4, 40.8, 41.0, 52.6, 55.3, 80.5, 81.2, 127.2, 127.3, 127.5, 128.6, 128.7, 129.3, 129.4, 129.7, 132.7, 133.3, 136.5, 143.8, 152.4, 156.3, 162.1, 169.9, 170.3, 171.8, HRMS calcd for $C_{34}H_{39}N_4O_{12}S$ $(M + H)^+$ 727.2285; found 727.2280.

15: ^{1}H NMR (125 MHz, $CDCl_3$): δ 1.59 – 1.73 (m, 3H), 1.88 – 1.92 (m, 1H), 2.03 (s, 3H), 3.40 – 3.45 (m, 1H), 3.45 – 3.52 (m, 1H), 3.68 (s, 2H), 3.71 (s, 2H), 3.75 (s, 3H), 4.63 – 4.67 (m, 1H), 5.80 (s, 2H), 5.82 (s, 2H), 6.28 (d, J = 8.0 Hz, 1H), 7.25 – 7.36 (m, 10H), 8.32 (br t, J = 5.5 Hz, 1H), 11.61 (br s, 1H). ^{13}C NMR (500 MHz, $CDCl_3$): . 23.4, 25.4, 29.6, 40.6, 41.0, 41.2, 52.1, 52.8, 80.8, 81.4, 127.5, 127.8, 128.8, 129.0, 129.6, 129.7, 132.9, 133.5, 152.7, 156.5, 162.9, 170.2, 170.6, 172.9. HRMS calcd for $C_{29}H_{35}N_4O_{11}$ $(M + H)^+$ 615.2302; found 615.2297.

ProTAME activation analysis

ProTAME was added to interphase *Xenopus* extract at 50 μM or cell growth media at 20 μM. For interphase extract, 800 μl of sample was collected at 0 min, 10 min, 20 min and 30 min after addition of proTAME and diluted to 8 ml with XB. For cell culture, approximately 800,000 cells were collected at 1 h, 2 h and 3 h after addition of proTAME and lysed in 400 μl lysis buffer as described above and subsequently diluted to 4 ml with lysis buffer. The diluted extract or cell lysate was extracted with 1.5 volume of ethyl acetate. The extracts were dried *in vacuo* and the dry extracts were resuspended in 200 μl of methanol for LC/MS analysis. LC/MS data were obtained using an Agilent series 1200 LC / 6130 MS system with a reversed-phase C18 column (Phenomenex Luna C18(2), 4.6 mm × 100 mm, 5 μm) and a CH_3CN/H_2O gradient solvent system beginning with 10% aqueous CH_3CN and ending at 100% CH_3CN at 20 min. 10 μl of each sample was injected for each analysis. The collected LC/MS profiles were further analyzed by

extracting specific ions such as 343 (TAME) and 727 (proTAME) in the positive ion MS mode.

Odyssey scanner for western signal quantification

Secondary antibodies coupled to fluorophores (anti-mouse Alexa-Fluor 750 and anti-rabbit Alexa-Fluor680, Invitrogen) were used to detect and quantify signals from rabbit anti-Cdc20 (Santa-Cruz, sc-8358) and mouse anti-GAPDH (AbCam, ab8245) antibodies on the same membrane using an Odyssey (Li-Cor Biosciences) scanner. Quantifications are reported as CDC20/GAPDH signal ratio, normalized to control treatment.

Cdc20/Cdh1 binding assay in HeLa cells

HeLa cells in DMEM 10% FBS were plated in T25 flasks at 20% confluence one day prior to the experiment. They were then synchronized by a double thymidine block (18 h for the first block, 8 h release and another 18 h for the second block, thymidine concentration: 2 mM). For analysis of Cdh1 binding, cells were released into 300 nM from the second thymidine block for 13 h and then washed into fresh medium. Six h later, cells were treated with 12 µM proTAME or proAAME or 0.06% DMSO for 2 h and then collected by trypin digrestion. For analysis of Cdc20 binding, cells were transfected with indicated siRNAs during the first release from thymidine block after two washes with DPBS (CellGro 21-030-CV) and addition of 6.3 ml OptiMEM. A volume (79 µl) of 20 µl

Control siRNA#3 or a 1:1 mix of 20 µl MAD2 siRNA and BubR1 siRNA (Dharmacon D-004101-01, 5'-GGAAGAAGAUCUAGAUGUA$_{UU}$-3') was mixed in 1381 µl OptiMEM in a tube, 23.7 µl OligoFectamine were mixed with 94.1 µl OptiMEM in a second tube. After 5 min incubation at RT, the tubes contents were mixed and siRNA-reagent complexes were allowed to form for 20 min at RT. The transfection mixes were added to cells in OptiMEM and FBS was added to 10% after 5 h transfection. Cyclin B1-Δ107 expressing adenovirus (1:100) was added at the start of the second thymidine block and kept in the medium for all subsequent steps. Cells were treated at 10 h after release with 100 nM okadaic acid, 25 µg/ml cycloheximide and 12 µM proTAME as indicatd. After 2 h treatment, cells were collected by mitotic shake-off. Cell pellets were washed twice with DPBS and flash-frozen with liquid nitrogen and stored at -80°C until use. Cell lysis and APC immunoprecipitation were performed as described above.

Live cell imaging

The imaging plate was mounted onto a motorized stage (Prior ProScan II) on a Nikon TE2000E PFS inverted microscope fitted with an incubation chamber maintained at 37C and supplied with 5% CO_2. A 20X Plan Apo 0.75 NA or 40X Plan Fluor 0.75 NA objective lens was used as indicated and images were collected with 2x2 binning. DIC or GFP fluorescent images were taken every 12 min (unless otherwise specified) for 36 h with a Hamamatsu ORCA cooled CCD camera and Nikon Elements Software. TIFF files of each image were exported from Elements and used to build stacks and Quicktime

movies with Metamorph imaging software (Molecular Devices). For manual analysis, mitotic duration is counted as the time between the first frame of chromosome condensation and the frame of chromosome segregation (anaphase) or decondensation (mitotic exit in the presence of nocodazole) or cell death (chromosomes shrinking to a small bright dot).

Emi1 knockdown and proTAME rescue

HeLa H2B-GFP cells were plated in glass-bottom 24-well plates at 20% confluence one day prior to the experiment. Cells were transfected with a pool of Emi1 siRNA (Dharmacon M-012434-01, 5'-GAAAGGCUGUCAUGUAUUG-3'; 5'-CAACAGACACUUAAUAGUA-3'; 5'-CGAAGUGUCUCUGUAAUUA-3'; 5'-GUACGAAGUGUCUCUGUAA-3') or Control#3 siRNA (described above) at 18.5 nM with DharmaFect3. After 24 h, cells were treated with 0.06% DMSO or 12 μM proTAME. Live cell imaging was set up as described above.

ProTAME dose-response

HeLa H2B-GFP cells were plated in a 24-well plate in DMEM 10% FBS at 20% confluence one day prior to experiment and synchronized by double thymidine block as described above. ProTAME was added to final concentrations of 780 nM, 3 μM or 12 μM and proAAME was added to a final concentration of 12 μM at 8 h after release from the second thymidine block. 0.06% DMSO was used as the negative control. Live cell

imaging was set up as described above.

Exogenous cyclin-GFP expression, live-cell imaging, and quantitation

HeLa H2B-RFP cells were transduced with cyclin B1-GFP or cyclin A2-GFP adenovirus for 40 h. Phenol Red-Free DMEM (Mediatech) supplemented with 10% FBS and 1:100 Penicillin-Streptomycin-Glutamine (Mediatech) was used as imaging medium. 20 μM proAAME, 20 μM proTAME or150 nM nocodazole was added 45 min prior to the start of imaging. Live cell imaging was set up as described above except that the cells were plated in a 8-well chambered coverglasses (NUNC Lab-tek 155411). Four positions per treatment group were imaged with DIC transmitted light, red fluorescence, and green fluorescence (Semrock GFP/HcRed "Pinkel" filter set) at 12 min intervals for 24 h. Stacks of red and green fluorescence were merged, saved as AVI video files and analyzed using ImageJ. For quantitation, the first GFP-positive cells that undergo mitosis in three separate movies were chosen, giving at least 30 cells quantitated for each treatment group. Mean intensity values for the green channel were collected for a cytoplasmic region of a cell upon mitotic entry, mitotic exit, or after 1 h of mitotic arrest. At the same time points, background mean green intensity was determined and individually subtracted from the cytoplasmic mean intensity. This background corrected mean intensity value was then used to determine the percentage of the original GFP signal remaining at the completion of division (for the control cells) or after 1 h of mitotic arrest (for the nocodazole and proTAME treated cells). The average values for all quantitated cells were plotted with the

error bars representing standard error of the mean.

Immunofluorescence

HeLa cells grown in DMEM + 10% FBS were plated on 25 mm glass coverslips in a 6-well dish at a density of 130,000/ml×3ml 48 h prior to treatment. They were then treated with 0.06% DMSO, 12 μM proTAME, 300 nM nocodazole or 300nM taxol for 2 h. The cells were washed twice with PBS and fixed with 3% paraformaldehyde for 15 min. The cells were then washed with PBS and permeabilized with PBS plus 0.5% Triton X-100 for 2 min. The cells were then washed with PBS and blocked with PBS plus 5% FBS for 1 h. CREST antisera diluted 1:50 into PBS was added to the cells and incubated at room temperature for 1 h. The cells were washed with PBS and incubated with 1:1000 anti-human-Alexa 568 (Invitrogen, A21090) and 1:100 anti-α-tubulin-FITC for 1 h. The cells were then washed with PBS and the nuclei were stained with 1 μg/ml Hoechst 33342. The cover slips were mounted in 0.1M N-propylgallate in 9:1 glycerol:PBS. Z-series images were taken on a Nikon TE2000 microscope with PerkinElmer spinning disk confocal device. Maximal Z-projection images of individual cells were made by Image J. To measure interkinetochore distances, a straight line was drawn across a kinetochore pair in the same confocal plane and pixel intensities along the line were plotted so that each kinetochore would be represented by a peak on the line. The interkinetochore distance was calculated as the distance between the peaks. Fifty-five kinetochore pairs from 5 cells treated with DMSO or proTAME were measured and the

p-value was calculated with a paired student test.

Mad2 knockdown and time point analysis

HeLa H2B-GFP cells were plated in a 24-well plate in DMEM + 10% FBS at 20% confluence one day prior to the experiment and synchronized by double thymidine block as described above. The cells were released from the first thymidine block into 200 µl OptiMem without FBS. Transfection was performed immediately after the first thymidine release. To prepare the transfection mixture for one well, 40 µl OptiMem was mixed with 2.5 µl of 20 µM Mad2 siRNA stock (GGAACAACUGAAAGAUUGGdTdT, synthesized by DHARMACON) or control (D-001210-01-20, DHARMACON), and 6.5 µl of OptiMem was mixed with 1 µl of Oligofectamine (Invitrogen, 12252-011). The two mixtures were left at room temperature for 5 min before being mixed together and incubated for additional 20 min and then added to the cells to a final volume of 250 µl. 4 h after transfection, 250 µl of DMEM + 20% FBS were added to cells. 8 h after the release, 500 µl of 4 mM thymidine in DMEM + 10% FBS was added to each well to make the final concentration of 2 mM and the cells were incubated for another 18 h before being released into growth medium. At 8 h after release, cells were treated 0.06% DMSO, 12 µM proTAME, 300 nM nocodazole or 12 µM proTAME plus 300 nM nocodazole in growth medium. Cell samples were collected at 4 h, 8 h, 10 h, 12 h, 14 h, 16 h and 20 h post-release and protein levels were analyzed by Western blot.

Cdc20 knockdown sensitization to proTAME treatment

HeLa H2B-GFP cells were plated in glass-bottom 24-well plates (Greiner Bio-One 662892) at 20% confluence one day prior to the experiment. Cells were transfected with DharmaFect3, following the manufacturer's protocol at a final concentration of 18.5 nM control siRNA#3 or a mix of 1.85 nM Cdc20 siRNA completed to 18.5 nM with control siRNA#3. After 24 h transfection, cells were treated with DMSO or 4 μM proTAME and live cell imaging was set up immediately as described above.

UbcH10 and Cdc27 knockdown and hesperadin treatment

HeLa H2B-GFP cells were plated in glass-bottom 24-well plates at 20% confluence one day prior to the experiment and synchronized by double thymidine block as described above. Cells were transfected with UbcH10 siRNA (Dharmacon D-004693-15, 5'-UAAAUUAAGCCUCGGUUGA$_{UU}$-3'), Cdc27 siRNA (Dharmacon J-003229-11, 5'-GGAAAUAGCCGAGAGGUAA$_{UU}$-3') or Control#3 siRNA (described above) at 18.5 nM with DharmaFect3, during the release from the first thymidine block. Cells were treated with 100 nM Hesperadin or DMSO 8 h after release from the second thymidine block and live cell imaging was set up as described above.

Measuring cycloheximide-sensitivity of drug-induced arrest

HeLa H2B-GFP cells were plated in a 24-well plate in DMEM + 10% FBS at 20% confluence one day prior to experiment and synchronized by double thymidine block as

synchronized above. At 8 h after release from the second block, cells were treated with 12 μM proTAME, 300 nM nocodazole or 150 nM taxol and 4 h later, cells were left untreated or treated with an addition of 25 μg/ml cycloheximide. Live cell imaging was set up as described above.

Measuring hesperadin-sensitivity of drug-induced arrest

HeLa H2B-GFP cells were plated in a 24-well plate in DMEM + 10% FBS at 20% confluence one day prior to experiment and synchronized by double thymidine block as described above. At 8 h after release from the second block, 100 nM hesperadin, 12 μM proTAME with or without 100 nM hesperadin, 300 nM nocodazole with or without 100 nM hesperadin or 150 nM taxol with or without 100 nM hesperadin were added to cells. Untreated cells were used as the control. Live cell imaging was set up as described above. For experiments with MG132, at 10 h after release from the second block, 3 μM MG132, or 3 μM MG132 plus 100 nM hesperadin, or 3 μM MG132 plus 100 nM hesperadin and 12 μM proTAME were added to cells. Alternatively, at 10 h after release from the second block, 10 μM MG132 with or without 25 μg/ml cycloheximide was added to the cells. 30 min after, cells were left untreated or treated with 100 nM hesperadin or 100 nM hesperadin and 12 μM proTAME. Live cell imaging was set up as described above.

Measuring Mad2-dependence of MG132-induced arrest

HeLa H2B-GFP cells were plated in a 24-well plate in DMEM + 10% FBS at 20%

confluence one day prior to experiment and synchronized by double thymidine block as described above. Mad2 siRNA transfection was performed as described above. At 10 h after release from the second block, 10 μM MG132 with or without 25 μg/ml cycloheximide was added to the cells. Live cell imaging was set up as described above. Manual analysis was focused only on cells that entered mitosis after MG132 addition.

Chromosome congression analysis

HeLa H2B-GFP cells were plated in 35mm glass-bottom dishes (MatTek) in DMEM + 10% FBS at 20% confluence one day prior to the experiment and synchronized by double thymidine block as described above. Drugs were added as follows to a final volume of 3 ml from 2X concentrated preparation in culture medium. DMSO (0.06%), proTAME (3 and 12μM) or 10nM Nocodazole were added 8 h after release from the second block, while MG132 (10μM) was added at 10 h. H2B-GFP was imaged for 4 hrs every 3 min at 40X magnification as described above.

Click-iT chemistry labeling of de novo-translated proteins

HeLa H2B-GFP cells (600,000) were plated in 3mL DMEM + 10% FBS in 6-well plates 24 h prior to synchronization. Cells were arrested in interphase by 2mM Thymidine treatment for 24 h. To label proteins translated in S/G2 phase, three hours after release from thymidine-block, the cells were washed once with warm DPBS with Mg^{2+}/Ca^{2+} and switched to filter-sterilized labeling medium (Methionine-free medium from Sigma,

catalog #D0422, supplemented with 10mL FBS pre-dialyzed against 1L DPBS, 2mM Glutamine and 568 μM L-Cysteine). After 30 min pre-incubation to deplete the remaining intracellular pool of Methionine, the methionine analog L-azidohomoalanine (AHA) was added at 250 μM (Invitrogen, catalog #C10102) and the cells were incubated for 3 h in the presence or absence of 25 μg/mL cycloheximide. To label proteins translated in mitosis, cells were treated with 300 nM nocodazole or 12 μM proTAME at 5 h after release from thymidine block and allowed to enter mitosis. Mitotic cells were collected by mitotic shake off, washed once in warm DPBS with Mg^{2+}/Ca^{2+} and switched to labeling medium. After 30 min pre-incubation, 250 μM AHA was added. Labeling was allowed to occur for 12 h in the presence or absence of 25 μg/mL cycloheximide. After labeling, the cells were collected by trypsinization (interphase cells) or mitotic shake-off (mitotic cells), washed twice with DPBS with Mg2+/Ca2+ and lyzed in 50 μL lysis buffer (Tris-HCl 50 mM pH 8.0, SDS 1% supplemented with 250 U/mL Benzonase, VWR, catalog #80108-806 and EDTA-free protease inhibitors, Roche). After 15 min on ice, cells were vortexed and centrifuged at 15,000g at 4C for 5 min. Supernatants were collected and protein concentrations were determined using the BCA assay (Pierce). Proteins (200 μg) were labeled with biotin-azide following the manufacturer's protocol (Invitrogen, catalog #B10184) and the protein reaction buffer kit (catalog #C10276). Labeled proteins were desalted with desalting columns (Thermo Scientific, catalog #89889) pre-washed with incubation buffer (NP-40 1%, SDS 0.1% in DPBS with Ca2+/Mg2+, with protease inhibitors). Ten percent of proteins were kept aside as total

protein control for western blots of specific proteins, and another 10% were conserved to run Streptavidin-HRP western blots to detect all labeled proteins. The remaining sample was incubated at room temperature with Neutravidin agarose resin pre-washed with incubation buffer (Thermo scientific, catalog #29200) to purify biotin-labeled proteins. The resin was washed once with incubation buffer and three times with wash buffer (NP-40 1% in DPBS with Ca2+/Mg2+, with protease inhibitors). Purified proteins were boiled in SDS-PAGE loading buffer and tested by western blotting.

Statistical analysis

For each indicated figure and conditions, the data sample size (N), median and average values are reported. Statistical analysis was performed using the software Jmp 8.0 (SAS Institute Inc.). Samples were compared two by two using the Mann-Whitney-Wilcoxon non-parametric statistical test. The *p* values are reported. The samples were considered statistically significantly different when *p* was inferior to 0.05. Very small *p* values were reported as zero by Jmp.

Supplemental References

Bryan, D.B.H., R.F.; Holden, K.G.; Huffman, W.F.; Gleason, J.G. (1977). Nuclear analogs of .beta.-lactam antibiotics. 2. The total synthesis of 8-oxo-4-thia-1-azabicyclo[4.2.0]oct-2-ene-2-carboxylic acids J Am Chem Soc 99, 2353-2355.

Folkmann, M.L., F.J. (1990). Acyloxymethyl Carbonochloridates. New Intermediates in Prodrug Synthesis. Synthesis, 1159-1166.

Kimata, Y., Baxter, J.E., Fry, A.M., and Yamano, H. (2008). A role for the Fizzy/Cdc20 family of proteins in activation of the APC/C distinct from substrate recruitment. Mol Cell 32, 576-583.

Kirkpatrick, D.S., Hathaway, N.A., Hanna, J., Elsasser, S., Rush, J., Finley, D., King, R.W., and Gygi, S.P. (2006). Quantitative analysis of in vitro ubiquitinated cyclin B1 reveals complex chain topology. Nat Cell Biol 8, 700-710.

Murray, A.W. (1991). Chapter 30 Cell Cycle Extracts. Methods Cell Biol 36, 581.

Saulnier, M.G.F., D.B.; Deshpande, M.S.; Hansel, S.B.; Vyas, D.M. (1994). An efficient method for the synthesis of guanidino prodrugs. Bioorg Med Chem Lett 4, 1985-1990.

Tangirala, R.S.A., S.; Agama, K.; Pommier, Y.; Anderson, B.D.; Bevins, R.; Curran, D.P. (2006). Synthesis and biological assays of E-ring analogs of camptothecin and homocamptothecin. Bioorg Med Chem 14, 6202-6212.

Verma, R., Peters, N.R., D'Onofrio, M., Tochtrop, G.P., Sakamoto, K.M., Varadan, R., Zhang, M., Coffino, P., Fushman, D., Deshaies, R.J., King, R.W. (2004). Ubistatins inhibit proteasome-dependent degradation by binding the ubiquitin chain. Science 306, 117-120.

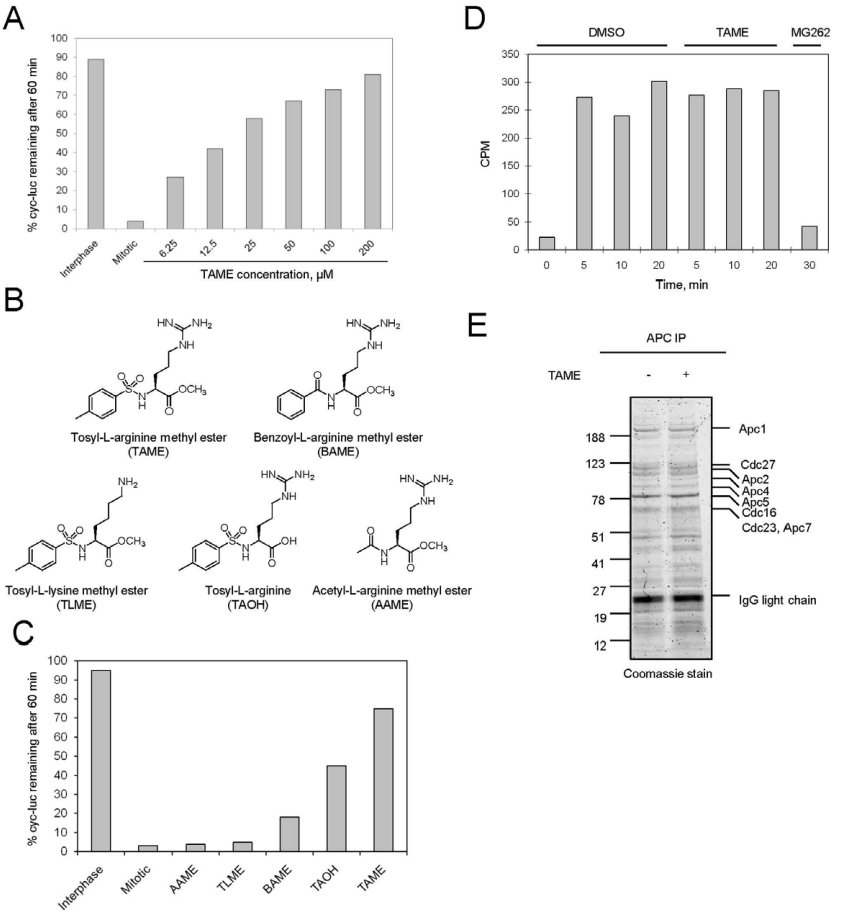

Figure S1: (A) TAME stabilizes cyclin B-luciferase (cycB-luc) reporter in mitotic *Xenopus* extract. Different concentrations of TAME were added to the extract containing the reporter. Samples were collected at 60 min and the remaining reporter level was measured by luminescence. Interphase extract was used as a negative control. (B) Structures of TAME derivatives. (C) The derivatives shown in (A) were tested in the luciferase assay at 200 μM. (D) TAME does not inhibit degradation of pre-ubiquitinated cyclin B. Baculovirus-expressed and purified ^{35}S-labeled cyclin B bound to unlabeled Cdk1 was first ubiquitinated by APC in an *in vitro* ubiquitination system and then added into *Xenopus* extract supplemented with DMSO, 200 μM TAME or 200 μM proteasome inhibitor MG262. At indicated time points, protein was precipitated and the level of radioactivity in supernatant was measured by scintillation counting. (E) TAME does not affect the composition of APC core subunits. Mitotic extract was treated with DMSO or 200 μM TAME. APC was immunoprecipitated and the subunits were resolved by SDS-PAGE and visualized by coomassie stain. Identity of subunits was confirmed by mass spectrometry.

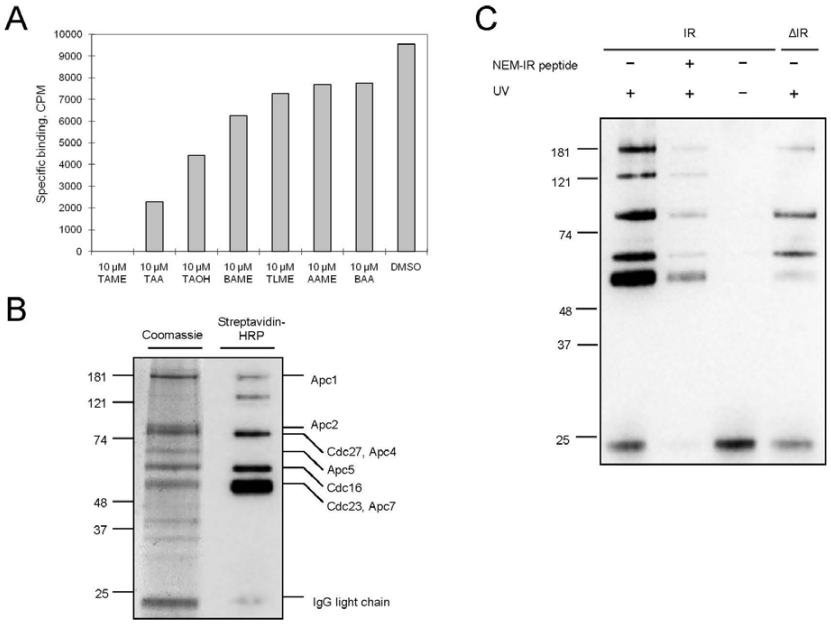

Figure S2: (A) The ability of TAME derivatives to compete with ^{3}H-TAME for binding to the APC correlates with their ability to inhibit cyclin B-luciferase degradation. Two hundred nM ^{3}H-TAME was added into interphase extract with 10 µM of unlabeled TAME derivatives before Cdc27 immunoprecipitation, and the amount of bound radioactivity was determined by scintillation counting. Specific binding was obtained by subtracting the value of mock IP (IP without Cdc27 antibody). The relative levels of competition correlate with the trends seen in the cyclin-luciferase assay as shown in Figure S1C. (B) Cdh1 C-terminal peptide crosslinks to the TPR subcomplex in an IR-dependent manner. An IR peptide coupled to a photocrosslinker labels a subset of APC subunits. Left: Coomassie stain of APC immunopurified from interphase *Xenopus* extract. Right: APC subunits crosslinked by the labeled IR peptide. Identity of APC subunits was confirmed by mass spectrometry. (C) Crosslinking is IR-dependent. The crosslinking assay was performed in the presence of excess unlabeled IR peptide with the N-terminal cysteine blocked with N-ethyl maleimide (NEM) (lane 2), no UV illumination (lane 3) or with labeled ΔIR peptide (lane 4).

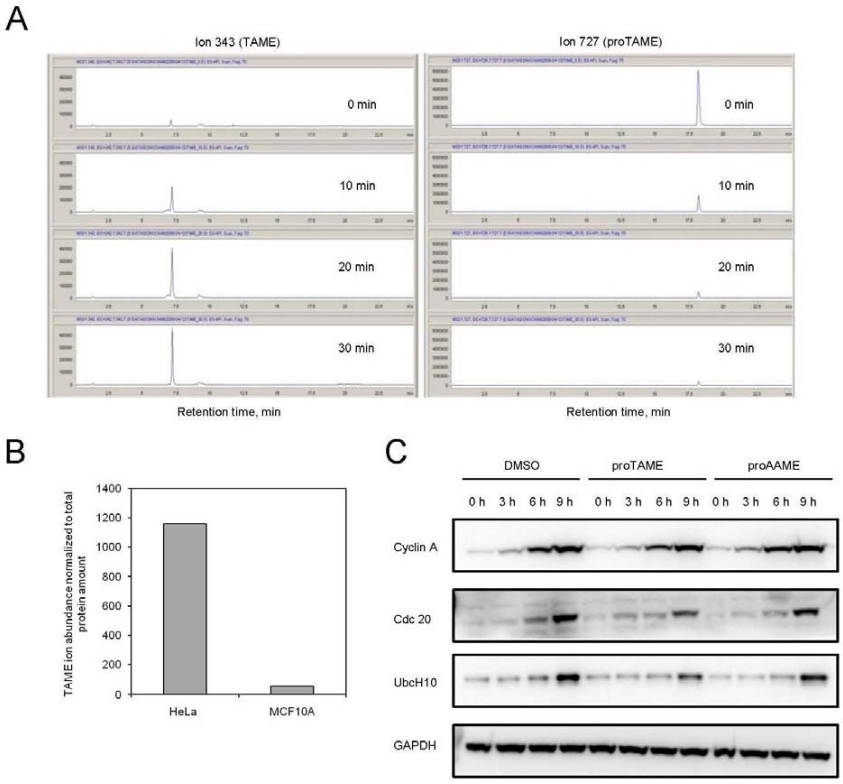

Figure S3: (A) ProTAME is converted to TAME in *Xenopus* extract. Fifty μM proTAME was added to interphase *Xenopus* extract and samples were collected at indicated time points. Ethyl acetate extraction was performed, and samples analyzed by liquid-chromatography-mass spectrometry (LC/MS). Chromatograms of the abundance of TAME and proTAME ion are shown. (B) ProTAME is efficiently activated in HeLa cells but not MCF10A cells. HeLa and MCF10A cells were treated with 20 μM proTAME. Cells were collected after 1 h and lysed. Ethyl acetate extraction was performed prior to LC/MS analysis. Quantitation of the abundance of TAME ion normalized to total protein level is shown. (C) ProTAME does not induce premature accumulation of APC substrates in G1 cells. HeLa cells were synchronized by double thymidine block, released into nocodazole for 13 h and washed out of nocodazole for 6 h. Cells were then treated with DMSO (0.06%), proTAME or proAAME (12 μM). Samples were collected at indicated time points and protein level was measured by immunoblot.

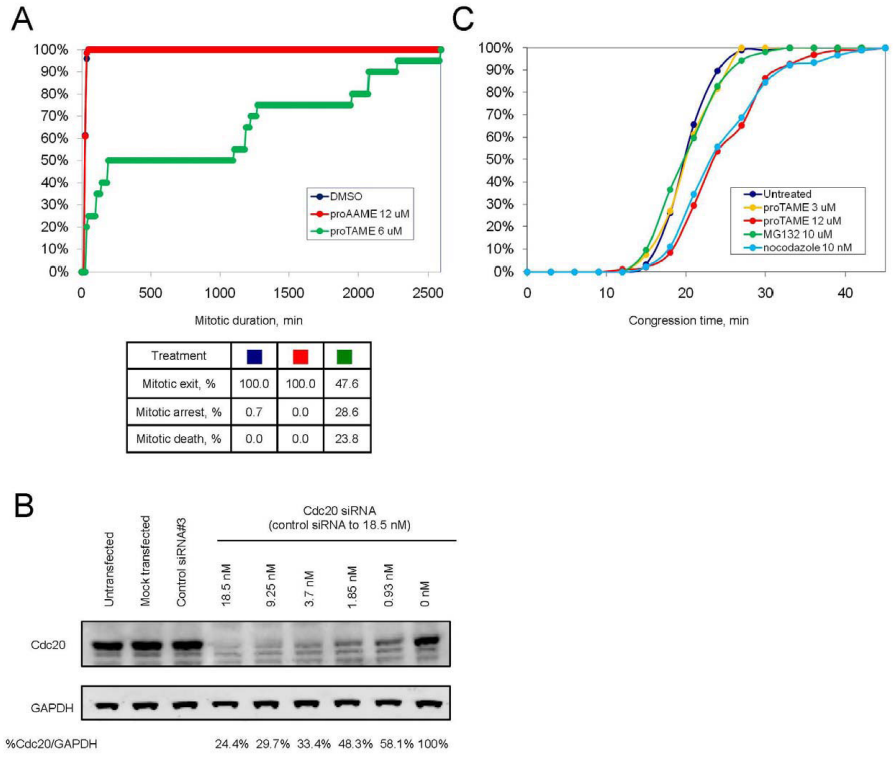

Figure S4: (A) ProTAME induces a mitotic exit delay in hTERT-RPE1 H2B-GFP cells. Asynchronous hTERT-RPE1 H2B-GFP cells were treated with 0.06% DMSO, 6 μM proTAME or 12 μM proAAME. Cells were imaged at 12 min interval. Cumulative frequency curves of mitotic duration and cell fate distribution are shown. (B) Cdc20 siRNA induces a dose-dependent knockdown of Cdc20. HeLa H2B-GFP cells were plated in 24-well plates and transfected with indicated siRNAs. Control siRNA was added to final 18.5 nM siRNA concentration in wells with decreasing Cdc20 siRNA concentration. Cells were lysed 48 h after transfection and lysates were subjected to western blotting to detect Cdc20 and GAPDH. Protein level quantification was performed on a LiCor Odyssey scanner as described in Material and Methods. (C) Twelve μM but not 3 μM proTAME induces a mild delay in chromosome congression. HeLa H2B-GFP cells were synchronized by double thymidine block and treated with 0.06% DMSO, 3 μM proTAME, 12 μM proTAME, 10 μM MG132 or 10 nM nocodazole at 8 h after release. Cells were imaged at 3 min interval and 40x magnification. The time between prophase and full metaphase congression was analyzed. Cumulative frequency curves of the congression time were plotted.

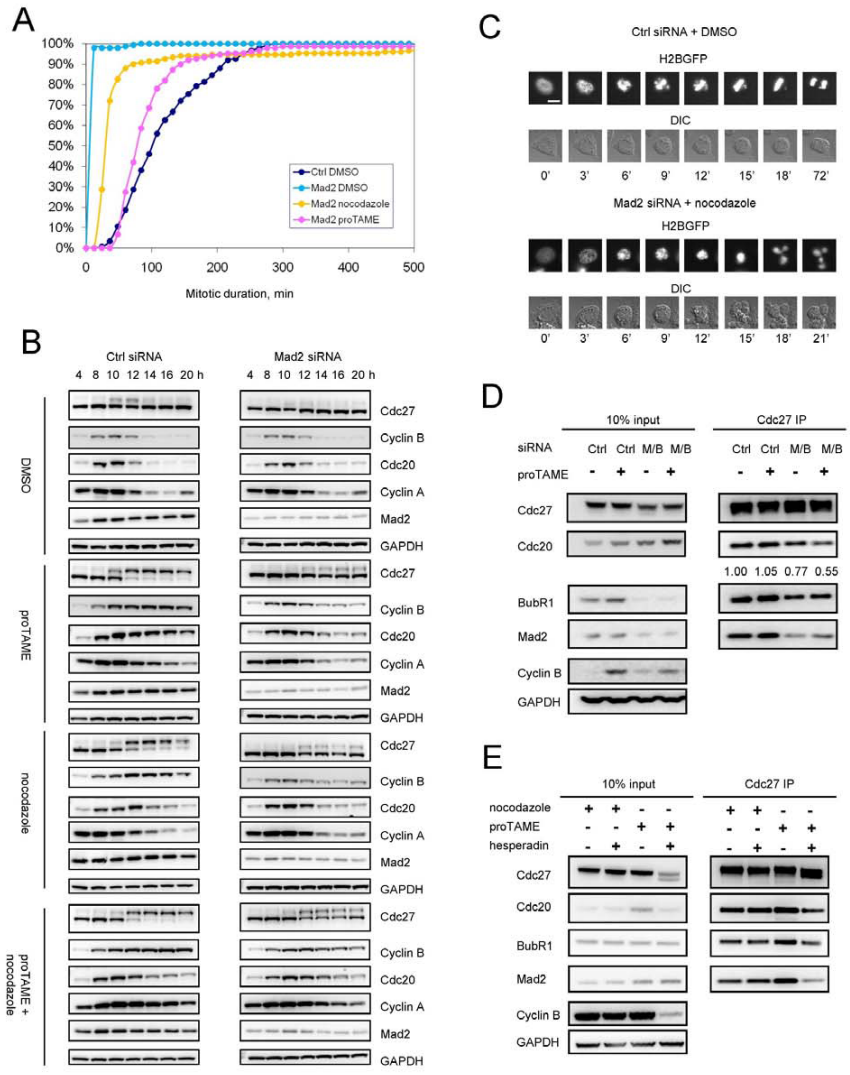
A
100%
90%
80%
70%
60%
50%
40%
30%
20%
10%
0%
0
100
200
300
400
500
Mitotic duration, min
Ctrl DMSO
Mad2 DMSO
Mad2 nocodazole
Mad2 proTAME
B
Ctrl siRNA
Mad2 siRNA
4 8 10 12 14 16 20 h
DMSO
proTAME
nocodazole
proTAME + nocodazole
Cdc27
Cyclin B
Cdc20
Cyclin A
Mad2
GAPDH
C
Ctrl siRNA + DMSO
H2BGFP
DIC
0' 3' 6' 9' 12' 15' 18' 72'
Mad2 siRNA + nocodazole
H2BGFP
DIC
0' 3' 6' 9' 12' 15' 18' 21'
D
10% input
Cdc27 IP
siRNA
Ctrl Ctrl M/B M/B
proTAME
- + - +
Cdc27
Cdc20
BubR1
Mad2
Cyclin B
GAPDH
1.00 1.05 0.77 0.55
E
10% input
Cdc27 IP
nocodazole
proTAME
hesperadin
Cdc27
Cdc20
BubR1
Mad2
Cyclin B
GAPDH

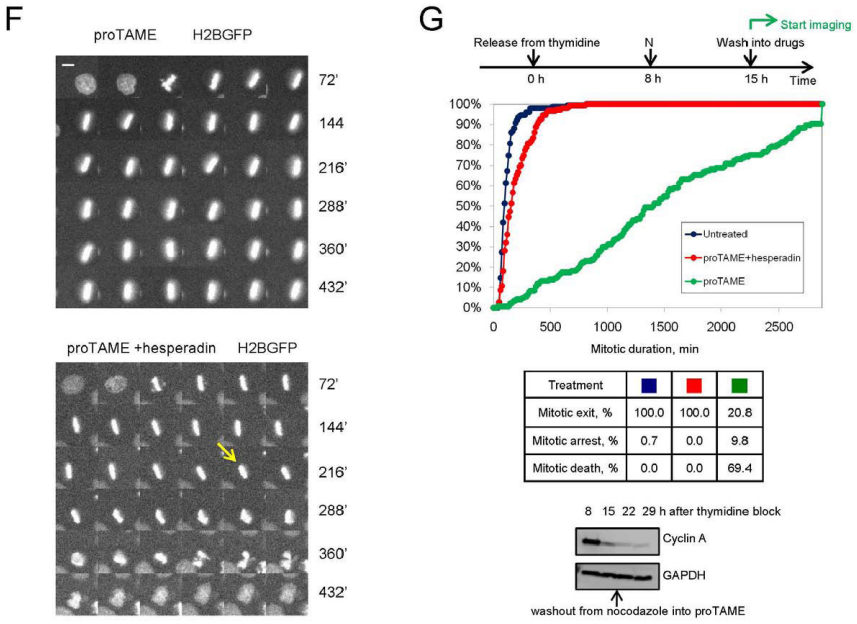

Figure S5: (A) Same experiment as shown in Figure 6A but with an expanded x-axis to better show the difference between short mitotic durations. (B) ProTAME-induced mitotic arrest is Mad2-dependent. HeLa H2B-GFP cells were transfected with indicated siRNAs between rounds of thymidine treatment. Following release, cells were treated with compounds and samples were collected at indicated time points. Protein levels were measured by immunoblot. (C) Mad2 knockdown efficiently overrides the spindle assembly checkpoint in the presence of nocodazole. Above: Control-siRNA-treated cells were treated with 0.06% DMSO. Below: Mad2 knockdown cells were treated with 300 nM nocodazole. Live imaging was done at 40x magnification and 3 min interval. Scale bar: 10 μm. (D) ProTAME inhibits Cdc20 association with human APC if the SAC is inactivated. Double thymidine synchronized HeLa cells were transfected with Mad2 and BubR1 siRNA, and infected with cyclin BΔ107 adenovirus. At 10.5 h after release from thymidine, cells were treated with indicated drugs for 2 h. M/B: Mad2/BubR1 siRNA. Numbers indicate the relative Cdc20 band intensity normalized to Cdc27. (E) Hesperadin overrides a proTAME-induced mitotic arrest. HeLa cells were synchronized with double thymidine block and treated with indicated drugs at 10 h after release for 1 h. Mitotic cells were collected and APC was immunoprecipitated from cell lysate. Protein levels were measured by Western blot. (F) Hesperadin induces deformation of the metaphase plate in proTAME-arrested cells. HeLa H2B-GFP cells were synchronized with double thymidine block and treated with 12 μM proTAME at 8 h after release and with 100 nM hesperadin at 10 h after release. For cells that have entered metaphase prior to hesperadin treatment, changes in the morphology of metaphase plate were analyzed and one representative cell is shown. The yellow arrow denotes the time of hesperadin addition. A representative cell arrested with proTAME alone is also shown for comparison. Scale bar: 10 μm. (G) Hesperadin overrides proTAME-induced mitotic arrest of cells released from nocodazole-induced arrest. HeLa H2B-GFP cells were synchronized with double thymidine block and treated with 300 nM nocodazole at 8 h after release from thymidine block. Cells were washed out of nocodazole at 15 h after release from thymidine block into growth medium, or 12 μM proTAME, or 12 μM proTAME and 100 nM hesperadin. Cells were imaged at 12 min interval. Cumulative frequency curves of mitotic duration and cell fate distribution are shown. Cell samples were collected at different time points as indicated and protein levels were measured by immunoblot. The top diagram shows timing of treatments. N: nocodazole.

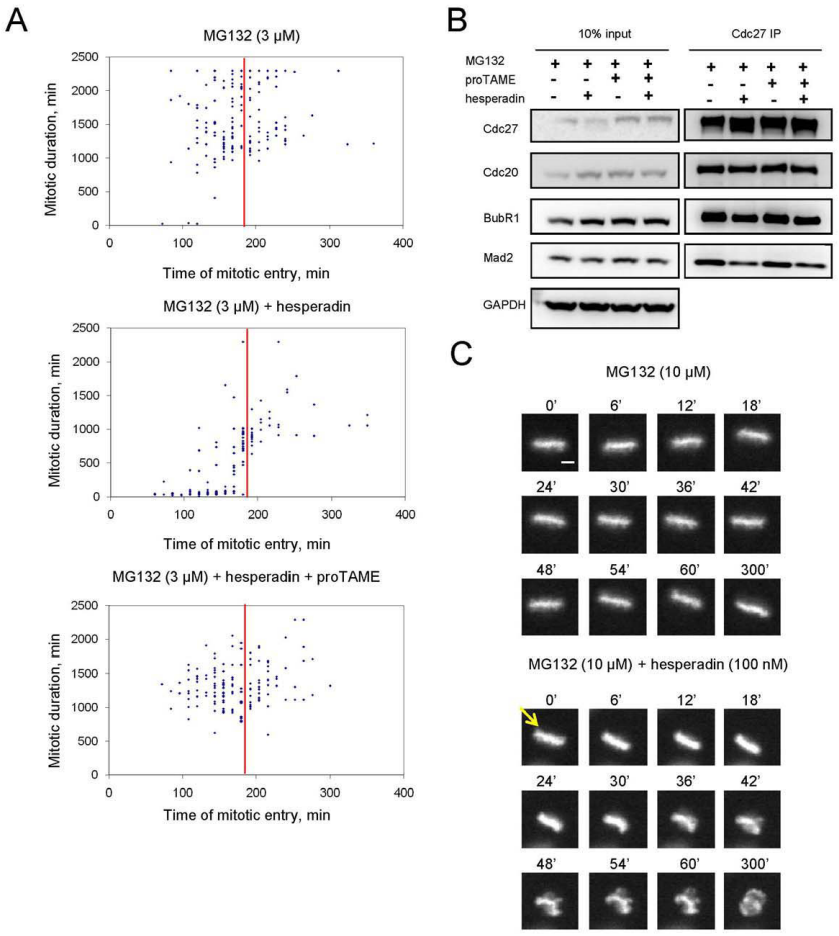

Figure S6: (A) Hepseradin overrides MG132-induced mitotic arrest. HeLa H2B-GFP cells were synchronized with double thymidine block and treated with indicated drugs at 10 h after release. Mitotic duration of each individual cell is plotted against its mitotic entry time point. The red line denotes the time of addition of MG132. (B) Hesperadin reduces the amount of Mad2/BubR1 bound to the APC in cells arrested in mitosis with MG132. HeLa cells were synchronized with double thymidine block and treated with indicated drugs at 10 h after release for 2 h. Mitotic cells were collected and APC was immunoprecipitated from cell lysate. Protein levels were measured by immunoblot. (C) Hesperadin induces deformation of the metaphase plate in MG132-arrested cells. HeLa H2B-GFP cells were synchronized with double thymidine block and treated with 10 μM proTAME at 10 h after release, and with 100 nM hesperadin at 11 h after release. For cells that have entered metaphase prior to hesperadin treatment, changes in the morphology of metaphase plate after hesperadin treatment were analyzed and one representative cell is shown. The yellow arrow denotes the time of hesperadin addition. A representative cell arrested with MG132 alone is also shown for comparison. Scale bar: 5 μm.

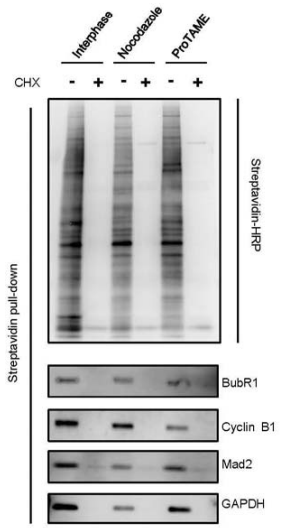

Figure S7: Proteins required for maintenance of the SAC are synthesized during prolonged mitotic arrest. HeLa H2B-GFP cells were arrested in interphase by a 24-hour thymidine block (2mM) and released in growth medium. To identify newly translated proteins in interphase cells, cells were switched to methionine-free labeling medium 3 hrs after release and de novo translated proteins were labeled by adding the methionine analog L-azidohomoalanine (AHA) at 250μM for 3hrs and collected by trypsinization. For labeling of proteins newly translated during mitosis, cells were released from thymidine block and nocodazole (300 nM) or proTAME (12μM) was added 5hrs after release. Seven hours later, mitotic cells were collected by shakeoff and switched to the labeling medium and incubated with 250μM AHA for 12 hours. A majority of cells remained in mitosis based on morphology. Following the labeling period, mitotic cells were collected by shake off. A labeling reaction including cycloheximide 25μg/mL as negative control was carried in parallel for each condition. Cells in nocodazole + cycloheximide slipped out of mitosis after the 12hrs incubation and were collected by trypsinization. Protein lysates were generated for each labeling condition, and newly synthesized proteins were labeled using biotin azide and purified with neutravidin-agarose resin as described in the Methods section. Purified proteins from equivalent amounts of total protein were eluted by boiling in SDS sample buffer, separated on SDS-PAGE gels and indicated proteins were detected by western blotting.